

Characterization of Jetting-Induced Disturbance Zone and Associated Ecological Impacts

by

Mohammed A. Gabr, Ph.D., P.E.

Roy H. Borden, Ph.D., P.E.

Raymond L. Denton

Alex W. Smith

Department of Civil, Construction and Environmental
Engineering
North Carolina State University

In Cooperation with
The North Carolina Department of Transportation
and
The Institute for Transportation Research and Education

North Carolina State University

Raleigh, North Carolina

August, 2004

CIVIL
ENGINEERING
RESEARCH

NC STATE UNIVERSITY

DEPARTMENT OF CIVIL ENGINEERING
NORTH CAROLINA STATE UNIVERSITY

Technical Report Documentation Page

1. Report No. FHWA/NC/2006-09	2. Government Accession No.	3. Recipient's Catalog No.	
4. Title and Subtitle Characterization of Jetting-Induced Disturbance Zone and Associated Ecological Impacts		5. Report Date August, 2004	
		6. Performing Organization Code	
7. Author(s) M.A. Gabr, R.H. Borden, R. L. Denton, and A. W. Smith		8. Performing Organization Report No.	
9. Performing Organization Name and Address Department of Civil, Construction, and Environmental Engineering CB 7908 Mann Hall North Carolina State University Raleigh, NC 27695-7908		10. Work Unit No. (TRAIS)	
		11. Contract or Grant No.	
12. Sponsoring Agency Name and Address North Carolina Department of Transportation Research and Analysis Group 1 South Wilmington Street Raleigh, North Carolina 27601		13. Type of Report and Period Covered July 2002 - June 2004	
		14. Sponsoring Agency Code 2003-15	
15. Supplementary Notes			
<p>Abstract. Research in this report presents the first study documented in literature to characterize the surface disturbance and associated ecological impact due to pile jetting process. The enclosed work describes development of phenomenological pile jetting model in various soil profiles through implementation of a laboratory experimental program, field testing program, and comprehensive data analyses. The physical phenomenon of jetting was observed in the laboratory and a model for computing disturbance created by jetted-pile installations was developed. Four test sites were chosen in different geographical locations in Eastern North Carolina to perform a total of 26 jetted pile installations. Ecological impacts of jetting on marine environment and tidal marches are discussed and presented.</p>			
17. Key Words ecological, disturbance, field testing, flow rate, imacct, jetting, piles, sand,		18. Distribution Statement	
19. Security Classif. (of this report) Unclassified	20. Security Classif. (of this page) Unclassified	21. No. of Pages 270	22. Price

Form DOT F 1700.7 (8-72)

Reproduction of completed page authorized

DISCLAIMER

The contents of this report reflect the views of the author(s) and not necessarily the views of the University. The author(s) are responsible for the facts and the accuracy of the data presented herein. The contents do not necessarily reflect the official views or policies of either the North Carolina Department of Transportation or the Federal Highway Administration at the time of publication. This report does not constitute a standard, specification, or regulation.

ACKNOWLEDGMENTS

The authors are grateful for NCDOT-Geotechnical and Construction Divisions for their support of the research work, their technical contributions, and facilitating of field work. Thanks are also due to Dr. Moy Biswas and the research and analysis group for their support of the research and facilitating the proposed work. The authors would like to also acknowledge the contributions of Dr. David B. Eggleston, Cynthia Huggett and Gayle Plaia of the Department of Marine, Earth & Atmospheric Sciences who evaluated the impact of pile jetting on infaunal macrobenthos (Chapter 9) and Dr. Stephen W. Broome, Department of Soil Science, who evaluated the influence of jetting on tidal marsh vegetation (chapter 10).

Executive Summary

Research in this report presents a systematic study to characterize the surface disturbance and associated ecological impacts due to pile jetting process. The work aimed at developing a pile jetting model for computing the size of associated debris zones and illustrating potential ecological impacts of the jetting process. The work encompassed laboratory and field testing programs, and comprehensive data analyses for the development of the phenomenological model. From the laboratory testing program, the physical phenomenon of jetting was observed and a model for computing the disturbance created by jetted-pile installations was presented. Field testing encompassed four test sites in different geographical locations of Eastern North Carolina. A total of 26 jetted pile installations were performed to aid in model development and verify the behavior observed during laboratory experimentations.

Data from laboratory study indicated that installation of piles using jetting approach stems from the simultaneous erosion of soils beneath the pile tip and transport of these soil particles through the annulus to the ground surface. The pile advances only after a sufficient area of soil has been eroded to cause a tip bearing capacity failure as side friction is reduced due to the return water and liquefaction jetting annulus. Optimization of water flowrate (Q_w) and jet nozzle velocity (V_j) for a given soil profile provides minimal debris zone dimensions for jetted installations. In general, higher jet velocities with longer flow rates will produce smaller debris zones. Given equal jetting parameters, the extent of the debris zone for sands with smaller average particle sizes ($D_{50} = 0.15$ mm) were approximately 100% further from the pile center than sands with larger average particle size ($D_{50} = 0.5$ mm).

Measurement of the debris zone in the field indicated that the diameter of the disturbed area created from the jetting process was generally equivalent to the jetted depth of pile. Furthermore, the volume of debris material measured around the annulus of pile was generally equal to, or slightly more in case of dense profiles than, the inserted volume of pile for a particular installation.

At sites where the process took place underwater, environmental sampling indicated slight variation in pH and dissolved oxygen during jetting. Turbidity increased after jetting but did not exceed 70 NTU. Turbidity approached 70NTU level only at Swans Quarter No. 5 installation. In this case, turbidity curtains were used during jetting at the site where the highest turbidity was measured around the pile. This is due to the fact that the curtain maintained the sediment confined to area around the pile. Sampling of sediments and infauna was performed at three sites several months after testing was completed. Only at one of three sites (i.e., Swan Quarter), the mean number of macrobenthic organisms was significantly lower at the impact area compared to sampling areas that were 5 m and 20 m upstream and downstream. The mean number of macrobenthic species did not vary significantly according to sampling area, including the impact areas, and at the White Oak River jetting had no statistically significant effect on the mean number organisms nor the mean number of macrobenthic species; however, species adapted to disturbed habitats (tube-building oligochaetes) had colonized the impact area and areas downstream. It seems that 4-9 months after jetting, the mean abundance and species composition of macrobenthos, primarily polychaetes and

molluscan bivalves, sometimes showed a negative response to jetting disturbances, however, this biological response to disturbance was isolated in space to < 5 m away from the general impact area, including downstream areas, and did not negatively alter the overall numbers of macrobenthic species. The spatially isolated nature of the impact on macrobenthos observed in this study is consistent with the scale of impact by jetting on the sediment thickness, where sediment thickness from a jetted piling declines to background levels at ~ 6 m from the impact area. For jetting performed on land, the long-term impact of elevation change on marsh vegetation is likely to be minimal even if the spoil deposits are not removed. The elevation changes due to uplift of the original surface plus the spoil deposit does not exceed the maximum elevation of some plant community in each marsh. While spoil deposited at each of the jetting installations was deep enough to bury existing vegetation, there was evidence of regrowth by shoots coming up through the spoil deposits or rhizomes growing into the affected area from the edges. At Swan Quarter, where the sandy spoil is very phosphorus deficient, applying and incorporating phosphate fertilizer would enhance establishment of vegetation.

A proposed phenomenological model provides an estimate of debris zone characteristics. The model was verified through data obtained from field testing. The results of the verification study indicate that the results from the model agree fairly with field data. In 11 cases, the model results over predicted the measured debris volume and diameters. In six cases, the model under predicted the measured values by approximately 20% on the average. A design procedure was outlined for implementing the proposed three-part jetting model that include insertion rate, volume and size of disturbance zone, and change in bedform due to under current velocities. A spreadsheet was developed and presented for determination of the insertion characteristics and debris volume and area.

Finally, as field jetting for construction is conducted in the future, monitoring of the installations, surveying of the disturbance zone, and documentation of employed pumps capacity should be performed to add data to the data base collected during this research. The addition of more jetting data with a larger variety of subsurface profiles will serve to further verify the proposed model for evaluating pile insertion rate and associated disturbance zone. Research should also be conducted to evaluate the environmental impact of alternative installation methods (such as driving) or foundation type (such as drilled shafts) so that engineers will have the ability to perform realistic cost-benefit analyses for structures to be installed in environmentally sensitive areas.

TABLE OF CONTENTS

TECHNICAL REPORT DOCUMENTATION PAGE	II
EXECUTIVE SUMMARY.....	IV
LIST OF FIGURES.....	XIV
CHAPTER 1 - INTRODUCTION.....	1
1.1 Background	1
1.2 Problem Statement.....	2
1.3 Objectives.....	2
1.4 Scope of Research.....	3
1.4.1 Chapter 1 – Introduction	3
1.4.2 Chapter 2 – Literature Review	3
1.4.3 Chapter 3 – Laboratory Experimental Program	3
1.4.4 Chapter 4 – Laboratory Jetting Results and Model Development.....	3
1.4.5 Chapter 5 – Field Testing Methodology.....	4
1.4.6 Chapter 6 – Data Acquisition and Test Monitoring	4
1.4.7 Chapter 7 – Results of Field Testing	4
1.4.8 Chapter 8 – Model Development and Verification for Field.....	4
1.4.9 Chapter 9 – Environmental Impact of Pile Jetting on Macrobenthos in North Carolina.....	4
1.4.10 Chapter 10 – Effects of Pile Jetting on Tidal Marsh Vegetation	4
1.4.11 Chapter 11 – Summary and Conclusions.....	4

CHAPTER 2 - LITERATURE REVIEW	5
2.1 State-of-the-art of Pile Jetting.....	5
2.1.1 Efficiency and Comparison of Pile Installation Methods.....	5
2.1.2 Variation of Subsurface Characteristics	6
2.1.3 General Installation Procedure (Tsinker, 1988)	7
2.1.4 Pile Installation Design Guidelines (Shestopal, 1959)	7
2.1.5 Summary of State-of-the-Art of Pile Jetting.....	9
2.2 Model Techniques for Determining effect of Jetting on Pile Capacity (Gunaratne et al., 1999)	10
2.2.1 Experimental Program for Model Testing.....	11
2.2.2 Testing Matrix and Pile Installation Methods	11
2.2.3 Lateral and Axial Load Testing of Jetted Piles (Gunaratne et al., 1999).....	14
2.2.4 Summary of Experimental Modeling of Jetted Pile Installations	14
2.3 Hydraulic Effects on Transport of Sedimentary Particles	14
2.4 Summary of Literature Review	16
CHAPTER 3 - LABORATORY EXPERIMENTAL PROGRAM	17
3.1. Mechanical Properties of Laboratory Test Soils	17
3.1.1 Index properties of Test Soils.....	17
3.1.2 Effective Angle of Internal Friction	19
3.1.3 Permeability of Testing Material.....	19
3.2 Laboratory Jetting Program.....	20
3.2.1 Fabrication of Model Test Piles	20
3.2.2 Jetting Test Chamber.....	21

3.2.3	Fabrication of Jetting Apparatus	22
3.2.4	Test Setup and Quality Control.....	23
3.2.5	Jet Testing Program.....	25
CHAPTER 4 - LABORATORY JETTING TEST RESULTS AND MODEL DEVELOPMENT		27
4.1	Insertion Characteristics and Refusal Depth.....	27
4.1.1	Insertion Rate Characteristics.....	27
4.1.2	Insertion Characteristics – Angled Jets	30
4.2	Debris Zone Characteristics.....	31
4.2.1	Debris Volume Analysis – Full Depth	31
4.2.2	Debris Area Analysis – Depth Control.....	31
4.2.3	Debris Zone Analysis - 45° Angled Jets – Full Tests	34
4.2.4	Debris Zone Evaluation – Depth Control Tests.....	36
4.3	Model Development	41
4.3.1	Debris Zone Modeling	41
4.3.2	Validation of Proposed Model with Laboratory Tests	42
CHAPTER 5 - FIELD TESTING METHODOLOGY.....		44
5.1	Test Locations.....	44
5.1.1	White Oak River.....	45
5.1.2	Cherry Branch Ferry Basin.....	46
5.1.3	Sampson County Bridge Replacement site	47
5.1.4	Swan Quarter Ferry Basin	47

5.2	Test Setup and Equipment	49
5.2.1	Equipment	52
5.2.2	Testing Procedure.....	54
5.2.2.1	Water Installations	55
5.2.2.2	Land Installation	57
5.2.2.3	Angled Jets	58
 CHAPTER 6 - DATA ACQUISITION AND TEST MONITORING.....		59
6.1	Insertion Rate Monitoring.....	59
6.2	Pump Performance Monitoring.....	59
6.3	Test Termination Criterion.....	60
6.4	Debris Zone Delineation and Volume Determination.....	60
6.5	Particle Size Distribution.....	62
6.6	Dispersivity Testing.....	62
6.7	Water Quality Monitoring	63
6.8	Summary of Data Acquisition and Test Monitoring.....	64
 CHAPTER 7 - RESULTS OF FIELD TESTING.....		65
7.1	Refusal Depth and Insertion Characteristics.....	65
7.2	Debris Zone Characteristics.....	67
7.2.1	Shape and Extent of Debris Zone.....	67
7.2.2	Volume of Debris Zone.....	68

7.2.3	Particle Size Distribution of Debris Zone	69
7.3	Water Quality Characteristics	71
7.3.1	White Oak River Site	71
7.3.1.1	Summary of Monitored Water Quality Parameters at White Oak River	75
7.3.2	Cherry Branch Ferry Basin.....	76
7.3.2.1	Summary of Monitored Water Quality Characteristics at Cherry Branch	78
7.3.3	Swan Quarter Ferry Basin	78
7.3.3.1	Summary of Monitored Water Quality Characteristics at Swan Quarter.....	81
 CHAPTER 8 - MODEL DEVELOPMENT AND VERIFICATION		82
8.1	Insertion Model	82
8.1.1	Insertion Model Validation	90
8.2	Debris Model Verification	92
8.3	Particle Transport Model	96
8.3.1	Model Rational.....	96
8.3.2	Proposed Approach	97
8.3.3	Turbidity and Transport Length: Underwater Jetting	101
8.4	Proposed Design Methodology	102
 CHAPTER 9 - ENVIRONMENTAL IMPACT OF PILE JETTING ON MACROBENTHOS IN NORTH CAROLINA		104
9.1	Sampling Locations and Testing Methods	104
9.2	Results for Given Sites	106

9.2.1	White Oak River.....	106
9.2.2	Swan Quarter Ferry Basin.....	111
9.2.3	Cherry Point Ferry Basin.....	115
9.3	Summary of Environmental Impact of Pile Jetting On Macrobenthos.....	121

CHAPTER 10 - EFFECTS OF PILE JETTING ON TIDAL MARSH

VEGETATION 123

10.1	Methods.....	123
-------------	---------------------	------------

10.2	Results for Given Sites.....	124
-------------	-------------------------------------	------------

10.2.1	Swan Quarter Marsh.....	124
--------	-------------------------	-----

10.2.2	White Oak River.....	127
--------	----------------------	-----

10.3	Summary of Effects of Pile Jetting On Tidal Marsh Vegetation	129
-------------	---	------------

CHAPTER 11 - SUMMARY AND CONCLUSIONS 131

REFERENCES..... 134

LIST OF TABLES

Table 2-1 K_T factor for various jet pipe material (Marine Structures Handbook, 1972) ...	9
Table 2-2 Volume of Water and Head Required for Pile Jetting (Marine Structures Handbook 1972).....	9
Table 2-3a,b Engineering Properties of Foundation Soil (Gunaratne et al., 1999)	11
Table 2-4 Nomenclature for Piles in the Testing Program (Gunaratne et al., 1999)	12
Table 3-1 Index Properties for Natural Soils Used in Laboratory Testing Program	18
Table 3-2 Permeability Information for Soils Used in Laboratory Testing.....	20
Table 3-3 Available Flowrate and Nozzle Velocity Configurations	23
Table 4-1 Description of Tests Conducted in Experimental Program.....	27
Table 6-1 Example Illustrating calculations of the Debris Volume, CB-1	62
Table 7-1 Summary of Field Testing Program	66
Table 7-2 Summary of Debris Zone Measurements	68
Table 8-1 SPT Hammer Efficiency Corrections (adapted from Clayton, 1990; from Coduto, 2001).	85
Table 8-2 Borehole and sampler correction factors (adapted from Skempton, 1986; from Coduto, 2001).	85
Table 8-3 Measured versus predicted insertion time for given tests.	92
Table 8-4 Summary of Debris Zone Verification	94
Table 9-1 Berger-Parker Diversity Index at White Oak River	111
Table 9-2 Berger-Parker Diversity Index at Swan Quarter	115
Table 9-3 Berger-Parker Diversity Index at Cherry Branch.....	121

Table 10-1 Plant species observed in marshes at Swan Quarter and White Oak River.	124
Table 10-2 Results of analyses of soil samples from Swan Quarter.....	127
Table 10-3 Results of analyses of soil samples from White Oak River marshes.	129

LIST OF FIGURES

Figure 2-1 Variation in Annulus Dimensions for Various Foundation Soil (Matlin, 1983).	7
Figure 2-2 Structure of Typical Jetted Pile Installation (Matlin, 1983).....	10
Figure 2-3 Lateral Load Capacity vs. Lateral Displacement at Point of Load Application (Gunaratne et al., 1999)	13
Figure 2-4 Elapsed Time of Jetting vs. Jetting Pressure – 2.5 ft Depth.....	13
Figure 2-5 Forces acting on a particle resting on a granular bed subject to a steady current (Allen, 1985).....	15
Figure 2-6 Lift force due to Bernoulli effect on granular bed subject to fluid shear.....	16
Figure 3-1 Grain Size Distribution Curves for Laboratory Jetting Tests.....	18
Figure 3-2 Direct Shear Test Results for Material Used in Laboratory Jetting.....	19
Figure 3-3 Saturation Tank and Specimen Basket.....	21
Figure 3-4 Overhead View of Saturation Tank with Specimen Basket in Place	22
Figure 3-5 Laboratory Jetting Apparatus and Various Nozzles.....	22
Figure 3-6 Free-fall of Specimen Soil for Desired Lift Height	24
Figure 3-7 Compaction of Individual Lift Height.....	24
Figure 3-8 Density Check at Midpoint of Lift Height	25
Figure 3-9 Flowchart for Tests Conducted with Vertical Jets – Full Depth.....	26
Figure 3-10 Angled Jet Nozzles for Jetting Modification	26
Figure 4-1 Depth of Insertion as a Function of Time for Various Water Flowrate and Jet Nozzle Velocity(Numbers on curves = Flow rate(ft ³ /min) – Nozzle velocity (ft/min))	28

Figure 4-2 Comparison of Pile Insertion Rates at Given Depths Due to Variation in Jetting Parameters	29
Figure 4-3 Depth of Insertion with Time for Various Water Flowrate and.....	31
Figure 4-4 Debris Volume with Increase in Jetted Pile Volume	32
Figure 4-5 Comparison of Debris Areas in Concrete Sand at Two Insertion Depths.....	33
Figure 4-6 Debris Area with Increase in Jetted Pile Volume	33
Figure 4-7 Immeasurable Debris Area Distribution for Cherry Branch Sand	34
Figure 4-8 Comparison of Debris Zone Volumes Due to Various Nozzle Orientations ..	35
Figure 4-9 Comparison of Debris Zone Areas Due to Various Nozzle Orientations	35
Figure 4-10 Correlations between Pile Insertion Rate and Debris Volume (Depth = 1.0 ft)	36
Figure 4-11 Correlations between Pile Insertion Rate and Debris Area (Depth = 1.0 ft)	37
Figure 4-12 Variation of Debris Volume “a-parameter” as a Function of	39
Figure 4-13 Debris Volume “b-parameter” Versus D_{50}	39
Figure 4-14 Debris Area “a-parameter” Versus D_{50}	40
Figure 4-15 Debris Area “b-parameter” Versus D_{50}	40
Figure 4-16 Debris Volume Validation of Proposed Model.....	42
Figure 4-17 Debris Area Validation of Proposed Model.....	43
Figure 5-1 Site map detailing the field testing locations	44
Figure 5-2 River and adjacent marsh area at White Oak River Site in Stella, NC	45
Figure 5-3 Cherry Branch Ferry basin, looking west to east, crane barge in foreground.	47
Figure 5-4 Sampson County Research Site	48

Figure 5-5 Swan Quarter Ferry Basin looking from Southwest to Northeast.....	49
Figure 5-6 Marshy area adjacent to ferry basin (shown after pile installations).	49
Figure 5-7 Steel Test Pile with plate welded onto bottom end.	50
Figure 5-8 Nozzle ends at the ends of the jet pipe, shown with 2 inch (5.08cm) nozzles.	51
Figure 5-9 Connection of the main jet pipes to water injection tee at upper end of pile..	51
Figure 5-10 American model 5220 crane used for maneuvering test piles.	52
Figure 5-11 Hale model centrifugal trash pump used at first jetting site.....	53
Figure 5-12 Myer’s Seth model DP150.....	53
Figure 5-13 Cornell model 4HC high pressure pump.....	54
Figure 5-14 Water meter used to monitor Hale pump and Myer’s Seth pump.....	55
Figure 5-15 Pump curve used to back-calculate flowrate from Cornell 4HC pump (Private Correspondence, Corenll Pump Company, Portland, Oregon, 2003).....	55
Figure 5-16 Pile placed into start position in the reference template.	56
Figure 5-17 Beginning to perform pre-jet survey.	57
Figure 5-18 Measuring the profile after a jetting installation.	58
Figure 6-1 Typical jetted pile installation with debris zone profile and extent.	60
Figure 6-2 Elliptical Distribution of Debris Area (from Smith, 2003).	61
Figure 6-3 WTW measurement systems, Multi-340i with probes.....	63
Figure 6-4 Orbeco-Hellige Model 966 turbidimeter.....	64
Figure 7-1 Typical Debris Zone Profiles (a) and the average of the profiles(b).....	67
Figure 7-2 White Oak River measured and NCDOT reported GSD	69

Figure 7-3 Cherry Branch Ferry basin measured and NCDOT reported GSD.....	70
Figure 7-4 Sampson County measured and NCDOT reported GSD	70
Figure 7-5 Swan Quarter Ferry basin measured and NCDOT reported GSD	71
Figure 7-6 Temperature Readings at WO-1.....	72
Figure 7-7 Turbidity Readings at WO-1	72
Figure 7-8 Dissolved Oxygen Readings at WO-1.	73
Figure 7-9 pH Readings at WO-1.....	73
Figure 7-10 pH readings at WO-3.	74
Figure 7-11 Dissolved Oxygen (DO) Content readings (1 Minute interval) at WO-3.	74
Figure 7-12 Turbidity readings at WO-3 installation site.....	75
Figure 7-13 Temperature Readings at CB-2.....	77
Figure 7-14 pH Readings taken at CB-2.....	77
Figure 7-15 Turbidity Readings at CB-7.	78
Figure 7-16 Turbidity Readings taken at SQ-3.....	79
Figure 7-17 DO readings taken at SQ-5.	80
Figure 7-18 Turbidity reading at SQ-5 (maximum).	80
Figure 7-19 Turbidity reading at SQ-6 (average).	81
Figure 8-1 Relationship between Insertion Parameter and Time for Insertion for Different soil densities.....	83
Figure 8-2 Insertion Parameter Characteristics for SC and SQ sites.....	84
Figure 8-3 SQ-1 Insertion Parameter, N_{cr} curve fitting.	86
Figure 8-4 SQ-2 Insertion Parameter, N_{cr} curve fitting	86

Figure 8-5	SQ-3 Insertion Parameter, N_{cr} curve fitting	87
Figure 8-6	SQ-9 Insertion Parameter, N_{cr} curve fitting	87
Figure 8-7	SQ-10 Insertion Parameter, N_{cr} curve fitting	88
Figure 8-8	SC-1 Insertion Parameter, N_{cr} curve fitting	88
Figure 8-9	Development of Slope Parameter, m equation.....	89
Figure 8-10	Example of pile insertion spreadsheet, from SQ-2.	91
Figure 8-11	Measured versus predicted insertion times.	92
Figure 8-12	Debris Volume Verification.....	95
Figure 8-13	Debris Diameter Verification.....	95
Figure 8-14	Effect of Current Speed on the Erosion and Deposition Characteristics for Specified Bed Particle Diameter (Open University. Oceanography Course Team 1999).....	97
Figure 8-15	Turbidity distribution with time.....	99
Figure 8-16	Example Spreadsheet for Pile Jetting Model.....	103
Figure 9-1	White Oak River: site sample locations	107
Figure 9-2	Mean (+ SE) total abundance and number of species of macrobenthic organisms ($> 500 \mu\text{m}$) collected with petite Ponar grab samples ($N = 5$) at the White Oak River in March 2004..	109
Figure 9-3	Mean (+ SE) total abundance of organisms within the dominant taxonomic groups ($> 500 \mu\text{m}$) collected with petite Ponar grab samples ($N = 5$) at the White Oak River in March 2004. See text for results of statistical analyses.....	110
Figure 9-4	Swan Quarter Ferry Terminal: site sample locations.....	112

Figure 9-5 Mean (+ SE) total abundance and number of species of macrobenthic organisms (> 500 μm) collected with petite Ponar grab samples (N = 5) at Swan Quarter in March 2004. See text for results of statistical analyses.....	113
Figure 9-6 Mean (+ SE) total abundance of organisms within the dominant taxonomic groups (> 500 μm) collected with petite Ponar grab samples (N = 5) at Swan Quarter in March 2004. See text for results of statistical analyses.	114
Figure 9-7 The size-frequency of the three dominant species of bivalves collected with a petite Ponar grab sampler at Swan Quarter in March 2004.....	116
Figure 9-8 Cherry Point Ferry Terminal: site sample locations	117
Figure 9-9 Mean (+ SE) total abundance and number of species of macrobenthic organisms (> 500 μm) collected with petite Ponar grab samples (N = 5) at Cherry Point in March 2004. See text for results of statistical analyses.....	119
Figure 9-10 Mean (+ SE) total abundance of organisms within the dominant taxonomic groups (> 500 μm) collected with petite Ponar grab samples (N = 5) at Cherry Point in March 2004. See text for results of statistical analyses.	120
Figure 10-1 . Irregularly flooded brackish-water marsh at Swan Quarter showing spoil from pile jetting installations.....	125
Figure 10-2 <i>Juncus roemerianus</i> patch along the shoreline at Swan Quarter.	125
Figure 10-3 <i>Spartina alterniflora</i> is present along small creeks at the Swan Quarter....	126
Figure 10-4 White Oak River spoil from pile jetting installation.....	128
Figure 10-5 Vegetation at White Oak River Marsh. <i>Spartina alterniflora</i> (center) growing in a drainage ditch, <i>Juncus roemerianus</i> , the previous year's seed stalks of <i>Spartina cynosuroides</i> and shrubs scattered across the marsh	128

CHAPTER 1 - INTRODUCTION

1.1 Background

With the increased demand for public transportation, rural development, and leisure activities, it has become likewise demanding for engineers to produce innovative methods to assure safe and economic designs of civil infrastructures. This demand has impacted environmentally sensitive areas which serve to ensure stability in the environment and achieve balance within our ecosystems. Achieving balance between public demand and environmental stability becomes more difficult with public expansion into undisturbed regions. The engineer is faced with providing designs that are functional and economical while at the same time environmentally friendly to ecologically sensitive areas such as the estuarine regions of eastern North Carolina.

At present, the NCDOT specifies the use of pre-stressed concrete piles in the coastal plain region of North Carolina due to the high corrosion resistance properties of concrete, as compared to steel piles (*Soils and Foundations Design Section Reference Manual* version 2001). Severe corrosion occurs due to the harsh saline environment present in the region. The method typically used to install the concrete foundation elements is dynamic driving through the subsurface profiles. The subsurface profiles of the coastal plain region are typically sedimentary in nature, and therefore contain interspersed layers of material of varying composition and relative density. Often layers of dense material located within softer sedimentary profiles make it difficult to drive piles to the required depth without inducing high compressive stresses into the concrete which potentially damages the pile. In these instances the use of water jetting to aid installation is required. The alternative is using drilled shaft. The advantages to using jetted piles in lieu of drilled shafts are many. Jetted piles are considerably less expensive to install per linear foot than drilled shafts and can be installed much faster. In addition, jetted piles can be positioned on land or over water with appropriate driving templates. Jetted piles can be removed and aligned if installed incorrectly from the design grade. Therefore, it is often economically desirable to use jetted, concrete piles with subsequent driving to achieve specified design criteria in lieu of drilled shaft foundations.

However, the construction methods mentioned here rarely address possible adverse effects on the environment surrounding such installations. While there is literature available on the structural performance of jetted pile foundations, little is published on the environmental impact as well as mechanics of installation of jetted piles. Tsinker (1988) presented empirical relationships for jetting piles in various soil types with emphasis on flowrates as a function of pile. Gunaratne et al. (1999) presented comparisons of load tests conducted on driven, bored and jetted piles with emphasis on pile capacity.

At the present, United States Army Corps of Engineers (USACOE), North Carolina Division of Water Quality, United States Fish and Wildlife Services, Division of Coastal Management, and Environmental Protection Agency restrict or prohibit jetting as a construction technique in eastern North Carolina. This is predominantly due to insufficient data and lack of specification-based contracts directing foundation

contractors to controlled and engineered jetting parameters. Knowledge of the debris zone created by the jetting process is currently unavailable to the regulatory agencies, engineers, and contractors who use jetting as a construction method.

Upon completion of jetting a pile, the ground surface surrounding the pile is normally inundated with water and overlain by debris exhumed from the annulus around the pile. In coastal or environmentally sensitive areas, debris from the annulus affects essentially the hydric soil layer adjacent the pile. These hydric soils are considered by federal regulation 40456 (August 14, 1991) to be layers that are saturated, flooded, or ponded long enough to develop anaerobic conditions in the upper stratum of the soil profile. These soils are composed of organic and mineral constituents necessary for many organisms to reproduce and develop. While environmental impacts of debris extruded from the jetted holes can be evaluated using present assessment techniques such as the Habitat Evaluation Procedure (HEP, 1981) and the Wetland Evaluation Technique (WET, Adamus et al 1991), the knowledge regarding the extent of such debris zone is missing. Therefore, in order to provide information needed for environmental impact, it is necessary to investigate the effects of jetting parameters on the volume and area of material debris as a function of pile installation depth and geometry.

1.2 Problem Statement

In order to investigate the impact of pile jetting on environmentally sensitive areas and the size of debris zone, it is necessary to first understand and evaluate in a controlled manner the impact of jetting parameters, such as insertion rate and flow characteristics, on disturbance zone. Such work is best conducted in the laboratory where testing parameters such as soil type and insertion rate are controlled. Once jetting mechanism are defined, it is necessary to conduct full scale field installations in areas that are similar to locations that are likely to be encountered during a typical construction project where pile jetting would be a viable foundation choice. It is also necessary to determine the combined effects of varying parameters such as jet water flow rate and jet nozzle velocity on the debris zone. In order to develop a model that correlates jetting parameters with pile installation and debris characteristics, an array of soils consisting of various material types and engineering properties will be implemented into an experimental program. The model will be developed during the laboratory and field testing and should enable the practicing engineer to specify jetting parameters, including insertion rate, water flow rate and soil grain sizes, which will effectively install the required pile and quantify the debris zone. The definition of the volume and area of the debris zone will assist in assessing environmental impacts associated with pile installation.

1.3 Objectives

The main objective of this research is to first understand and define the inter relationship between jetting parameters, pile installation and disturbance zone characteristics. Through laboratory jetting experiments with model size piles, jetting parameters required to achieve a given installation depth will be defined as well as associated disturbance area and volume. Based on the lab data, a model will be

developed. The model will be further developed and verified using a series of full-scale jetted pile installations to verify the developed model. Specifically, the following objectives are pursued in this research:

- 1) Develop an experimental testing program in the laboratory to evaluate debris zone characteristics and understand mechanics of jetted pile installations.
- 2) Develop a model for jetted pile installations while minimizing size of disturbance zone.
- 3) Develop a full-scale field testing program and measurement techniques to evaluate pile installation rates and associated debris zone characteristics. In conjunction with field testing, collect data related to environmental impact.
- 4) Characterize and define disturbance due to jetted pile installations.
- 5) Assess effects of varying jetting parameters on pile installation rates, debris zone volumes, debris zone areas, and installation depths.
- 6) Evaluate environmental impacts associated with pile jetting.
- 7) Compare results from field jetting installations with estimations at representative sites made using the proposed model for determining debris volume and extent.
- 8) Expand the proposed model to include insertion parameters for full size piles.
- 9) Recommend a procedure by which specifications can be developed for pile jetting practices if feasible.

1.4 Scope of Research

1.4.1 Chapter 1 – Introduction

An introduction to the jetting problem as related to environmentally sensitive areas is given. The benefits and drawbacks of using jetted piles in comparison to other foundation options is discussed.

1.4.2 Chapter 2 – Literature Review

Current state-of-the-art field practices are also reviewed. Literature detailing particle transport theory is discussed.

1.4.3 Chapter 3 – Laboratory Experimental Program

The experimental program is developed and presented providing insight on the materials implemented in the testing program. Physical properties of the soil and classification tests conducted to obtain these properties are described. The methodology behind construction of the test samples is presented as well as the results of investigation into the mechanics of jetting presented.

1.4.4 Chapter 4 – Laboratory Jetting Results and Model Development

Tests conducted in the experimental program were analyzed and relationship between jetting characteristics, such as debris zone surrounding jetted piles, and the mechanics of installation are developed for various soils used in the program. A model for pile jetting is developed for implementation to full-scale jetted pile installations. The model requires

input of soil index properties and allows the engineer to predict the debris zone characteristics for a set of jetting parameters and given pile dimensions.

1.4.5 Chapter 5 – Field Testing Methodology

A field testing program is developed to determine the effects of various soil profiles approach parameters on the volume and extent of debris zone created by jetting. Testing apparatuses and field locations are discussed.

1.4.6 Chapter 6 – Data Acquisition and Test Monitoring

Methods of data acquisition and soil/water samples collection from field testing are presented. A data analysis procedure was adapted so that test results could be compared with laboratory results.

1.4.7 Chapter 7 – Results of Field Testing

Tests conducted in the field test program were analyzed and presented. Results from each test at the various locations are summarized. Observations and trends gathered from the analysis are discussed.

1.4.8 Chapter 8 – Model Development and Verification for Field

A three-part model is introduced which encompasses the identified three important aspects of jetting. The first component is an insertion model which details the jetting parameters required for successful insertion of a pile. The second component provides the debris volume and area extent produced by jetting to a given depth. The third model component addresses the particle transport length caused by underwater current, if present.

1.4.9 Chapter 9 – Environmental Impact of Pile Jetting on Macrobenthos in North Carolina

Impact of jetting on infaunal macrobenthos is assessed after sampling at three sites: White Oak River, Cherry Point Ferry basin, and Swan Quarter Ferry basin. Abundance and species diversity of infaunal macrobenthos as a function of distance away from pile jetting operations are analyzed and GIS maps of each site are created.

1.4.10 Chapter 10 – Effects of Pile Jetting on Tidal Marsh Vegetation

Jetting effects on vegetation at Swan Quarter and White Oak River are analyzed by inspecting and listing each plant species. In determining impact on zone of plant species within tidal marshes two major environmental factors: elevation relative to tidal inundation and salinity, are discussed.

1.4.11 Chapter 11 – Summary and Conclusions

Conclusions derived from the pile jetting testing research program are summarized in this section.

CHAPTER 2 - LITERATURE REVIEW

Pile jetting has been predominantly used in areas consisting of sands and gravels to install bridge foundations, dock piles, bulkheads and fence posts. However, after an extensive search for literature on the environmental impacts of jetting, it is realized that environmental disturbance due to pile jetting has not been reported in past literature. The purpose of this research is not to perfect the art of pile jetting, but to investigate the volume and area of debris created by the jetting process in order to be able to environmentally evaluate its impact.

In order to understand the fundamental practice of jetting, literature from Tsinker(1988) and Matlin(1983) has been reviewed. Their research consisted of performance monitoring of jetted piles as well as installation guidelines for jetting piles in various soil profiles with the main objective being assuring full depth installation.

An in-depth investigation into capacity and performance monitoring of bored, driven, and jetted piles has been conducted by Gunaratne et al. (1999) demonstrating the effect of the installation method on the service integrity of structural piles. Their research encompassed a detailed small-scale experimental program as well as a dimensional analysis and evaluation of their findings. In addition, a study on the hydraulic effects of fluid velocity on particle transport by Allen(1985) is reviewed to provide an understanding on how particles are initially suspended and transported by fluids.

2.1 State-of-the-art of Pile Jetting

Even though pile jetting has been an effective means of installing piles for many structural applications, the state-of-practice of pile jetting is hardly accepted as a suitable means for pile installation in ecologically sensitive areas. This is due to non-regulated and specification- deficient contracts encompassing the jetting installation processes where knowledge of associated disturbance is missing. For this reason, regulatory agencies need to understand impact of pile installation methods to ensure minimal disturbance to ecologically sensitive areas.

2.1.1 Efficiency and Comparison of Pile Installation Methods

A comprehensive review of pile jetting has been conducted by Tsinker (1988). Tsinker documented the significance in time savings from pile jetting as compared to dynamic methods of pile installation. As expected, the energy savings and noise reduction in using pile jetting as opposed to dynamic driving methods is a positive component of jetting practices. Some may argue that pollution from dynamic and vibratory pile installation methods could divert migrating fish species from traveling to spawning estuaries.

Jetted piles can be effectively installed in most sand and gravel soil strata as well as subsurface profiles encompassing clay and peat materials. Jetted piles can easily be positioned on land or over water with appropriate driving templates. Also, jetted piles can be removed and aligned if installed incorrectly from the design grade. Water jetting

of piles is beneficial as compared to dynamic driving in that piles are installed before any stress conditions develop within the pile section. If not efficiently controlled and designed, driving piles with dynamic methods may lead to development of stresses within the pile section above the allowable stresses considered in design and fabrication.

Excessive cost and time associated with dynamic driving methods are significantly reduced with jetting. Commonly, a combination of jetting and driving is employed. Jetted pile applications consist of discharging a stream of water at the base of the pile and/or along the pile sides to erode the surrounding soils (Tsinker, 1988). Continued water erosion and removal of the surrounding soils allows the pile to penetrate through soil layers until a sufficient distance above the permanent tip elevation is reached. At this point, dynamic methods are used for the last few feet of installation to achieve final pile set.

2.1.2 Variation of Subsurface Characteristics

In jetting piles within sand formations, Tsinker noted that water flow rate is more important than the jet velocity, whereas in gravel or clay materials, the jet velocity is vital in loosening soil particles from around the pile. In both conditions, an effective jetting program is only successful if the jet velocity is sufficient to loosen soil and an appropriate flow rate of water is used to displace the soil from below the pile tip and carry them along the pile sides to the ground surface (Tsinker, 1988). If either of these two jetting parameters is insufficient, the pile will not penetrate the soil. Air can be often implemented into jetting applications to insure that soil particles are effectively transported to the ground surface.

Variation in soil type also affects the dimensions of the jet-affected zone surrounding the pile. Layers of clay encountered in predominantly uniform sand profiles may cause a blanketing effect of the return water streaming from the jet pipe nozzles (Tsinker, 1988). Due to this phenomenon, downward movement of the pile would discontinue at lesser depth than would a similar pile in a uniform sand stratum without the clay layer. It is therefore inferred that sufficient volume of return water must be maintained in order to insure continual pile insertion. Also, in cemented sands and clay materials, the jet velocity must be sufficient to fracture the matrix into smaller diameter masses in which the flow of water can transport the material above ground. A schematic of pile jetting through various soil strata along with variation in return water annulus dimensions are shown in Figure 2.1 (Tsinker, 1988). Tsinker also recognized effects of large boulders, cobbles, or debris on the effectiveness of pile jetting. As mentioned earlier, Tsinker stressed the importance of achieving essential volume flow rates of water to maintain adequate transport of subsurface materials to the ground surface.

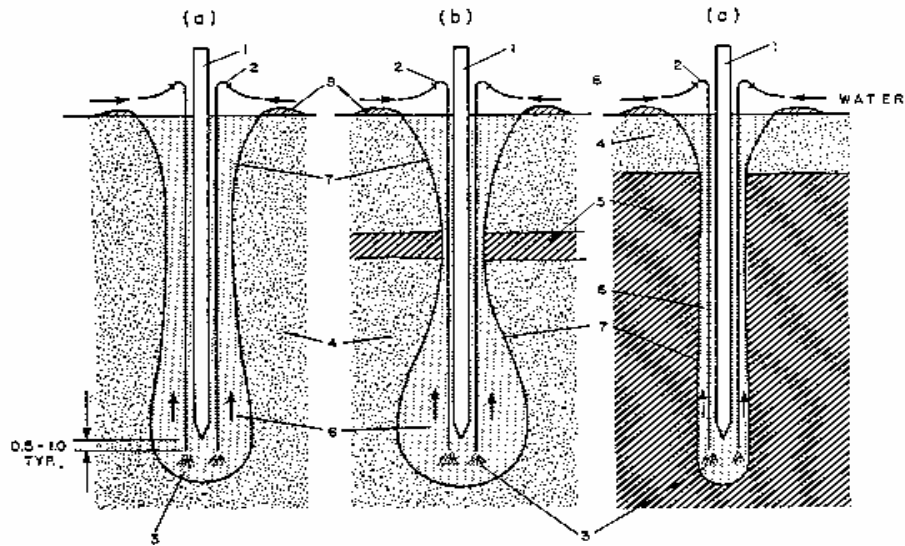


Figure 2-1 Variation in Annulus Dimensions for Various Foundation Soil (Matlin, 1983).
 (a) Uniform Sand; (b) Sand with Clay Stratum; (c) Sand with Underlain Clay: 1 – Pile; 2 – Jet Pipe; 3 – Water Jet; 4 – Sand; 5 – Clay; 6 – Loose Sand; 7 – Return Annulus; 8 – Particle Deposition

2.1.3 General Installation Procedure (Tsinker, 1988)

Pile jetting is a relatively simple application requiring equipment such as a “centrifugal pump equipped with a flow meter and pressure gage, a minimum of two steel jet pipes connected to the pump....and a winch for handling the jet pipes” (Tsinker, 1988). Tsinker suggested that pipe diameters between 2 and 4 inches (50 and 100mm) are sufficient to carry the flow of water to the jet nozzles to increase the velocity of water exiting the jet hose. Two jet pipes are often mounted on either side of the pile to achieve balance and symmetry during pile installation. Prior to lowering the pile to the desired depth, the pump is engaged and the jet pipes are lowered to the ground surface and allowed to penetrate the soil stratum. Operators then successively lower and raise the jet pipes through the soil column to loosen material within that section. The pile is then lowered into position and allowed to penetrate the soil column freely while the jet nozzles liquefying the soil.

2.1.4 Pile Installation Design Guidelines (Shestopal, 1959)

Shestopal (1959) conducted numerous jetting investigations for pile installation using steel pipes as model test piles. Through correlations gathered from research data, he developed empirical equations for determining water quantities and jet water

velocities to install piles of various length and diameter. He also considered the effects of jetting piles in soil stratum with elevated and deep ground water profiles.

Shestopal provided the following empirical equation for predicting the required flow rate to install a pile of given diameter to a desired depth of penetration in a uniform sand stratum (groundwater table below pile tip):

$$\frac{Q}{D} = 530(D_{50})^{1.3} l^{0.5} + 0.1\pi l k \quad \text{Eq. 2.1}$$

Where: Q = flow rate of water, (m^3/h)

D = pile diameter or width, (m)

D_{50} = average size of soil particles, (mm)

l = installation depth of pile, (m)

k = filtration coefficient (permeability), (m/day)

The following empirical equation is for installation of jetted piles within a uniform saturated sand stratum (Shestopal, 1959):

$$\frac{Q}{D} = 530(D_{50})^{1.3} l^{0.5} + 0.017\pi l k \quad \text{Eq. 2.2}$$

For jetting piles in non-uniform soil stratum, the average filtration coefficient (permeability) should be determined from the following:

$$k = \frac{\sum k_n l_n}{l} \quad \text{Eq. 2.3}$$

Where: k_n = filtration coefficient for soil layer n , (m/day)

l_n = length of soil layer n , (m)

l = installation depth of pile, (m)

In order to determine the required pump capacity, head loss within the jetting system water supply hoses may be calculated from the following equation:

$$H = \frac{Q^2 l_h}{K_T} \quad \text{Eq. 2.4}$$

Where: H = head loss in jetting system, (m)

Q = flow rate of water, (m^3/h)

l_h = length of water supply hoses, (m)

K_T = empirical coefficient due to hose material obtained from Table 2.1

Table 2-1 K_T factor for various jet pipe material (Marine Structures Handbook, 1972)

Jet Pipe Internal Diameter (mm)	Rubberized Hose Material	Rubber Hose Material
33	33	50
50	133	200
65	567	850
76	1333	2000

In order to select an efficient jetting system, Tsinker (1988) suggests: 1) selecting the appropriate water volume flow rate and head to drive the proposed pile (Table 2.2, or Eqs. 2-1) to 2-4); 2) determining pressure losses foreseen in the hoses and jet pipes of the system; and, 3) specifying competent pump.

Table 2-2 Volume of Water and Head Required for Pile Jetting (Marine Structures Handbook 1972)

Soil Type	Depth of Pile Driving (m)	Head at Nozzle Tip (MPa)	Pile Section Diameter			
			300-500 mm		500-700mm	
			Jet Pipe Internal Diameter (mm)	Flow Rate of Water (m^3/min)	Jet Pipe Internal Diameter (mm)	Flow Rate of Water (m^3/min)
Silt; Silty Sand	5-15	0.4-0.8	37	0.4-1.0	50	1.0-1.5
Fine Sand; Soft Clay; Sand	15-25	0.8-1.0	68	1.0-1.5	80	1.5-2.0
Sand and Hard Sand Loam	5-12	0.6-1.0	50	1.0-1.5	68	1.5-2.0
Sand with Gravel	15-25	1.0-1.5	80	1.5-2.5	106	2.0-3.0
CONVERSIONS MPa to psi: multiply by 145.04 m^3/min to ft^3/min : multiply by 35.31						

2.1.5 Summary of State-of-the-Art of Pile Jetting

A review of literature on installation of piles yielded some findings beneficial to this research program. Fundamental mechanics of a jetted pile installation in sand is shown in Figure 2.2. Tsinker (1988) described the structure of the jet hole with three distinctive zones. Immediately beneath the pile tip, the sand structure is significantly

altered from in situ conditions. Infiltration of jet water into this zone results in a mixture of sand particles and water. Within Zone 2, excess water from the sand-water mixture rises to the surface while lubricating the pile sides. Tsinker also realized a third zone in the jet hole structure consisting of a sand-water mixture at high pore pressures stemming from water infiltration into the hole sides.

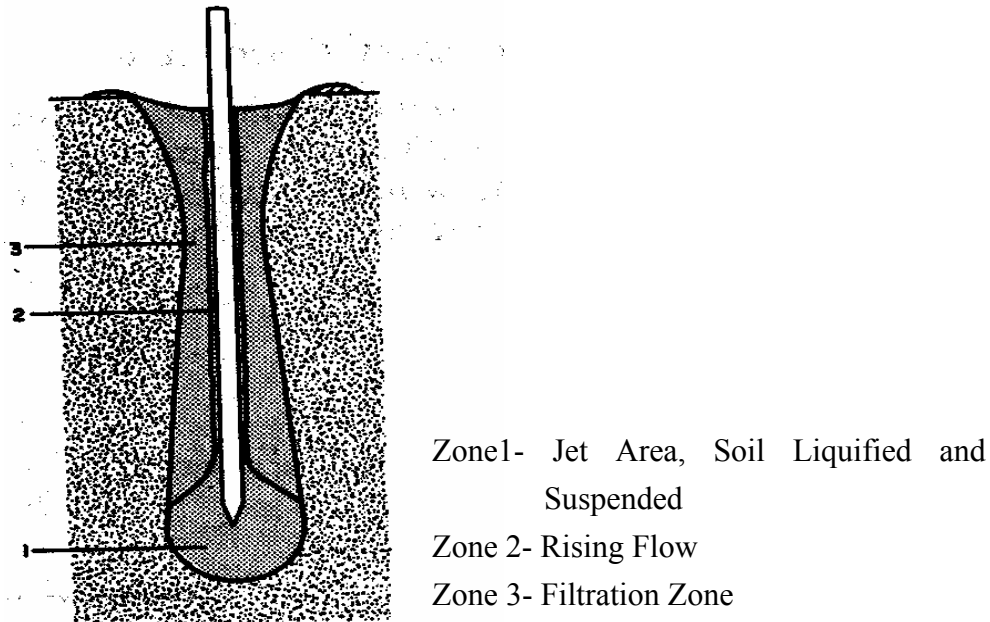


Figure 2-2 Structure of Typical Jetted Pile Installation (Matlin, 1983)

Tsinker (1988) conducted research on capacity effects of jetting piles within dry and water-bearing sands. From that research, he suggested that “concrete piles jetted into dry sand have six to nine times more capacity than identical piles jetted into water-bearing sand.” Furthermore, he noted that subsequent dynamic driving does not significantly increase the capacity of piles jetted in dry sand stratum. He suggested that this is due to the inability of dry sands to densify by liquefaction. Densification in unsaturated profiles may occur due to settlement of loose sand around the pile and subsequent compaction of the material due to water force from the jets. This densification is not as profound as that seen in saturated sands where dynamic driving methods invoke liquefaction. Also, although washing of some fines from the jetted column occurs, Tsinker stated that “sandy soils granulometric composition” is not altered significantly.

2.2 Model Techniques for Determining effect of Jetting on Pile Capacity (Gunarathne et al., 1999)

An investigation into the effects of pile jetting on pile capacity was conducted by Gunaratne et al. (1999) under sponsorship by Florida Department of Transportation. This study encompassed model piles installed using jetting techniques, pre-forming and

dynamic driving methods. Pre-forming refers to the method of pre-drilling a hole prior to pile installation in order to penetrate a denser layer which would be difficult or impossible to penetrate by other methods. The specific purpose of their research was to determine the effect of jetting pressure on the lateral capacity and skin friction of piles. Furthermore, an objection was to determine the zone of influence of jetting on soils adjacent to existing foundations and explore strength variation due to jetting and pre-forming. Surface effects due to the jetting process were not studied.

2.2.1 Experimental Program for Model Testing

Gunaratne et al. (1999) conducted an experimental program using model aluminum piles installed into a 90% sand + 10% kaolin mixture with jetting, pre-forming, and dynamic installation methods. Laboratory testing of the soil material used in the experimental program yielded the results shown in Table 2.3.

2.2.2 Testing Matrix and Pile Installation Methods

The experimental program consisted of an excavated 26.26 ft² (2.44 m²) by 7.0 ft (2.13m) deep test pit filled to 5.97 feet (1.82 m) in successive lifts with the mixture of masonry sand and kaolinite. Each lift was compacted to 103.2 lb/ft³ (16.2 kN/m³) or 94.3 lb/ft³ (14.8 kN/m³) based on the desired relative density of the test. Next, two 5.0 ft (1.52 m) long aluminum shafts, 2 in. x 2 in. (50.8 mm x 50.8 mm), 1/16 in. (1.6 mm) wall thickness were instrumented with strain gauges and installed into the testing medium by either dynamic driving or jetting. Piles were jetted through saturated and unsaturated test specimens at various jetting pressures to expedite installation due to increased flow rate and velocity of the jet water. The nomenclatures for tests within the testing program are shown in Table 2.4 below. The first symbol in the test description denotes the saturation condition (i.e. “U” for unsaturated, “S” for saturated) and the second symbol denotes the installation method (i.e. “D” for driven, “J” for jetted).

Table 2-3a,b Engineering Properties of Foundation Soil (Gunaratne et al., 1999)

	Mas. Sand	Kaolinite
D ₅₀ (mm)	0.25	N/A
□ _d Max, (lb/ft ³)	111.7	N/A
□ _d Min, (lb/ft ³)	88.0	N/A
PI	N/A	22
LL	N/A	60

Soil Material	% Passing No. 40 Sieve	% Passing No. 200 Sieve	Spec. Gravity, G _s	Opt. Moist. Content, OMC (%)	□ _d @ OMC. lb/ft ³	□ @ □ _d = 94.7 lb/ft ³	□ @ □ _d = 103.7 lb/ft ³
90% Masonry Sand + 10% Kaolinite	88.2	10.2	2.68	10.2	112	35	38
CONVERSIONS: lb/ft ³ to kN/m ³ divide by 6.4 mm to inch multiply by 0.0394							

Table 2-4 Nomenclature for Piles in the Testing Program (Gunaratne et al., 1999)

Unit Weight (lb/ft ³)	Condition	Driven Piles	Jetted Piles			
			Jetting Pressure			
			25 psi	50 psi	75 psi	100 psi
103.7	Unsaturated	UD ₁	UJ ₁₁	UJ ₁₂	UJ ₁₃	UJ ₁₄
	Saturated	SD ₁	SJ ₁₁	SJ ₁₂	SJ ₁₃	SJ ₁₄
94.7	Unsaturated	UD ₂	UJ ₂₁	UJ ₂₂	UJ ₂₃	UJ ₂₄
	Saturated	SD ₂	SJ ₂₁	SJ ₂₂	SJ ₂₃	SJ ₂₄
CONVERSIONS: lb/ft ³ to kN/m ³ divide by 6.4 psi to kPa multiply by 6.895						

The water jet system used to install jetted piles consisted of two stainless steel pipes with inside diameters of 0.16 in. (4 mm) extending to the pile tip and fastened to the pile head. Water was pressurized with a “booster” pump and fed into a 0.75 in. (19.05 mm) reinforced hose which was reduced and coupled to the two steel jet pipes. Each pile was jetted to 2.5 ft (0.75 m) and then impact driven 0.833 ft (0.254 m) to the required tip elevation.

Upon completion of model pile installation and dissipation of excess pore water pressure, lateral load testing of the piles was conducted. The piles were monitored with Linearly Varying Displacement Transducers (LVDT) and strain gauges connected to a data acquisition system to monitor the displacement and loading information. From Figure 2.3, Gunaratne et al (1999) realized that lateral load capacity for jetted piles decreases with increased jetting pressure. This holds true for both saturated and unsaturated conditions. Also, lateral capacity for saturated conditions is significantly less than that of for unsaturated conditions with similar jetting parameters. Overall, for similar jetting parameter tests, lateral displacements at failure with saturated conditions seem to be greater than for lateral load tests conducted in unsaturated conditions.

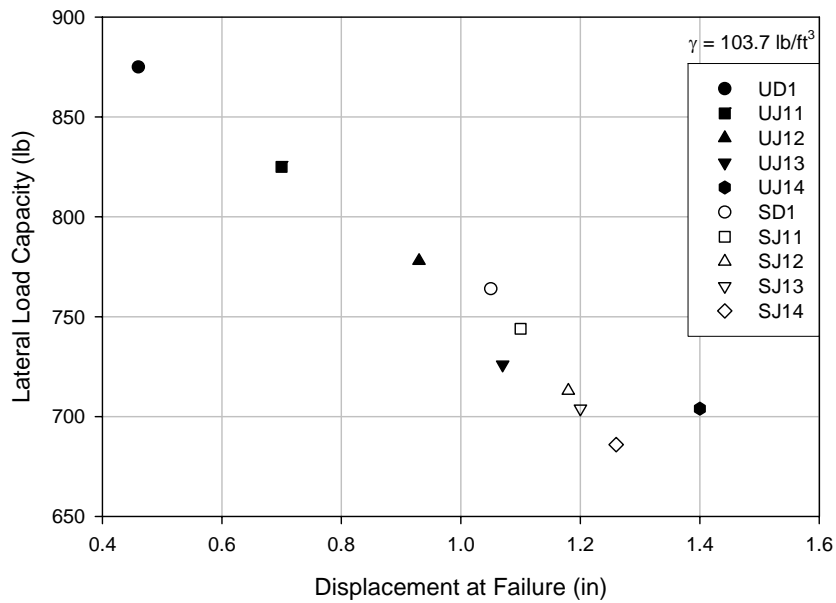


Figure 2-3 Lateral Load Capacity vs. Lateral Displacement at Point of Load Application (Gunaratne et al., 1999)

Results for tests using $\gamma = 94.7$ pcf samples were similar in trend to those observed using the $\gamma = 103.1$ pcf samples. Figure 2.4 displays the required jetting time to reach the desired model-pile tip elevation (0.75 m) prior to impact driving to final pile set for lateral load testing (Gunaratne et al., 1999).

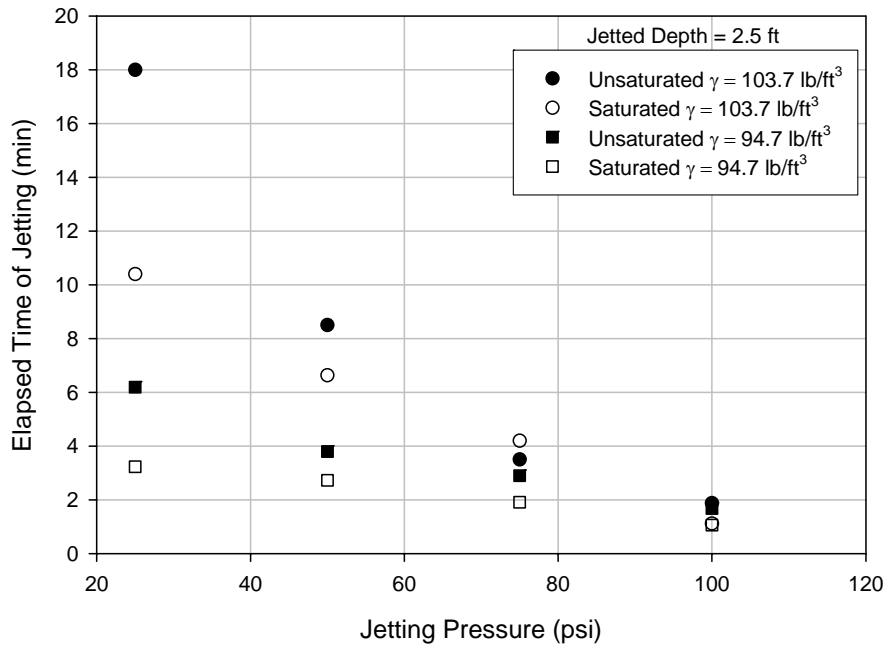


Figure 2-4 Elapsed Time of Jetting vs. Jetting Pressure – 2.5 ft Depth (Gunaratne et al., 1999)

From Figure 2.4, it is shown that for equal depth of driving, the pile installation rate is dependent on both material density and saturation conditions. For equal material density at low jetting pressures, installation rates through saturated soils are nearly double that for unsaturated soils. However, as jetting pressure is increased, the installation rate seems to become more dependent on soil density rather than saturation conditions in the jetting stratum.

2.2.3 Lateral and Axial Load Testing of Jetted Piles (Gunaratne et al., 1999)

Lateral and axial load testing of both jetted and dynamically driven model-piles were conducted to determine effects of spacing and the installation methods on pile capacity. The piles were tested at axial displacements of 0.5 in (12.7 mm) and laterally tested to displacements of 1 inch (25.4 mm). Axial capacities of piles driven with jetting and dynamic driving were shown to have higher capacities at spacing of 3 times diameter (3D) than similar piles driven at a spacing of 5D in unsaturated conditions. This is believed to be due to the overlapping influence of densification zones surrounding the piles at closer spacing. Dynamic driving of the piles to achieve final set at this close spacing was believed to have overridden the jetting effects. Gunaratne et al. (1999) also stated that the axial capacity of jetted piles in saturated soil conditions does not affect the axial load behavior of adjacent driven piles.

Lateral load testing of the model piles was conducted under saturated and unsaturated conditions. In general, Gunaratne et al. (1999) suggested that lateral load capacity in unsaturated conditions increased with greater spacing between jetted piles as tested in the experimental program. Higher lateral load capacities were also obtained in existing piles where jetting was implemented at a spacing of 5D rather than 3D. At closer spacing, reduction in lateral confinement surrounding existing piles may occur due to jetting, and therefore lower capacity.

2.2.4 Summary of Experimental Modeling of Jetted Pile Installations

Through research funded by Florida Department of Transportation, Gunaratne et al. (1999) developed design charts for capacity of piles installed with various methods. Conclusions drawn from their research include: lateral stability of jetted piles is significantly less than lateral stability of piles mechanically driven to the same installation depth; jetting further than 5D from existing piles in unsaturated conditions and 3D in saturated conditions seems to have little effect on axial and lateral load capacity; and, installation rates of jetted piles are influenced by jetting pressures and flow rates as well as material density and saturation conditions within the jetting stratum.

2.3 Hydraulic Effects on Transport of Sedimentary Particles

In order to understand the effects of fluid and flow properties on sediment transport, a review of literature provided by Allen (1985) was conducted. This review was undertaken to determine if available jetting parameters from the experimental program could be used to predict the transport of the soil particles emitted from the jetting annulus due to the underwater currents. Transport of soil particles by fluids involves two distinct parts. The first consists of an initial force required to initiate

particle motion. The next involves forces necessary to move soil particles along a velocity vector. These forces must initiate movement and entrain the soil particles within the fluid current for successful transport (Allen, 1985). Allen states that grain size, fluid properties, and flow characteristics together determine the “entrainment threshold and the modes and rate of sediment transport.” As shown in Figure 2.5, the forces acting on an idealized spherical particle of greater density than the shearing fluid, in contact with a bed of similar spherical particles are a fluid drag force (F_D), lift force (F_L), particle buoyant weight (F_w), and interparticle cohesion (F_C) from grain to grain contact.

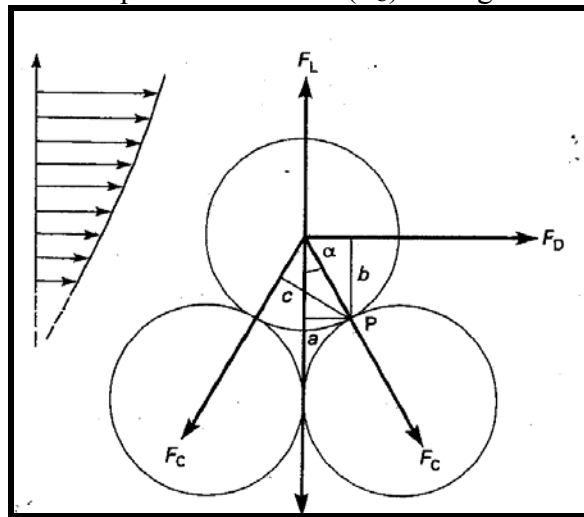


Figure 2-5 Forces acting on a particle resting on a granular bed subject to a steady current (Allen, 1985)

Applying Newton’s First law, the following force balance was given (Allen, 1985):

$$aF_L + bF_D = aF_w + cF_C \quad \text{Eq. 2.5}$$

where: a, b, and c are the moment arm lengths from P

P is the downstream pivot point on grain surfaces

The effects of inter-particle cohesion between sand and gravel particles is neglected which results in only the fluid drag, fluid lift, and particle buoyant weight acting on the soil grain. Within clay or silt profiles, the inter-particle forces become important due to adhesion of particles through van der Waals or electrostatic forces.

The fluid drag force may be specified as the mean bed shear stress or through definition of the drag coefficient involving mean fluid velocity at the particle-fluid interface. The lift force may be defined through application of the Bernoulli equation. Since the velocity on the upper surface of the soil particle in Figure 2.6 is greater than at the particle interface between the soil particles, a pressure gradient exists which provides a lifting force beneath the upper soil particle. Therefore, the particle weight or specific gravity, particle size, and interparticle cohesion all contribute to efficiency of a given fluid velocity to initiate soil particle transport (Allen, 1985).

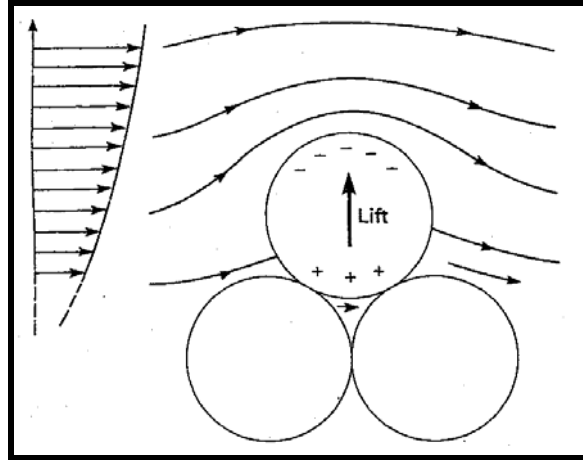


Figure 2-6 Lift force due to Bernoulli effect on granular bed subject to fluid shear
(Allen, 1985)

2.4 Summary of Literature Review

The literature review presented the state-of-the-art of pile jetting techniques implemented for installation of various length and diameter piles as presented by Tsinker (1988). These developed techniques encompassed variations in subsurface materials as well as jetting pump capacity requirements. Nearly ten years later, research conducted by Gunaratne et al. (1999) brought forth important aspects of model testing and experimental program development for evaluating impact of jetting on pile capacity. Lateral load test results from jetted and driven piles were presented and compared as well as pile installation rates as a function of jetting pressure and flow rate variations. Literature on the effects of water currents and the initiation of erosion and transport has been reviewed. However, there was no information attained from literature on the impact of pile jetting on surface debris zone volumes, debris zone areas, and the effect of these characteristics on surface environments. The focus of the current research is to quantify the debris zone and its characteristics due to variation in soil type and jetting parameters for successful pile installation. In addition, sampling the surrounding environment while jetting is conducting in the field will provide data for investigating the ecological impact of the problem. Sampling will include obtaining water and sediment specimens when jetting underwater and sediment specimens when jetting on land.

CHAPTER 3 - LABORATORY EXPERIMENTAL PROGRAM

An experimental program was developed to quantify jetting induced disturbance and pile insertion characteristics for jetted pile installations and to provide a setting in which a detailed study of jetting parameters could be conducted for several soil types. Index properties of test materials were measured. Testing included sieve analysis for grain size, maximum and minimum index density tests, direct shear tests, and permeability tests. The prototype jetting experiments were performed using model concrete piles in samples that were 5ft × 5ft × 4.5ft. Once a soil sample was prepared, its surface was surveyed to establish a pre-installation baseline. After pile jetting, the soil surface was again surveyed to evaluate size of the disturbance zone. This program enabled the researchers to vary jetting parameters in a controlled setting to determine the relationship between these parameters and the zone of disturbance and model pile insertion characteristics.

3.1. Mechanical Properties of Laboratory Test Soils

3.1.1 Index properties of Test Soils

Four different soils were used in the laboratory test program: a well-graded coarse Concrete Sand, a uniform graded Mortar Sand, a uniform Cherry Branch Ferry Basin dredged sand, and a 90/10 Mortar Sand/Kaolinite mixture. These soil types exhibited desired properties with respect to grain size uniformity and gradation as it is inferred that soil particle size and gradation will have an impact on pile insertion depth, pile insertion rate, and debris volume characteristics (Allen,1985). Selections of soils used in this research were predominantly based on the particle size distribution and characteristics of the distribution curves. The grain size distribution curves for each material used in the testing program are shown in Figure 3.1. The maximum and minimum index densities were determined for the Concrete Sand, Mortar Sand, and Cherry Branch Sand used in the testing program. The maximum dry densities of the soils were determined in accordance with ASTM D 4253 using a vibratory shake table. The minimum dry densities for the natural soils were determined in accordance with ASTM D 4254 using the “funnel pouring device” to fill the specified material mold. Also, specific gravities of the soils were determined in accordance with ASTM D 854. The maximum and minimum index densities of test materials are shown in Table 3.1. Also each soil type was defined by USCS using the Coefficient of Uniformity (C_u) and Coefficient of Curvature (C_c).

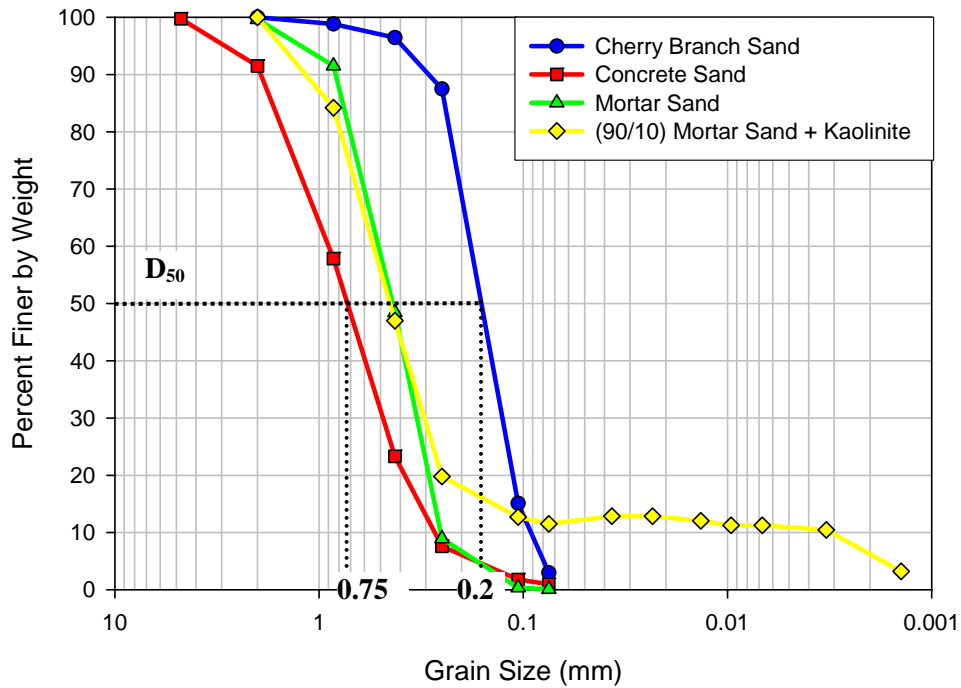


Figure 3-1 Grain Size Distribution Curves for Laboratory Jetting Tests

Table 3-1 Index Properties for Natural Soils Used in Laboratory Testing Program

Soil Type	Max. Dry Density, ρ_{dmax} (pcf)	Min. Dry Density, ρ_{dmin} (pcf)	Min. Void Ratio, e_{min}	Max. Void Ratio, e_{max}	Specific Gravity	C_u / C_c	USCS	
Concrete Sand	114.81	94.10	0.44	0.76	2.65	3.28 / 0.91	SW	
Mortar Sand	107.98	90.10	0.49	0.79	2.58	1.79 / 0.88	SP	
Cherry Branch Sand	102.00	82.00	0.60	0.99	2.61	2.00 / 1.04	SP	
Mortar Sand + Kaolinite (90/10)	N/A						176.07 / 56.60	SW-SM

3.1.2 Effective Angle of Internal Friction

To determine strength properties of the test soils, direct shear tests were conducted on specimens compacted to dry densities corresponding to 50% relative density since relative densities range from 50 to 70 percent within the upper soil stratum where jetting would routinely be used for pile installation. Also normal stresses ranging from 250 psf (12 kPa) to 2000 psf (96 kPa) were used to develop the failure envelope for each sand type. These normal stresses cover the range of vertical effective stresses within a saturated soil stratum of 20 to 40 feet (6.1 to 12.2 m) below the ground surface. These depths are consistent with jetted pile installations that were planned to be conducted in field settings as an extension to the laboratory research. The effective angles of internal friction for each test are shown in Figure 3.2. These friction angle ranged from 30° for the sand + kaolinite mix to 42° for the concrete sand, with the soil retrieved from the dredged basin material having $\phi' = 34^\circ$.

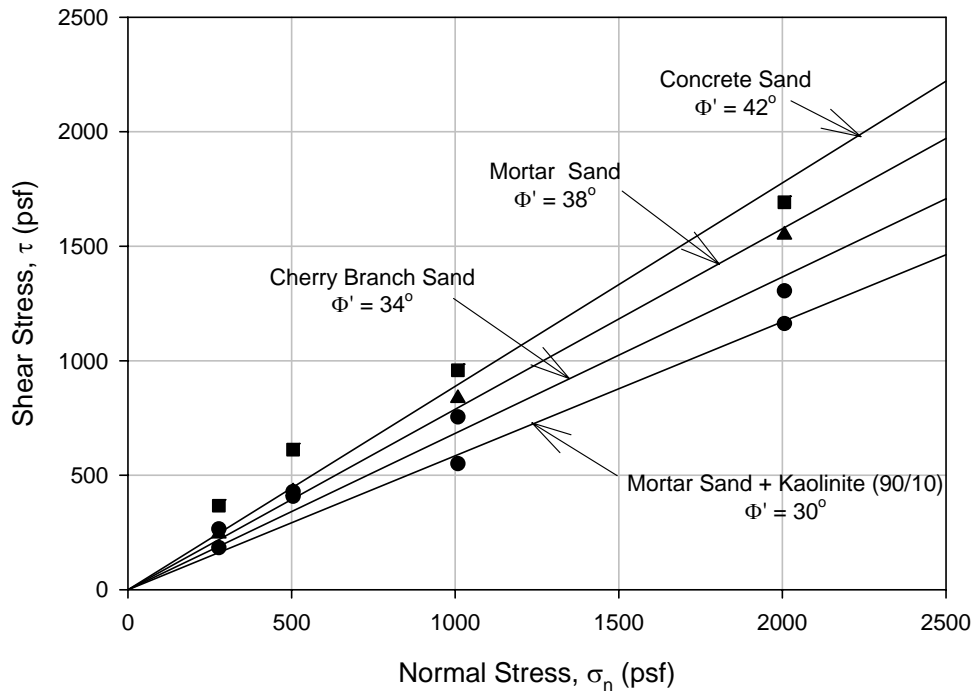


Figure 3-2 Direct Shear Test Results for Material Used in Laboratory Jetting

3.1.3 Permeability of Testing Material

Falling head permeability tests were conducted on test samples. Required masses of each soil material were determined to yield relative densities between 50% and 70%, which are consistent with threshold values deemed appropriate for the experimental program. Each specimen was simultaneously subjected to 10 psi (69 kPa) confining pressure and specimen pressure (headwater). Permeability values, along with pertinent

test information, are shown in Table 3.2, and were in the range of 1 to 5×10^{-4} ft/s for the sand soils and decreased by nearly one order of magnitude when kaolinite was added.

Table 3-2 Permeability Information for Soils Used in Laboratory Testing

Soil Type →	Concrete Sand	Cherry Branch Sand	Mortar Sand	Mortar Sand + Kaolinite (90/10)
Relative Density, D_r (%)	57	72	63	
Void Ratio, e	0.56	0.71	0.65	0.56
No. of Pore Volumes for Constant k	11	21	10	4
Permeability, k ft/s (cm/s)	1.5×10^{-4} (10^{-2})	2.8×10^{-4} (10^{-2})	5.2×10^{-4} (10^{-2})	2.7×10^{-5} (10^{-3})

3.2 Laboratory Jetting Program

A series of jetted pile installations were performed in the various test sands, and a model was developed based on the laboratory results. The laboratory jetting program was performed in the Constructed Facilities Laboratory(CFL) on North Carolina State University's Centennial Campus. The jetting program consisted of fabrication of model test piles, a jetting test chamber, and jetting apparatus. The laboratory scale jetting system encompassed aspects of full-scale jetting processes. Also, of key importance was development of a method to repeatedly construct test specimens with similar index densities in order to provide a basis of comparison for each jetted pile insertion with various jetting parameters.

3.2.1 Fabrication of Model Test Piles

Three solid model test piles were constructed of 5000 psi (34500 kPa), 28 day compressive strength concrete, formed with 0.667 ft (0.204 m), 0.5 ft (0.153 m), and 0.333 ft (0.102m) inside diameter PVC water pipe. Each test pile was 8 feet (2.438 m) in length and reinforced with one A36 steel No. 8 rebar extending the entire length of the test pile. Steel hooks were placed in the top of each test pile. These hooks extended from the pile head so each could be connected to chains suspended from an overhead crane. The steel reinforcement provided sufficient tensile support to the pile so each could be lifted at the head without excessive cracking of the concrete. After concrete placement, the test piles were allowed to cure for seven days to develop adequate strength before the forms were removed.

Each test pile was marked from the pile tip at 2-inch (50mm) increments so that insertion rate information could be obtained during each jetting procedure. These insertion rates were compared between each test to determine jetting parameter effects and installation and debris characteristics in the various soil types.

3.2.2 Jetting Test Chamber

A 5 ft x 5 ft x 4.5 ft (1.52 m x 1.52 m x 1.37 m - length x width x height) steel box was fabricated to efficiently conduct jetting tests without unnecessary climbing and bending over the box sides. This box was fabricated as a tank used to saturate the soil specimens used in the laboratory jetting program. A 3 ft x 3 ft x 4 ft (0.91 m x 0.91 m x 1.22m - length x width x height) steel frame specimen basket was fabricated with steel channels for specimen containment as shown in Figure 3.3. The frame allowed routine movement of large soil specimens with an overhead crane. The interior of the frame was lined with a geotextile and geogrid layer, which allowed the saturation water to permeate the soil specimens. The saturation tank and specimen basket are shown in Figure 3.3 and Figure 3.4.



Figure 3-3 Saturation Tank and Specimen Basket



Figure 3-4 Overhead View of Saturation Tank with Specimen Basket in Place

3.2.3 Fabrication of Jetting Apparatus

To install model test piles in the various testing media, it was necessary to fabricate a jetting apparatus that would allow controlled water flow rates and jet nozzle velocities. The jetting apparatus used in laboratory testing and the various nozzles implemented in the program are shown in Figure 3.5.



Figure 3-5 Laboratory Jetting Apparatus and Various Nozzles

Variations in jetting parameters provided a means of comparison between tests for final depth of installation, volume and area of debris zones, and pile insertion rate. The jetting apparatus consists of two 5 ft (1.52 m) long, 0.8125 inch (20.6 mm) inside-diameter jet pipes connected with galvanized tees, forming a single jetting system. Also, the available flow rates and nozzle velocities for each nozzle configuration are shown in Table 3.3. The nozzle diameter ranged from 0.5 - 0.813 inch (1/2 to 13/16 inch), which yielded jetting velocities in the range of 186-980 ft/min depending on the flow rate.

3.2.4 Test Setup and Quality Control

Comparison testing involved jetting piles with various jetting parameters through specimens compacted to equal relative densities. The laboratory procedure to produce 50-70 % relative density for one lift thickness was as follows:

Allow soil to free-fall from material box producing an un-compacted height of approximately 18 inches. Level the surface.

Table 3-3 Available Flowrate and Nozzle Velocity Configurations

	Water Flow Rate 1.337 ft ³ /min			Water Flow Rate 2.674 ft ³ /min		
Nozzle Diameter (inch)	Jet	Nozzle	Velocity	Jet	Nozzle	Velocity
	(ft/min)			(ft/min)		
0.500	490			980		
0.625	313			326		
0.813	186			372		
CONVERSIONS: ft ³ /min to m ³ /min multiply by 0.0283 inch to mm multiply by 25.4 ft/min to m/min divide by 3.281						

- i. Using a vibratory jack hammer with 8" plate, compact the lift for five minutes starting from the edge of the specimen basket while following a circular motion until the center is reached.
- ii. Adjust the moisture content to aid in compaction as needed.
- iii. Determine dry density from the midpoint of the layer (6 inches) using nuclear density gage.

This specimen preparation sequence is illustrated in Figures 3.6 through 3.8.



Figure 3-6 Free-fall of Specimen Soil for Desired Lift Height



Figure 3-7 Compaction of Individual Lift Height



Figure 3-8 Density Check at Midpoint of Lift Height

Upon completion of specimen preparation and quality control, the saturation tank was filled with water until the water surface and specimen surface coincided. The Concrete, Cherry Branch, and Mortar sands were allowed to inundate for an hour, whereas the Mortar Sand/Kaolinite mixtures were allowed to inundate for 24 hours. Saturated conditions are consistent with coastal groundwater conditions found in Eastern North Carolina. A reference beam was set above the test box and used for pre and post testing surveying of the samples surface.

3.2.5 Jet Testing Program

In order to quantify both the magnitude and extent of disturbance and the insertion rate as a function of jetting parameters, a series of “full-depth” tests was conducted. These full-depth tests involved maintaining a consistent water flowrate and jet nozzle velocity for each test. After completion of specimen preparation and inundation, the jetting apparatus was connected to the selected test pile such that the jet nozzles were flush with the pile tip. The jetting nozzles were located at the edge of the pile on opposite sides. The pile was then lowered into place and allowed to settle under self weight at the specimen surface. During jetting, the test pile penetrated the specimens until refusal. From these tests, maximum insertion depth and debris zone characteristics for the experiment jetting parameters were acquired. The flowchart in Figure 3.9 demonstrates the test matrix for vertical jet testing used in the laboratory program.

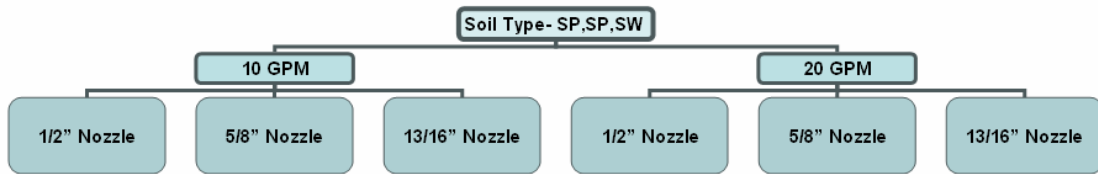


Figure 3-9 Flowchart for Tests Conducted with Vertical Jets – Full Depth

Even though the majority of laboratory jetting involved the vertical jetting apparatus, modifications involved jet nozzles angled at 45° from the vertical pipes to determine if jet nozzle orientation affected the insertion and debris zone characteristics of jetted piles. These nozzles were oriented so the jet water flowed directly under the pile tip. The orientations of the jet streams used in these tests are shown in Figure 3.10. Data produced from these tests were compared to similar jetting parameter tests using vertical nozzles.



Figure 3-10 Angled Jet Nozzles for Jetting Modification

CHAPTER 4 - LABORATORY JETTING TEST RESULTS and MODEL DEVELOPMENT

A majority of the jetting experiments were conducted on the eight inch diameter pile which consistently reached insertion refusal prior to encountering the specimen depth limit while initial jetting of the four inch and six inch diameter piles penetrated the entire sample depth. The water flow rates (Q_w) and jet nozzle velocities (V_j) varied between tests to determine the effects of these parameters on pile installation and debris zone characteristics. Table 4.1 provides information on testing parameters.

Table 4-1 Description of Tests Conducted in Experimental Program

Concrete Sand		Mortar Sand		Cherry Branch Sand		Mortar + Kaolinite	
Full Tests	Depth Control Tests	*Full Tests	*Depth Control Tests	Full Tests	Depth Control Tests	Full Tests	Depth Control Tests
$(Q_w - V_j)$ (ft ³ /min - ft/min)	$(Q_w - V_j)$ (ft ³ /min - ft/min)	$(Q_w - V_j)$ (ft ³ /min - ft/min)	$(Q_w - V_j)$ (ft ³ /min - ft/min)	$(Q_w - V_j)$ (ft ³ /min - ft/min)	$(Q_w - V_j)$ (ft ³ /min - ft/min)	$(Q_w - V_j)$ (ft ³ /min - ft/min)	$(Q_w - V_j)$ (ft ³ /min - ft/min)
1.337-313	1.337-490	1.337-186	1.337-313	1.337-186	1.337-186	1.337-186	1.337-186
1.337-313	2.674-372	1.337-186	1.337-490	1.337-313	1.337-313	1.337-313	1.337-490
1.337-490	2.674-626	1.337-490	2.674-372	1.337-490	1.337-490	1.337-490	2.674-372
2.674-372	2.674-980	2.674-626	2.674-980	1.337-490	2.674-372		2.674-980
2.674-626		2.674-626		2.674-372	2.674-626		
2.674-626		2.674-980					
2.674-980							
CONVERSIONS: ft ³ /min to m ³ /min multiply by 0.0283 ft/min to m/min divide by 3.281							

* A full test was run by continually jetting the pile into the sample. In comparison, a depth control test was run incrementally where the test is stopped after pre-specified insertion depth was reached and the disturbance zone was measured.

4.1 Insertion Characteristics and Refusal Depth

4.1.1 Insertion Rate Characteristics

Piles were jetted into various sand specimens compacted to consistent relative densities to provide a basis of comparison between tests with variations in water flow rate (Q_w) and jet nozzle velocity (V_j). Insertion properties (i.e. Pile Insertion Rate, and Refusal Depth) were measured as a function of water flow rate (Q_w) and jet nozzle

velocity (V_j). Visual observations regarding water returning from the pile annulus with soil particles was documented.

Insertion depth versus time graphs shown in Figures 4.1a-d for each soil type indicate that with equal Q_w , higher jet nozzle velocities enable the pile tip to penetrate to greater depths as compared to tests performed using lower jet nozzle velocities. Greater depth of insertion indicated that erosion efficiency and particle lifting ability increased with higher jet velocities. For example, in the case of concrete sand having $D_{50}=0.75$ mm, at a $Q_w = 2.674$ ft³/min only when $V_j = 980$ ft/min did pile insertion exceed 2 ft

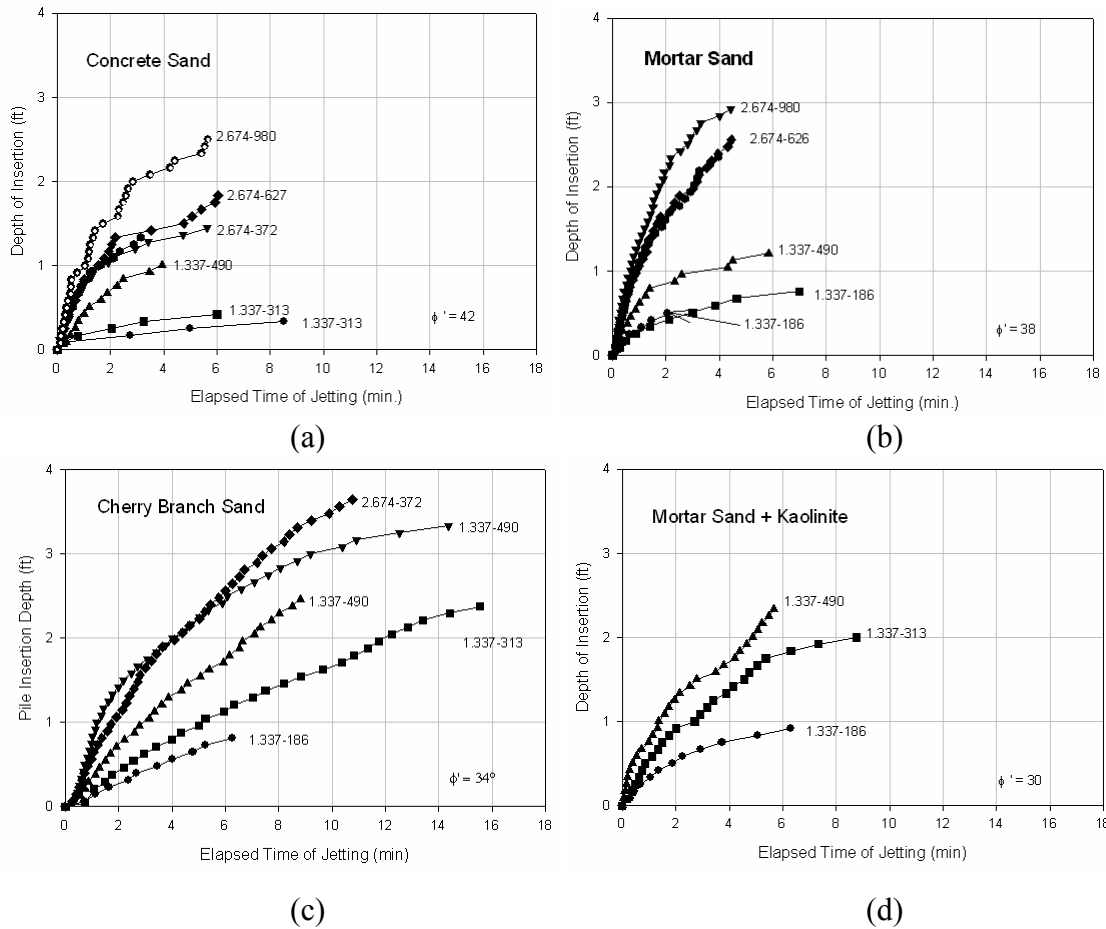


Figure 4-1 Depth of Insertion as a Function of Time for Various Water Flowrate and Jet Nozzle Velocity (Numbers on curves = Flow rate(ft³/min) – Nozzle velocity (ft/min))

In contrast, a $V_j = 370$ ft/min was all that was needed to exceed 2ft in the Cherry Branch sand having $D_{50} = 0.2$ mm. Accordingly, it is recognized that particle lift by a fluid medium is dependent on the velocity of fluid, particle diameter, and specific gravity of the particle. For equal jetting parameters, it is expected that greater insertion depths may be obtained in soil profiles with smaller average particle sizes as opposed to soil profiles with larger average particle sizes.

Using the same jetting velocity, the average insertion rate, at one foot insertion, is approximately 0.7 ft/min (0.20 m/min) in the Cherry Branch sand, in comparison to approximately 0.3 ft/min (0.08 m/min) in the Concrete Sand. The effective angle of internal friction (ϕ), determined by direct shear testing, is 42° and 34° for the Concrete and Cherry Branch Sand, respectively. Thus, tip bearing capacity of the Concrete Sand at this depth increment is greater than tip bearing capacity of the Cherry Branch Sand. For equal depths of insertion, a larger eroded area needs to be accomplished beneath the pile tip in Concrete Sand to cause a bearing capacity failure and advancement of the pile. With equal jetting parameters, longer time intervals are necessary to erode greater areas in soils with higher friction angle materials, therefore decreasing the pile insertion rate. Depths of insertion were chosen for each soil type based on the attainable insertion depth of the lowest Q_w and V_j relationship. Furthermore, as shown in Figure 4.2, for a given depth, the pile insertion rate is dependent on both Q_w and V_j . For equal Q_w , increases in V_j will provide higher insertion rates for any depth of insertion.

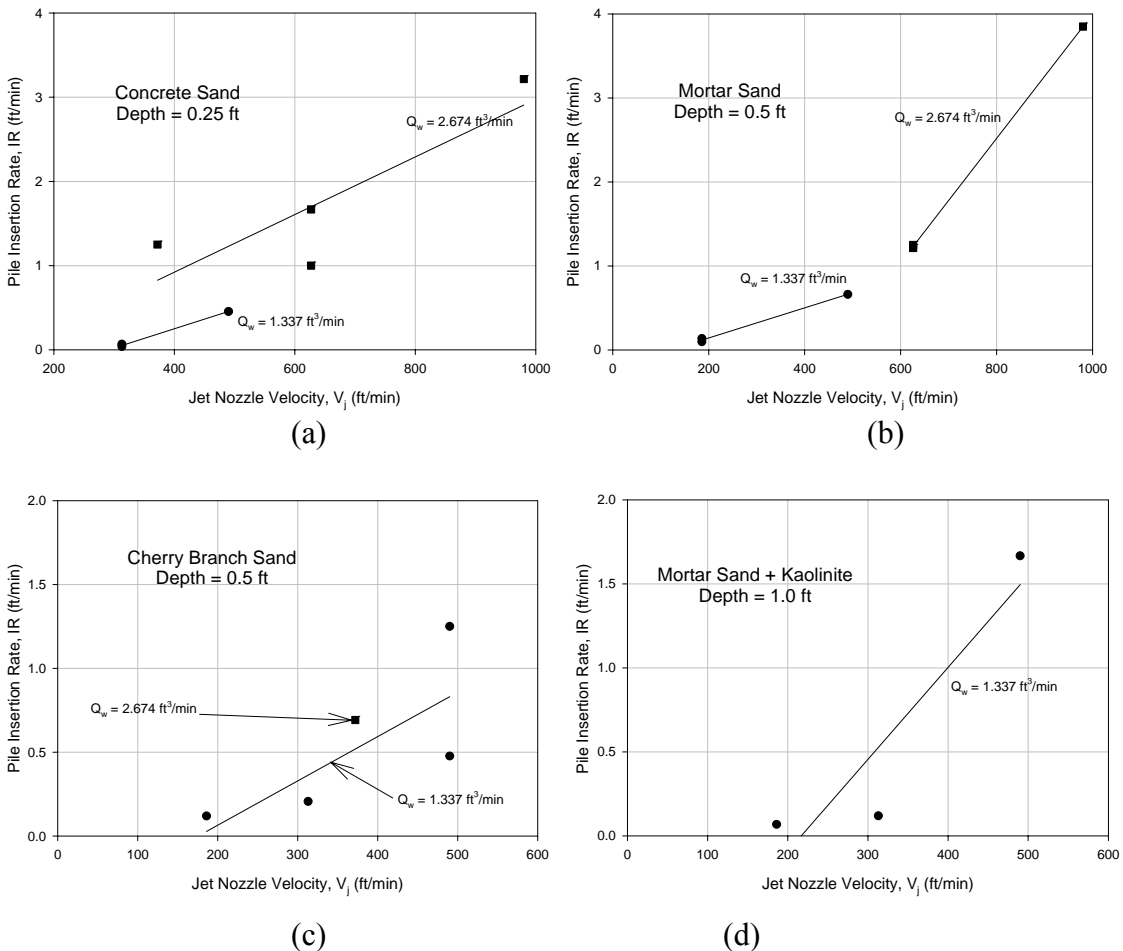


Figure 4-2 Comparison of Pile Insertion Rates at Given Depths Due to Variation in Jetting Parameters

Assuming continuity, jet nozzle velocity is linearly dependent on the jet nozzle area and water flow rate through the nozzle by the following equation:

$$Q_w = A_j V_j \quad \text{Eq. 4.1}$$

where:

Q_w = water volume flowrate (L^3/T)

A_j = jet nozzle area (L^2)

V_j = jet nozzle velocity (L/T)

The pile insertion rate, IR, is based on both Q_w and V_j for a given depth in the soil stratum. Since the bearing resistance of a uniform soil profile increases with depth, the dimensions of the jetted pile are important when comparing installation characteristics. Equation 4.2 provides a direct relationship between the pile dimensions, insertion rate, and therefore indirectly the jetting parameters, at a specified depth within the soil profile.

$$Q_p = IR \times A_p \quad \text{Eq. 4.2}$$

where:

Q_p = pile volume flowrate (L^3/T)

IR = pile insertion rate (L/T)

A_p = pile area (L^2)

The pile volume rate is the volume of pile (Area * Length) inserted per given time.

4.1.2 Insertion Characteristics – Angled Jets

As a form of practice modification, 45° angled jet nozzles were implemented into the jetting system to determine jet nozzle orientation effects on pile insertion characteristics. These tests were conducted in Mortar Sand specimens to compare the final depth of pile insertion and insertion rates with those obtained using vertical nozzle orientations. The depth of insertion as a function of time for the comparison tests are shown in Figure 4.3. Comparing insertion depths and rates for equal jetting parameters in Mortar Sand in Figure 4.3, the angled jetting system is seen to provide greater depth of insertion and insertion rate capabilities. For example, for Q_w of 1.337 ft³/min (0.038 m³/min) and V_j of 490 ft/min (149 m/min), the vertical jets provide a depth of insertion at six minutes of 1.25 ft (0.38 m), whereas the angled jetting system provides a depth of insertion at six minutes of 2.75 ft (0.84 m). However, as will be discussed in conjunction with the field test data there are practical limitations related to the ability to install and use angled jet nozzle in the field.

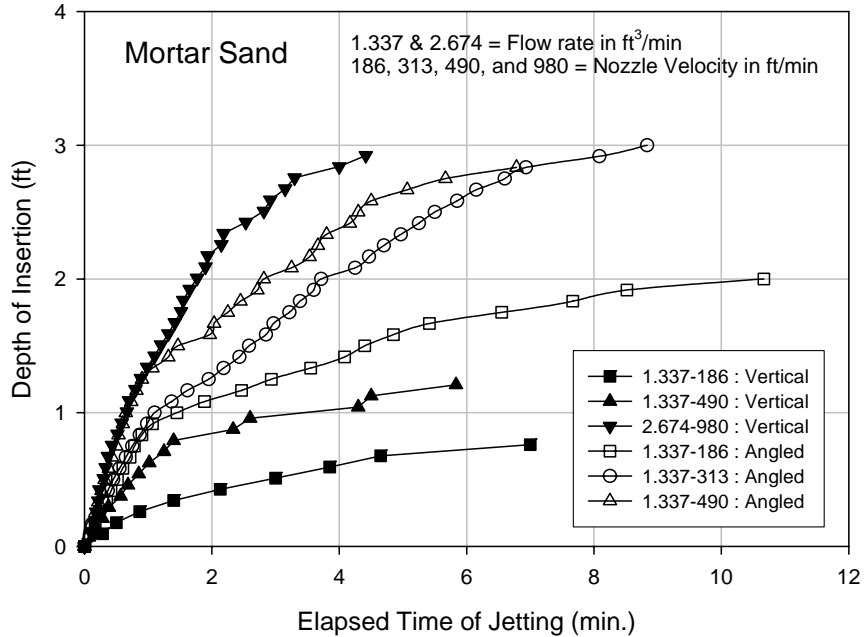


Figure 4-3 Depth of Insertion with Time for Various Water Flowrate and Jet Nozzle Orientation.

4.2 Debris Zone Characteristics

4.2.1 Debris Volume Analysis – Full Depth

Upon termination of jetting, debris volumes (V_{debris}) were determined based on final survey of the sample surface. The debris volumes were determined for each full test to establish the relationship between the total volume of pile jetted into the specimen and the quantity of material exiting the jetting annulus. As shown in Figure 4.4, data indicated that the debris volume exiting the annulus increases linearly with depth of pile installed. These relationships are plotted with best-fit lines through the data for each soil type.

4.2.2 Debris Area Analysis – Depth Control

Upon termination of jetting, debris areas (A_{debris}) were determined based on final survey of the sample surface shown in Figure 4.5. The debris areas were determined for each full test to establish the relationship between the total volume of pile jetted into the specimen and the distribution of material ejected from the annulus to the sample surface. The debris areas calculated for each full depth test followed similar distribution with jetted pile volume as the debris volume quantities.

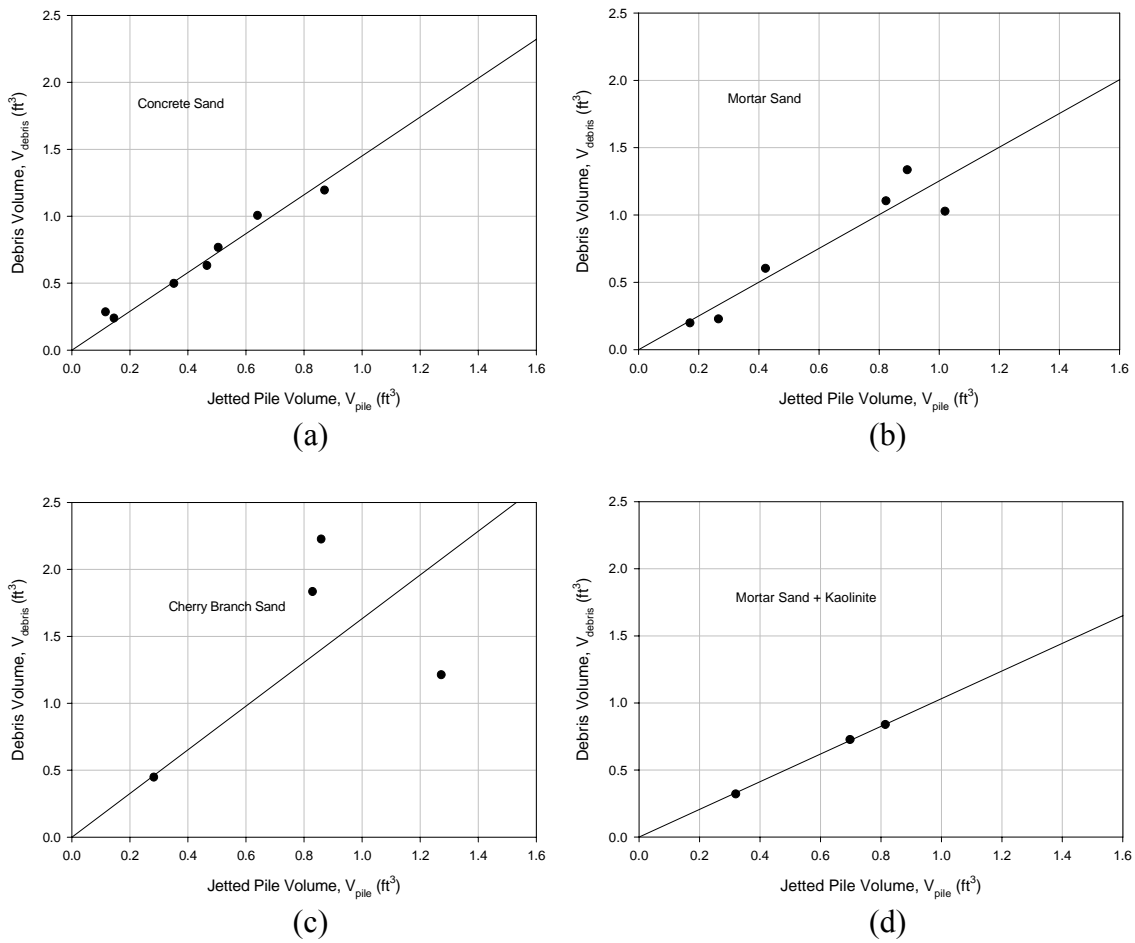


Figure 4-4 Debris Volume with Increase in Jetted Pile Volume

Figure 4.5 a & b displays the debris area distributions for a jetted pile in Concrete Sand to a depth of approximately 36 inches (0.91 m) and 14 inches (0.36 m) respectively. As might logically be expected, as the depth of pile penetration increases, so does the lateral extent of the debris area and the total debris volume. It should be stated that the measuring system used in the experimental program was precise to 0.039 inches (1mm). It should also be noted that smaller particles would have traveled further than the debris zones shown in Figure 4.5. However, due to the boundary constraints of the test box setup, these extents were not determined. The debris areas (A_{debris}) for each full depth test conducted on the various sand types, with the exception of the Cherry Branch Sand are shown in Figure 4.6.

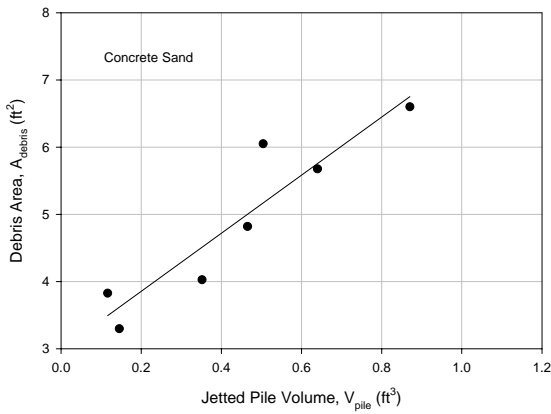


(a) 36 inch installation depth

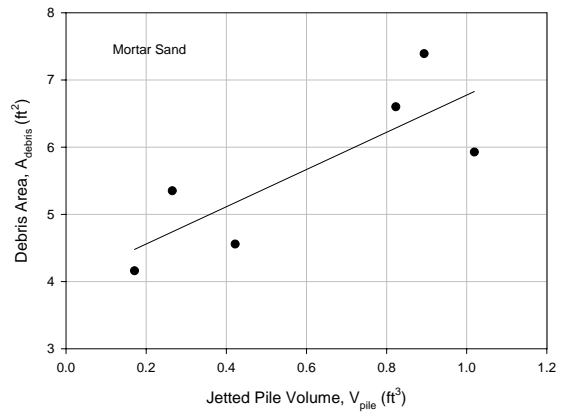


(b) 14 inch installation depth

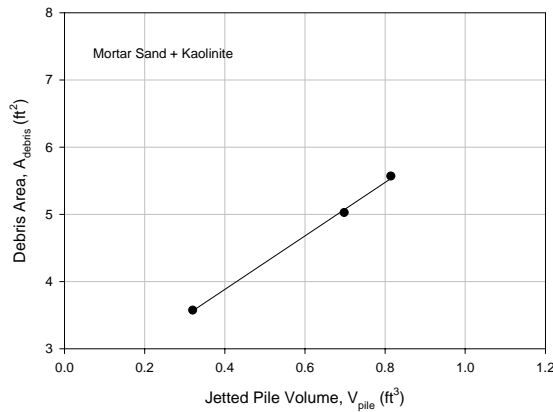
Figure 4-5 Comparison of Debris Areas in Concrete Sand at Two Insertion Depths



(a)



(b)



(c)

Figure 4-6 Debris Area with Increase in Jettted Pile Volume

The ability to attain greater depths of insertion with lower values of Q_w and V_j for the Cherry Branch Sand as compared to the “coarse grained” sand types has been presented. However, insertion rates for the Cherry Branch tests were lower at greater depths due to using the lower values of Q_w and V_j as compared to those needed to reach the same depth in the sands with larger average grain sizes.

It was visually observed during the experiments that the smaller particles were lifted from the jetting annulus and displaced over the specimen boundaries by increasing volumes of water. The relative small size Cherry Branch Sand particles were easily transported with the low jet nozzle velocities. This point is illustrated in Figure 4.7 where fine particles are seen near the boundary of the test box.



Figure 4-7 Immeasurable Debris Area Distribution for Cherry Branch Sand

4.2.3 Debris Zone Analysis - 45° Angled Jets – Full Tests

Even though the insertion rate and final depth of insertion for piles jetted with 45° angled jets are greater than those installed using vertical jet nozzle, the data presented in Figures 4.8 and 4.9 demonstrate that angled jets have negligible effect on the size of the debris zone as compared to that created using the vertical jet nozzle orientations. Therefore, it is believed that employing angled jets will benefit insertion rates while resulting in similar sized debris zones to those produced by vertical jets when compared at equal depths insertion. As shown in Figure 4.8, debris zone volume increased linearly with jetted pile volume using either nozzle orientation. Similar trend was observed for the debris zone area as shown in Figure 4.9.

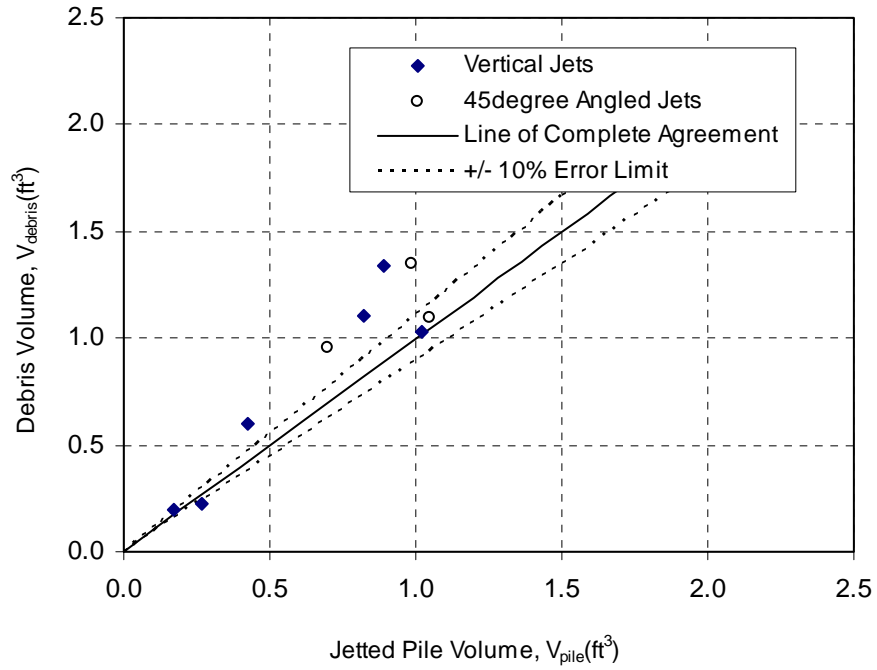


Figure 4-8 Comparison of Debris Zone Volumes Due to Various Nozzle Orientations

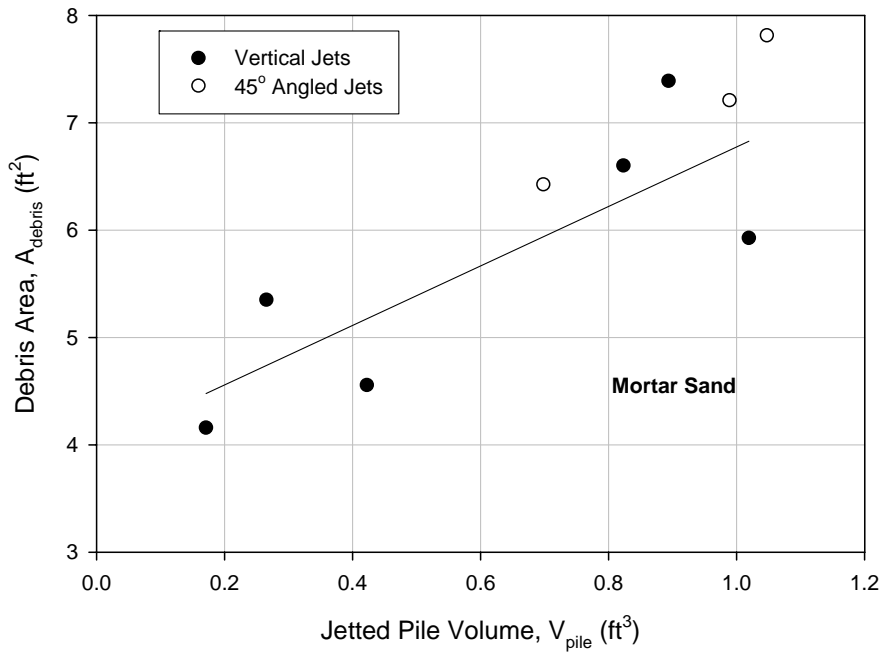


Figure 4-9 Comparison of Debris Zone Areas Due to Various Nozzle Orientations

4.2.4 Debris Zone Evaluation – Depth Control Tests

From full-depth tests, it is not possible to compare debris volumes and jetting parameters for equal depths of insertion since pile insertion rate varies for a given depth increment depending on jetting parameters. In order to establish a relationship between debris zone area and jetting parameters for a given insertion depth, “depth-controlled” tests were conducted. Depth-control tests were conducted primarily to optimize jetting parameters for installing a pile in a given soil type. Optimum jetting parameters are defined as a combination of water flow rate and jet nozzle velocity allowing adequate pile insertion rate while generating minimum debris volume. There are many combinations of Q_w and V_j that will sufficiently install a pile to the required depth. However, due to the need to obtain a reasonable insertion rate, there will exist an optimum Q_w and V_j , that will minimize surface impacts. Figure 4.10 shows the jetting data plotted as normalized values.

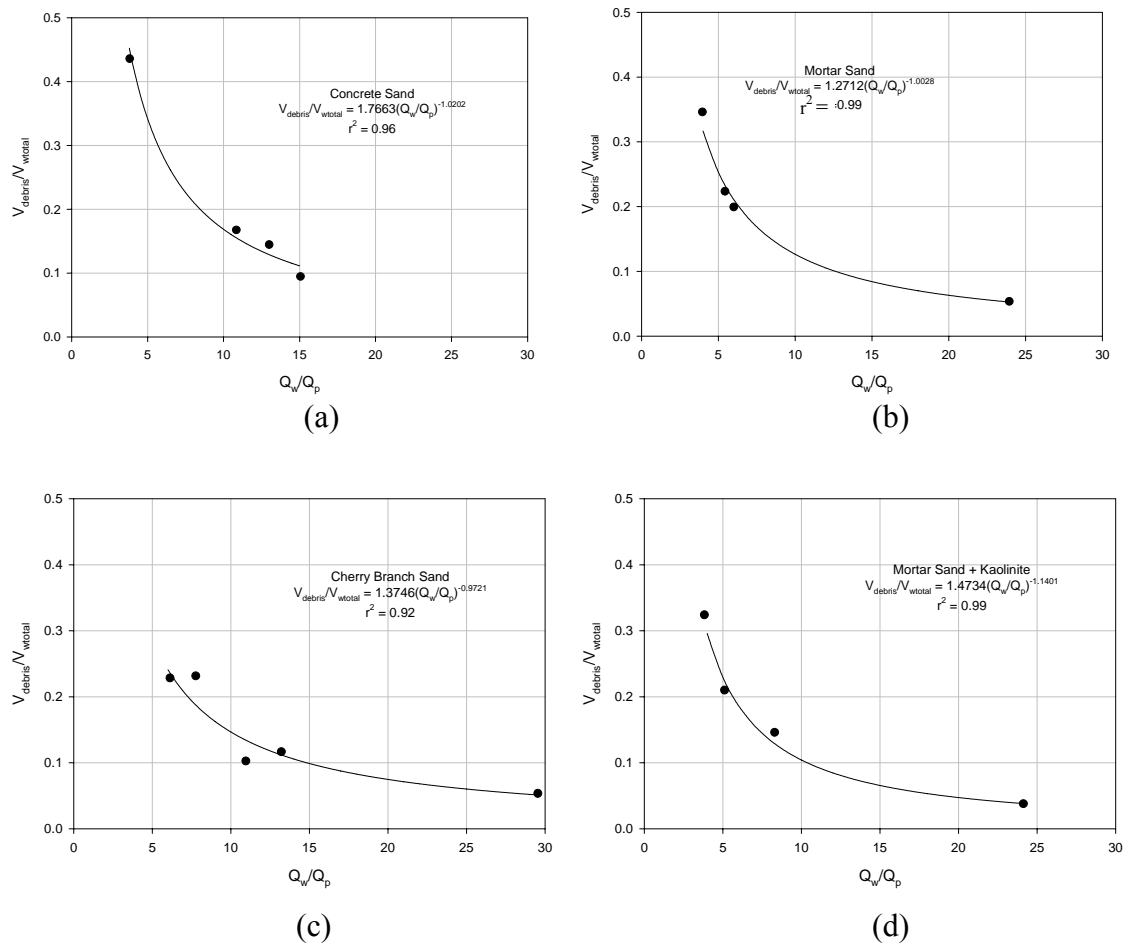


Figure 4-10 Correlations between Pile Insertion Rate and Debris Volume (Depth = 1.0 ft)

In this case, the Q_w was normalized with respect to pile volume insertion rate (Q_p) and the volume of debris was normalized with respect to the volume of water (V_w). In

Figure 4.11, the area of debris is multiplied by the pile diameter and normalized with respect to V_w . It may be inferred from Figures 4.10 and 4.11 that the total volume of water (V_{wtotal}) along with Q_w/Q_p at a given depth has a distinct effect on the debris volume (V_{debris}) and debris area (A_{debris}) surrounding jetted pile installations. Since Q_p depends on both jetting parameters, (Q_w , and V_j) normalizing Q_w with Q_p takes into account V_j required to achieve the insertion depth. Therefore, to achieve faster insertion rates for a given Q_w at a specified depth, the Q_w/Q_p ratio must be minimized resulting in higher required values of V_j .

As shown in Figure 4.10, the debris volume is a function of the characteristics of the soil thru which the pile is jetted. Therefore, it is expected that variations in particle size and characteristics of the different soils would lead to dissimilar debris zone quantities for the same jetting parameters.

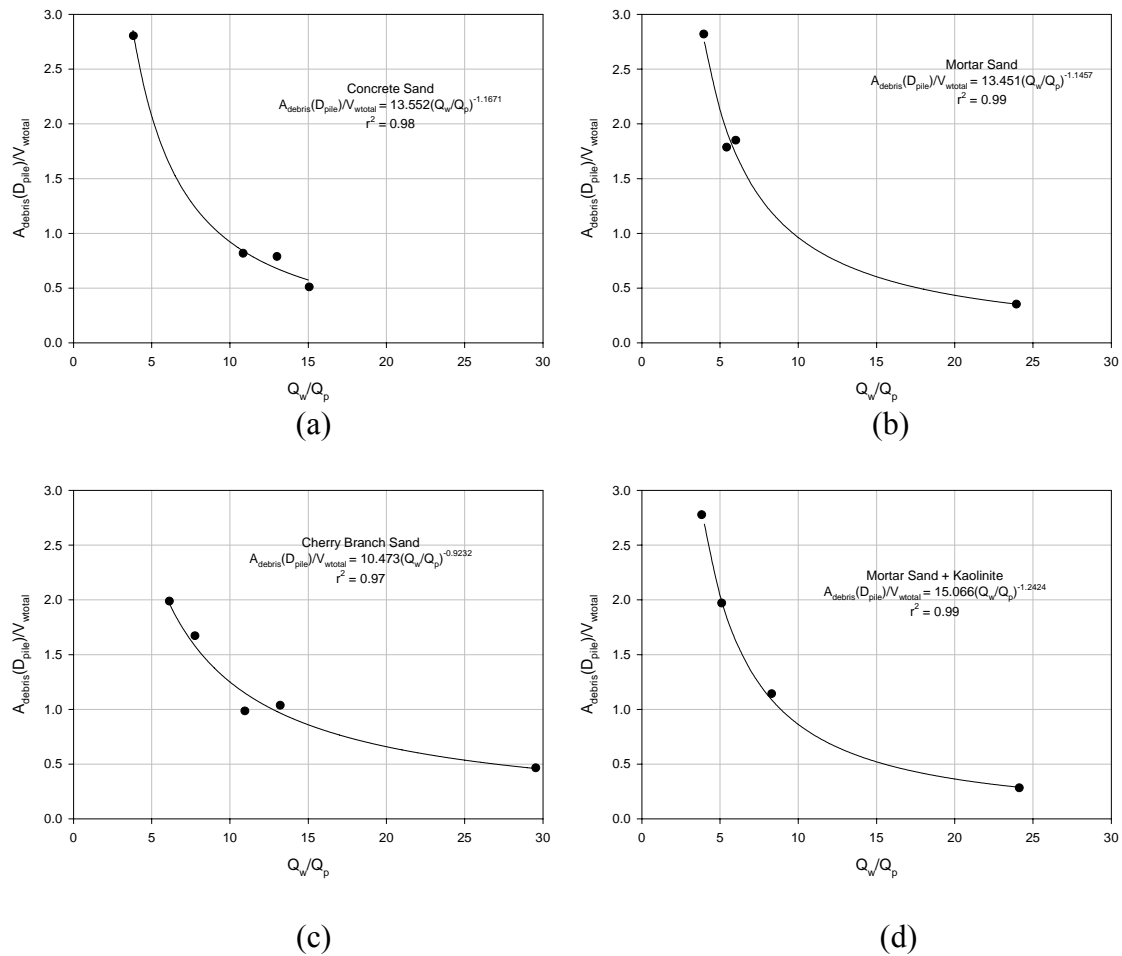


Figure 4-11 Correlations between Pile Insertion Rate and Debris Area (Depth = 1.0 ft)

In Figure 4.11, the debris area is multiplied by the pile diameter (D_p) and normalized by the total volume of water. This normalization was used to develop the

relationship between the pile diameter and the total volume of water necessary to jet the pile to the cutoff depth.

The debris volume for each soil type can be expressed by the following equation:

$$V_{\text{debris}} = V_{\text{wtotal}} \times a_{\text{volume}} \left(\frac{Q_w}{Q_p} \right)^{b_{\text{volume}}} \quad \text{Eq. 4.3}$$

where:

V_{debris} = debris volume (L^3)

V_{wtotal} = total volume of jetted water (L^3)

a_{volume} = Volume parameter dependent on the characteristics of grain size distribution

b_{volume} = D_{50} dependent volume parameter

Q_w = Water flowrate (L^3/min)

Q_p = Pile volume insertion rate (L^3/min)

The debris area for each soil type can be expressed by the following equation:

$$A_{\text{debris}} = \left(\frac{V_{\text{wtotal}}}{D_{\text{pile}}} \right) \times a_{\text{area}} \left(\frac{Q_w}{Q_p} \right)^{b_{\text{area}}} \quad \text{Eq. 4.4}$$

where: A_{debris} = debris area (L^2)

V_{wtotal} = total volume of jetted water (L^3)

D_{pile} = pile diameter (L)

a_{area} = GSD dependent area parameter

b_{area} = D_{50} dependent area parameter

Q_w = water volume flowrate (L^3/min)

Q_p = pile volume insertion rate (L^3/min)

Using the regression parameters from Figure 4.10 for the natural soils, Figures 4.12 & 4.13 shows the dependency of debris volume a-parameter (used in Eq 4.3) on grain size distribution (GSD) and jetting parameters based on test results obtained in this study. In Figure 4.12, the coefficient of curvature (Cc) is defined as $(D_{30})^2 / (D_{60}D_{10})$.

It seems that debris area is dependent upon the jetting parameters pile insertion rate and the total volume of water required to insert the pile. Figures 4.14 & 4.15 provide the dependency of debris area “a and b” parameters on grain size distribution (GSD) characteristics and jetting parameters.

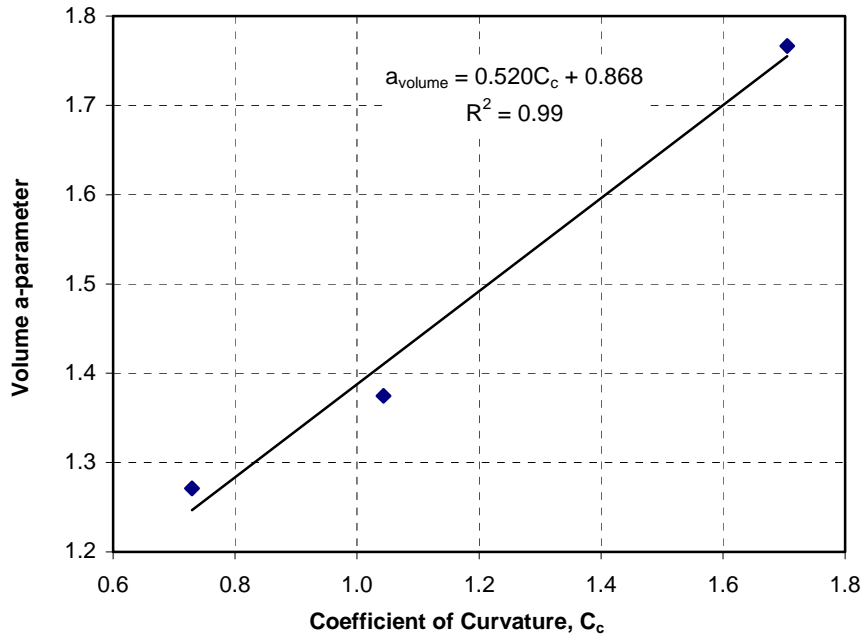


Figure 4-12 Variation of Debris Volume “a-parameter” as a Function of C_c

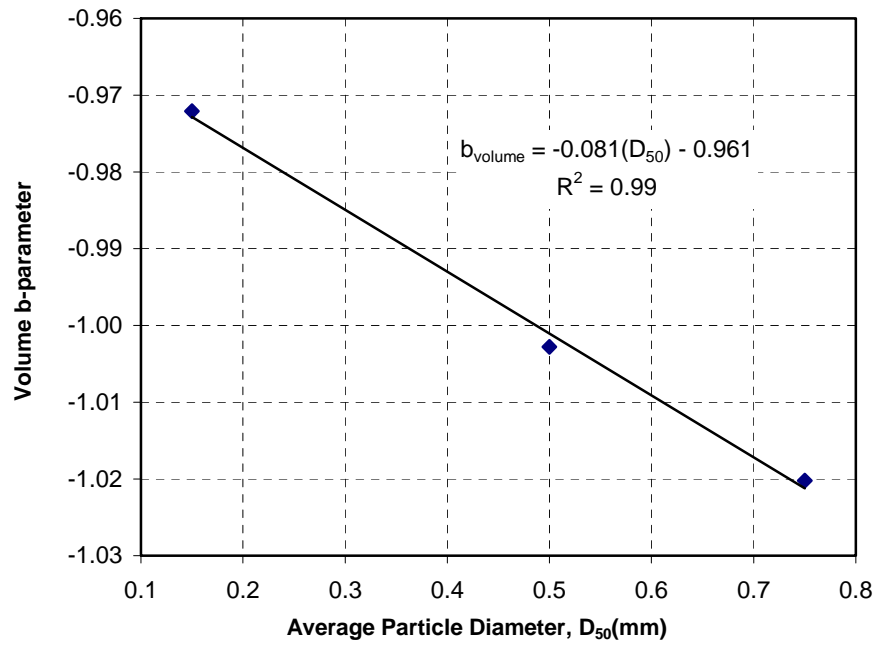


Figure 4-13 Debris Volume “b-parameter” Versus D₅₀

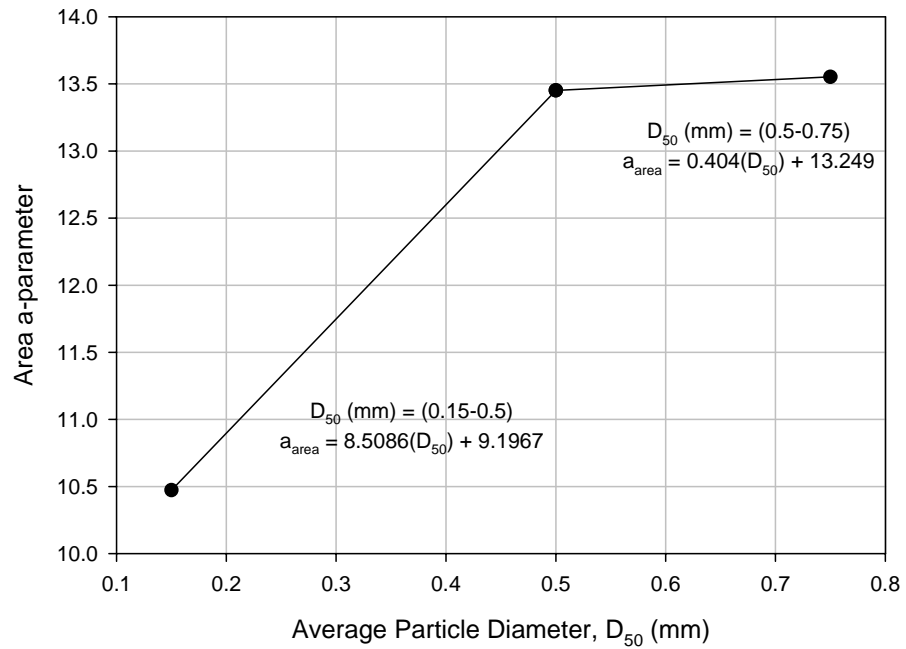


Figure 4-14 Debris Area “a-parameter” Versus D_{50}

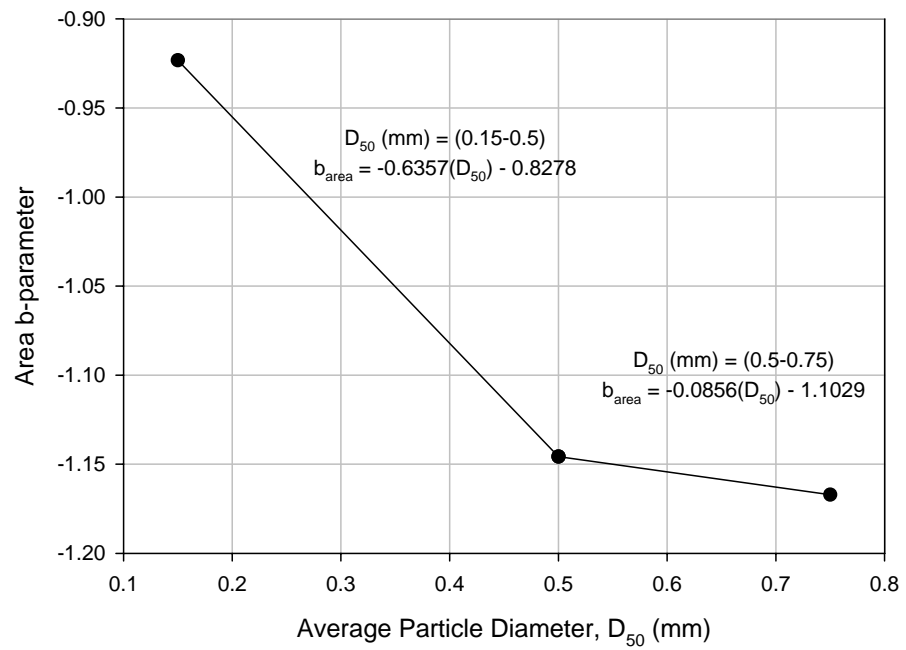


Figure 4-15 Debris Area “b-parameter” Versus D_{50}

4.3 Model Development

4.3.1 Debris Zone Modeling

From Section 4.2.4 it was shown that the debris volume (V_{debris}) and debris area (A_{debris}) follow power relationships with the total volume of water (V_{wtotal}) and jetting parameters required to achieve a given depth of insertion. The following empirical equations provide the relationship between jetting parameters and debris zone for various soil types used in the testing program.

$$V_{\text{debris}} = V_{\text{wtotal}} a_{\text{volume}} \left(\frac{Q_w}{Q_p} \right)^{b_{\text{volume}}} \quad \text{Eq. 4.5}$$

where: V_{debris} = total volume of soil material transported to ground surface (L^3)
 V_{wtotal} = total volume of water required to jet a pile to a given depth with available jetting parameters (L^3)
 a_{volume} = parameter based on C_c
 b_{volume} = parameter based on D_{50}

and

$$a_{\text{volume}} = 0.520(C_c) + 0.868 \quad \text{Eq. 4.6}$$

$$b_{\text{volume}} = -0.081(D_{50}) - 0.961 \quad (D_{50} \text{ in mm}) \quad \text{Eq. 4.7}$$

(inches to mm multiply by 25.4)

In order to estimate the debris area, the following equation is proposed:

$$A_{\text{debris}} = \left(\frac{V_{\text{wtotal}}}{D_{\text{pile}}} \right) a_{\text{area}} \left(\frac{Q_w}{Q_p} \right)^{b_{\text{area}}} \quad \text{Eq. 4.8}$$

where: A_{debris} = debris distribution on ground surface from jetted pile installation (L^2)
 V_{wtotal} = total volume of water required to jet a pile to a given depth with available jetting parameters (L^3)
 D_{pile} = diameter of jetted pile (L)
 a_{area} = parameter based on D_{50}
 b_{area} = parameter based on C_c

In cases where $D_{50} < 0.5$ mm, the a_{area} and b_{area} parameters are calculated as follow:
(inches to mm multiply by 25.4)

$$a_{\text{area}} = 8.5086(D_{50}) + 9.1967 \quad (D_{50} \text{ in mm}) \quad \text{Eq. 4.9}$$

$$b_{\text{area}} = -0.6357(D_{50}) - 0.8279 \quad (D_{50} \text{ in mm}) \quad \text{Eq. 4.10}$$

For $D_{50} > 0.5$ mm

(inches to mm multiply by 25.4)

$$a_{\text{area}} = 0.404(D_{50}) + 13.249 \quad (D_{50} \text{ in mm}) \quad \text{Eq. 4.11}$$

$$b_{\text{area}} = -0.085(D_{50}) - 1.1029 \quad (D_{50} \text{ in mm}) \quad \text{Eq. 4.12}$$

4.3.2 Validation of Proposed Model with Laboratory Tests

The validation using laboratory data was mainly to ensure that equations developed from test data were accurately coded in the model spreadsheet. Using Equations 4.5 and 4.8, the debris zone volume (V_{debris}) and debris zone area (A_{debris}) were estimated based on the final depth of insertion obtained in the laboratory tests. These model estimated values were then compared to the actual values of debris zone quantities for the given soil types. Figure 4.16 & 4.17 present the line of 100% agreement between the actual debris zone quantities from laboratory tests (V_{lab} and A_{lab}) and the estimated debris zone quantities (V_{model} and A_{model}) from implementation of the empirical model (Boundary effects encountered in the Cherry Branch Sand full-depth tests produced immeasurable debris area properties).

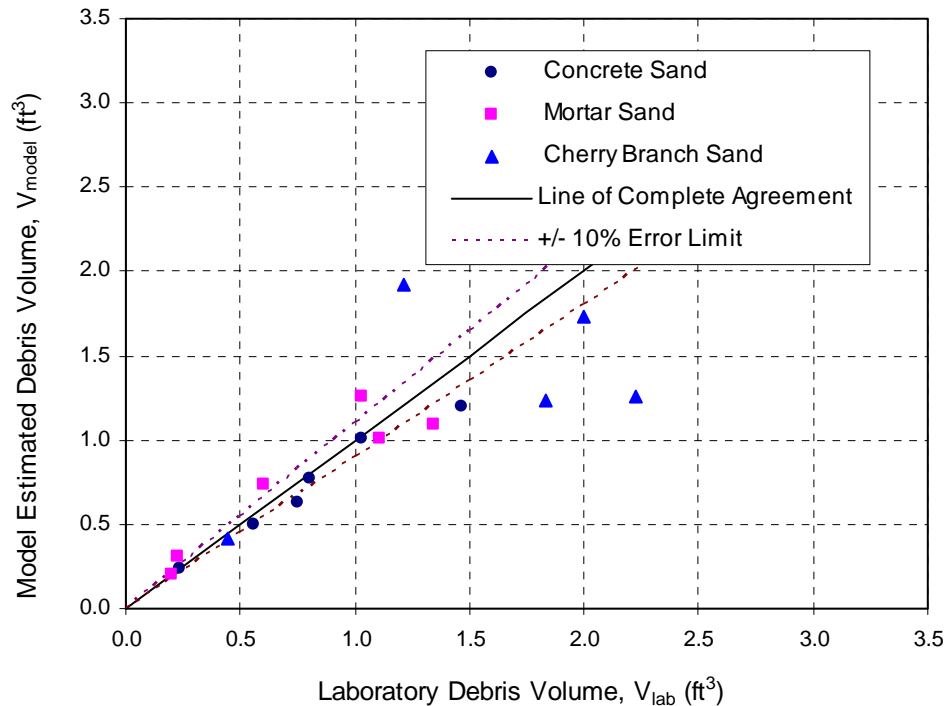


Figure 4-16 Debris Volume Validation of Proposed Model

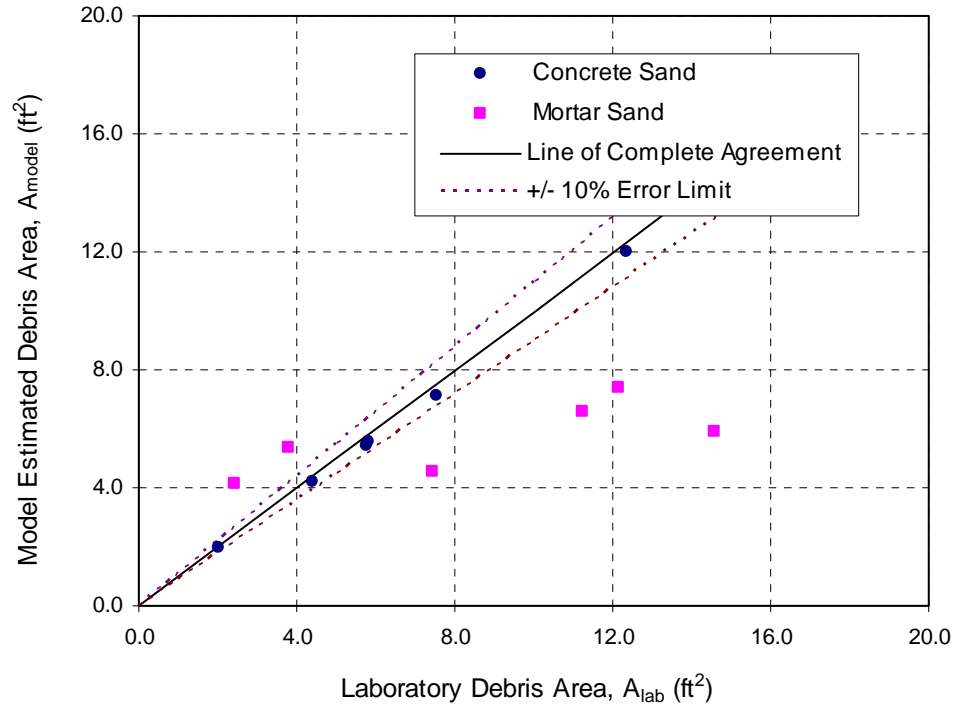


Figure 4-17 Debris Area Validation of Proposed Model

In Figures 4.16 & 4.17, the proposed model is seen to provide a reasonably good estimation of debris volume and area observed in laboratory data. Some scatter exists between the model and actual values due to the regression of test parameters based on results from several tests having various soil types and jetting parameters. Overall, the model should provide accurate estimations of debris zone for jet-driven piles within the range of q_{app}/σ'_v achieved in laboratory testing.

CHAPTER 5 - FIELD TESTING METHODOLOGY

A total of 26 full-scale jetting pile installations at four different test sites were performed to expand the data base developed during laboratory testing, obtain data for the validation/modification of the laboratory based models, and assess the impact of jetting on the surrounding environment. The test sites were selected based on the characteristics of the subsurface profile at each of the potential sites and also the ease with which the jetting research could be implemented given construction schedules and field crew availability. The field testing was conducted in coordination with NCDOT bridge maintenance Division 2 forces. It should be acknowledged that the bridge maintenance division was indispensable for fabrication and implementation of the jetting system used to conduct the field work. The four Sites selected for field testing and testing dates are as follows:

- i. White Oak River (6 installations) June 16-20, 2003
- ii. Cherry Branch Ferry Basin (9 installations) Sept. 3-10, 2003
- iii. Caeser Swamp, Sampson County (1 installation) Oct. 27, 2003
- iv. Swan Quarter Ferry Basin (10 installations) Nov. 3-6, 2003

5.1 Test Locations

The test locations of the test sites are identified in Figure 5.1. Each test location is described separately in following sections.

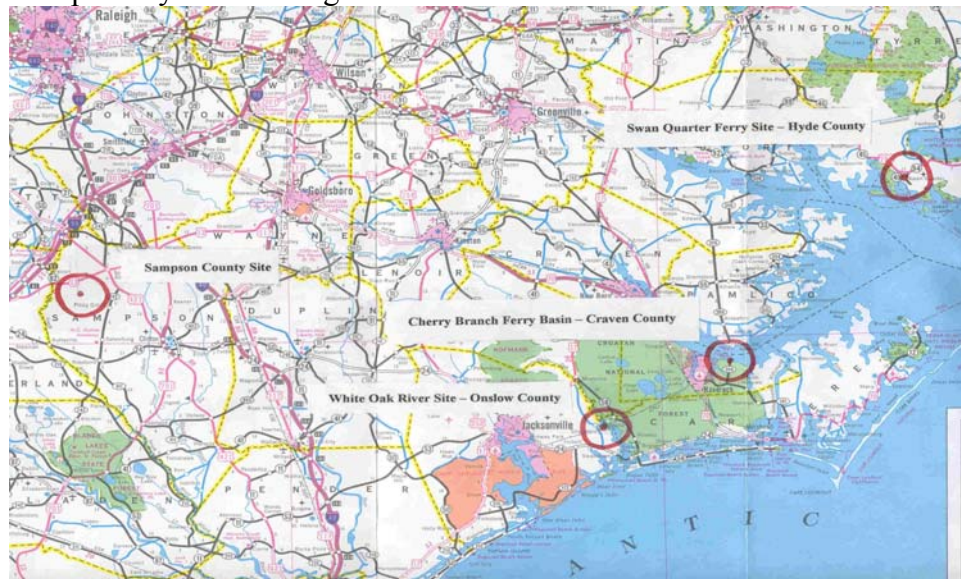


Figure 5-1 Site map detailing the field testing locations

5.1.1 White Oak River

The first testing site was in Stella, North Carolina, at the White Oak River. The White Oak River is located within the coastal plain region and is a tidally controlled river. However, the water in the area of testing was found to have no salinity content. The site had previously been the subject of NCDOT subsurface investigation (NCDOT state project 8.2160801, TIP No. B-2938) which consisted of 42 Standard Penetration Test (SPT) borings along with periodic samples taken within the borings for grain size distribution, Atterberg limits, and natural moisture content determinations. Based on results from the NCDOT subsurface investigation, the site was found to have an upper layer of very soft alluvium muck which extended to depth of 5 to 20 feet (1.5m to 6m). Standard penetration testing performed in the muck layer yielded SPT N-values ranging from weight of hammer (WOH) to 2 blows per foot (30cm). The muck layer was underlain by a layer of loose to medium dense, alluvial, silty, fine to coarse sand which was approximately 6.5 feet (2m) in thickness. SPT N-values in this layer ranged from 3 to 17 blows per foot. Below the sand layer was medium to very dense silty, fine to coarse sand of the Coastal Plain Undivided formation, which extended until boring termination at depths of 65 to 100 feet (19.5 to 30m). SPT N-values in this layer generally increased with depth and ranged from 14 to 100 blows per foot (30cm).

The general conditions at the site were wet and marshy on the land adjacent to the river. The marshy area was covered with native grasses and needle rush. The White Oak site provided areas to test which were located both in the water and on land (in marshy areas). Three pile installations were performed in the river adjacent to an existing road crossing, and three installations were performed adjacent to the existing roadway alignment in the marshy area. Figure 5.2 below shows a photograph of the river and adjacent marsh setting at the White Oak river site.



Figure 5-2 River and adjacent marsh area at White Oak River Site in Stella, NC

5.1.2 Cherry Branch Ferry Basin

The second site was located at the Cherry Branch Ferry Basin in North Carolina. The subsurface conditions at Cherry Branch Ferry Basin were previously investigated by the NCDOT in September of 1997. The site is described as being located in the Coastal Plain Physiographic Province and underlain by recent alluvial and marine deposits of Pliocene to Miocene age (NCDOT state project 6.171034, TIP No. F-2801). The investigation consisted of seven SPT borings. Four of the borings were located within the ferry basin along the western bulkhead, and three were located in the ferry basin along, what is now, the eastern bulkhead in the basin. The depth of the water in the basin ranged from 7 to 9 feet (2.1 to 2.75 m).

The profile along the western side of the basin is composed of an upper layer of very soft organic (muck and sand) deposits ranging from 5 to 21 feet (1.5 to 6.4m) in thickness. The organic content of this deposit was found to be between 19 and 55 percent with a natural water content of 172 to 187 percent. The organic soils were underlain by 2.5 to 12.5 feet (.76 to 3.8 m) of alluvial loose to medium dense fine to coarse sand. The Yorktown Formation of Pliocene age underlies the surficial sediments at an elevation of -25 to -35 feet. Soils with the Yorktown Formation generally consist of 15 to 20 feet (4.6 to 6.1 m) of medium stiff to stiff sandy clay and clayey sandy silt underlain by approximately 4 feet (1.2 m) of loose to medium dense slightly clayey fine sand. The Pungo River Formation of Miocene age underlies the Yorktown Formation at an elevation of approximately -55 feet and consist of stiff phosphatic sandy silty clay.

The profile along the eastern side of the basin consists of an upper layer of the Yorktown Formation which is composed of 7 to 8 feet (2.1 to 2.4 m) of very loose to loose fine to coarse sand underlain by 15 to 17 feet (4.6 to 5.2 m) of loose to medium dense fine sand with shell fragments. The granular sediments are underlain by 17 to 21 feet (4.6 to 6.4 m) of medium stiff to stiff silty sandy clay and clayey sandy silt. An approximately 5 foot (1.5m) thick layer of medium dense fine sand underlies the cohesive deposits. The Pungo River formation underlies the Yorktown Formation and consists of 10 feet (3m) of medium stiff to stiff phosphatic sandy silty clay underlain by a 0.5 to 1.5 feet (.15 to .5 m) thick layer of indurated limestone. The limestone is underlain by loose to dense fine to coarse sand. It should be noted that, at the time of the subsurface investigation, the borings on the eastern side were performed along an embankment which has now been removed for the construction of what is now the eastern bulkhead in the basin.

Nine test pile installations were performed at Cherry Branch, each being conducted in the basin. Figure 5.3 shows an overall view of the Cherry Branch Ferry Basin.



Figure 5-3 Cherry Branch Ferry basin, looking west to east, crane barge in foreground.

5.1.3 Sampson County Bridge Replacement site

The third site was located in Sampson County, approximately 8 miles north of Salemburg, North Carolina. The subsurface investigation of this site was reported by NCDOT in January of 2003. The site was described in the report as being located in the Coastal Plain Physiographic Province and being underlain by recent alluvial soils and Cretaceous age sediments of the Black Creek Formation (NCDOT state project 5.2852).

The upper layer of the subsurface is composed of approximately 6 feet (1.8m) of very loose to loose fine to coarse brown clayey sand fill. The fill was underlain by very loose to dense coarse sand with gravel to a depth of 16 feet (4.9m). Beneath the coarse sand was stiff to hard micaceous silty clay extending to boring termination at a depth of 64 feet (19.5m). It is noted that during the test pile installation, the pile refused at a depth of 16 feet (4.9m) on a layer that contained .75 to 1 inch (1.9 to 2.5 cm) diameter gravel particles which was at least 1 foot (.3 m) thick. Based on the difficulty of installing the test pile and the description in the NCDOT report it is assumed this layer of gravel has a SPT N-value greater than 50. Only one test pile installation was performed at this site due to space constraints and hanging power lines. Figure 5.4 shows an overall view the Sampson County research site.

5.1.4 Swan Quarter Ferry Basin

The fourth test site is located at the Swan Quarter Ferry Basin in Swan Quarter, North Carolina. The ferry basin is adjacent to the Pamlico Sound and provides transportation to Roanoke Island.



Figure 5-4 Sampson County Research Site

This site had been previously investigated by NCDOT with a report dating March of 2000. According to the report, the ferry basin is located in the tidewater portion of the Lower Coastal Plain and is underlain by mixed marine and fluvial sediments of Quaternary to Tertiary age. The water depth in the ferry basin ranges from 10 to 17 feet (3 to 5.2m) in depth (NCDOT State Project 6.081008, F-3305).

A total of four SPT borings were made to investigate the site. Based on the borings, the NCDOT report stated that the site generally had an upper layer of approximately 20 feet (6.1m) in thickness of very soft fine sandy, silty clay and clayey fine sandy silt. The upper layer was underlain by loose to dense fine sand, and fine to coarse sand with interbedded thin layers (1 to 2 feet thick) of very dense sand and very soft clayey, sandy silt to a depth of 50 to 60 feet (15.2 to 18.3m). Below the sand deposit, soils consisted of alternating beds of medium stiff to stiff silty sandy clay and medium dense clayey fine to coarse sand. At the time of jetting tests, @ 1 to 3 foot (.3 to .9 m) layer could be dredged material of fill consisting of silty sand and oyster shells was observed at some of the locations of the test piles. No SPT testing was performed on the fill, but it was assumed that the fill was relatively dense, as it took considerable effort for the research piles to penetrate this upper layer of fill.

The area where jetting of test piles occurred consisted of the basin itself along with a lower lying marshy area covered with native grasses and bushes. A total of ten test pile installations were performed, six of which were conducted in the basin and four were conducted in the lower lying marshy area adjacent to the basin. Figures 5.5 and 5.6 show a general view of the site at Swan Quarter.



Figure 5-5 Swan Quarter Ferry Basin looking from Southwest to Northeast



Figure 5-6 Marshy area adjacent to ferry basin (shown after pile installations).

5.2 Test Setup and Equipment

*Initially, it was determined that a concrete pile should be used for the field testing since it is the most frequently jetted pile in the geographical area of the research. However, it was pointed out by the Division 2 officials that continually handling concrete piles would be tedious work as lifting long concrete sections is dangerous work due to the large bending moments induced in the piles during erection. Further, removing the research piles after installation would be difficult unless lifting hooks were cast into the concrete, in which case there was still no guarantee that removal without damaging the

pile was possible. This issue was resolved by using a 40-foot (12.2m) long, 2-foot (.61m) diameter, steel pipe pile section filled with a mixture of sand and water. This allowed the steel pipe pile to simulate the weight of a concrete pile with similar dimensions, therefore inducing the same bearing stresses when erected. A steel plate was welded on the bottom end of the pipe pile. The pile was placed on a trailer which was then passed over highway scales, and by trial and error (filling the pipe pile with sand and water), until the target weight of approximately 18,800lb (8530 kg) was achieved. Using the steel pipe section was very beneficial in that, the pile could be lifted easily without fear of damaging it, and the pile could be extracted by a vibratory hammer if it became difficult to remove after jetting. This enabled the use of the same pile for all tests. Figure 5.7 is a photograph of the closed-end steel test pile.



Figure 5-7 Steel Test Pile with plate welded onto bottom end.

The jetting system frame was composed of two, 2.5 inch (6.35cm) galvanized steel pipes which extended from the bottom of the pile up 34 feet (10.4m) to where they were connected together with a combination of elbows and a union. At the connection, a tee was placed so that the water source could be introduced to the two main jet pipes via a single hose. The end of each jet pipe was threaded so that it could accept different diameter straight or angled nozzles with diameters ranging from 1.5 to 2.5 inches (3.81 to 6.35cm). Since the same pile was used for all installations, the main jet pipes were welded to the test pile. Figure 5.8 shows the nozzles (bottom end) of the main jet pipes and Figure 5.9 shows the connection of these pipes at the upper end of the pile.



Figure 5-8 Nozzle ends at the ends of the jet pipe, shown with 2 inch (5.08cm) nozzles.



Figure 5-9 Connection of the main jet pipes to water injection tee at upper end of pile.

The tee at the top of the pile was connected to the 2.5 inch (6.35cm) or 4 inch (10.16cm) diameter flexible hose supplying water from the jetting pump.

5.2.1 Equipment

The mechanical equipment needed to perform the actual pile jetting installations consisted of a crane capable of maneuvering the large pile and a water pump capable of producing the flow rates, while withstanding the back pressure, needed to install the pile. The crane used to lift and maneuver the pile during installation was an American model 5220, as shown in Figure 5.10.



Figure 5-10 American model 5220 crane used for maneuvering test piles.

During the course of the research, three different pumps were used, as it became evident that higher flow rates were needed. The first pump used was a Hale model centrifugal trash pump powered by a diesel engine capable of producing flowrates in the range of 250 to 450 gallons per minute (950 to 1500 liters per minute). The pump was equipped with a 6-inch (15.24cm) diameter suction hose and a 2.5-inch (6.35 cm) diameter discharge hose. This pump, shown in Figure 5.11, was used at the first site but not used for the remainder of the research as it became evident that a higher capacity pump was needed.



Figure 5-11 Hale model centrifugal trash pump used at first jetting site.

The second pump used was a Myer's Seth model DP150 centrifugal trash pump equipped with a 6-inch (15.24-cm) diameter suction hose and an interchangeable 2.5-inch or 4-inch (6.35-cm or 10.16-cm) diameter discharge hose. The Myer's Seth delivered flowrates of 300 to 700 gallons per minute (1135 to 2650 liters per minute) and could sustain a maximum dynamic head pressure of approximately 60 psi (414 kPa) at operating speed of 1,200 to 2,100 Rpm. The Myer's Seth model DP150, shown in Figure 5.12, was only used at the second site as still higher flow rates and head pressure were deemed necessary for full depth installation of the test piles.



Figure 5-12 Myer's Seth model DP150

The third pump used was a Cornell model 4HC equipped with a 200 horse-power diesel engine, as shown in Figure 5.13.



Figure 5-13 Cornell model 4HC high pressure pump.

The 4HC produced flow rates ranging from 1200 to 1450 gallons (4540 to 5490 liters) per minute. The 4HC is a specialized high pressure pump which is capable of sustaining dynamic head pressure in excess of 150psi (10034 kPa). The 4HC was the only pump capable of inserting the test pile its entire length and was used for the remaining two test sites.

The first two trash pumps used were outfitted with a flow meter (Figure 5.14) so that the total amount of water delivered over a given time period (flowrate) could be monitored. The maximum capacity of the water meter was 900gpm so it was not compatible with the 4HC high pressure pump. For the 4HC, the total dynamic head pressure was monitored along with the engine RPM to determine the flowrate from a pump curve provided by the manufacturer and shown in Figure 5.15 as provided by the manufacturer. As shown in Figure 5.15, for a constant engine speed, the backpressure is inversely proportional to the flowrate output of the pump.

5.2.2 Testing Procedure

Two different methods were used for installing the piles; one for installations on land and the other for installations in water.



Figure 5-14 Water meter used to monitor Hale pump and Myer's Seth pump

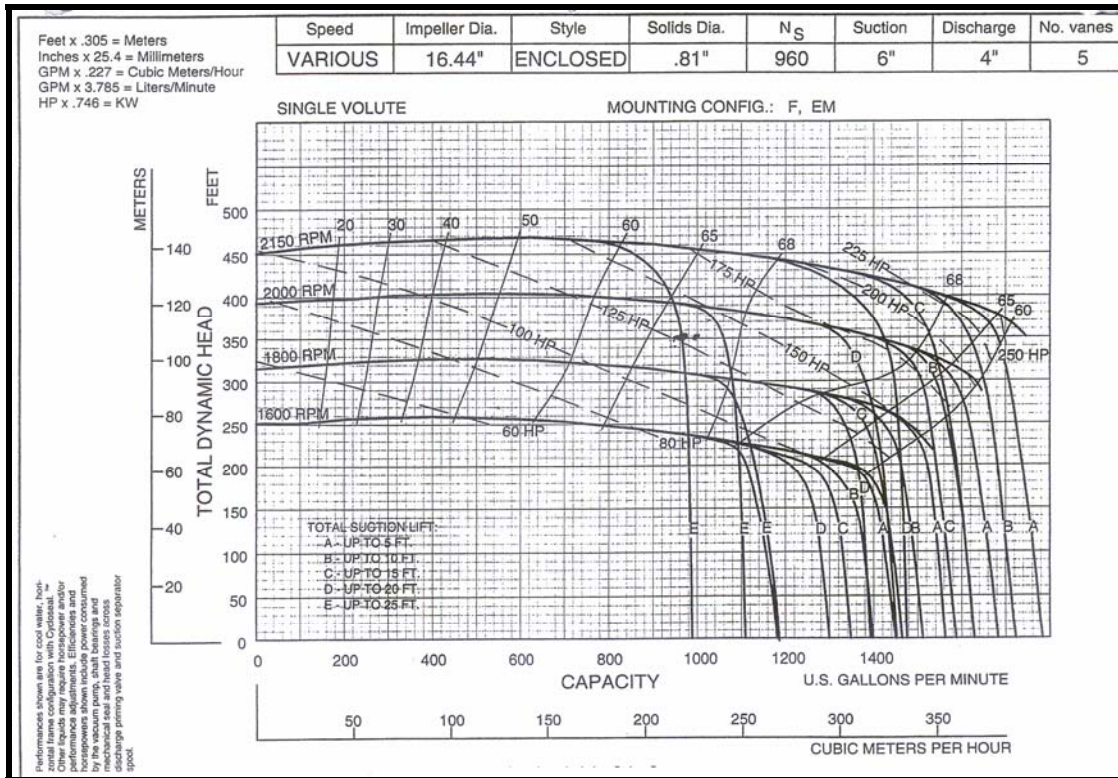


Figure 5-15 Pump curve used to back-calculate flowrate from Cornell 4HC pump (Private Correspondence, Corenll Pump Company, Portland, Oregon, 2003)

5.2.2.1 Water Installations

Testing performed in the water required a frame of steel 12x53 H-piles to be installed around the test pile insertion area in order to provide a working area for monitoring and data collection. This system of H-piles was referred to as the reference

template. The template individual members were installed using a vibratory hammer prior to the test pile installation. The template consisted of four H-piles driven in a square pattern with dimensions that measured approximately 35 feet by 35 feet (10.7m by 10.7m). The four free standing piles were connected by four beams, which were attached around the perimeter by a temporary weld. The template was then used to support a 40-foot (12.2 m) long aluminum scaffold, which was moved around by the crane, as needed, to support the researchers as they worked around the test pile.

After the assembly of the reference template, the discharge hose of the pump was attached to the main jet pipe assembly of the test pile and the pile was marked in 2 foot (.61m) increments to facilitate measuring the rate of installation. At this time, the desired nozzles were also attached to the ends of the main jet pipes. The test pile was then moved into position at the center of the template and lowered until the nozzles were almost in contact with the soil bed below the water surface. Figure 5.16 shows the pile being placed into position within the reference template.

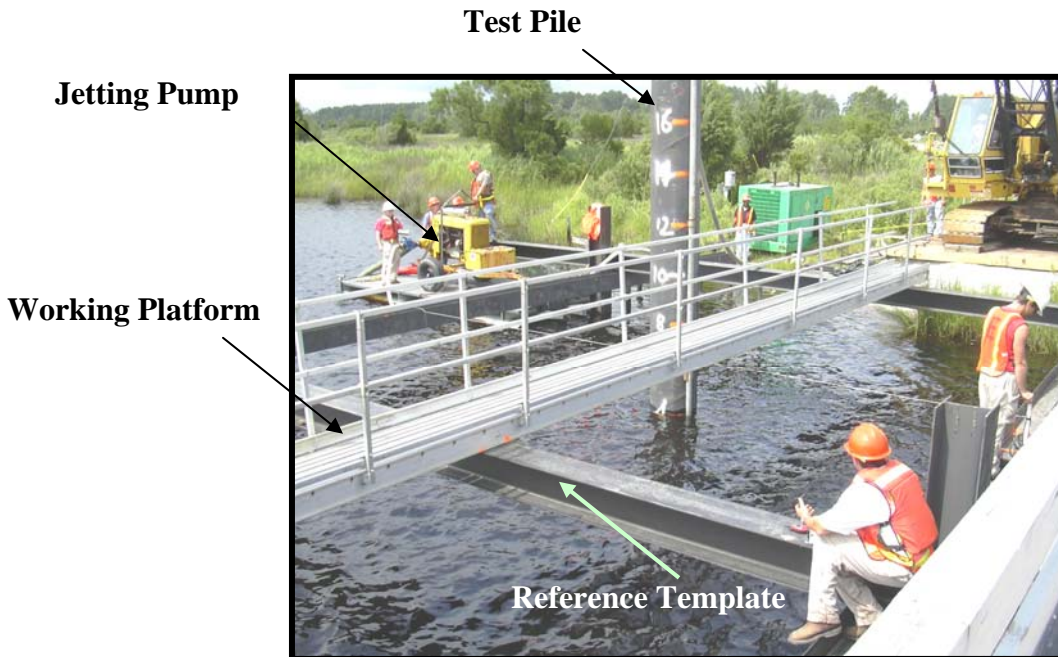


Figure 5-16 Pile placed into start position in the reference template.

Once the pile was placed into position, a careful survey was taken of the ground surface profile below the water surface. This was accomplished by utilizing the reference template as a datum, (taken as the top of the railing on the walkway platform) and the distance to the submerged ground surface was measured with a survey rod that was outfitted with a rigid rubber bottom plate. Readings were made in horizontal increments of one foot extending in the four cardinal directions from the pile (i.e. in site North, South, East, and West directions). The survey rod's rubber foot was 8-in x 10-in x 1-in (20.3-cm x 25.4-cm x 2.5-cm) in dimension. The rubber foot allowed the rod to be lowered onto a bed of soft sediment and rest there without significant penetration. The pre-jet survey was taken prior to disturbance of the soil from the test pile installation, as illustrated in Figure 5.17.



Figure 5-17 Beginning to perform pre-jet survey.

After jetting, the same technique was used to measure the distance to the soil surface from the reference template. The differences between the pre-jet and post-jet readings were used to determine the change in elevation of the submerged mud line.

After completion of the pre-jetting measurements, the jetting hose (pump discharge) was connected to the pump, and the pump was positioned at the water source. The pump was then activated and the crane operator allowed the pile to be lowered into the subsurface under its own weight, and the action of the water jets, applying just sufficient tension to the top of pile to keep it plumb. The pile was allowed to sink until it was observed that no further insertion was taking place or until a desired termination depth was reached, as will be discussed in the Chapter 7.

5.2.2.2 Land Installation

The land installations were simpler than those in water because neither the reference template nor the scaffold was needed. The procedure for determining a reference for a pre-jet survey was established by placing a series of “taught” string lines marked in 1 foot (30cm) horizontal increments to facilitate measuring from a fixed reference point. The string lines were attached to iron silt fence stakes which were driven in a cross pattern approximately 30 feet by 30 feet (9.1m by 9.1m). One such string line is shown in Figure 5.18 while post-jetting measurements were being made.

The procedure for the installation of a pile on land was similar to a water installation. After completion of the pre-jetting measurements, the jetting hose (pump discharge) was connected to the pump and the pump was positioned at the water source.



Figure 5-18 Measuring the profile after a jetting installation.

The pump was then activated and the crane operator allowed the pile to be lowered into the soil profile under its own weight and the action of the water jets, applying just sufficient tension to the top of pile to keep the pile plumb. It was also important for land installations to make sure that jets were activated prior to lowering the jets into the soil profile. The same termination criteria were used on land as for under water tests.

5.2.2.3 Angled Jets

The modification proposed as a results of the laboratory program of using angled jet nozzles to increase the insertion rate and depth was also explored during field testing. The process of configuring the jetting system with the nozzles consisted of screwing a 45 degree elbow to each jet nozzle with the desired outlet diameter. The nozzles were tightened and directed toward the center of the pile. This technique was tried in 3 successive attempts at location WO-6 (at White Oak site). In each attempt, the nozzles were not capable of withstanding the stresses applied upon them while the pile was being lowered through the soil profile. In each attempt, when the pile was extracted, the nozzles were severely crimped, damaged, or missing altogether. After three attempts, it was reasoned that, without a better design of jet nozzle and connection, using the 45 degree angled jets was not a feasible option when jetting in full scale field applications, especially since White Oak site was one of the softest profile types encountered in the field testing program.

CHAPTER 6 - DATA ACQUISITION AND TEST MONITORING

The data acquisition and field monitoring programs were adapted from techniques developed during the laboratory portion of the research. The data gathered consisted of monitoring the insertion rate of the test pile during installation, monitoring the pump performance for determination of water flowrate and pressure, determining depth of termination or refusal, surveying the ground surface profile before and after jetting for determination of the debris volume and area extent, and determining the grain size distribution of the debris material created by the jetting installation. In addition, water quality parameters associated with jetting in the water, including pH, dissolved oxygen, turbidity and salinity were monitored.

6.1 Insertion Rate Monitoring

The insertion rate of each test pile was monitored for each field installation. In general, recording the insertion procedure was performed manually and by video camera. At the beginning of the test, a stopwatch was started at the moment the jets began dispensing water and the pile was allowed to penetrate the soil. A researcher visually monitored the process of the pile being inserted and recorded the times coinciding with the one foot increments as marked on the pile. The process of recording the insertions for each increment continued until the cessation of the test. This information was used to determine the pile insertion rate for each increment of pile and also the average insertion rate of the entire pile length.

6.2 Pump Performance Monitoring

The process of monitoring the pump during pile installations was important because pump performance directly affected the installations of the test piles. During field testing at the first two sites, a flow meter was attached in-line to the discharge end of the pump. The monitoring of water discharge volume over a given time period made determining the flowrate straight forward. At the third and fourth sites, the Cornell 4HC pump, which had a significantly higher flowrate output (> 1200 gpm, 4500 lpm), was used. However, as the flow meter was not adequate for reading flowrates above 900 gallons per minute (3400 liters per minute), it was not used. Instead, the pump curve provided by the manufacturer (see Fig 5.15) was used to estimate flow rates. To use the curve, the engine speed (RPM) was monitored along with the pump backpressure, and the height of suction lift was measured. The height of the suction lift was determined by measuring the vertical distance between the surface of the water source to the bottom of the suction intake on the rear of the pump. During the duration of the all the tests, the appropriate parameters dependent upon which pump was used, were monitored continuously, so that the flowrate, velocity, and or pump back pressure could be determined for the purpose of model development.

6.3 Test Termination Criterion

The test termination criterion varied depending upon the individual test installation. In general, the test was terminated when no further advancement of the pile was possible under the action of the jetting apparatus with constant flowrate and pressure. From the laboratory experimentation, it was observed that an increased total volume of water would negatively affect (increase) the amount of debris generated from a pile installation, therefore termination was reached when the pile no longer advanced even if return water was still being generated around the annulus of the pile. In some cases the pile was advanced until the jetting hose connection near the top of the pile at 34 feet (10.4m) reached the ground surface. The pile was not advanced beyond this point to prevent damage to the jetting apparatus. By analyzing the insertion data from the various field tests, an empirical model relating insertion rate to water flowrate, backpressure, and relative density of the subsurface profile (based on SPT N-value) was developed.

6.4 Debris Zone Delineation and Volume Determination

After installation of each test pile, a survey was conducted to determine the change in elevation of the ground surface profile. The method for conducting the survey after jetting was the same as described for the pre-jet survey (Sections 5.2.2.1 and 5.2.2.2). Once the change in elevation was computed for the ground surface profile, the initial and final elevations at each point along the ground surface were tabulated in data sheets in Microsoft Excel™. With this information, the elevation change at each location along the ground surface was determined. In order to determine the volume of material deposited within the debris zone (V_{debris}), numeric integration of the average height of deposited material around the pile was conducted. Figure 6.1 illustrates a typical jetted pile installation with the shape of the debris profile as a function of distance away from the pile.

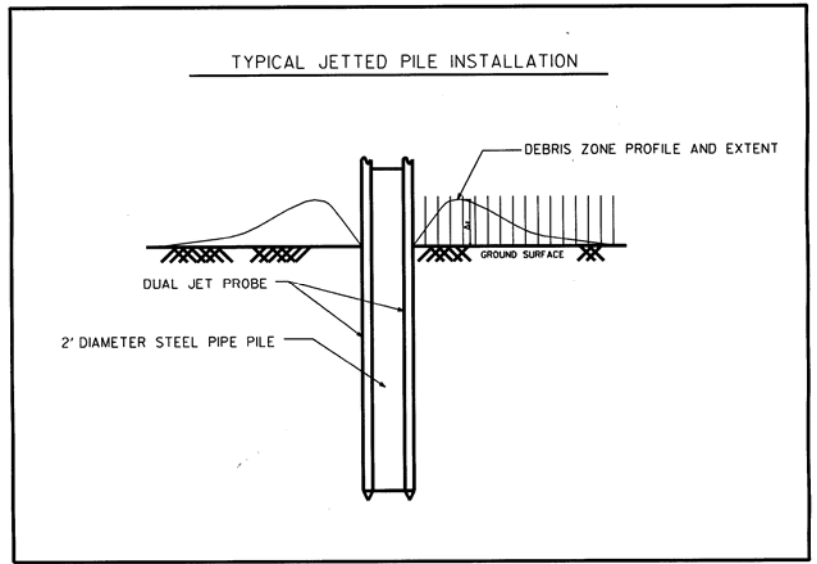


Figure 6-1 Typical jetted pile installation with debris zone profile and extent.

The volume integration was conducted in all four cardinal directions (north, south, east and west) and averaged. The general shape of the debris area was usually symmetrical which validated this approach. The area of the debris zone (A_{debris}) was calculated from the following equation assuming a shape of an elliptical area as shown in Figure 6.2:

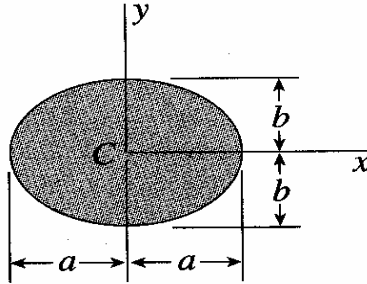


Figure 6-2 Elliptical Distribution of Debris Area (from Smith, 2003).

$$A_{debris} = \pi ab \quad \text{Eq. 6.1}$$

where: a = radial distance of debris zone extent in east and west direction
 b = radial distance of debris zone extent in north and south direction

However, it was subsequently determined that reporting the diameter of the debris zone would be more appropriate since calculation of the area introduces a square of the error produced when measuring the extent of the debris zone. The diameter of the debris zone was expressed in terms of the longest dimension extending from the center of the pile. In this case, referring to Figure 6.2, the diameter of the debris zone reported, (D_{debris}) would be:

$$D_{debris} = 2a \quad \text{Eq. 6-2}$$

where: a = radial distance of debris zone extent in direction of maximum extent.

Accordingly, the surface effects of pile jetting could be quantified and compared with results predicted from the debris zone model. To illustrate the spoil volume calculations, the surveyed profile case of CB-1, Appendix D, Figure D-2, will be used. The volume is calculated for each spoil increment in the four directions (North South, East, West) assuming concentric circles. The zero in the “Distance Column” in Table 6.1 designates the pile edge and the one foot interval thereafter designates the surveyed point. So, for example in the north direction, the spoil thickness is 0.7 ft at the pile edge and 0.5 ft one foot in the north direction. Assuming the shape of the spoil to be a circle (the radius of the circle is 2 ft but the pile inside the spoil circle has a radius of 1 ft), the volume of the spoil using the surveyed data is estimated as follows:

$$\text{Volume}_{\text{first increment, north direction}} = (0.7+0.5)/2 * ((\text{PI} * (2\text{ft})^2) - (\text{PI} * (1\text{ft-pile diam})^2)) = 5.65\text{ft}^3$$

This process is repeated for the four directions for all incremental points surveyed. Based on data in Table 6.1, the volume for north, south, east and west directions are 179, 38, 77, and 45 ft³, respectively. The average value of the four directions (in this case 85 ft³) is then reported as the spoil volume.

Table 6-1 Example Illustrating calculations of the Debris Volume, CB-1

Dist (ft)	Pre and Post Jetting Difference in Elevation				Debris Volume per One ft increment			
	North	South	East	West	North	South	East	West
0	0.7	0.5	0.3	0	xxxxxxx	xxxxxxx	xxxxxxx	xxxxxxx
1	0.5	0.5	0.2	0	5.6548668	4.712389	2.356194	0
2	0.4	0.5	0.3	0	7.0685835	7.853982	3.926991	0
3	0.5	0.2	0.6	0.1	9.8960169	7.696902	9.896017	1.099557
4	0.4	0.2	0.4	0.2	12.72345	5.654867	14.13717	4.24115
5	0.4	0.1	0.3	0.4	13.823008	5.183628	12.09513	10.36726
6	0.3	0	0.1	0.1	14.294247	2.042035	8.168141	10.21018
7	0.3	0.1	0.1	0.1	14.137167	2.356194	4.712389	4.712389
8	0.3	0	0.1	0.1	16.022123	2.670354	5.340708	5.340708
9	0.1	0	0.1	0.1	11.938052	0	5.969026	5.969026
10	0.3	0	0.1	0	13.194689	0	6.597345	3.298672
11	0.3	0	0	0	21.676989	0	3.612832	0
12	0.1	0	0	0	15.707963	0	0	0
13	0.1	0	0	0	8.4823002	0	0	0
14	0.1	0	0	0	9.1106187	0	0	0
15	0	0	0	0	4.8694686	0	0	0

6.5 Particle Size Distribution

Collected samples of the debris material extending around the pile circumference were obtained for particle size distribution determination and dispersivity testing. Particle size distribution tests were performed in accordance with ASTM D 422. Based on the laboratory testing, it was determined that a significant portion of the material being replaced by the pile must be removed for successful installation. The particle size distribution of the debris zone should be representative of the subsurface soils present at a specific jetting location. With this understanding, the particle size distribution tests were utilized primarily to confirm that the subsurface soils at a particular jetting installation site were consistent with the subsurface soils described and characterized by the NCDOT geotechnical reports and boring logs. It was imperative to confirm this information, as data from the NCDOT geotechnical reports was used to develop the insertion model.

6.6 Dispersivity Testing

Dispersivity testing was performed on samples obtained from the debris areas that exhibited cohesive characteristics during field inspection. The dispersivity testing was performed in accordance with ASTM D 4221 (double hydrometer method). According to

ASTM D 4221, dispersive clays are those which normally deflocculate when exposed to water of low-salt concentration, the opposite of aggregated clays that would remain flocculated in the same soil-water system. Generally dispersive clays are highly erosive. Decker (1977) indicated that that dispersivity determined from the method ASTM D 4221 has about 85% reliance in predicting dispersive performance (85% of dispersive clays show more than 35% dispersion).

The purpose of the dispersivity testing was to evaluate the duration that fine particles remain in suspension and the expected distribution of fines in the water column during jetting. Results of the testing, however, indicated that the dispersion of the test samples obtained from the field were below 35%, which indicates that fine-size particles were non-dispersive.

6.7 Water Quality Monitoring

Water quality monitoring was conducted at each underwater jetting site to evaluate the effects of pile jetting on the surrounding environment. A system of monitoring stations was set in increasing distances from the test pile at each installation. A typical station consisted of a stationary buoy, which was used as a marker so that the same location could be sampled for a series of water quality tests. Generally, the buoys were spaced 25 to 50 feet (7.6 to 15.2 m) apart and extended radially away from the pile in the direction of the naturally flowing tide (if present). A pre-jet water quality reading was taken at each sample station to establish a baseline for future readings prior to performing any jetting activities. During jetting, the parameters were also monitored, and afterwards readings were taken over a period of up to approximately two hours until the readings returned to the pre-jet conditions.

Five parameters were chosen to monitor water quality. These were temperature, pH, dissolved oxygen content (DO), salinity, and turbidity. The device used to measure pH, DO, salinity, and temperature was a Multi 340i hand-held set manufactured by WTW measurement systems as shown in Figure 6.3.



Figure 6-3 WTW measurement systems, Multi-340i with probes.

The Multi 340i utilizes a hand-held central processing unit with a series of interchangeable, submersible probes. Each probe is capable of measuring a different water quality parameter. To measure with the 340i, the specified probe for the parameter of interest was attached to the handheld device and the other end was submerged to the desired depth and location. The measurement was digitally displayed on the handheld unit and was manually recorded. The process was repeated until all the parameters were measured at a given site.

A separate device was required to measure turbidity. Turbidity is a measure of cloudiness due to suspended particles and is measured using the intensity of light that can pass through a sample. The darker or cloudier a sample is, the less light will pass, corresponding to a higher turbidity reading. Turbidity is expressed in standard units called Nephelometric Turbidity Units (NTU). The turbidity readings taken at each test site were measured with an Orbeco-Hellige portable model 966 unit shown in Figure 6.4.



Figure 6-4 Orbeco-Hellige Model 966 turbidimeter.

The process of measuring turbidity consisted of collecting a 50mL water sample at the location of interest and placing it into a small glass container which was then inserted into the turbidity device. The device has an internal light source which shines through the sample, and the turbidity reading is displayed on a digital display. A telescoping, 16-foot (4.88m) long bailing device was used to obtain samples at the specified location.

6.8 Summary of Data Acquisition and Test Monitoring

Each parameter measured during the field testing has been summarized along with the procedure for measuring that parameter. The results obtained from all test monitoring and data acquisition will be discussed in detail in the following chapter.

CHAPTER 7 - RESULTS OF FIELD TESTING

A total of 26 pile installations were performed in the four different soil profiles as described earlier. During the course of testing, as the relationship between the measured parameters and pile insertions became clearer, some variations in procedure were introduced to facilitate collection of data, omit unnecessary samplings, and/or increase measurements in some areas. These variations will be explained and justified. A summary of the field testing program with applied jetting parameters is presented in Table 7.1.

7.1 Refusal Depth and Insertion Characteristics

As shown in Table 7.1, six installations were performed at the White Oak testing site. The depth of insertions ranged from 20 to 25 ft. However, the upper 15 to 20 ft of the profile at the site consisted of very soft muck deposits which could be penetrated by the self weight of the test pile. With this in mind, it is evident that the pumping system employed at this site was not sufficient for installing the piles beyond 6 to 9 ft in depth. Appendix I contains data illustrating the standard penetration resistance with depth for tested sites.

A variety of nozzle sizes ranging from 2.5" down to 1.5" were used, which in turn gave a range of velocities from 650 to 1800 fpm, respectively. Nozzle velocities were calculated by dividing the pump flowrate by the total area of the jet nozzles. From observing the range of insertion depths, it becomes apparent that even with an increase in velocity, the insertion depth will not increase significantly unless sufficient flowrate is provided to carry the debris material up through the annulus surrounding the pile.

Based on the observations of pump performance and insertion depths achieved at White Oak, it was determined that a larger pump capable of delivering a higher flowrate would be needed for the future sites. At the next site, Cherry Branch, a larger pump was acquired which delivered flowrates up to 90.5 cfm (677 gallon/min). With the new pump, the test piles could be jetted to depths of up to 16 feet. Since this was still less than the available length of the pile, a larger pump was pursued for the next sites. Based on conversations with different pump manufacturers it was determined that a high pressure pump would be the most suitable for jetting where the flow rate and jetting velocity are maintained while sustaining pressures in excess of 150 psi. A new pump was secured which could tolerate the high pressures deemed necessary. It was equipped with a pressure gauge which could be monitored continuously during the installation. A pump curve provided by the manufacturer allowed the flowrates to be back-calculated based on pump pressure and engine speed.

The high pressure pump was used for the remainder of the field testing at Sampson County and Swan Quarter. At Sampson County, one installation was performed, and the depth of insertion reached 16 feet. At this depth the pile refused, and no increase in pump output would advance the pile.

Table 7-1 Summary of Field Testing Program

Location	Test ID	Type of Test Land (L) or Under Water (UW)	Flowrate (ft ³ /min)	Nozzle Velocity (ft/min)	Back Pressure (psi)	Jetted Depth (ft)
White Oak	WO-1	UW	48.7	715	NM*	6
White Oak	WO-2	UW	35.5	1446	NM	7
White Oak	WO-3	UW	44.5	653	NM	9
White Oak	WO-4	L	52.1	1194	NM	6
White Oak	WO-5	L	47.2	693	NM	6
White Oak	WO-6	L	43.0	1753	NM	6
Cherry Branch	CB-1	UW	42.0	963	NM	10
Cherry Branch	CB-2	UW	44.0	645	NM	10.5
Cherry Branch	CB-3	UW	77.0	1129	NM	16
Cherry Branch	CB-4	UW	77.4	1774	NM	16
Cherry Branch	CB-5	UW	81.3	1863	NM	14
Cherry Branch	CB-6	UW	77.7	1140	NM	14
Cherry Branch	CB-7	UW	82.2	3349	NM	10
Cherry Branch	CB-8	UW	89.4	1311	NM	12
Cherry Branch	CB-9	UW	90.5	2074	NM	10
Sampson County	SC-1	L	179.0	4102	125	16
Swan Quarter	SQ-1	UW	192.5	4412	112.5	30
Swan Quarter	SQ-2	UW	179.0	2626	100	33
Swan Quarter	SQ-3	UW	139.0	2039	98	30
Swan Quarter	SQ-4	UW	165.8	2432	100	26.5
Swan Quarter	SQ-5	UW	184.5	4228	75	34
Swan Quarter	SQ-6	UW	173.8	7081	75	25
Swan Quarter	SQ-7	L	192.5	7843	75	34
Swan Quarter	SQ-8	L	160.4	3676	75	32
Swan Quarter	SQ-9	L	165.8	3800	125	31.5
Swan Quarter	SQ-10	L	175.0	2567	78	32.5

* NM= Not Measured

The pile was withdrawn, and at the base of hole a 1- foot-thick layer of gravel was observed. A sample was retrieved for particle size distribution analysis, and it was estimated that the layer would likely exhibit an SPT N-value in excess of 50 bpf. This value was used in the model to represent a refusal point.

At Swan Quarter, a total of ten field installations were performed, with insertion depths ranging from 26.5 feet to 34 feet. At these locations refusal was not encountered, but the tests were terminated to avoid damage to the jetting frame mounted on the top of the test pile. From observing the pump characteristics during insertion, it was determined that maintaining pump pressure was important for successful installation of the pile. It was observed that when the pile reached a depth coinciding with a denser layer the pump pressure increased allowing the pile to advance further. This indicates that the effective area the jet nozzle may be reduced during the jetting process. If a sufficiently dense profile is encountered during the insertion process, it appears that the open end of the

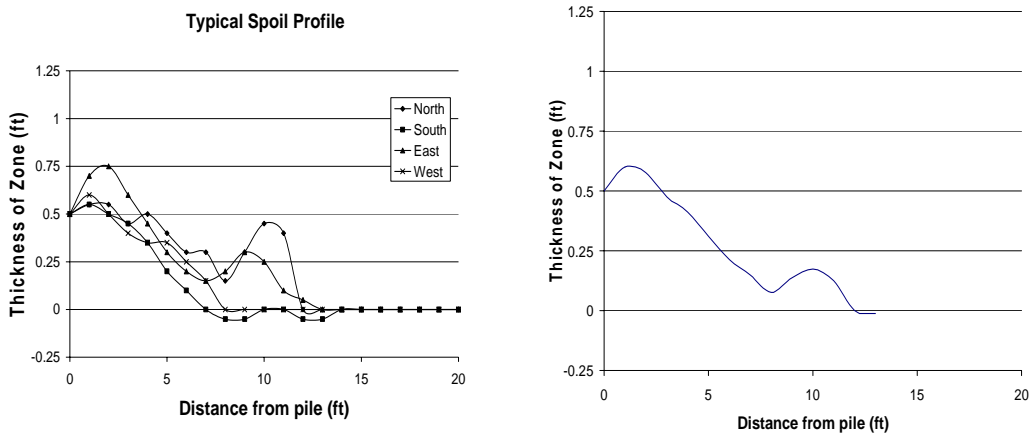
nozzles become partially blocked by the soil, thereby reducing the effective cutting area of the nozzles while increasing the cutting velocity. This action explains the need for an increased pump pressure as the pump is maintaining a constant volume through a reduced cross-sectional area. Furthermore, it explains why a pump incapable of sustaining increasing backpressures will not be sufficient for successful pile installations. It was determined that monitoring pump pressure along with flowrate is more appropriate than simply monitoring flowrate, and back-calculating velocity based upon nozzle area. If the pump is not capable of maintaining a constant volume under increased backpressure then return water (and therefore advancement of pile) is ensured up to the threshold capacity of the pump.

7.2 Debris Zone Characteristics

During the installation of each jetted pile, the debris zone created around the perimeter of the pile was surveyed using the previously described methods. From analyzing the debris zones, several characteristics were observed with respect to their shape and extent.

7.2.1 Shape and Extent of Debris Zone

Generally, the debris zone extended radially outward in all directions from the annulus around the pile, consistent with the flow of return water. It should be noted that in a few occasions the return water exited the ground surface at a location other than around the perimeter of the pile. This was most likely due to soft zones located in the vicinity of the installation that provided another return path with less resistance than the annulus around the pile. In either instance, the debris zone created by the return water was generally a “blunted” cone shape, which was thicker at the source of the return water and tapered as it extended away from the return water source. Figure 7.1 shows a typical debris zone profile measured at Swan Quarter-9 during field testing. In Figure 7.1(a), each line on the plot represents a different direction measured out from the pile. Figure 7.1(b) shows the average of the four measured profiles.



a) Typical Debris Zone Profiles

b) the average of the profiles

Figure 7-1 Typical Debris Zone Profiles (a) and the average of the profiles(b).

For the particular installation shown in Figure 7.1, the radial extent of the debris zone approaches 15 feet (4.57m), equating to a debris zone diameter of approximately 30 feet (9.14m). This is an important observation because the depth of insertion of the pile at this location was 31.5 feet (9.6m). The trend of the diameter of the debris zone approximating the jetted depth of pile was repeatedly observed in almost all of the field pile installations.

7.2.2 Volume of Debris Zone

An interesting trend observed was that the volume of the displaced soil accumulated in the debris zone usually approximated the volume of pile jetted into the ground. This is intuitive, as it would be expected that the amount of displaced soil from pile insertion should at least be equal to the total volume of inserted pile. Generally the measured debris volume was slightly more than the pile volume. An explanation for this occurrence is that the debris zone material is re-deposited at higher void ratio than the original site void ratio of the soil profile. It would follow, that a debris zone measured at a location where dense subsurface soils are present may have a higher ratio of debris zone volume to inserted pile volume than at a location of loose subsurface profile. Table 7.2 summarizes the volume and extent of debris measured at each test location. Test locations where volume and extent of debris were not determined have been omitted.

Table 7-2 Summary of Debris Zone Measurements

	Measured		
	$V_{\text{debris}}(\text{ft}^3)$	$A_{\text{debris}}(\text{ft}^2)^1$	$D_{\text{debris}}(\text{ft})$
CB-1	84.71	412.33	22.91
CB-2	30.15	238.76	17.44
CB-3	69.12	314.16	20.00
CB-4	74.14	313.37	19.97
CB-5	53.72	469.70	24.45
CB-6	28.50	146.90	13.68
CB-7	49.09	306.31	19.75
CB-8	51.60	358.14	21.35
CB-9	51.25	296.88	19.44
SQ-7	176.16	530.14	25.98
SQ-8	146.40	530.14	25.98
SQ-9	107.60	449.25	23.92
SQ-10	131.55	449.25	23.92
WO-1	109.01	320.44	20.20
WO-2	104.73	392.70	22.36
WO-3	57.92	343.22	20.90
WO-4	69.43	251.32	17.89

CB = Cherry Branch
 SQ = Swan Quarter
 WO = White Oak

¹ A_{debris} is calculated using equation 6.1

7.2.3 Particle Size Distribution of Debris Zone

Representative samples were taken from each of the debris zone locations where sampling was possible. The bulk samples were obtained using a shovel from the debris pile with care exercised to sample the whole depth. Each sample was approximately 1 lb and sample location was adjacent to the jetted pile. These samples were tested for particle size analysis in accordance with ASTM D 422. The particle size distributions were compared with particle size distributions provided by NCDOT subsurface reports for borings in the same area. Figures 7.2 through 7.5 illustrate the comparison between the NCDOT – obtained grain size distributions and distributions generated from the debris zone samples.

The grain size distributions provided in NCDOT reports are similar to the distributions generated from the samples collected from the respective debris zones, with only a slight increase in the mean particle size for the collected samples. This implies that the entire range of particle sizes within the soil profile was removed during installation of the pile. This confirms the observations made through the laboratory testing phase of the research. The disparity between the mean particle sizes is accounted for in that the finer silt and clay size particles have been washed outside of the measurable debris zone within the return water.

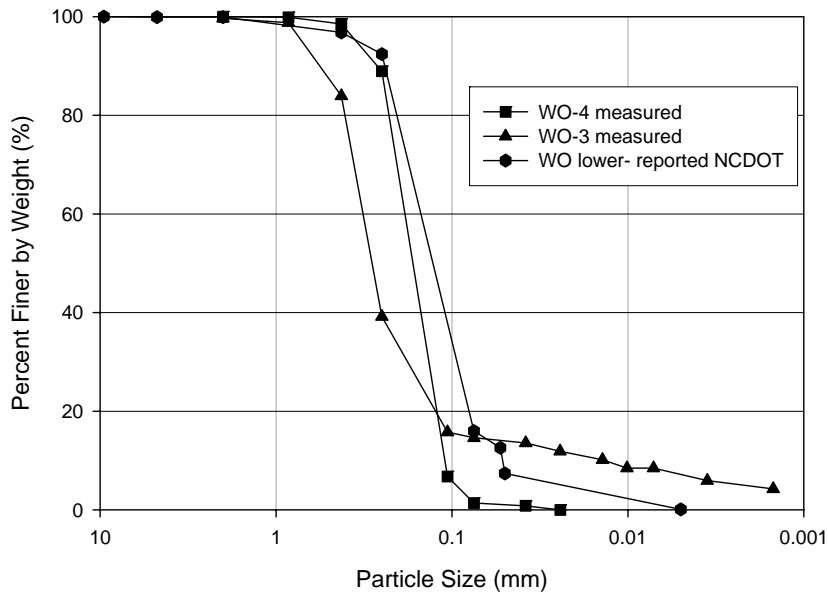


Figure 7-2 White Oak River measured and NCDOT reported GSD

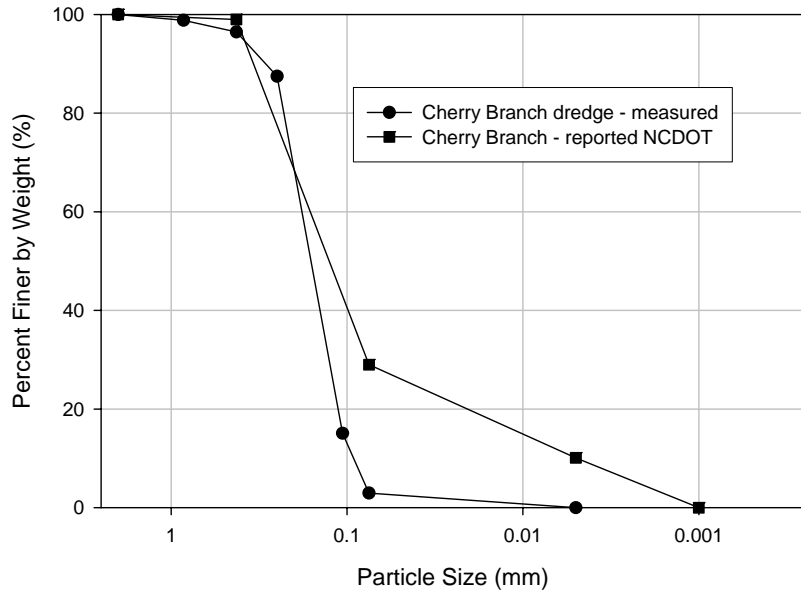


Figure 7-3 Cherry Branch Ferry basin measured and NCDOT reported GSD

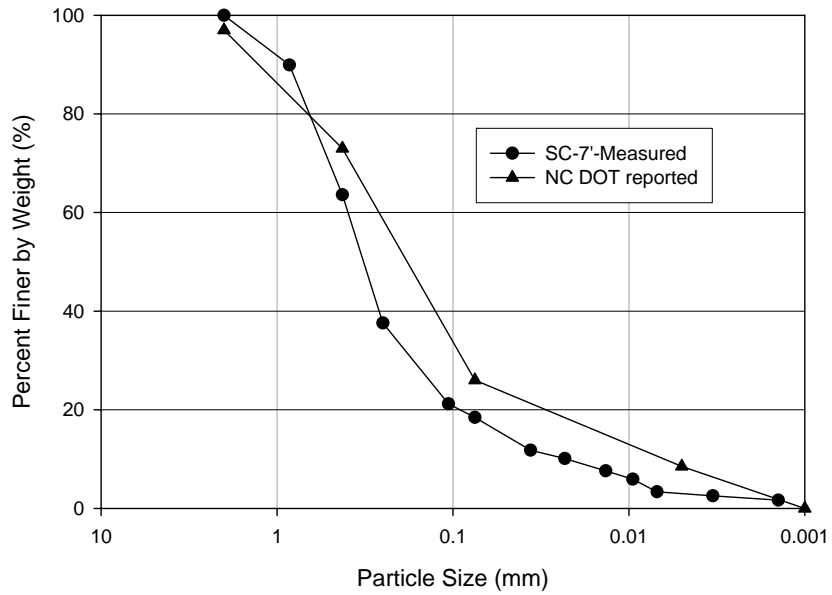


Figure 7-4 Sampson County measured and NCDOT reported GSD

measure the water quality characteristics in the immediate vicinity of the pile (within 10 feet, (3m)) in order to capture the effects of jetting on the environment surrounding the installation area. Figures 7.10 through 7.12 present readings taken in a subsequent test, WO-3.

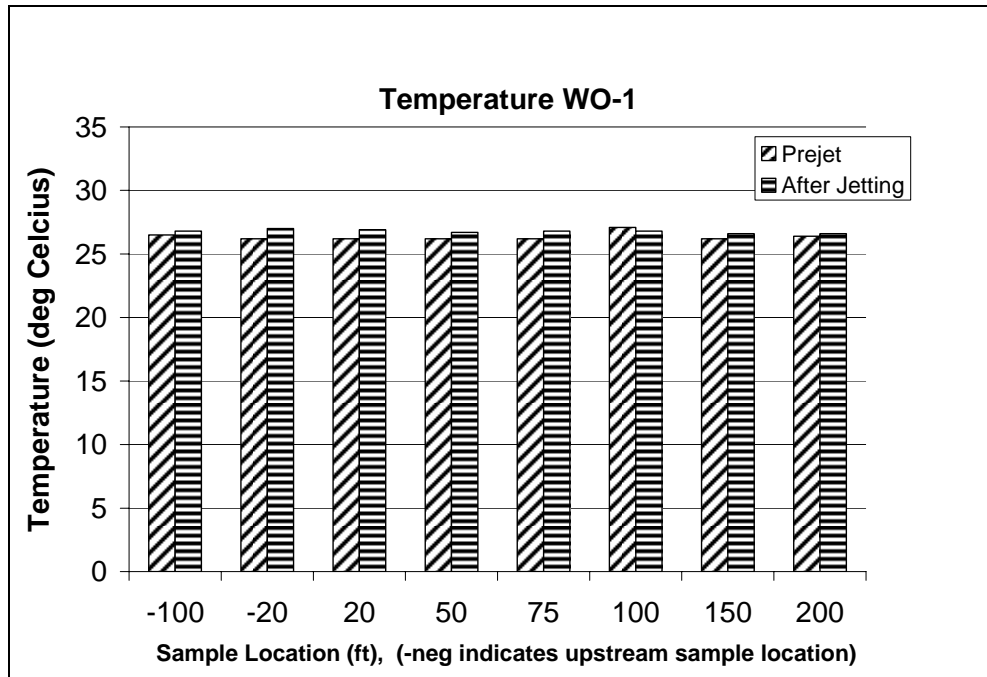


Figure 7-6 Temperature Readings at WO-1.

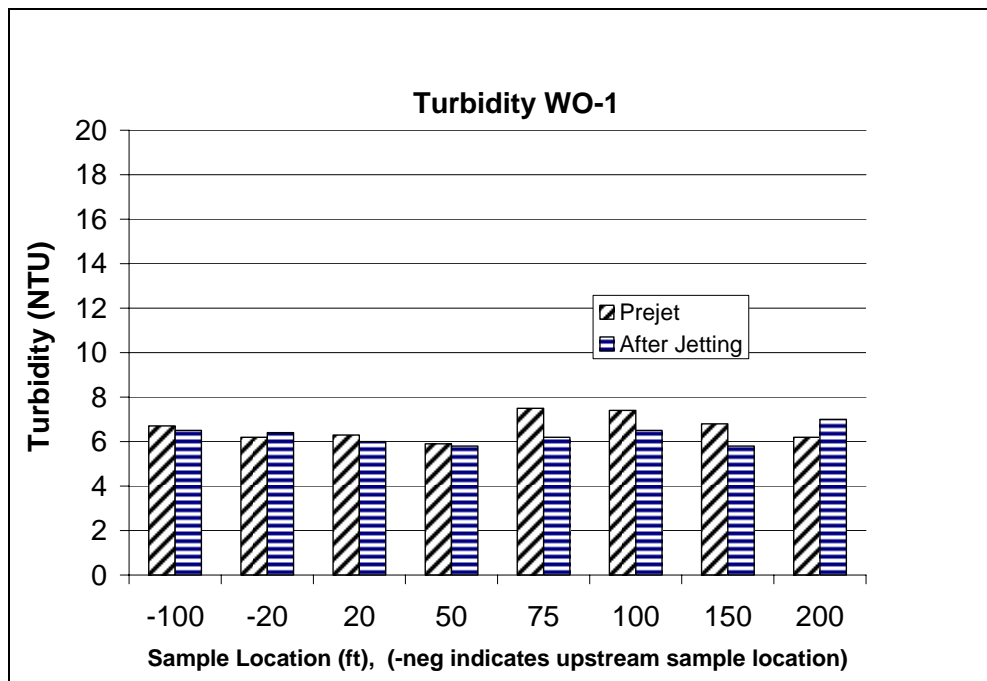


Figure 7-7 Turbidity Readings at WO-1

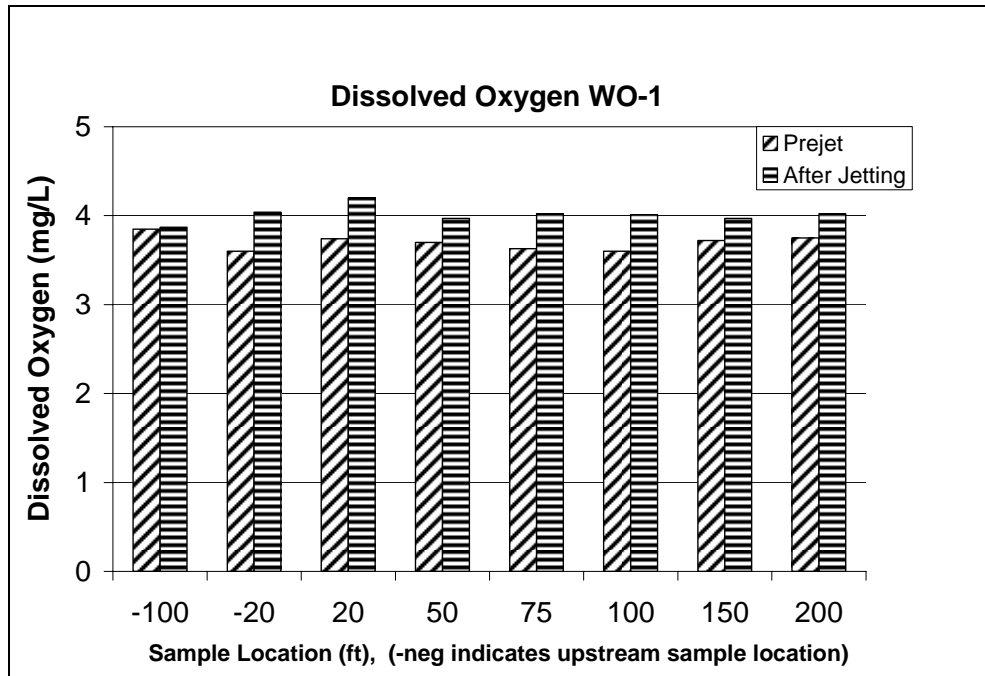


Figure 7-8 Dissolved Oxygen Readings at WO-1.

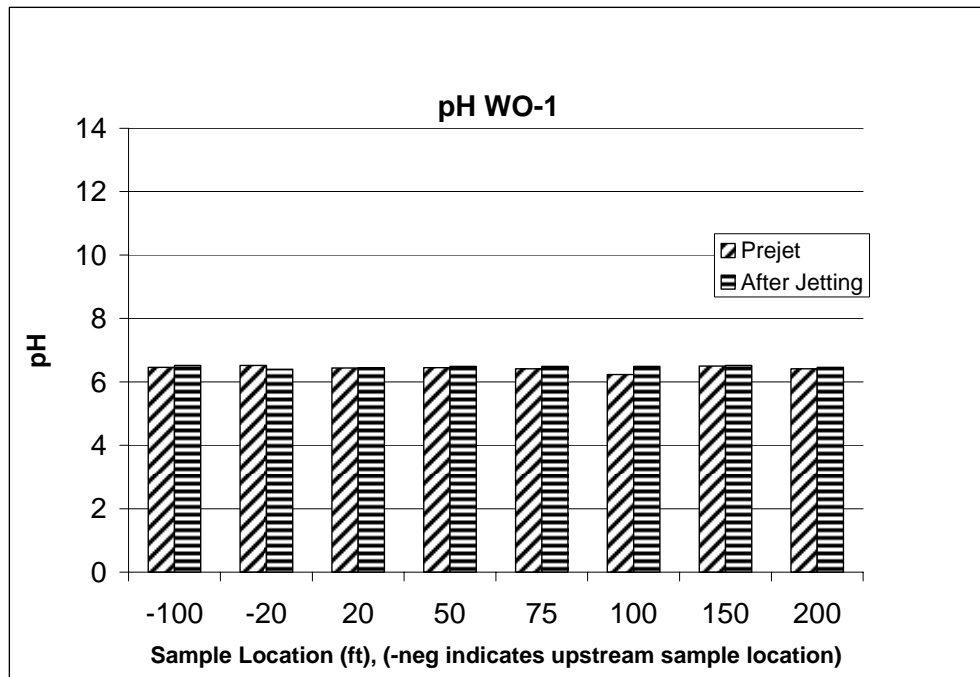


Figure 7-9 pH Readings at WO-1.

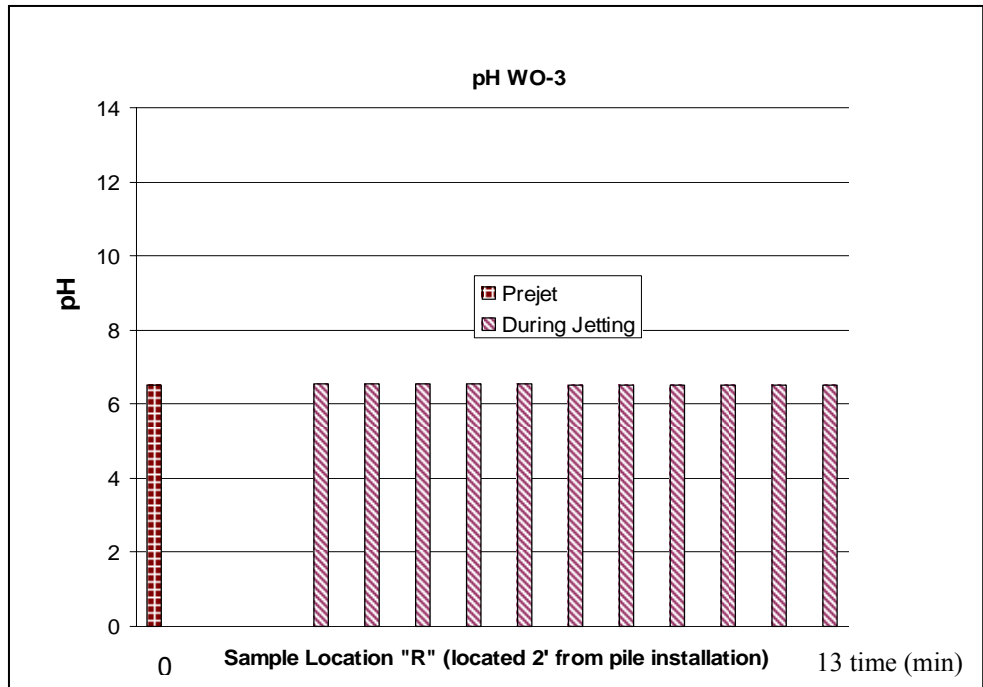


Figure 7-10 pH readings at WO-3.

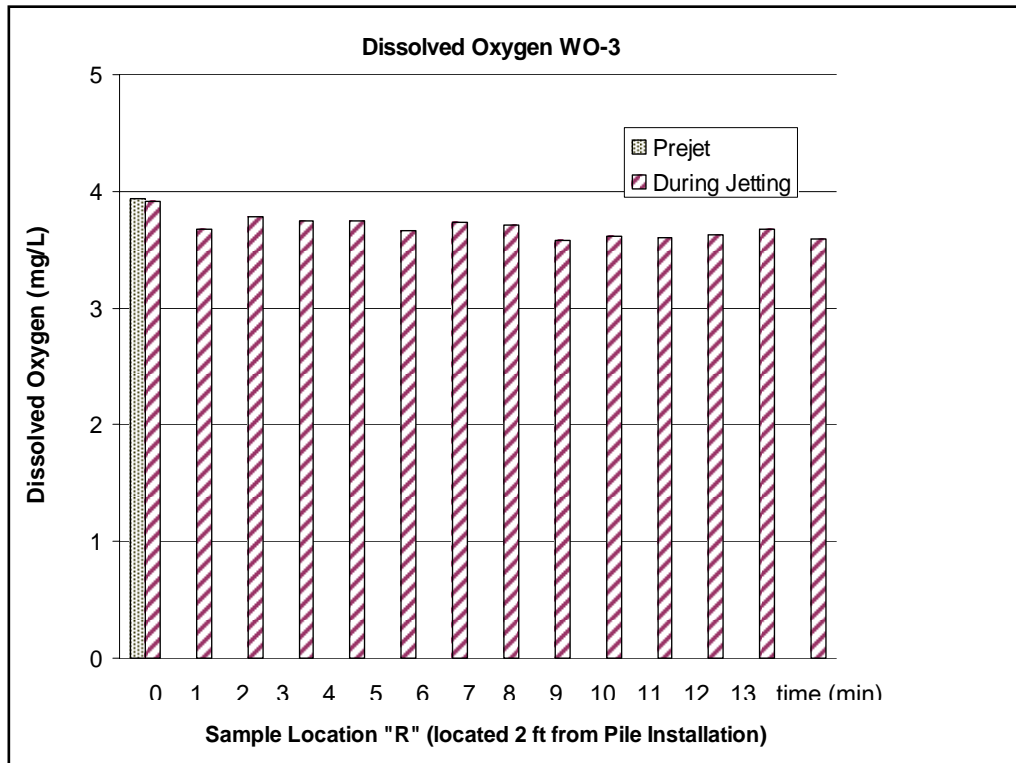


Figure 7-11 Dissolved Oxygen (DO) Content readings (1 Minute interval) at WO-3.

Similar to the readings taken at WO-1, Figure 7.10 shows the negligible effect that jetting had on the pH of the water column around the test pile at WO-3. Figure 7.11 shows the dissolved oxygen content (DO) measured within 2 feet (2.44m) of the pile installation at test location WO-3. Data also show that during testing, an insignificant decrease in dissolved oxygen content occurred. The DO readings at WO-3 were taken at 1 minute intervals beginning immediately at the start of the pile installation and continued for 13 minutes. It is difficult to discern the reason for the different DO measurement but it could be due to the differences in flow velocity around the pile during jetting.

Figure 7.12 illustrates the turbidity readings taken at WO-3. The readings were all taken within the first five minutes of jetting, thereby representing “worst” case values. The initial pre-jet value of 6.4 NTU increased to a maximum value of 21.8 NTU at a distance of 2 feet (.61m). The outer 8 foot readings were considerably lower, indicating that turbidity decreased as a function of distance from the pile installation location. This is may be expected since more particles fall out of suspension as the distance from the discharge annulus increases and velocity of the particles decrease.

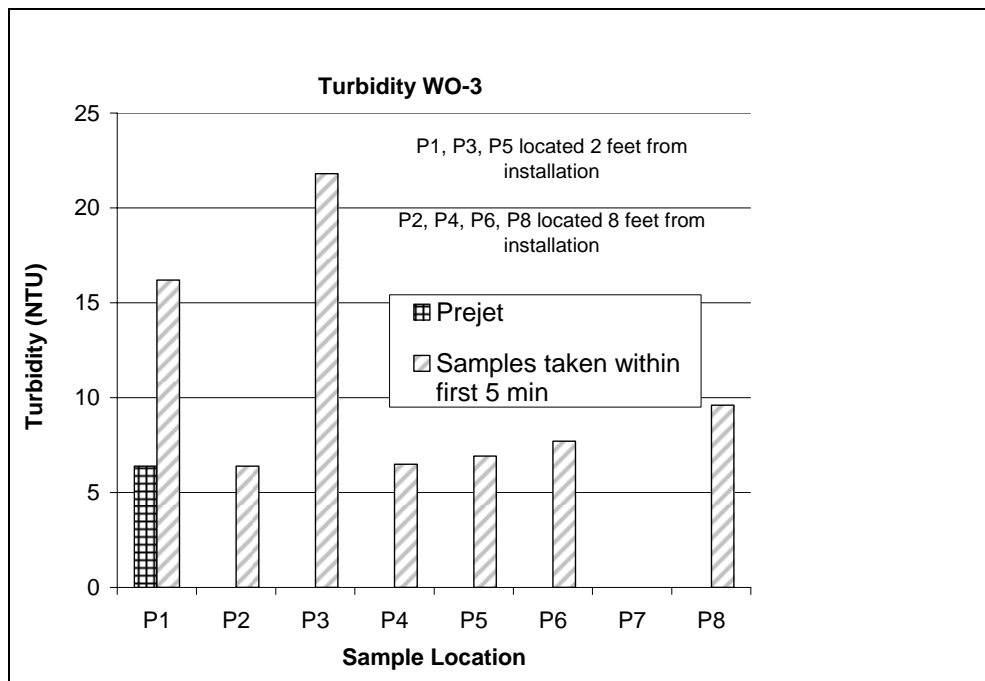


Figure 7-12 Turbidity readings at WO-3 installation site.

7.3.1.1 Summary of Monitored Water Quality Parameters at White Oak River

Analysis of the water quality data from the three underwater installations at White Oak River produced the following observations. A comparison of pre-jet and post-jet data show that temperature and pH were not significantly changed pre-jet and post-jet.

Salinity was not detected at the White Oak site, so no measurements overtime were made. Dissolved oxygen content was observed to slightly increase at some installations and to slightly decrease at others. These fluctuations were on the order of ± 1 mg/L (ppm). Turbidity readings indicated that an increase occurred in the immediate vicinity of the pile installation and that turbidity decreased as the distance from the installation location increases. Data indicated that for the jetting parameters employed and for existing field conditions at the White Oak site, increased turbidity increase was not detectable beyond 20 feet (6.1m) from the pile.

7.3.2 Cherry Branch Ferry Basin

At the Cherry Branch Ferry Basin, nine tests were conducted underwater, which afforded the opportunity to collect more water quality data. Similar to White Oak River, the pre-jet and post-jet pH and temperature readings were nor significantly different. Figure 7.13 shows the change in temperature with location while Figure 7.14 shows the change in pH.

The pre and post-jet salinity readings were consistently at 9 ppm with a fluctuation of ± 0.5 ppm. The dissolved oxygen readings were consistent with the behavior observed at White Oak River (pre- and post-jet readings at 4.5 mg/L with variations of ± 1.5 mg/L) with the exception of some spikes (+2mg/L) in DO around areas where prop-wash from boating activity in the ferry basin disturbed the water. Turbidity was the most influenced parameter at Cherry Branch. Readings were taken in two opposing directions from each pile installation due to the swaying motion of the current in the ferry basin.

The turbidity levels at Cherry Branch was measurable at a farther distance from the pile than at White Oak River. This may be explained by the fact the jetting flowrates and velocites used at Cherry Branch were greater in magnitude than those used at the White Oak river site. From review of particle transport literature it follows that a greater flowrate and velocity should in fact produce a greater distance of particle transport. Figure 7.15 illustrates turbidity readings from a typical pile installation at Cherry Branch. All data are included in Appendix F.

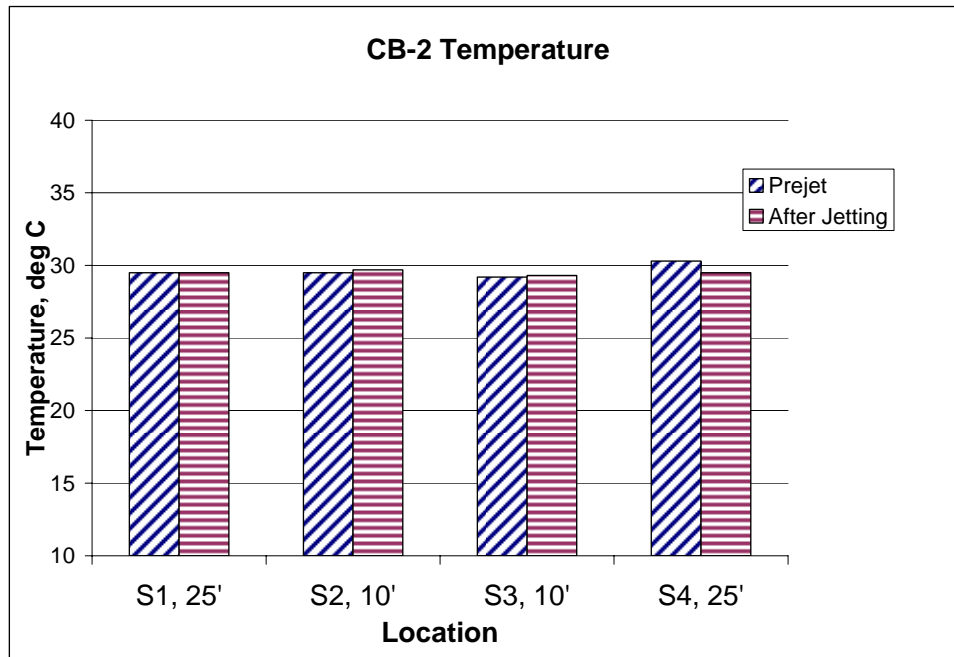


Figure 7-13 Temperature Readings at CB-2.

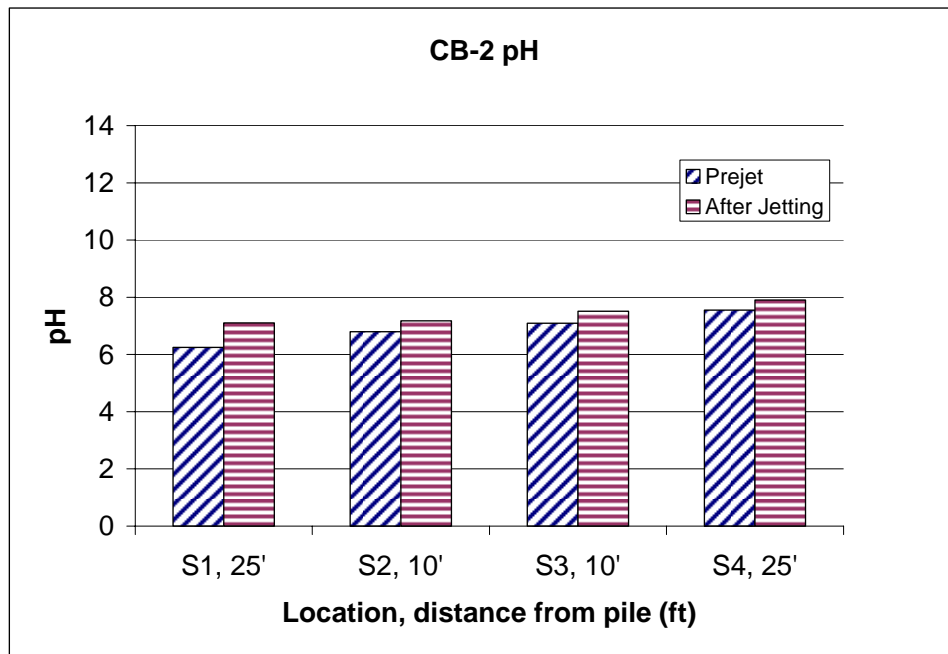


Figure 7-14 pH Readings taken at CB-2.

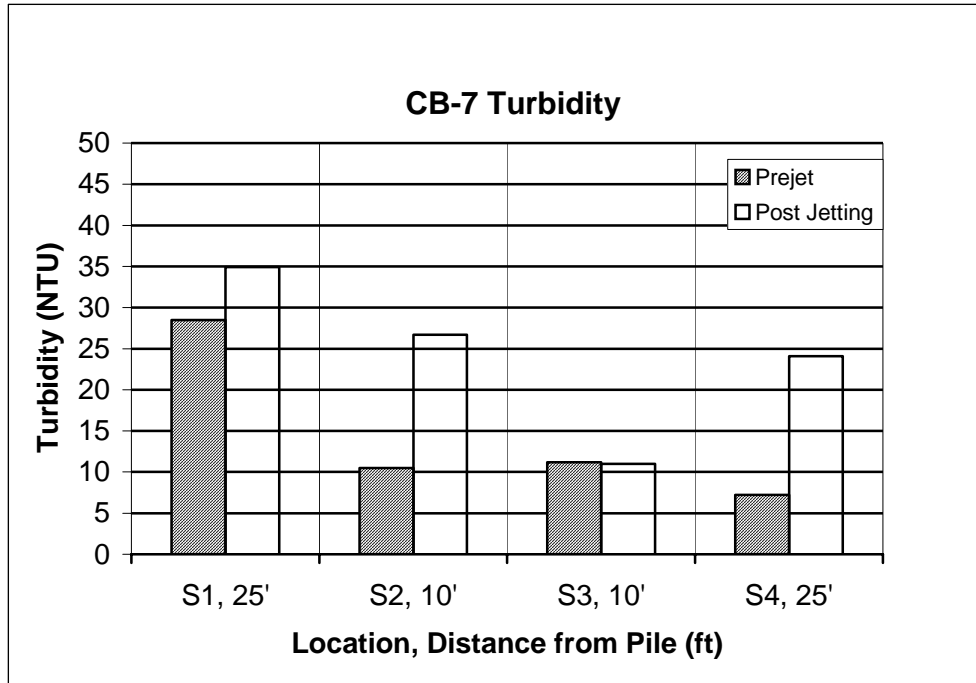


Figure 7-15 Turbidity Readings at CB-7.

7.3.2.1 Summary of Monitored Water Quality Characteristics at Cherry Branch

From the installations performed at Cherry Branch, it was determined that pile jetting had negligible short term effects on the temperature, salinity, and pH. Dissolved oxygen content changed by ± 1 mg/L. The turbidity of the surrounding water was affected within a 25 foot (7.62m) diameter area. Comparing results from the White Oak River site and Cherry Branch, it is confirmed that increased jetting flowrates and velocities increases the area impacted by turbidity.

7.3.3 Swan Quarter Ferry Basin

The underwater jetting sites at Swan Quarter differed from the previous sites in that the jetting area was surrounded and contained by a turbidity curtain, as mandated by the Division of Water Quality (DWQ). The purpose of the water quality testing at this site was twofold. First, to evaluate if the turbidity curtain was successful in containing the debris created from the jetting activities. Secondly, to determine the amount of time required for the area inside the curtain to return to the baseline conditions based on readings taken prior to the jetting activities.

Figure 7.16 shows the turbidity readings taken at SQ-3 as a function of location and time. The readings taken at location “C” were inside of the turbidity curtain at a distance of 10 feet (3m) from the pile installation.

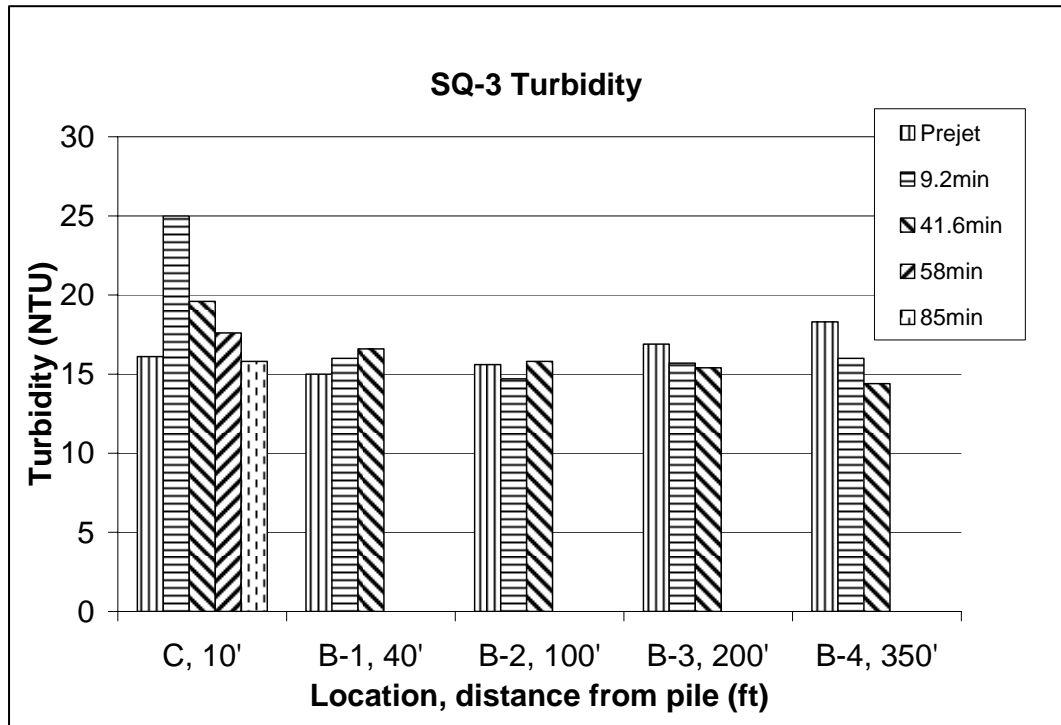


Figure 7-16 Turbidity Readings taken at SQ-3.

The other “B” locations were outside of the turbidity curtailed zone. From observation of the reported data, it is evident that the turbidity curtain had the positive effect of containing the turbid water created by the pile installation. It is on the other hand important to note that the test site was within the ferry basin with no perceivable levels of current velocities. The post-jet turbidity levels inside the turbidity curtain returned to the background levels after approximately 85 minutes (time elapsed after cessation of jetting). Figure 7.17 is an example of typical DO data taken from the Swan Quarter site. Notice that the post-jet levels are slightly increased from the pre-jet DO levels (similar behavior to the previous two sites). Monitored turbidity levels varied at the different test sites mostly due to differences in the mean grain size of the upper layers of soil. Figures 7.18 and 7.19 illustrate the maximum and average turbidity values, respectively. Measured maximum values were approximately 70 NTU. This value was measured after 15 min during the jetting process.

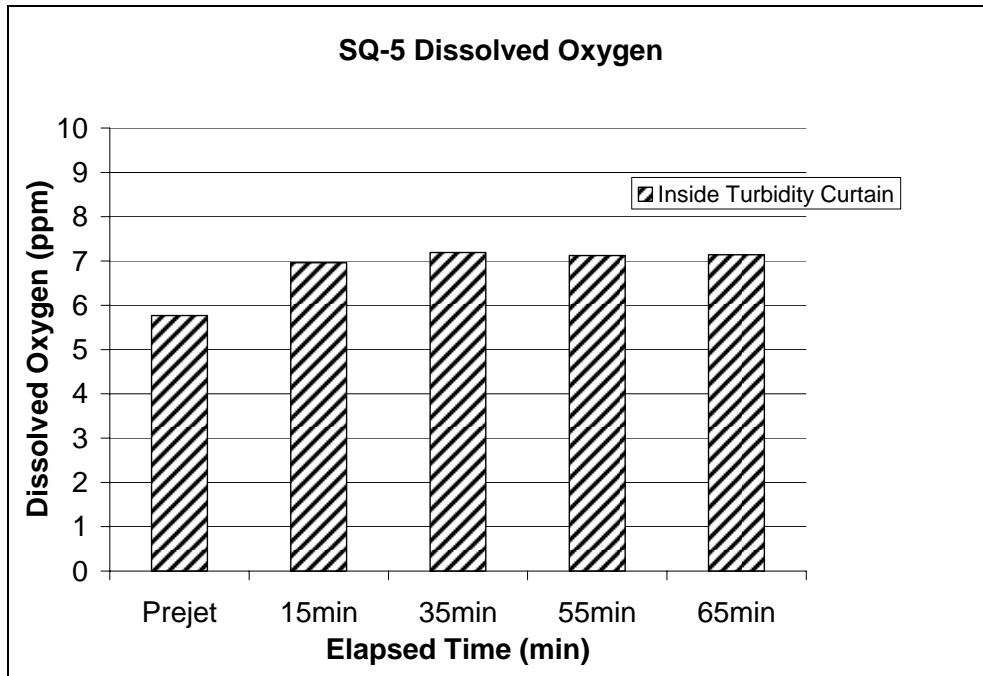


Figure 7-17 DO readings taken at SQ-5.

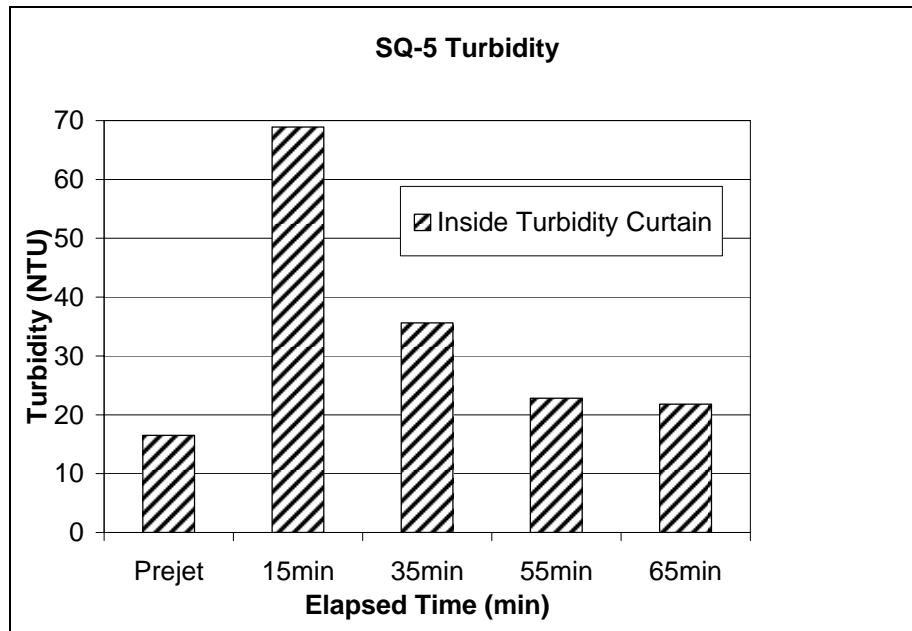


Figure 7-18 Turbidity reading at SQ-5 (maximum).

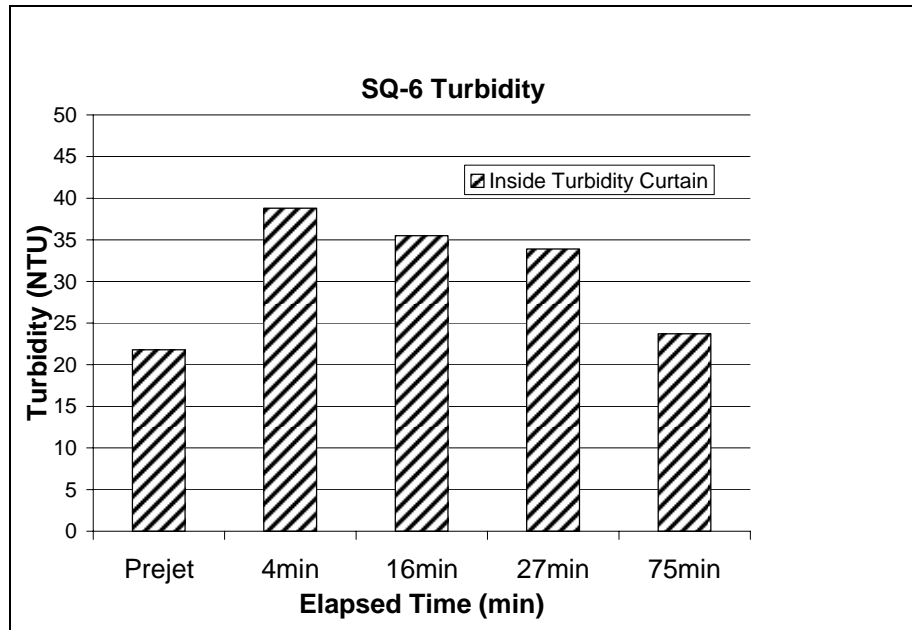


Figure 7-19 Turbidity reading at SQ-6 (average).

7.3.3.1 Summary of Monitored Water Quality Characteristics at Swan Quarter

Based on the monitored water quality parameters at Swan Quarter, it was determined that the dissolved oxygen content was shown to have a short term increase after the installation of jetted piles and temperature levels were not affected by jetting. The turbidity curtain proved to be an effective barrier for containing debris created from the process of pile jetting. However, such observation is limited to the tidal conditions observed in the ferry basin. One advantage of using the turbidity curtain in the ferry basin was that the absence of tidal made it easy to keep the curtain anchored in place.

From observation of the turbidity data, levels caused by jetting ranged from 20 to 70 NTU and took approximately 65 to 85 minutes to return to the baseline levels after cessation of the jetting procedure. These values are the highest recorded from any of the research sites due to a combination of finer grained soils and higher jetting velocities and flowrates employed. In addition, keeping the particles trapped inside the turbidity curtain had the effect of concentrating the fines and thus increasing the turbidity readings.

CHAPTER 8 - MODEL DEVELOPMENT AND VERIFICATION

The purpose of this chapter is to present a jetted pile insertion-rate model based on measured field data and to verify the relationships (based on work reported in literature) describing the debris volume transported to the ground surface and its lateral extent. Further, a model is proposed which accounts for the change in the shape of debris area under varying tidal/current conditions.

8.1 Insertion Model

As previously discussed in Chapter 7, higher pump pressure was needed for successful full depth pile installation. Since increased pressure was proven to be a major factor contributing to pile advancement, it was desired to incorporate this pump parameter into the proposed model. Further, as discussed in chapter 7, it was hypothesized that pump back pressure changed as a function of soil density which is also related to the hydraulic conductivity of the subsurface profile. This is explained in that, a stiffer profile will provide more resistance to the outflow of water from the jet pipes and will erode more slowly, thereby increasing pump pressure. For this reason, it follows that for an insertion parameter pump pressure should be used in lieu of velocity, since flow rate and therefore velocity, are not constant. In addition, while pump pressure is read from a gage, velocity cannot be readily calculated during a particular jetting installation if adjustment in the field is needed. In order to simplify model development, factors impacting insertion rate are lumped into a single term in which pile geometries and jetting parameters are normalized. The following insertion parameter (IP) is proposed based on the functional relationship between insertion rate and pump pressure, flow rate and pile geometry, as was observed from laboratory and field testing:

$$\frac{I_v / Q_w}{P_b / P_a} (L/D) = \text{Insertion Parameter, (min)} \quad \text{Eq. 8.1}$$

where:

- I_v = jetted volume of pile (L^3)
- Q_w = pump flowrate ($L^3/T(\text{minutes})$)
- P_b = pump back pressure (F/L^2)
- P_a = atmospheric pressure (F/L^2)
- L = jetted length of pile (L)
- D = diameter of pile (L)

Conceptually, it should be possible to develop a relationship between the IP and time required for pile insertion for various soil types as depicted in Figure 8.1.

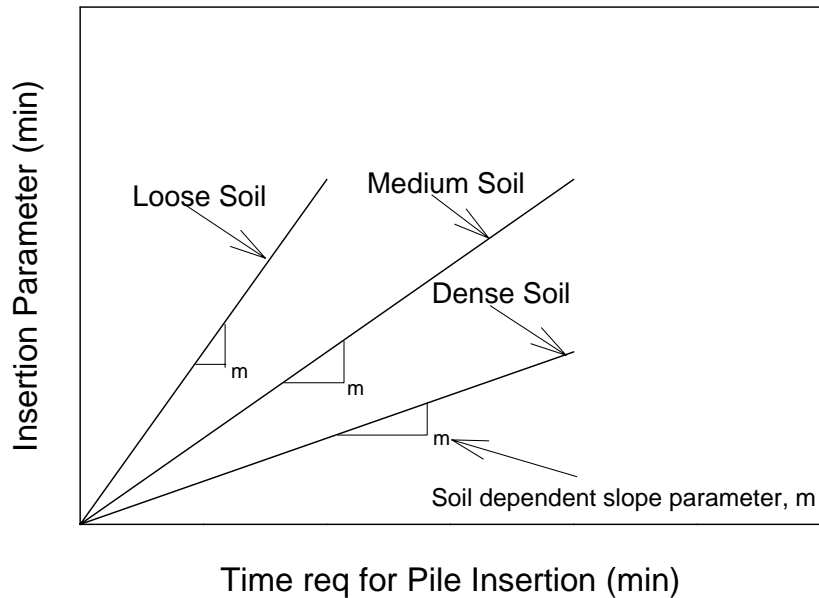


Figure 8-1 Relationship between Insertion Parameter and Time for Insertion for Different soil densities.

Inspecting the trends presented in Figure 8.1, the following observations are advanced:

- i. An increase in I_v results in an increased insertion time.
- ii. An increase in Q_w results in a reduced insertion time.
- iii. An increase in the L/D ratio results in an increased insertion time.
- iv. An increase in P_b results in a reduced insertion time.
- v. A denser material produces an increased insertion time for an equal insertion parameter in comparison to that required for a less dense material.

The following equation is proposed to describe the time required to insert a given pile:

$$\frac{\text{Insertion Parameter, IP}}{\text{slope parameter, } m} = \text{time (t) required to install pile, (min)} \quad \text{Eq.8.2}$$

where, m = Slope parameter dependent on soil characteristics

In order to prove the validity of the proposed relationships, the data collected from the field research at the Sampson County and the Swan Quarter sites were plotted in terms of insertion parameter versus time as shown in Figure 8.2. Data for White Oak

River and Cherry Branch were omitted from the insertion modeling data set as pump pressure (P_b) was not measured at these two sites.

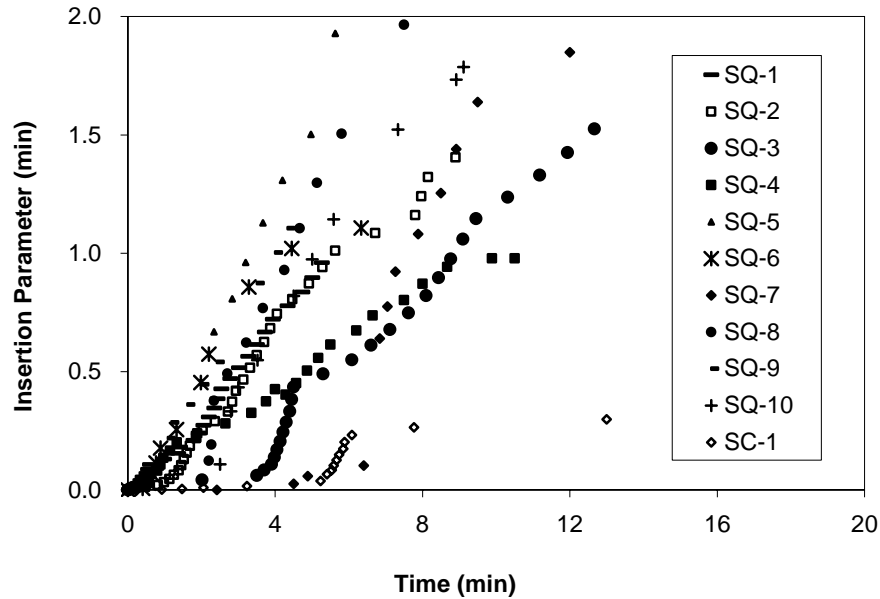


Figure 8-2 Insertion Parameter Characteristics for SC and SQ sites.

Each symbol in Figure 8.2 represents a different jetting test. Notice that each plot has a unique slope, m , which was expected since each test was conducted at a different location with soil characteristics differing from one location to another. Each plot can also be isolated into separate segments representing different layers in a non-homogeneous soil profile.

Six test locations were selected at which a high degree of certainty in the subsurface profile existed. These data were used to model the relationship between soil characteristics and the slope parameter, m , introduced in Equation 8.2. The data from each test selected were plotted, and isolated into different segments based on the average Standard Penetration Test (SPT) N -value corresponding to each segment. N -values were determined from NCDOT subsurface investigation reports provided to the research group. SPT N -value was selected as the criterion which to represent different soil characteristics as it is an index measure of soil composition and relative density. The N -value used for the insertion modeling will be referred to as N_{cr} signifying that it has been corrected for hammer efficiency, borehole diameter, and sampling method. This N_{cr} value is not the N_{60} value which also considers a rod-length correction given that such a lower corrected N -value could lead to unconservative insertion time productions. An overburden stress correction need not be applied because it is already accounted for in the L/D ratio in the insertion parameter term. The following equation is recommended to compute N_{cr} from the standard field N -value (adapted from Coduto, 2001).

$$N_{cr} = \frac{E_m C_B C_S N}{0.6} \quad \text{Eq. 8.3}$$

where: N = standard field uncorrected N-value, and
 Em, CB, and Cs are given in Tables 8.1 and 8.2.(from Coduto, 2001)

Table 8-1 SPT Hammer Efficiency Corrections (adapted from Clayton, 1990; from Coduto, 2001).

Country	Hammer Type	Hammer Release Mechanism	Hammer Efficiency, E_m
Argentina	Donut	Cathead	.45
Brazil	Pin Weight	Hand Dropped	.72
China	Automatic	Trip	.60
China	Donut	Hand Dropped	.55
China	Donut	Cathead	.5
Colombia	Donut	Cathead	.5
Japan	Donut	Tombi Trigger	.78-.85
Japan	Donut	Cathead(2 turns)	.65-.67
UK	Automatic	Trip	.73
USA	Safety	Cathead(2 turns)	.55-.60
USA	Donut	Cathead(2 turns)	.45
Venezuela	Donut	Cathead	.43

Table 8-2 Borehole and sampler correction factors (adapted from Skempton, 1986; from Coduto, 2001).

Factor	Equipment Variables	Value
Borhole Diameter Factor, C_B	65-115 mm (2.5-4.5 in)	1.00
	150 mm (6 in)	1.05
	200 mm (8in)	1.15
Sampling Method Factor, C_S	Standard Sampler	1.00
	Sampler without liner	1.20

Figures 8.3 to 8.7 show data from tests performed at Swan Quarter (SQ) while the lone SC plot, Figure 8.8, is for data from the Sampson County site. Figure 8.9 shows the relationship between the slope parameter m, and N_{cr} . As shown earlier in equation 8.1, the pump pressure is normalized with respect to the atmospheric pressure but still the data used to develop Figure 8.9 was for pump capable of sustaining dynamic head pressure in excess of 150psi. Collecting data on pump used by the contractors is recommended to further verify the proposed insertion model.

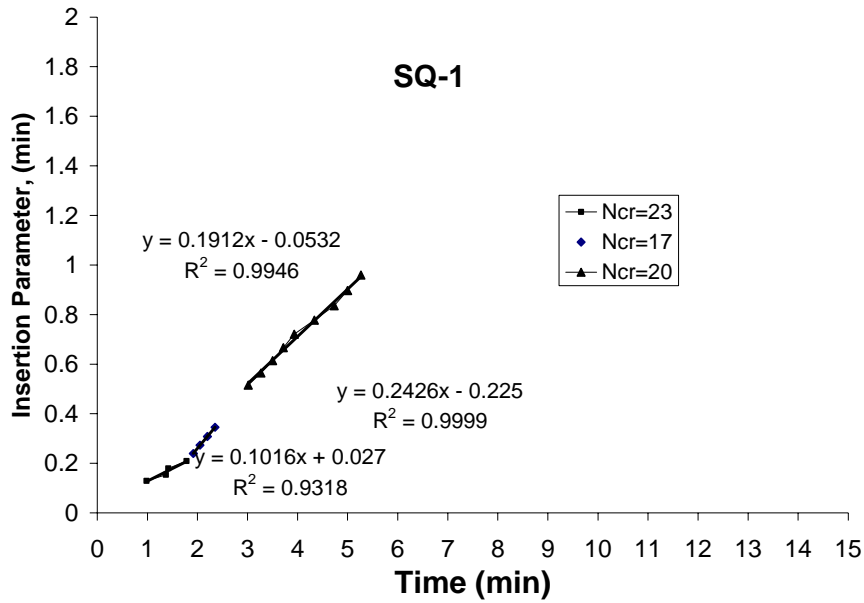


Figure 8-3 SQ-1 Insertion Parameter, N_{cr} curve fitting.

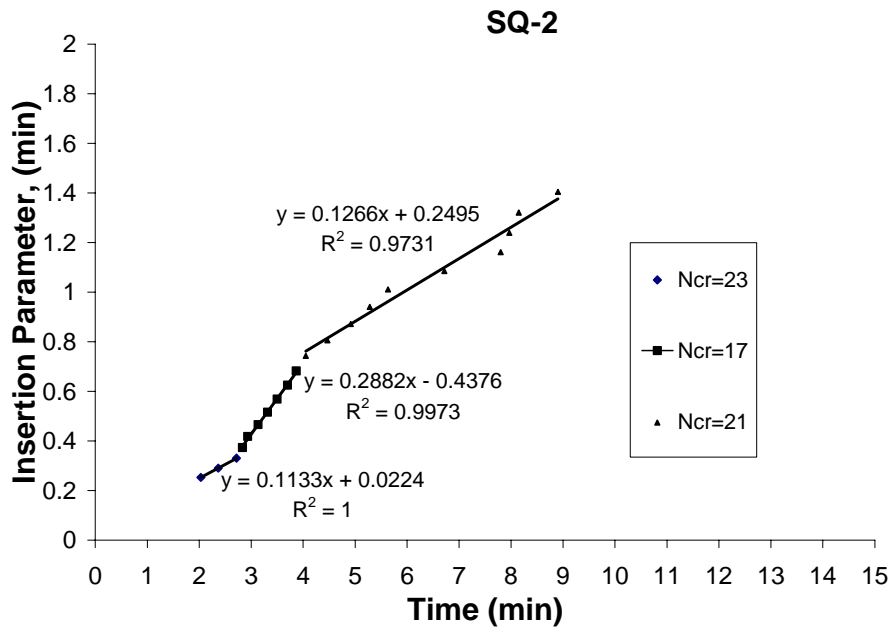


Figure 8-4 SQ-2 Insertion Parameter, N_{cr} curve fitting

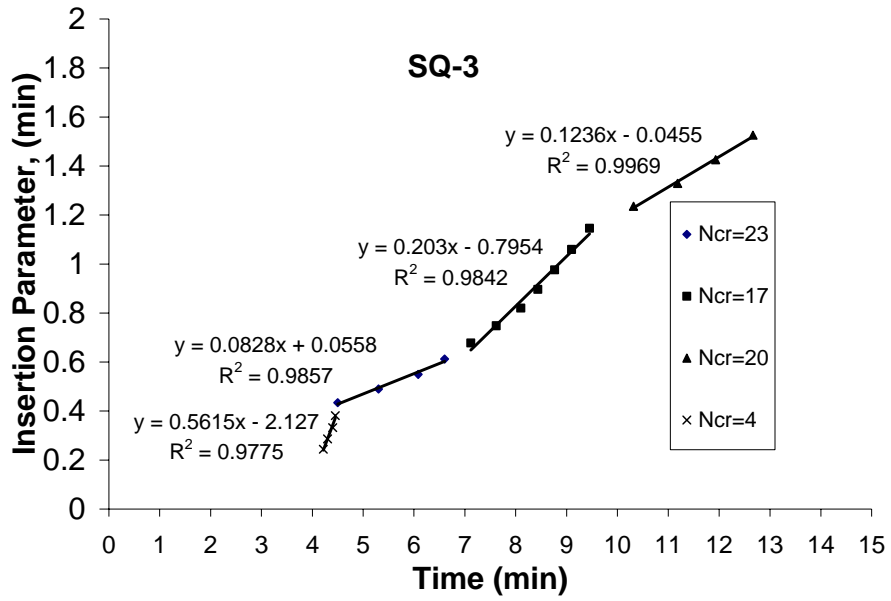


Figure 8-5 SQ-3 Insertion Parameter, N_{cr} curve fitting

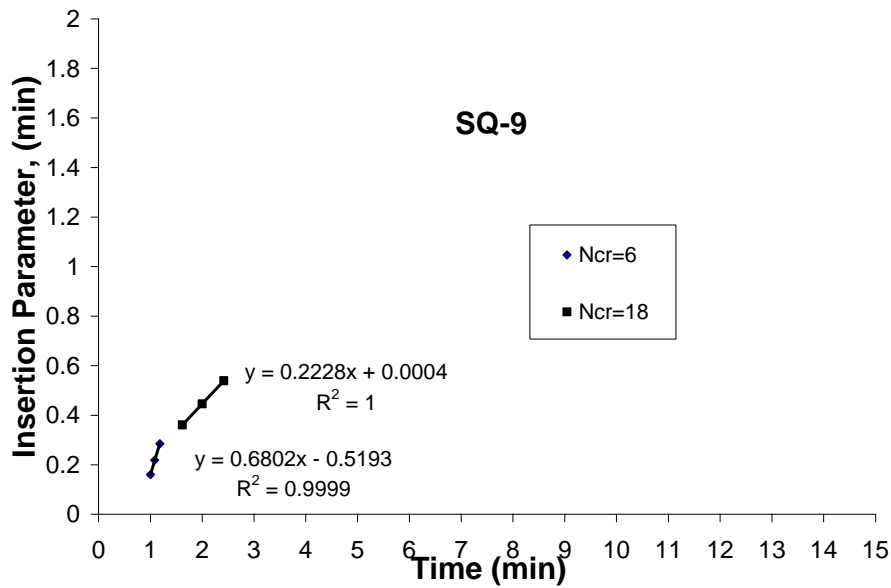


Figure 8-6 SQ-9 Insertion Parameter, N_{cr} curve fitting

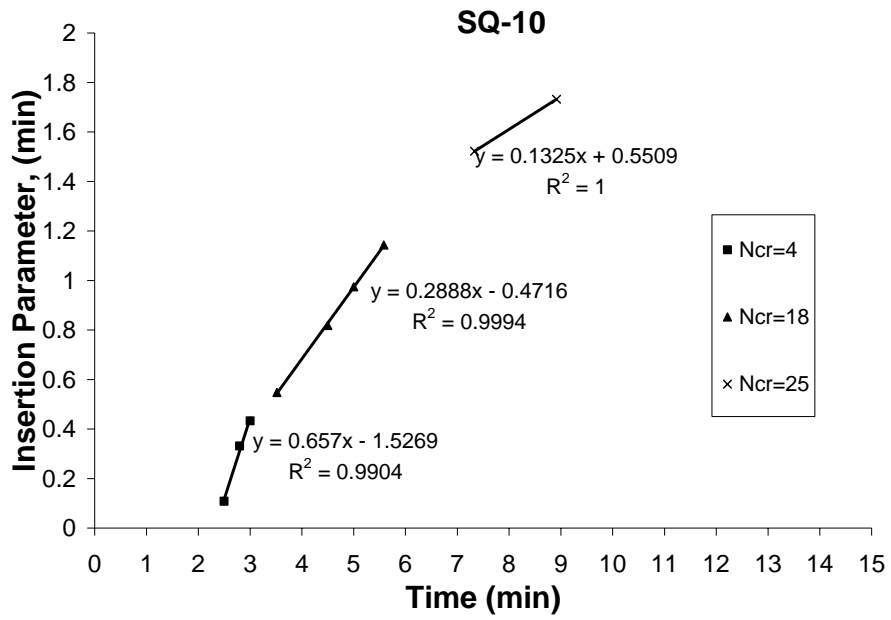


Figure 8-7 SQ-10 Insertion Parameter, N_{cr} curve fitting

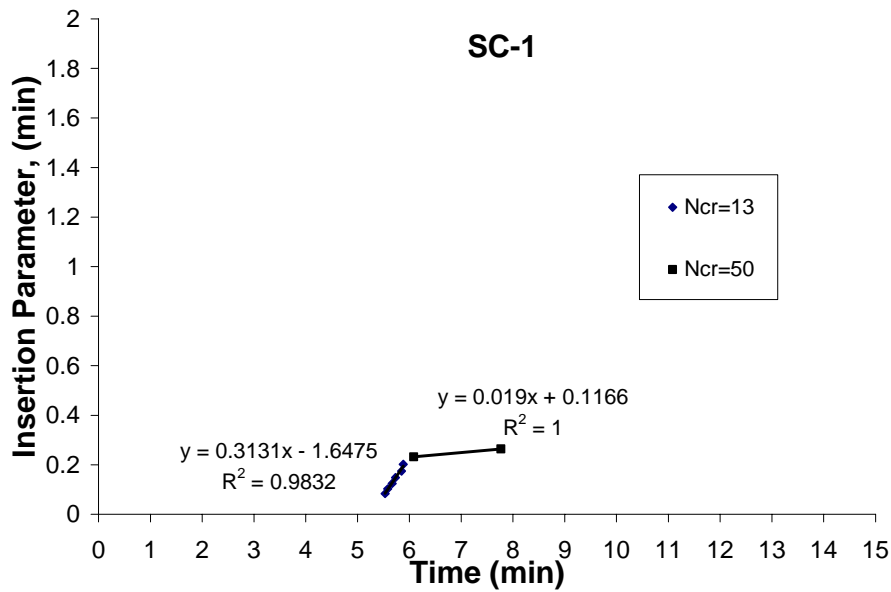


Figure 8-8 SC-1 Insertion Parameter, N_{cr} curve fitting

The slope parameters developed from Figures 8.3 to 8.8 were plotted in Figure 8.9 against their respective SPT N_{cr} values to develop the relationship between the N_{cr} value and slope parameter, m . Based on the data presented in Figure 8.9, Equation 8.4 was developed as follows:

$$\text{slope parameter, } m = 0.92e^{-0.0085(N_{cr})} \quad \text{Eq. 8.4}$$

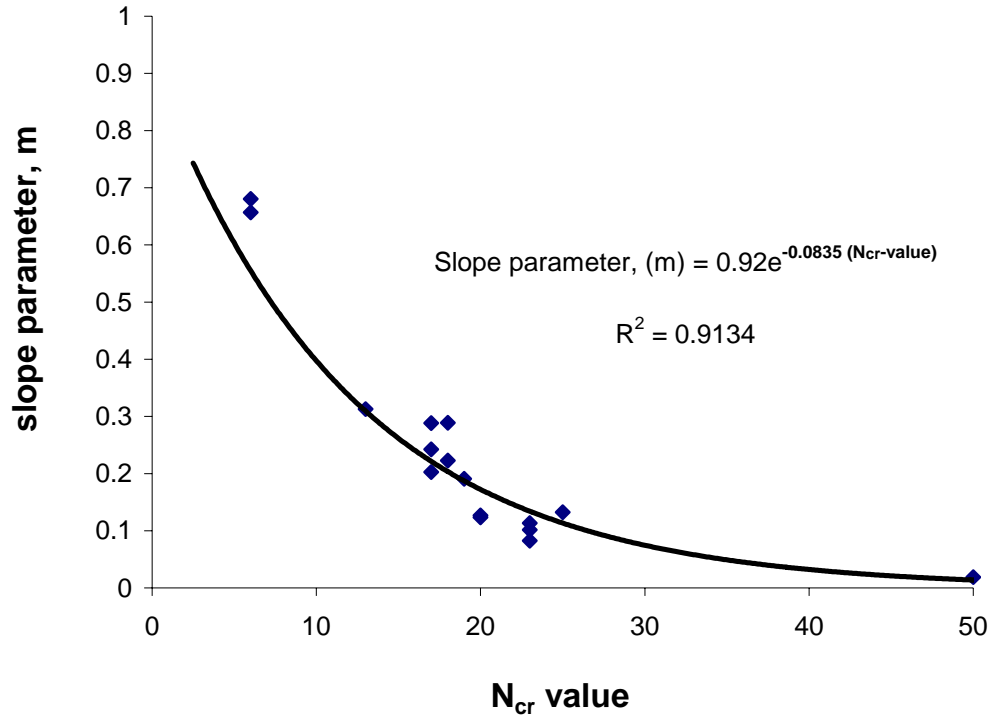


Figure 8-9 Development of Slope Parameter, m equation.

The model is applied by determining the slope parameter, m , after inputting the specific N_{cr} value describing a soil profile (or a segment there of) into Equation 8.4. After the slope parameter is computed, the insertion parameter (IP) is computed using equation 8.2. The required installation time for a given set of injection characteristics is the estimated using equation 8.3.

After determination of the required pile installation time, for a given IP, the debris volume and its lateral extent are estimated as follows:

$$V_{w\text{total}} = Q_w \times \text{time} \quad \text{Eq. 8.5}$$

and,

$$Q_p = I_v / \text{time} \quad \text{Eq. 8.6}$$

where:

V_{wtotal} = total volume of injected water

Q_p = average pile volume insertion rate

I_v = inserted volume of pile, (defined previously)

8.1.1 Insertion Model Validation

A pile jetting spreadsheet was developed in Microsoft ExcelTM so that each soil profile could be separated into discrete 1 foot (.3m) depth increments. Evaluating the soil profile in several increments provides a higher level of precision, and hopefully accuracy, in the case where a non-homogeneous soil profile is analyzed. The time required for insertion of each discrete increment is given by:

$$\text{Incremental insertion time (min)}_i = \left(\frac{\text{insertion parameter}}{m} \right)_{0 \text{ to } i} - \left(\frac{\text{insertion parameter}}{m} \right)_{0 \text{ to } i-1} \quad \text{Eq. 8.7}$$

The total time required to insert a pile length through the entire profile from 0 to i , is given by the equation:

$$\text{Total time req. (min)} = \sum_{i=1}^n \text{Incremental insertion time} \quad \text{Eq. 8.8}$$

Alternatively, for a homogeneous soil profile where the average N_{cr} value is constant, the time required to insert the entire pile can be calculated from equation 8.2 using the average N_{cr} value. A sample insertion spreadsheet is provided in Figure 8.10.

The estimated insertion time for each test was compared to the actual times measured during the field installations. Table 8.3 illustrates the computed values based on the proposed model and the measured values from the actual field tests. Figure 8.11 is a graphical representation of the data presented in Table 8.3. As shown in Figure 8.11, the computed versus measured times agree reasonably well.

Qw (ft³/min) 179
 D (ft) 2
 A (ft²) 3.14
 Pb (psi) 100
 Pa (psi) 14.7

Depth (ft)	N value	m	L/D	lv (ft ³)	Insertion Parameter	Time req (min)	Prev Increment	Incremental Insertion time
0.001	2	0.77495	0.0005	0.00314	0.0	0.0	0.0	0.000
1	2	0.77495	0.5	3.14	0.0	0.0	0.0	0.002
2	2	0.77495	1	6.28	0.0	0.0	0.0	0.005
3	2	0.77495	1.5	9.42	0.0	0.0	0.0	0.008
4	2	0.77495	2	12.56	0.0	0.0	0.0	0.012
5	2	0.77495	2.5	15.7	0.0	0.0	0.0	0.015
6	2	0.77495	3	18.84	0.0	0.1	0.0	0.018
7	2	0.77495	3.5	21.98	0.1	0.1	0.1	0.022
8	2	0.77495	4	25.12	0.1	0.1	0.1	0.025
9	2	0.77495	4.5	28.26	0.1	0.1	0.1	0.028
10	2	0.77495	5	31.4	0.1	0.2	0.1	0.032
11	2	0.77495	5.5	34.54	0.2	0.2	0.2	0.035
12	2	0.77495	6	37.68	0.2	0.2	0.2	0.038
13	2	0.77495	6.5	40.82	0.2	0.3	0.2	0.042
14	23	0.134196	7	43.96	0.3	1.9	1.6	0.259
15	23	0.134196	7.5	47.1	0.3	2.2	1.9	0.279
16	21	0.158586	8	50.24	0.3	2.1	1.8	0.252
17	19	0.18741	8.5	53.38	0.4	2.0	1.8	0.227
18	17	0.221472	9	56.52	0.4	1.9	1.7	0.204
19	15	0.261726	9.5	59.66	0.5	1.8	1.6	0.182
20	13	0.309296	10	62.8	0.5	1.7	1.5	0.163
21	14	0.284518	10.5	65.94	0.6	2.0	1.8	0.186
22	15	0.261726	11	69.08	0.6	2.4	2.2	0.212
23	16	0.240759	11.5	72.22	0.7	2.8	2.6	0.241
24	17	0.221472	12	75.36	0.7	3.4	3.1	0.274
25	18	0.20373	12.5	78.5	0.8	4.0	3.6	0.310
26	19	0.18741	13	81.64	0.9	4.7	4.3	0.351
27	20	0.172397	13.5	84.78	0.9	5.5	5.1	0.396
28	21	0.158586	14	87.92	1.0	6.4	5.9	0.447
29	22	0.145882	14.5	91.06	1.1	7.4	6.9	0.504
30	23	0.134196	15	94.2	1.2	8.6	8.1	0.567
31	24	0.123445	15.5	97.34	1.2	10.0	9.4	0.637
32	25	0.113556	16	100.48	1.3	11.6	10.9	0.715
33	26	0.104459	16.5	103.62	1.4	13.4	12.6	0.802

Σ 7.2
 (min)

Figure 8-10 Example of pile insertion spreadsheet, from SQ-2.

Table 8-3 Measured versus predicted insertion time for given tests.

Test 1-D	Measured Time (min)	Predicted Time (min)
SQ-1	4.67	5.21
SQ-2	7.05	7.21
SQ-3	8.22	5.75
SQ-4	6.75	5.65
SQ-9	3.63	5.64
SQ-10	6.95	9.76
SC-1	0.85	0.99

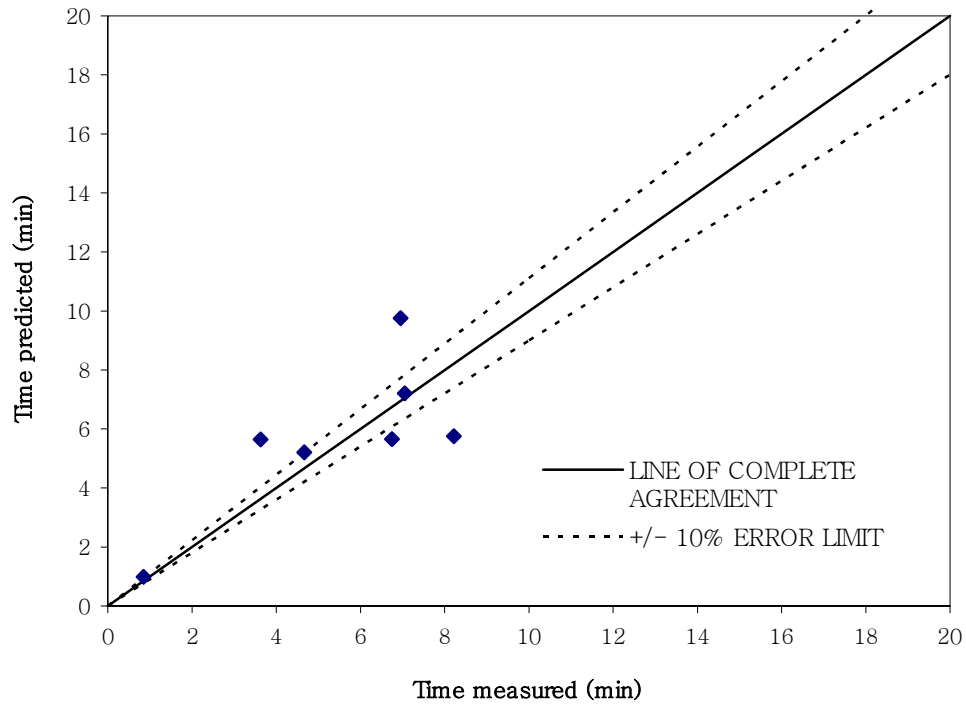


Figure 8-11 Measured versus predicted insertion times.

8.2 Debris Model Verification

The primary purpose of this section is to investigate the validity of the laboratory based debris model providing volume and area extent of the disturbance zone. The following equations are proposed for predicting debris volume and extent, as was presented in chapter 4:

$$V_{\text{debris}} = V_{\text{wtotal}} \times a_{\text{volume}} \left(\frac{Q_w}{Q_p} \right)^{b_{\text{volume}}} \quad \text{Eq. 8.9}$$

where : $V_{\text{debris}} = \text{debris volume (L}^3\text{)}$

$$\begin{aligned}
V_{\text{wtotal}} &= \text{total volume of jetted water (L}^3\text{)} \\
a_{\text{volume}} &= \text{GSD-dependent volume parameter} \\
b_{\text{volume}} &= D_{50}\text{-dependent volume parameter (with } D_{50} \text{ in mm)} \\
Q_w &= \text{water volume flowrate (L}^3\text{/min)} \\
Q_p &= \text{pile volume flowrate (L}^3\text{/min)}
\end{aligned}$$

and

$$a_{\text{volume}} = 0.520(C_c) + 0.868 \quad \text{Eq. 8.10}$$

$$b_{\text{volume}} = -0.081(D_{50}) - 0.961 \quad \text{Eq. 8.11}$$

The area of the debris zone is given by:

$$A_{\text{debris}} = \left(\frac{V_{\text{wtotal}}}{D_{\text{pile}}} \right) a_{\text{area}} \left(\frac{Q_w}{Q_p} \right)^{b_{\text{area}}} \quad \text{Eq. 8.12}$$

where: A_{debris} = debris distribution on ground surface from jetted pile installation (L^2)
 V_{wtotal} = total volume of water required to jet a pile to a given depth with available jetting parameters (L^3)
 D_{pile} = diameter of jetted pile (L)
 a_{area} = parameter based on D_{50} (with D_{50} in mm)
 b_{area} = parameter based on C_c

For $D_{50} < 0.5$ mm

$$a_{\text{area}} = 8.5086(D_{50}) + 9.1967 \quad \text{Eq. 8.13}$$

$$b_{\text{area}} = -0.6357(D_{50}) - 0.8279 \quad \text{Eq. 8-14}$$

For $D_{50} > 0.5$ mm

$$a_{\text{area}} = 0.404(D_{50}) + 13.249 \quad \text{Eq. 8-15}$$

$$b_{\text{area}} = -0.085(D_{50}) - 1.1029 \quad \text{Eq. 8-16}$$

To verify the model, the debris volume and lateral extent from each test were measured and compared with the computed debris volume and extent from the equations proposed herein. Table 8.4 is a summary of the comparative results. The error in volume and diameter predictions is presented (debris area is computed from a measured diameter; therefore any error in measurement is squared by the area computation.)

For eleven of the seventeen cases presented in Table 8.4, the debris volume was over predicted by 30% or less. In 5 of the cases, the debris volume was overpredicted;

however it was within 20% of the measured values. Similar trend was observed for the diameter calculations. The gross over prediction is mainly in areas where measurements occurred under water and where it was difficult to visually discern the presence of a disturbed volume and the associated height.

Table 8-4 Summary of Debris Zone Verification

Measured			Predicted			Percent Difference	
V _{debris}	A _{debris}	D _{debris}	V _{debris}	A _{debris}	D _{debris}	V _{debris}	D _{debris}
84.71	412.33	22.91	46.47	207.72	16.26	45%	29%
30.15	238.76	17.44	49.73	228.53	17.06	-65%	2%
69.12	314.16	20.00	72.67	314.22	20.00	-5%	0%
74.14	313.37	19.97	73.80	326.31	20.38	0%	-2%
53.72	469.70	24.45	64.73	287.19	19.12	-20%	22%
28.50	146.90	13.68	64.87	288.75	19.17	-128%	-40%
49.09	306.31	19.75	46.04	203.05	16.08	6%	19%
51.60	358.14	21.35	56.81	260.86	18.22	-10%	15%
51.25	296.88	19.44	47.05	214.08	16.51	8%	15%
176.16	530.14	25.98	162.11	726.45	30.41	8%	-17%
146.40	530.14	25.98	151.21	668.47	29.17	-3%	-12%
107.60	449.25	23.92	146.99	637.65	28.49	-37%	-19%
131.55	449.25	23.92	154.61	690.44	29.65	-18%	-24%
109.01	320.44	20.20	88.22	379.94	21.99	19%	-9%
104.73	392.70	22.36	118.70	508.89	25.45	-13%	-14%
57.92	343.22	20.90	130.75	580.09	27.18	-126%	-30%
69.43	251.32	17.89	121.77	540.55	26.23	-75%	-47%

The predicted debris diameter, D_{debris} was computed from the following equation:

$$D_{\text{debris}}(\text{predicted}) = \sqrt{\frac{4(A_{\text{debris}})}{\pi}} \quad \text{Eq. 8.17}$$

Figures 8.12 and 8.13 are graphical representations of the computed and measured debris data. As mentioned earlier, and for comparative purposes, the measured and predicted debris diameters were compared in lieu of the debris areas. The reason is that the measured debris area is computed from a measured diameter; therefore any error in measurement is squared by the area computation.

Figures 8.12 and 8.13 illustrate that the computed debris volumes and lateral extent represented by the diameter agree fairly with the measured values. The debris volume regression in Figure 8.12 shows that the predicted values were on the average 40% larger than measured for cases that over predicted the debris volume. If one is to ignore the two cases where the debris volume is over predicted by more than 100%, the predicted values are then less than 20% on the average larger than the measured values.

The model yielded data within 20% of the measured volumes for the six cases where the debris volume was under predicted.

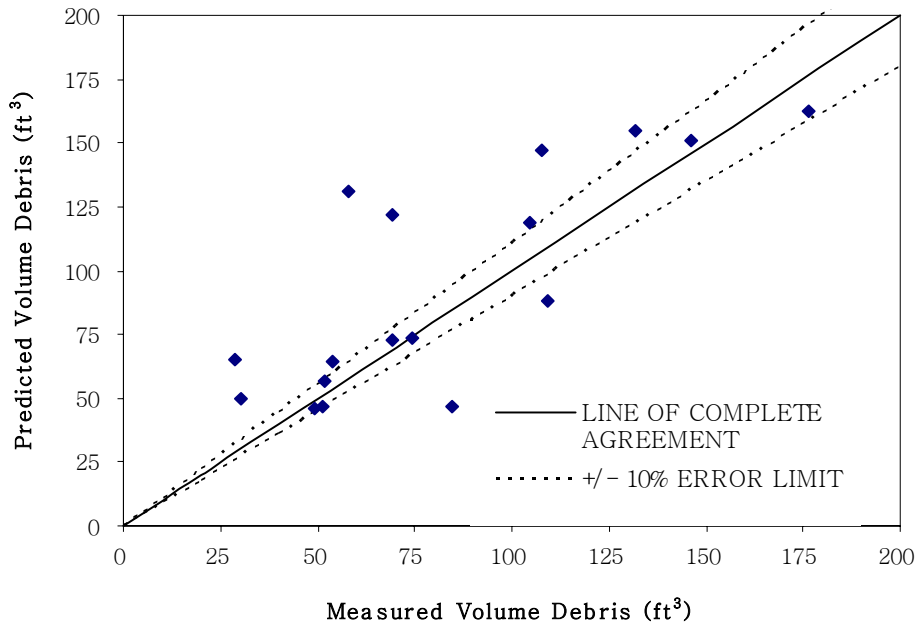


Figure 8-12 Debris Volume Verification

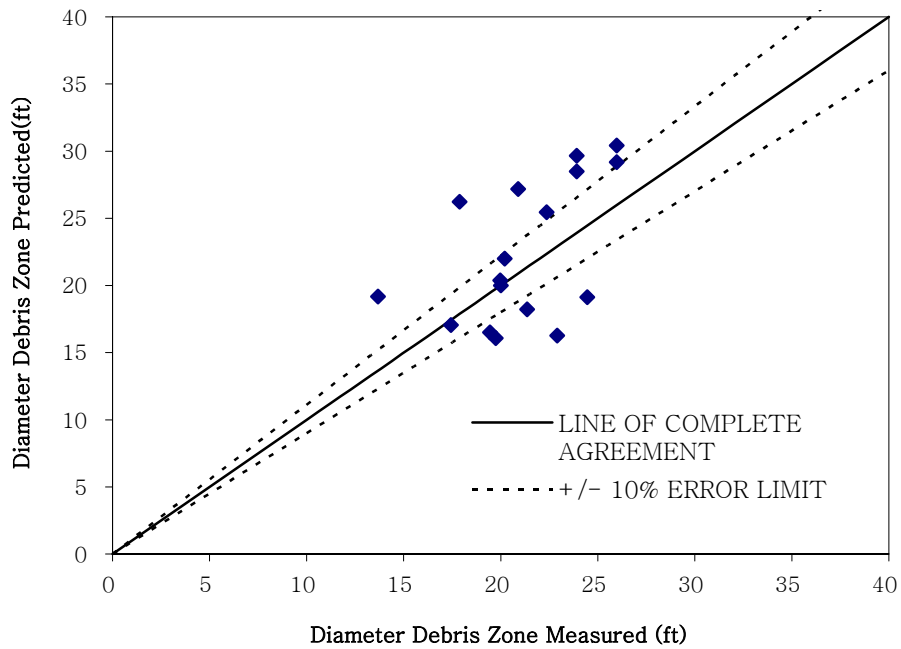


Figure 8-13 Debris Diameter Verification

The debris diameter regression in Figure 8.13 shows that the predicted values were on average within 20% of the measured values for the 11 cases where the diameter was over predicted. For the 6 cases where the diameter was under predicted, the predicted values were also on the average within 20% of the measured values.

8.3 Particle Transport Model

Particle transport modeling literature was reviewed in order to capture the effects of current on changing the shape of the debris zone around the pile. To this end, the literature review was centered on fluid flow and sediment transport in marine environments. In addition, double hydrometer laboratory testing was conducted on several samples of varying grain size distribution to determine the effects of grain size on turbidity.

8.3.1 Model Rational

Two main sources for fluid flow in the pile-jetting scenario are described. The first is the flow from the jets themselves. This fluid experiences maximum velocity upon exiting the jetting nozzles, and subsequently flows in a turbulent manner around the base of the pile, before flowing along annulus of the pile to the ground surface. The velocity of importance for zone of disturbance calculations is the exit velocity of the jetting fluid upon reaching the ground surface. This exit velocity is always less than that of the nozzle jet velocity, and is assumed to decrease as the pile insertion depth increases.

The second source of fluid flow is that of water current, which may or may not be present in all jetted pile locations. This source is either from river or tidal velocities, which may vary during the course of pile installation, but may play a major role in the determination of the environmental impact boundaries.

Jetting of a pile produces an additional layer of soil on the area surrounding the pile. This layer will be referred to as a bedform and will be of varying dimensions based on jetting velocities and flow rates, as have been described previously. When piles are jetted in locations with sub current, the current supplemental flow and velocity affect the dimensions of these bedforms. Additionally, the quality of the water in the area, i.e. turbidity, salinity, pH, and dissolved oxygen levels can be affected due to the disturbance of the mud line. This facet of model development is focused solely on the transport of sediment. There are three main scenarios which may exist when jetting a pile under water:

- i) The first scenario involves jetting when no current flow is acting. An example of this scenario would be the case of a tidal inlet in between high and low tide. For this scenario, the proposed debris zone model will describe the deposition of the bedform.
- ii) The second scenario can be described as an extension of the first scenario. Jetting occurs in still water, and then sometime later currents are introduced which have sufficient velocity to re-suspend the pre-described bedform and alter the shape and distribution of that bedform.
- iii) The third scenario is the case in which jetting occurs simultaneously with water currents which possess sufficient velocity to alter the bedform shape. Since the

proposed debris zone model should adequately describe the bedforms created by the first scenario, consideration will be given to the second and third scenarios respectively.

8.3.2 Proposed Approach

For the second scenario, in which currents must re-suspend a previously deposited bedform, the primary mechanism which governs the migration of the bedform is that of the initiation of particle movement. This is an important consideration because, although many particles can be transported at low fluid velocities, Newtonian physics dictates higher velocities are required in order to initiate erosion and movement. Figure 8.14 (from Open University Oceanography Course Team, 1999) illustrates typical current velocities required to initiate erosion (particle movement) for different particle sizes.

Referring to Figure 8.14, current speed is analogous to flow velocity. The curve corresponding to erosion provides the velocity required for the initiation of movement for each particle size. Above this line, particle movement is likely to occur, while below this line particles may have the ability to be transported if already in motion, but are not subjected to forces sufficient to initiate movement. For scenario two, the current velocity values must lie above the erosion line in order to displace a pre-deposited bedform.

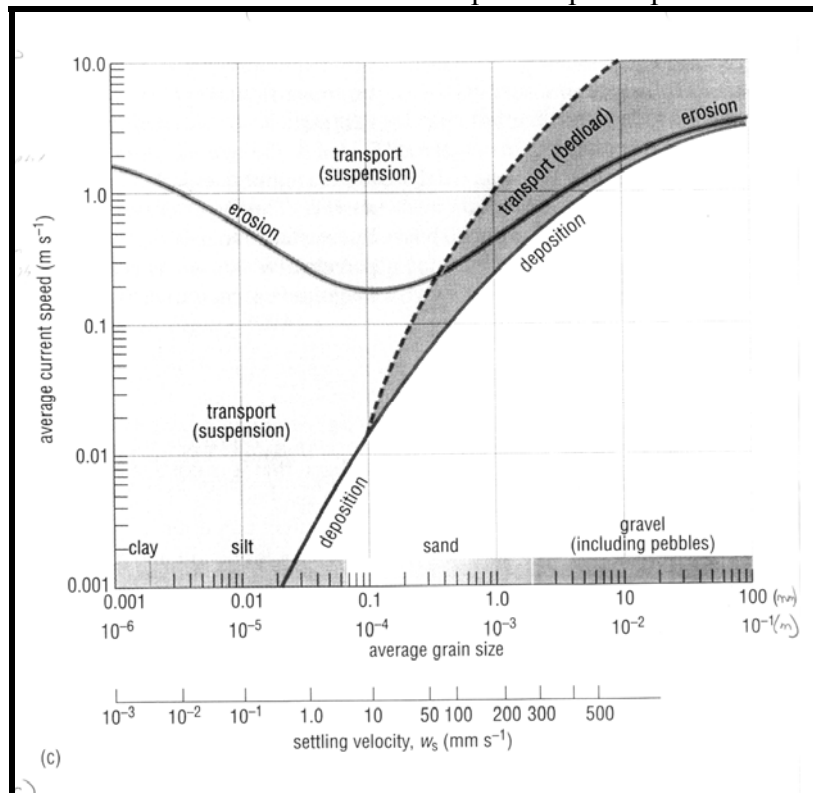


Figure 8-14 Effect of Current Speed on the Erosion and Deposition Characteristics for Specified Bed Particle Diameter (Open University. Oceanography Course Team 1999)

Note that the range of current velocities near the mud-line required to initiate erosion for clay to fine gravel-sized particles (grain sizes which can typically be jetted

through) ranges from approximately 0.2 to 2 meters per second. It should also be noted that the range of current velocities required to initiate erosion for the bedform deposited by the jetting process will also likely have an effect not only on the bedform produced by jetting but also on the all the surrounding ocean, river, or basin floor. Therefore, when jetting in this type of environment, the impacts associated with jetting are not likely to be as significant (or identifiable) because of the dynamic nature of occurring basin floor migration. Accordingly, perhaps the important scenario to consider is the third, in which jetting occurs simultaneously with naturally occurring water currents.

For analysis of bedform alteration due to simultaneous jetting and surface currents, it is important to understand Figure 8.14. One of the key points to note regarding Figure 8.14 is the variation in current velocity for erosion and deposition as a function of particle size. For gravel-sized particles, the current velocities that fall between erosion and deposition occur in a narrow band, suggesting that a small reduction in current speeds can cause the immediate deposition of eroded particles of this size. Conversely, for silt and clay-sized particles, fluctuations in current velocity over three cycles of a log scale can affect the erosion of particles, but have no effect on the deposition, i.e. particles already in motion will stay in suspension and be transported. Even for sand – sized particles, the range of current velocity that will not erode but transport sediment already in motion spans one-log cycle.

Velocities used for jetting are well above those required to initiate erosion. Thus, almost all particles will experience transport some distance from the jetted pile, as described by the debris zone and lateral extents model. Further, the water current velocity is normally relatively constant compared with jetting velocities, and may not be subject to significant dissipation. Thus, soil particles that enter suspension due to erosion caused by jetting velocities may be transported significant distances by water currents that otherwise do not have sufficient velocity to erode these particles. These particles will be shifted downstream altering the dimensions of the debris zone and may potentially cause unwanted turbidity in the surrounding water.

Equations of sediment transport length and deposition thickness are presented here. These equations are taken from Van Rijn(1984, a,b,c) on Sediment Transport, Parts I through III (1984). The equations were verified by extensive comparison to flume and field data, and are as follows:

$$\Delta / d = 0.11 (D_p / d)^{0.3} \cdot (1 - e^{-0.5T}) \cdot (25 - T) \quad \text{Eq. 8.18}$$

$$\Delta / \lambda = 0.015 (D_p / d)^{0.3} \cdot (1 - e^{-0.5T}) \cdot (25 - T) \quad \text{Eq. 8.19}$$

where:

- Δ = bed form height signifying the height of the disturbance zone
- d = flow depth signifying the depth impacted by current velocity
- D_p = particle diameter of disturbed sediments
- T = velocity dependent transport stage parameter

λ = bed form length signifying the length of the plume formed by the transported sediments.

The two equations in tandem can be used to solve for bed form height and length given that flow velocities, flow depth, and grain size distribution are known. The flow depth (d) is the height of the column of fluid moving, at the flow velocity of concern, carrying suspended sediment. Particle diameter (D_p), is the diameter of the particle size of concern, and is assumed to be D_{30} for evaluation of finer particle distribution (turbidity). Laboratory test data from a turbidity study conducted as a part of this research validates this assumption.

Figure 8.15 illustrates the relationship between turbidity and the characteristic D_{30} particle size. Notice that as D_{30} decreases, the amount of time required for turbidity dissipation increases. So, for this study, D_{30} will be used as the particle size of interest with regard to turbidity.

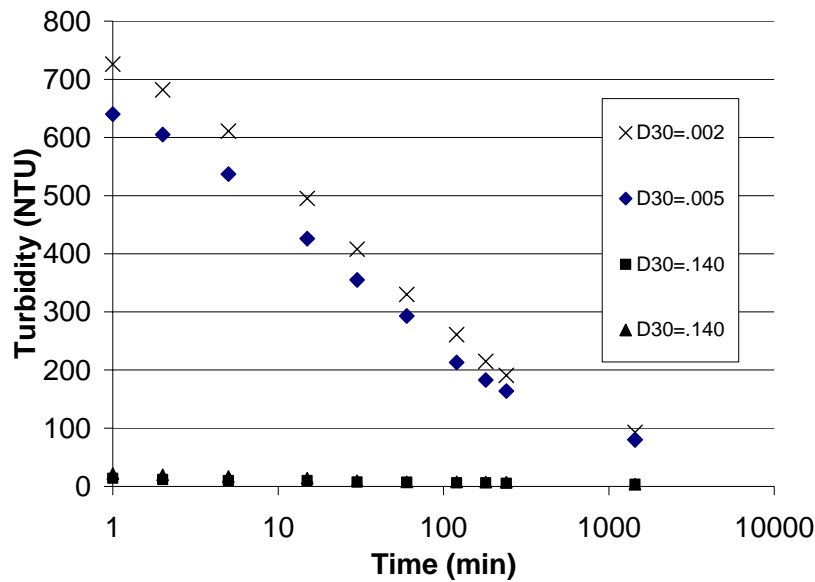


Figure 8-15 Turbidity distribution with time.

While variations in the height, or thickness, of created bedforms are important characteristic to consider, perhaps of more interest for an environmental focus is the variation in bedform length. This is typically the more critical value because it dictates the extent of impact a jetted pile may have on the surrounding area. Combining Equations 8.18 and 8.19 yields a simplified equation for bedform's length as follows:

$$\lambda = 7.3(d) \quad \text{Eq.8.20}$$

where:

λ = bedform length
d = flow depth

This equation demonstrates that the single factor affecting the lateral extent of debris zone due to current near the mud-line is the depth of flow; that is the height of the column of fluid moving at the flow velocity of concern carrying suspended sediment. Although this seems like a simplistic solution, when one considers the determination of a value for the depth of flow, the analysis becomes distinctly more complex.

Utilization of complete depth of basin water (i.e. depth of the river, ocean, or basin at the point of pile jetting) for the value of flow depth, could be in many cases lead to a significant overestimate, since the disturbed particles are rather suspended within a fraction of the height near the mud line. Conversely, utilization of a flow depth comparable to that of one obtained on land with a similar jetted pile will underestimate this bedform length, since this scenario does not take into consideration the presence of additional water that contributes to an increase in flow depth. No direct calculations exist for the determination of this flow depth, but it is expected to be related to the jetting exit velocity, and particle size diameter. Increases in a jetting exit velocity will result in the propulsion of particles further off the surface, thus increasing the flow depth. Additionally, decreases in the particle size diameter will also result in a greater flow depth since these particles are more likely to mix in a greater portion of the water depth, as opposed to remaining fairly close to the mud line as was indicated from data in the laboratory turbidity testing (Figure 8.15).

When considering this information in tandem with the goal of environmental impact evaluation, it is important to note the limitations associated with estimating sediment transport length based on Equations 8.18 through 8.20. These equations only estimate the sediment transport length based on an assumed flow depth. For any given grain size distribution this flow depth will vary for each particle size present in the distribution, since each specific particle size will be propelled into the water column at different heights. For the sand size and larger particles, within a given grain size distribution, it is logical to assume that the flow depth is roughly equivalent to the height of the thickest part of the measurable debris zone since these particles tend to stay very close to the ground surface and settle out immediately upon leaving the jetting annulus. Thus, the lateral debris zone extents would be expected to shift in the direction of the current velocity the amount dictated by Equation 8.20.. Considering the maximum thicknesses measured from the field research to be approximately 1 foot the shift of the debris zone would likely be less than 10 feet laterally in the direction of current velocity. However, keep in mind that as pile diameter and depth increase, the thickness of the measurable debris zone will also increase.

For this reason, it is appropriate to consider that the major impact of the surface water current to be the transport of smaller particle sizes (D_{30} and smaller) in the form of turbidity. In case of clay-size particles, it can be conservatively assumed that flow depth will approach the entire thickness of the water column above the jetting application. This assumption, however, needs further investigation for confirmation.

It is logical, however, to assume that as the distance from the pile increases, the turbidity level will decrease as more particles settle out of suspension. This assumption was confirmed by monitoring the turbidity levels with increasing distance from the pile during the field testing. The observed increases in turbidity returned to background levels after approximately 1 hour and the initial magnitude of the turbidity at locations were controlled primarily by the particle size distribution of the soil being transported to the surface in the return water. Areas of finer grain-size distribution soils exhibited higher initial magnitudes of turbidity than those with coarser grain size distributions. This was also confirmed by laboratory turbidity testing (see Figure 8.15).

8.3.3 Turbidity and Transport Length: Underwater Jetting

No research has been reported in the literature to determine the magnitude of turbidity caused by various particle sizes and jetting exit velocities underwater. This is maybe primarily because of the difficulty associated with determining an exit velocity which is not constant and cannot be readily measured or determined from continuity equations. From the field research, the maximum turbidity observed was on the order of approximately 70 NTU, as measured data was collected at Swan Quarter at a location with soil having very fine particle distribution (>96% silt and clay size particles) and where the greatest values of jetting flowrates and velocities were utilized during testing were employed. The lower end of the scale was approximately 20 NTU where predominantly sand soils were tested.

In considering the available research data, it is appropriate to be conservative when estimating the turbidity and sediment transport length. The following approach is proposed to estimate turbidity magnitude and transport length:

- Estimate the initial magnitude of turbidity based on grain size distribution of the site soil. A value on the order of 20 NTU should be expected as the minimum for any jetting application, including profiles comprised entirely of sand-sized or larger particles. This value should be expected to increase up to approximately 70 NTU as the percentage of silt and clay size particles in the distribution approach 100%.
- Use Equation 8.20 to estimate the transport length of the sediment plume using the estimated depth of disturbance zone as the flow depth.
- In areas where the current velocity exceeds the deposition velocity of the sand sized particles (from Figure 8.14) it is appropriate to consider that a shift in the measurable debris zone will take place in the direction of the current velocity.

It should be noted that the turbidity magnitude is an estimate based on observed turbidity levels during field testing performed for this research. It is recommended, in general, that a test pile be installed before production begins at underwater jetting sites to

determine if the magnitude of the turbidity is exceeding what is acceptable to local marine officials.

8.4 Proposed Design Methodology

In this section, the proposed three part jetting model is presented in the context of a design methodology. The procedure for implementing the model is described as follows:

1. Perform an appropriate subsurface investigation of the proposed jetting site and determine SPT N-values as a function of depth within the soil profile along with representative soil sampling for grain size distribution testing.
2. Separate the soil profile into layers based on the distribution of equal SPT N-values and use Equation 8.4 or Figure 8.9 to determine the slope parameter, m , for each layer. Then use Equations 8.1 and 8.2 to determine the predicted time required to insert a given pile based on a user-specified insertion parameter. The insertion parameter is determined based on the proposed pile dimensions and the specified pump characteristics.
3. Use the time required to insert the pile to calculate the total volume of water (V_{total}) and the pile volume insertion rate, Q_p , from Equations 8.5 and 8.6. Then use Equations 8.9 through 8.17 to calculate the volume and lateral extent of the debris zone created by the installation.
4. Estimate the initial magnitude of the turbidity based on grain size distribution data of the site. A value on the order of 20 NTU should be expected as the minimum for any jetting application, including profiles comprised entirely of sand-sized or larger particles, and this value should increase up to approximately 70 NTU as the percentage of silt and clay size particles in the distribution approach 100%.
5. If tidal currents are expected in the area of jetting, use Equation 8.20 to conservatively estimate the transport length of the sediment plume using flow depth equal to highest expected thickness of the disturbed zone around the pile. In this case, the volume of the sediments due to jetting is assumed to be re-distributed due to current velocity.

A Microsoft Excel spreadsheet has been formulated to perform the calculations in steps 1 through 3. An example of this spreadsheet is given in Figure 8.16.

Jetting Model Spreadsheet

Qw (gal/min)	1200	Cc	1.05
Diam (ft)	2	D50 (mm)	0.17
A (ft ²)	3.14	Total Depth(ft)	30
Pb (psi)	100		
Pa (psi)	14.7		

C_c = Coeff of Curvature of the grain size distribution
 $C_c = (D_{30})^2 / (D_{10} * D_{60})$
 Q_w = Pump Flowrate
 A = Area of Pile
 P_b = Pump pressure
 P_a = Atmospheric Pressure

Depth (ft)	N value	m	L/D	lv (ft ³)	IP	Time req (min)	Prev Increment	Incremental Insertion Time (min)
0.1	30	0.0935	0.05	0.314	0.0000	0.0002	0.0000	0.0002
1	30	0.0935	0.5	3.14	0.0014	0.0154	0.0002	0.0152
2	30	0.0935	1	6.28	0.0058	0.0616	0.0154	0.0462
3	30	0.0935	1.5	9.42	0.0129	0.1385	0.0616	0.0770
4	30	0.0935	2	12.56	0.0230	0.2463	0.1385	0.1078
5	30	0.0935	2.5	15.7	0.0360	0.3848	0.2463	0.1385
6	30	0.0935	3	18.84	0.0518	0.5542	0.3848	0.1693
7	30	0.0935	3.5	21.98	0.0705	0.7543	0.5542	0.2001
8	30	0.0935	4	25.12	0.0921	0.9852	0.7543	0.2309
9	30	0.0935	4.5	28.26	0.1165	1.2469	0.9852	0.2617
10	30	0.0935	5	31.4	0.1439	1.5394	1.2469	0.2925
11	30	0.0935	5.5	34.54	0.1741	1.8627	1.5394	0.3233
12	30	0.0935	6	37.68	0.2072	2.2167	1.8627	0.3541
13	30	0.0935	6.5	40.82	0.2431	2.6016	2.2167	0.3848
14	30	0.0935	7	43.96	0.2820	3.0172	2.6016	0.4156
15	30	0.0935	7.5	47.1	0.3237	3.4636	3.0172	0.4464
16	30	0.0935	8	50.24	0.3683	3.9408	3.4636	0.4772
17	30	0.0935	8.5	53.38	0.4158	4.4488	3.9408	0.5080
18	30	0.0935	9	56.52	0.4661	4.9876	4.4488	0.5388
19	30	0.0935	9.5	59.66	0.5194	5.5572	4.9876	0.5696
20	30	0.0935	10	62.8	0.5755	6.1575	5.5572	0.6004
21	30	0.0935	10.5	65.94	0.6345	6.7887	6.1575	0.6311
22	30	0.0935	11	69.08	0.6963	7.4506	6.7887	0.6619
23	30	0.0935	11.5	72.22	0.7611	8.1433	7.4506	0.6927
24	30	0.0935	12	75.36	0.8287	8.8668	8.1433	0.7235
25	30	0.0935	12.5	78.5	0.8992	9.6211	8.8668	0.7543
26	30	0.0935	13	81.64	0.9726	10.4062	9.6211	0.7851
27	30	0.0935	13.5	84.78	1.0488	11.2221	10.4062	0.8159
28	30	0.0935	14	87.92	1.1279	12.0687	11.2221	0.8467
29	30	0.0935	14.5	91.06	1.2099	12.9462	12.0687	0.8774
30	30	0.0935	15	94.2	1.2948	13.8544	12.9462	0.9082

Σ 14 TOTAL TIME (min)

Qw (ft ³ /min)	Q _p (ft ³ /min)	V _{utotal} (ft ³)	Q _w /Q _p	a _{volume}	b _{volume}	a _{area}	b _{area}	Predicted		
160.41666	6.80	2222.48	23.59	1.41	-0.97	11.37	-0.94	V _{debris}	A _{debris}	D _{debris}
								144.26	655.44	28.89

Q_p must be ≥ A_{pile} * 1 foot : for the pile to be advanced into the soil

Figure 8-16 Example Spreadsheet for Pile Jetting Model.

The use of the spreadsheet requires that the user input the soil profile N-values, pump characteristics, pile geometry, and total depth of insertion. The output results include insertion time, debris area volume and diameter influenced by deposition.

CHAPTER 9 - ENVIRONMENTAL IMPACT OF PILE JETTING ON MACROBENTHOS IN NORTH CAROLINA

by

Dr. David B. Eggleston, Cynthia Huggett and Gayle Plaia
NC State University
Department of Marine, Earth & Atmospheric Sciences
Raleigh, NC 27695-8208
919-515-7840 (o), 515-7802 (FAX)
eggleston@ncsu.edu

The impact of jetting on infaunal macrobenthos within each jetting site was assessed as well as upstream and downstream of each jetting site. Suspended sediment from jetting operations could (1) smother and suffocate macrobenthic organisms, especially those that suspension-feed (e.g., clams), (2) alter community structure from relatively deeply buried species with large biomass (e.g, clams) to relatively shallow-dwelling species of low biomass (e.g, tube-building polychaetes), or (3) have relatively little long-term impact to macrobenthos because of rapid recolonization. Estuarine macrobenthic organisms such as clams and mussels are excellent bioindicators of estuarine health because they are generally sessile and integrate overlying water quality through their suspension-feeding activities. The objectives of the proposed study were to quantify the (1) abundance and species diversity of infaunal macrobenthos as a function of distance away from pile jetting operations, and (2) create GIS maps of each study site.

9.1 Sampling Locations and Testing Methods

Sediments and infauna were sampled at three sites (WOR, SQF and CPF) during March 29, 31 and 30, 2004 respectively. These dates were chosen to correspond with peak abundance of early juvenile clams in this region of North Carolina (Eggleston, unpubl. data), which increase our chances of identifying recolonization of areas disturbed by jetting. Each site had at least one group of 2-6 pilings jetted into the sediment—pilings were removed from the sediment after initial placement. At sites where there was more than one impact area, the area that was least affected by factors other than jetting (e.g., boat propeller wash, pilings, bulkheads) was chosen for sampling. Upon arrival at a site, the jetted area (area impacted by sediments due to jetting, IA) was located and markers were placed 5 and 20 meters upstream (U5 and U20) and downstream (D5 and D20) from the impact area. Sampling according to distance from the jetting site, as well as upstream and downstream of the jetting site, was intended to identify the likely spatial scales of impact. Five benthic samples were randomly taken at each area, starting at D20 and proceeding upstream, using a petite Ponar grab sampler (15.24 cm X 15.24 cm X ~7 cm deep) from a small (6 m) boat. We chose a distance of 5 m and 20 m from each impact area because the sediment thickness from a jetted piling declines to background levels at ~ 6 m from the IA. We chose a sample size (N) of five because our previous

experience with estuarine macrobenthos in similar systems indicates homogeneous variances are achieved at $N = 5-9$. Thus, a total of 25 grab samples (U20 = 5; U5 = 5; IA = 5; D5 = 5; D20 = 5) were taken at each site for a total of 75 grab samples. Each sample was washed through a 500 micron sieve, and then packed into 250ml plastic bottles with 10% buffered formalin. Information concerning sediment depth, as well as sediment color and characteristics, was recorded for each grab. For each sampling site, surface water temperature, salinity, and dissolved oxygen were measured using a YSI 85, pH was measured using an Acumet AP61, water depth was measured using a Hondex hand-held depth sounder, and turbidity was measured using an Orbeco-Hellige Portable Model 966, which measures in units of NTU (nephelometric turbidity units).

Chain of custody for samples followed EPA and NC DWQ protocols. State laboratory certification by the NC DWQ is NOT required for estuarine and marine benthic sample processing. Sample jars were labeled on the outside and inside of each jar to ensure proper tracking of a given sample as it was processed. All organisms were classified to species whenever possible with both Olympus dissecting and compound microscopes, using taxonomic keys by Fox and Bynum (1975), Day (1973), Roback (1980), NC DWQ (1997), Milligan (1997) and Epler (2001). To ensure quality of macrobenthic taxonomic identification and enumeration, a second taxonomist conducted occasional spot checks of previously sorted samples.

For a given site (WOR, SQF, CPF), we tested whether or not the mean total abundance, total number of species, as well as total number of polychaetes, crustaceans, mollusks, and insects varied significantly between the five sampling stations (20 m downstream, D20; 5 m downstream, D5; Impact area, IA; 5 m upstream, U5; 20 m upstream, U20) with a 1-way ANOVA (ANOVA=Analysis Of Variances). We hypothesized an increasing gradient in macrobenthic response variables with distance from each impact area, particularly upstream of an impact area. In cases where the variances of a given response were heterogeneous, the assumption of homogeneous variances was met after $\log(x+1)$ transformation of the response variable. *Post hoc* multiple comparison tests were conducted with a Ryan's *Q*-test, as recommended by Day and Quinn (1989).

Initially, we also planned to assess the scale of jetting impacts on macrobenthos with an index of biotic integrity (IBI; Kerans and Karr 1994). Generation of IBI values require minimally impacted sites that can be used to set expected values. In this study, there was no impact of jetting on the mean number of macrobenthic species as detected by ANOVA analyses. Thus, IBI analyses were not necessary.

Although the total numbers of animals or total numbers of species might not differ between impact and control sites upstream and downstream of the impact area, the impact area could harbor different dominant species, some of which may be more indicative of disturbed environments (e.g., tube-building oligochaete worms) than others. Thus, "Berger-Parker Diversity Indices" (Berger and Parker 1970) were used to assess dominance by a particular species as a function of distance from an impact area. For example, if jetting negatively impacted macrobenthos at the impact area, then we hypothesized that the impact area would be dominated by a single, or particular suite of species reflecting recent colonization, whereas sampling stations further upstream and

downstream of the impact area would be less dominated by a single species reflecting a more stable benthic community over time.

9.2 Results for Given Sites

A total of 75 benthic grab samples produced at least 10 families and 57 species (Appendix J-1). Insects, crustaceans, polychaetes, and mollusks contained the largest number of species (Appendix J-1). The White Oak River had the lowest average salinity and was essentially freshwater (0.12 ppt), followed by Cherry Point (2.78 ppt) and Swan Quarter (8.98 ppt) (Appendix J-2). Swan Quarter and Cherry Point had ~ 10 times the number of organisms and ~ twice the number of species compared to the White Oak River (see below). Dissolved oxygen levels at all locations (WO = 8.37 mg DO/l; CB = 8.89 mg DO/l; SQ = 9.86 mg DO/l) were well above hypoxic levels (2-4 mg DO/l). Water temperature was highest at the White Oak River (16 °C), followed by Cherry Point (13.52 °C) and Swan Quarter (12.86 °C). Average water depth was shallowest at the White Oak River (0.69 m), followed by Cherry Point (2.53 m) and Swan Quarter (2.81 m). Average turbidity was lowest at the White Oak River (NTU = 8.76) and highest at Cherry Point (NTU = 16.88) and Swan Quarter (NTU = 14.43) (Appendix J-2). The average depths to which the Ponar grab penetrated into the sediment to take a macrobenthic sample were similar between sampling locations, and ranged from an average low of 5.0 cm at Swan Quarter to a high of 6.3 cm at Cherry Point (Appendix J-2).

9.2.1 White Oak River

The White Oak River location was adjacent to NC Highway 1442 near Stella, NC as shown in Figure 9.1. The river was ~100 m wide at this site. The impact area (IA) consisted of 3 jetted areas on the west side of the river adjacent to the bridge about 7m from shore. Except for the bridge, the shore was natural salt marsh. This was a relatively freshwater site with very tannic water. The sediments from all cores were dark brown to black silt and clay with no visible redox potential layer and large amounts of organic debris. The sediment was browner at the IA and upstream of the IA than other sampling stations.

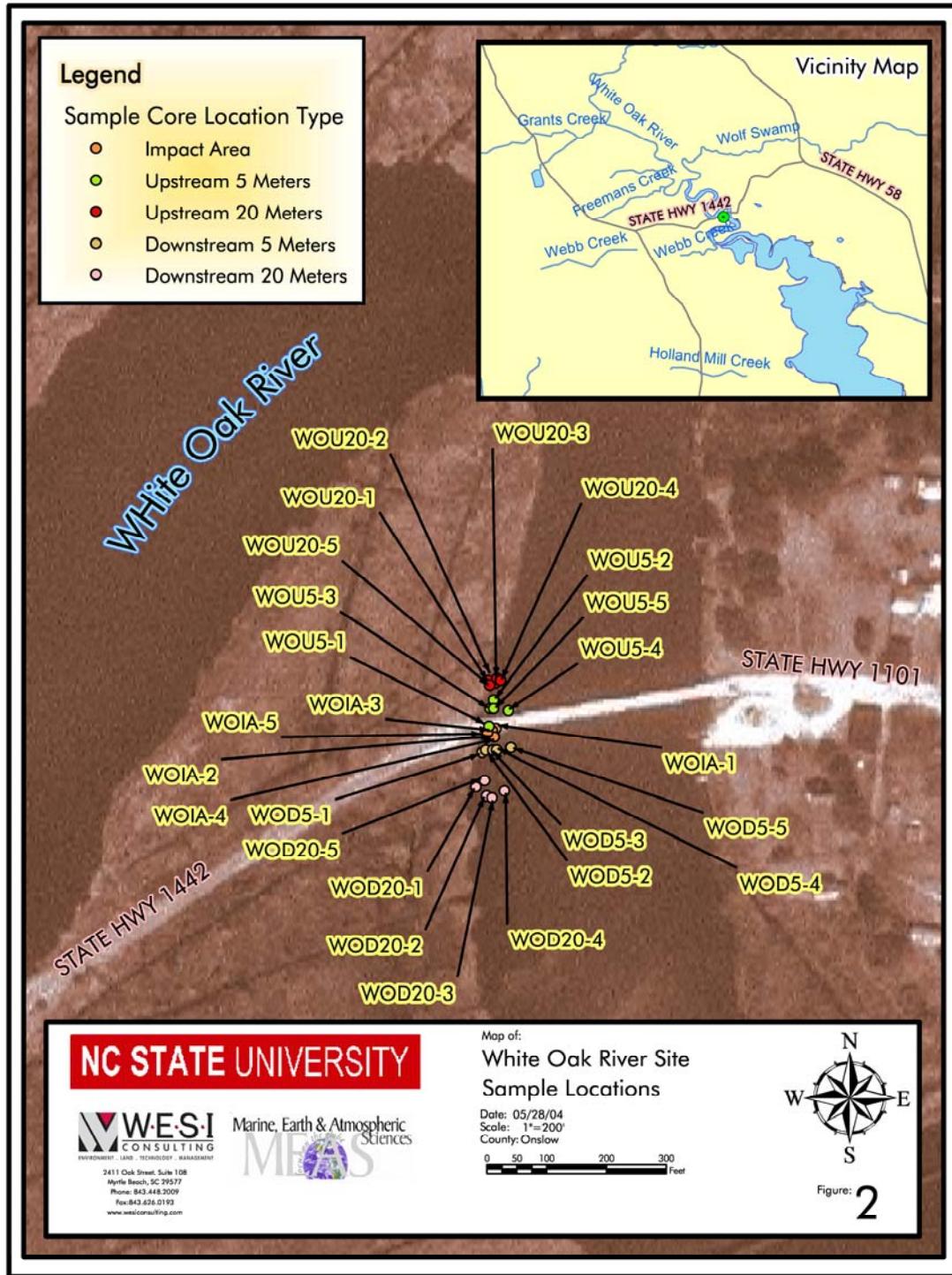
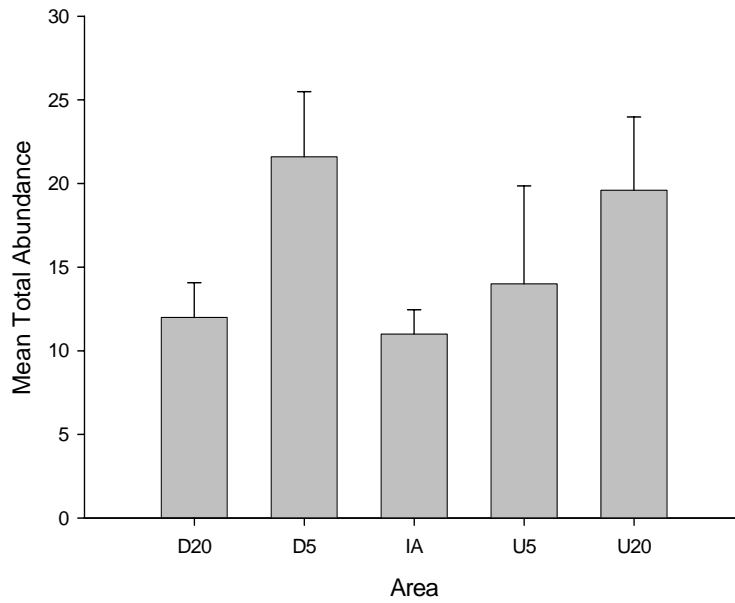


Figure 9-1 White Oak River: site sample locations

Figure 9.2 depicted that the mean total abundance of organisms per grab sample was lower in the IA and D20 sampling stations than other stations; however, the trend was not statistically significant (1-way ANOVA; $F = 1.47$, $df = 4, 25$, $P = 0.24$). As shown in Figure 9.3 the mean number of species per grab sample was similar across all sampling stations, and did not differ significantly from each other (1-way ANOVA; $F = 0.25$, $df = 4, 25$, $P = 0.91$). Although we expected to see the largest decrease in mean abundance and diversity of macrobenthos in the impact area and the station located 5 m downstream of the IA, the White Oak was not the case. We examined the response of the dominant taxonomic groups for evidence of an impact from jetting. Although the mean abundance of polychaetes and mollusks per grab sample was lowest in the impact area than other sampling stations as shown in Figure 9.3, the trend was not statistically significant (1-way ANOVA; both $P > 0.64$). The mean abundance of crustaceans was highest at the IA compared to other sampling stations, and the mean abundance of insects in the IA was somewhat similar to the mean abundance in other sampling stations—none of these trends were statistically significant (1-way analysis of variances (ANOVA); both $P > 0.25$).

The IA and downstream sites were all dominated by *Tubifex tubifex*, an oligochaete species of worm that is indicative of disturbed benthic habitats, whereas the upstream sites were dominated by insects as depicted in Table 9.1. Thus, the combined evidence from the ANOVA and Berger-Parker diversity analyses suggests that jetting may have negatively impacted primarily polychaete and molluscan species of macrobenthos only within the immediate impact area (i.e., not > 5 m away from the IA), although this trend was not statistically significant at an alpha level of 0.05, and that species adapted to disturbed habitats (tube-building oligochaetes) had colonized the impact area and areas downstream of the IA. The mean numbers of species appeared to be unaffected by the jetting disturbance.

White Oak River Total Abundance



White Oak River Number of Species

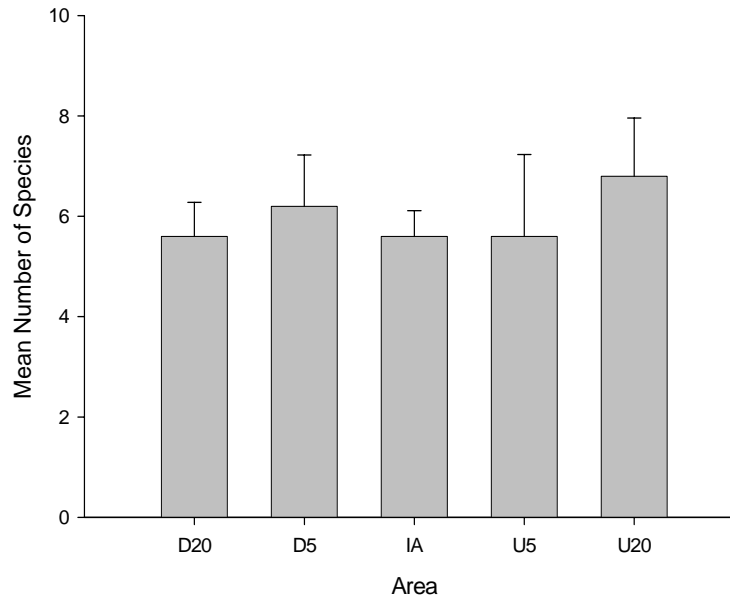


Figure 9-2 Mean (+ SE) total abundance and number of species of macrobenthic organisms (> 500 μm) collected with petite Ponar grab samples (N = 5) at the White Oak River in March 2004..

White Oak River

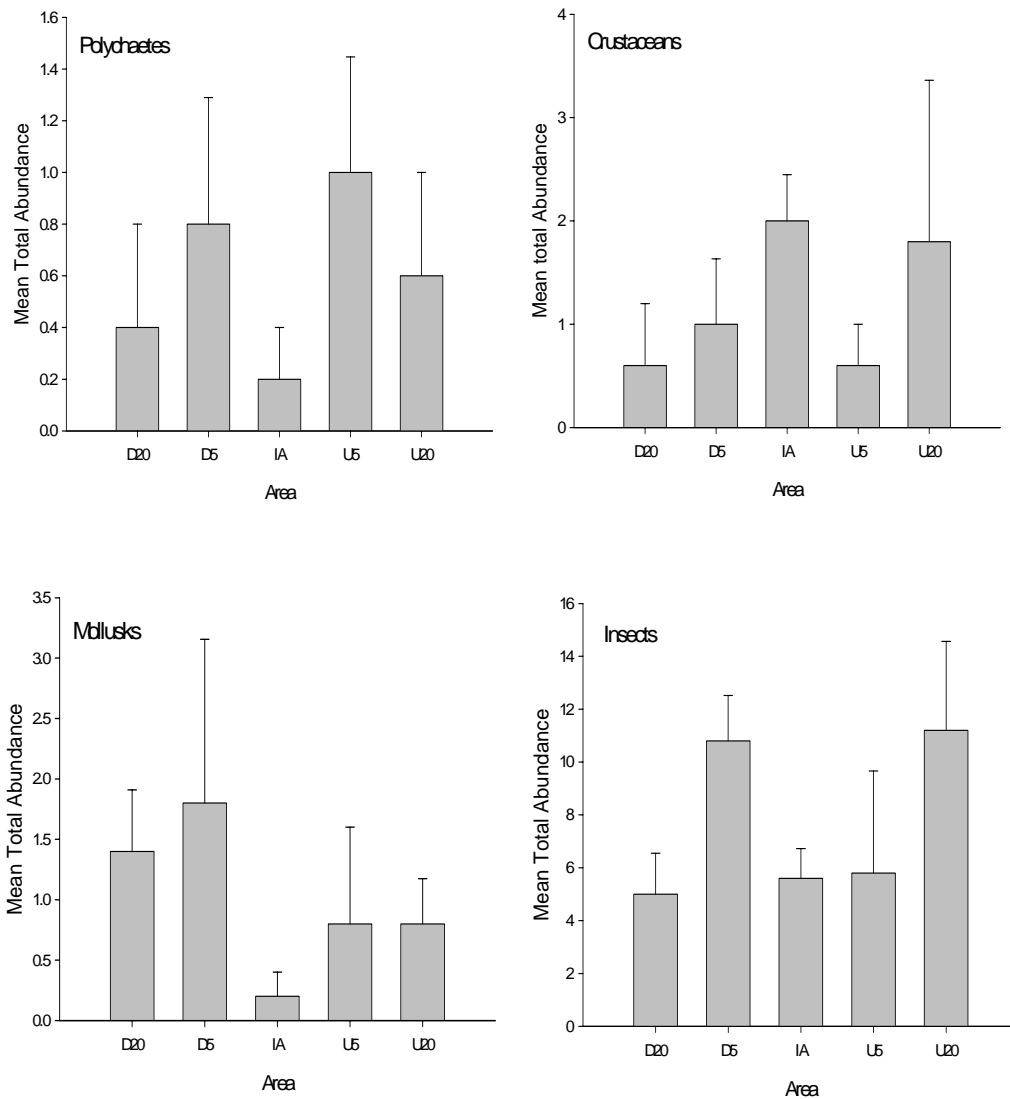


Figure 9-3 Mean (+ SE) total abundance of organisms within the dominant taxonomic groups (> 500 μ m) collected with petite Ponar grab samples (N = 5) at the White Oak River in March 2004. See text for results of statistical analyses

Table 9-1 Berger-Parker Diversity Index at White Oak River

Site	Area	# of Sp	N	Nmax	d	1/d	Dominant species
WO	D20	11	60	16	0.267	3.750	<i>Tubifex sp.</i>
	D5	10	108	32	0.296	3.375	<i>Tubifex sp</i>
	IA	11	55	13	0.236	4.231	<i>Tubifex sp</i>
	U5	14	70	18	0.257	3.889	<i>P. halterale</i>
	U20	14	98	19	0.194	5.158	<i>Micropsectra sp.</i>

9.2.2 Swan Quarter Ferry Basin

The Swan Quarter Ferry terminal basin was ~ 100m wide and oriented SW (entrance) to NE as shown in Figure 9.4. The basin was surrounded by natural marsh except for the ferry docks and, in some places adjacent to the IA, oyster shell. The IA was located in a somewhat irregular line ~ 7 m from shore. The current appeared to flow around the basin in a counterclockwise motion. Therefore, the downstream sites were located in the northwest corner of the northern end of the ferry basin, and the upstream sites in the southeast end. Except for the IA, sediment consisted of a 1cm or less brown layer over grey or black silt. The IA was noticeably sandier. Less organic debris was found at Swan Quarter than Cherry Branch or the White Oak River. Grab samples attempted less than 5m from the shore were unsuccessful due to the bottom being covered with oyster shell.

As shown in Figure 9.5, the mean abundance of macrobenthic animals per grab sample varied significantly with sampling area (1-way ANOVA; $F = 14.24$, $df = 4, 25$, $P = 0.0001$), and was significantly lower at the impact area (IA) than the other areas. Conversely, the mean number of macrobenthic species per grab sample did not vary significantly according to sampling area (1-way ANOVA; $F = 2.52$, $df = 4, 25$, $P = 0.07$). The pattern in mean abundance by sampling area was likely driven by polychaetes, since the mean abundance of polychaetes per grab sample varied significantly with sampling area (1-way ANOVA; $F = 14.31$, $df = 4, 25$, $P = 0.0001$), and was significantly lower in the impact area than any other areas. The mean abundance of mollusks also varied significantly according to sampling area (1-way ANOVA; $F = 7.93$, $df = 4, 25$, $F = 0.001$), and was significantly higher at the area 20m upstream of the impact area, compared to all of the other sampling areas of Figure 9.6. Figure 9.6 presented that no crustaceans were collected in upstream stations at Swan Quarter and there were significantly fewer crustaceans 5m downstream of the impact area than within the impact area, or 20 m downstream of the impact area. No insects were collected 5 m downstream and upstream of the impact area. The mean abundance of insects per grab sample was, however, significantly higher in the impact area than either 20 m upstream or downstream of the impact area.

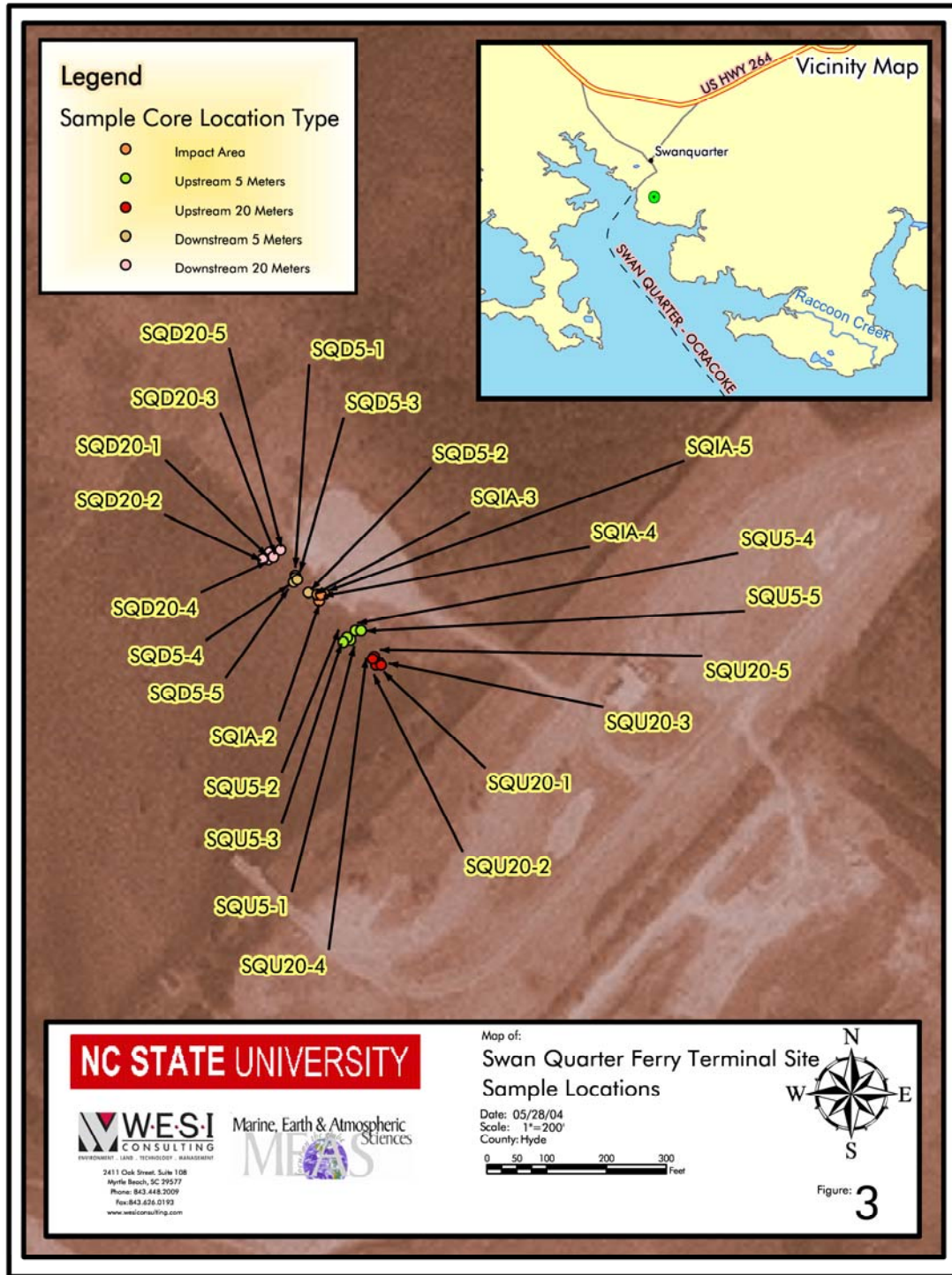


Figure 9-4 Swan Quarter Ferry Terminal: site sample locations.

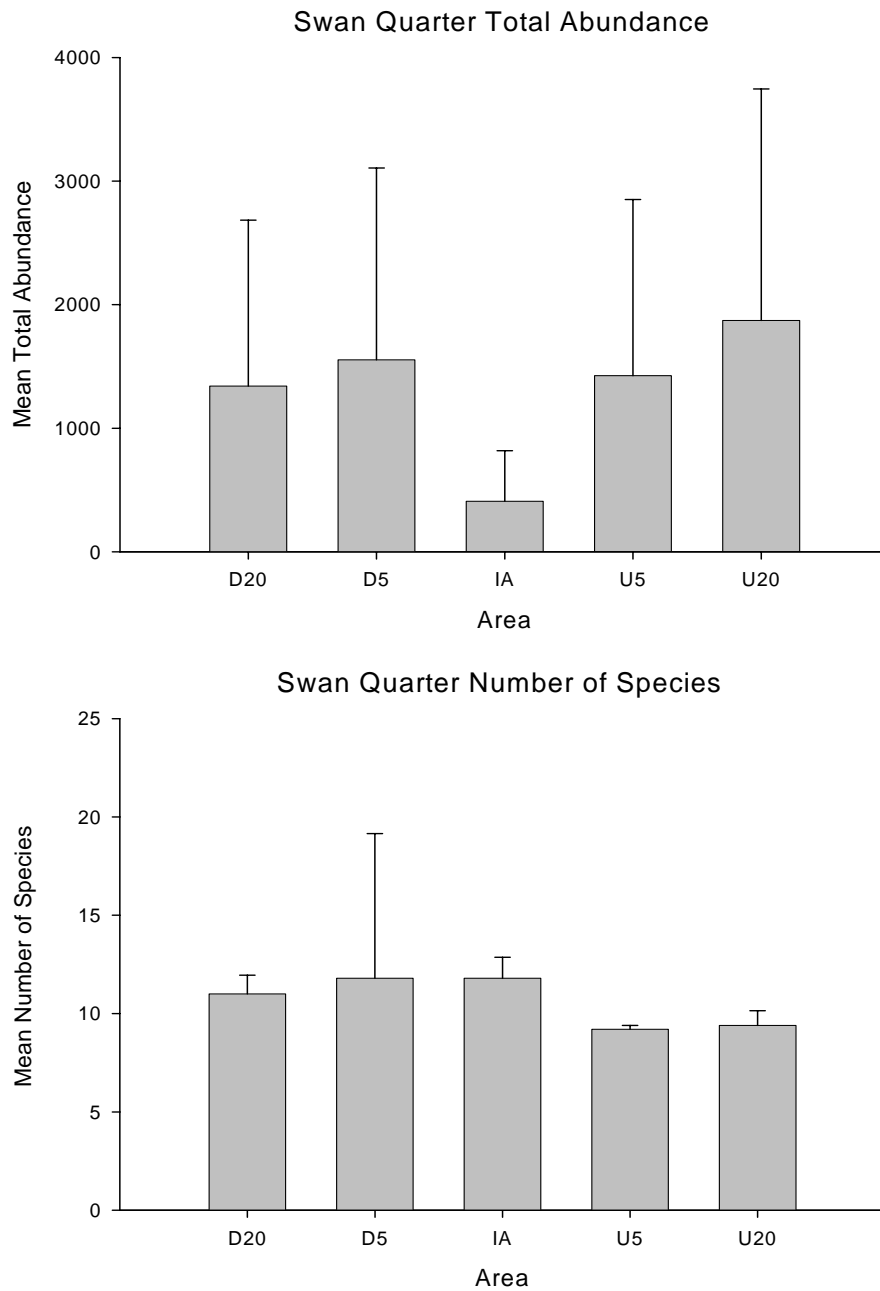


Figure 9-5 Mean (+ SE) total abundance and number of species of macrobenthic organisms (> 500 μ m) collected with petite Ponar grab samples (N = 5) at Swan Quarter in March 2004. See text for results of statistical analyses.

Swan Quarter Ferry Basin

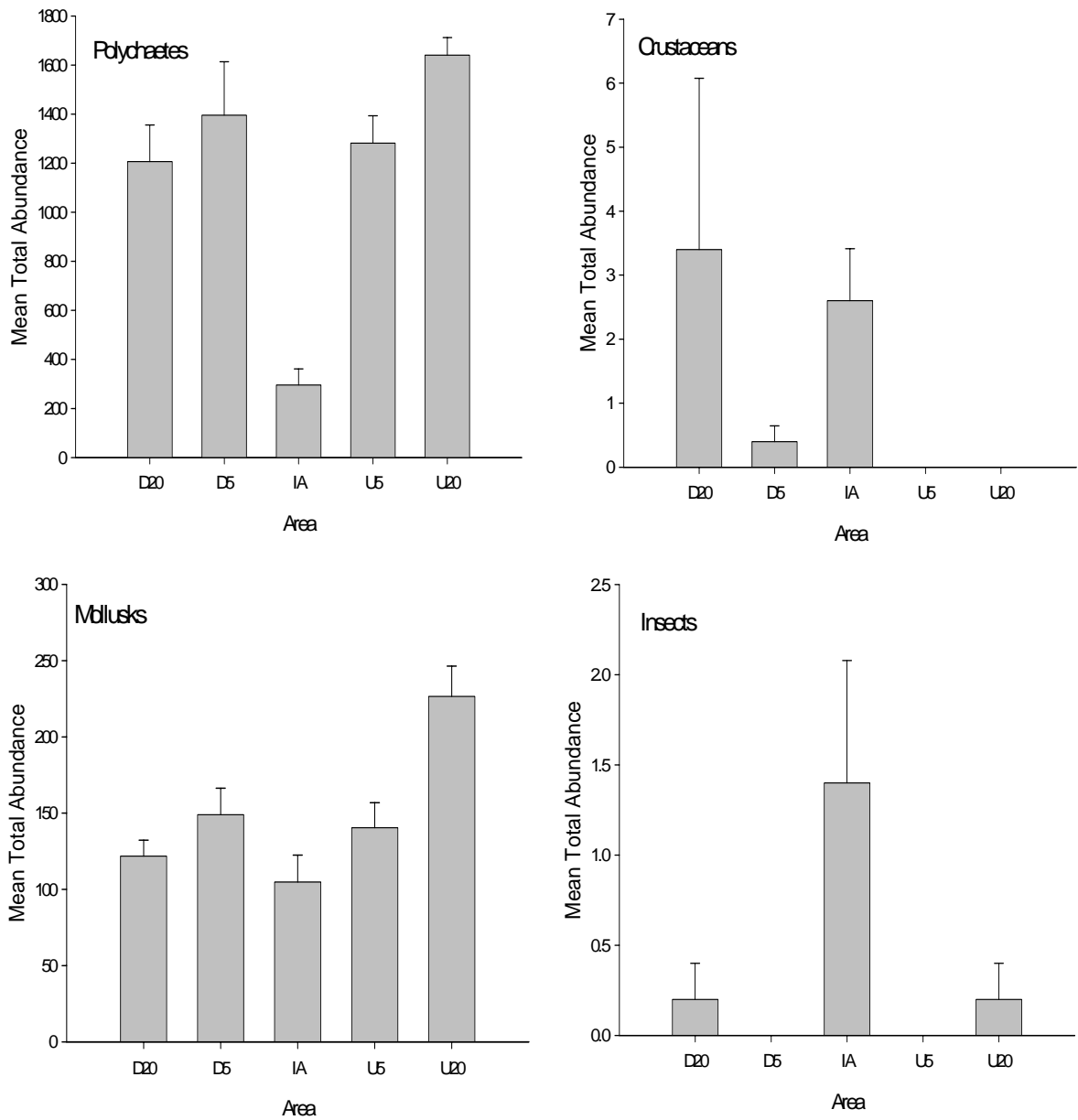


Figure 9-6 Mean (+ SE) total abundance of organisms within the dominant taxonomic groups (> 500 μ m) collected with petite Ponar grab samples (N = 5) at Swan Quarter in March 2004. See text for results of statistical analyses.

With the exception of the impact area, all sampling areas at Swan Quarter were dominated by the polychaete, *Mediomastus californiensis*, while the impact area was dominated by the polychaete, *Scolecopides viridis* as described in Table 9.2. Thus, the combined evidence from ANOVA and Berger-Parker diversity indices suggests that jetting may have negatively impacted the relative abundance and dominance of polychaetes, with significantly lower overall abundances of polychaetes in the impact area, and a shift from *M. californiensis* to *S. viridis* after jetting disturbance in the IA.

Although the mean abundance of mollusks did not vary according to sampling area, there was enough variation in size-frequency within the three major species of bivalves (*Macoma balthica*, *M. mitchelli*, *M. lateralis*) to assess the effects of jetting on bivalve size-frequencies. In this case, the size-frequency of *M. balthica* was similar between the impact area, and 20 m upstream and downstream of the IA as indicated in Figure 9.7. Conversely, the size-frequency of *M. mitchelli* and *M. lateralis* in the IA was generally restricted to smaller individuals compared to 20 m upstream and downstream of the IA, suggesting that these species of bivalves had recently colonized the impact areas.

Table 9-2 Berger-Parker Diversity Index at Swan Quarter

Site	Area	# of Sp	N	Nmax	d	1/d	Dominant species
SQ	D20	16	6709	4029	0.601	1.665	<i>M. californiensis</i>
	D5	17	7766	4734	0.610	1.641	<i>M. californiensis</i>
	IA	29	2045	1016	0.497	2.013	<i>S. viridis</i>
	U5	12	7126	4371	0.613	1.630	<i>M. californiensis</i>
	U20	13	9364	5245	0.560	1.785	<i>M. californiensis</i>

9.2.3 Cherry Point Ferry Basin

The Cherry Point Ferry Basin was ~75m wide, and oriented north-south with the entrance at the north end as presented in Figure 9.8. The basin was completely enclosed by a seawall and contained 3 impact areas (IAs). The two IAs along the sides of the basin could not be sampled because the seawall and barges were blocking the sampling area. Thus, the middle IA was sampled. A slight current was flowing into the basin and ferry traffic created wave action. The sampled IA consisted of 2 jetted areas. Downstream was located towards the southern end of the ferry basin. Sediment at the downstream sites consisted of a <1cm brown layer over black silt with a great deal of organic debris. The sediment surfaces of most samples were densely covered with tubes from tube-worms. At the IA, the brown sediment layer was noticeably deeper (2-5cm). The upstream sites contained a ~2cm brown layer of sediment.

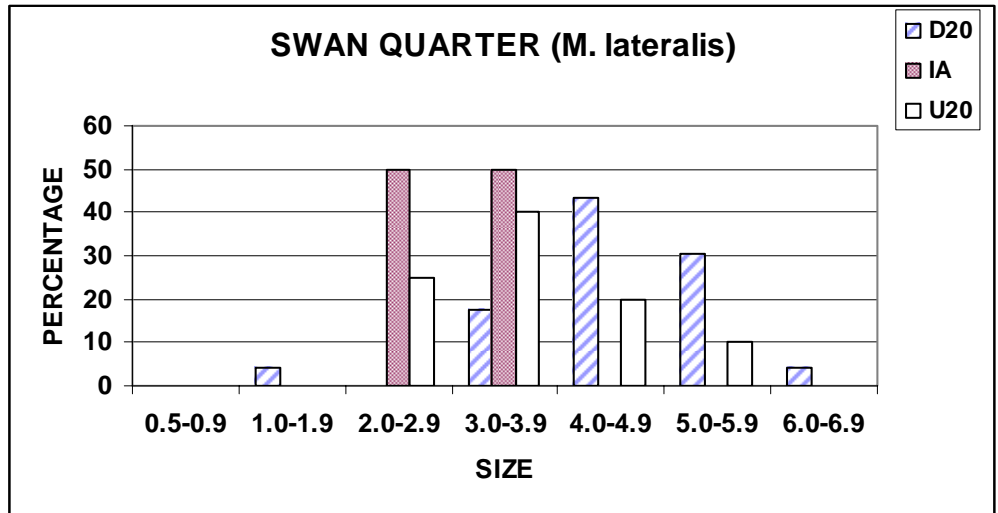
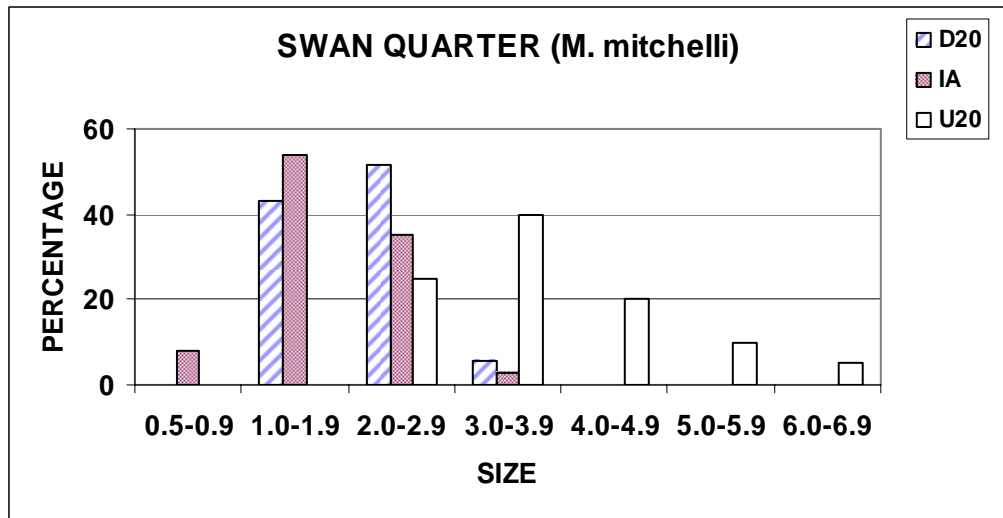
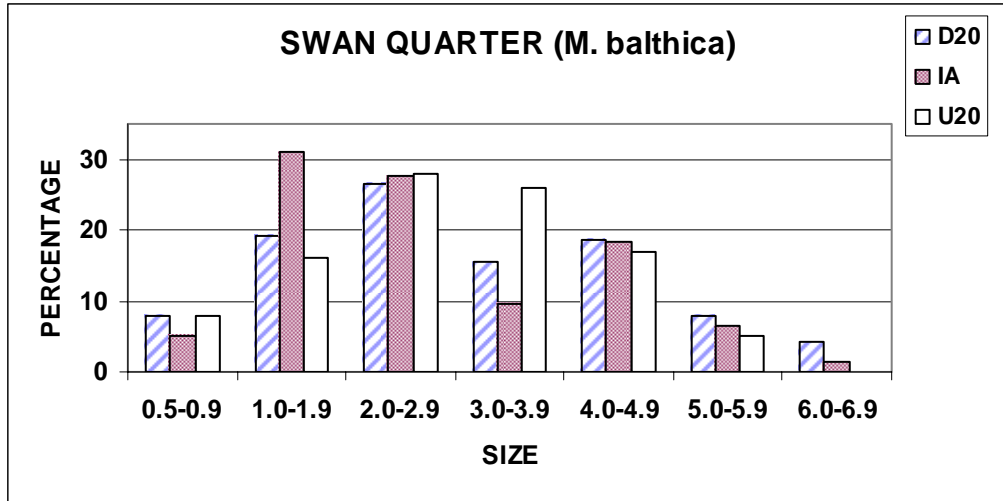


Figure 9-7 The size-frequency of the three dominant species of bivalves collected with a petite Ponar grab sampler at Swan Quarter in March 2004.

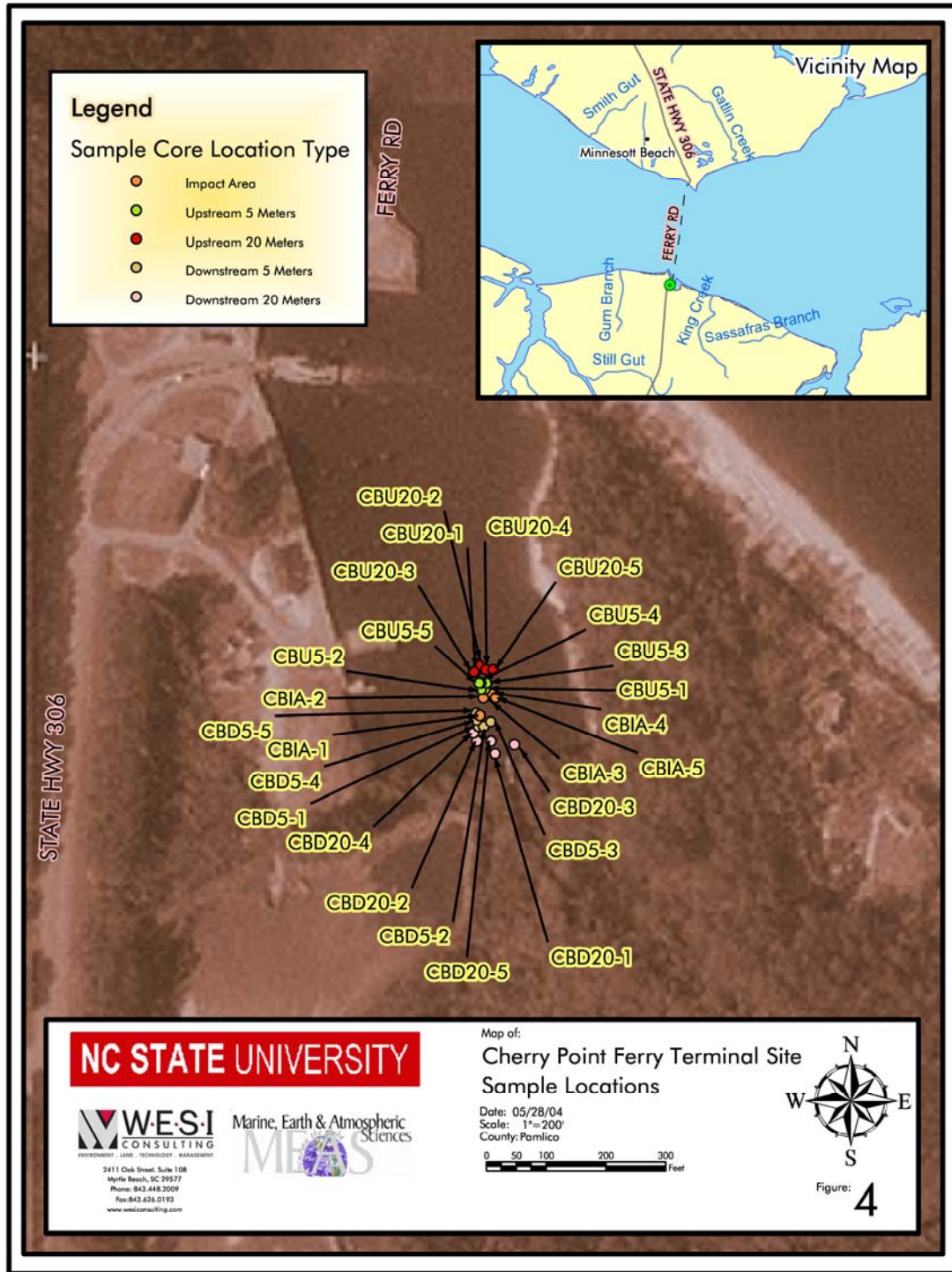


Figure 9-8 Cherry Point Ferry Terminal: site sample locations

Figure 9.9 showed that the mean total abundance of organisms and the mean total numbers of species per grab were similar between sampling areas, and did not differ significantly (two-way ANOVA, all $p > 0.39$). When examined by taxonomic groups, there may have been an impact of jetting on mollusks, but not polychaetes, insects, or crustaceans. For example, the mean number of mollusks per grab varied significantly according to sampling area (1-way ANOVA; $F = 9.54$, $df = 4, 25$, $P = 0.0001$), with lowest abundances 20 m downstream of the IA, followed by the IA and 5 m downstream of the IA, and highest abundances upstream of the IA. Although the mean number of crustaceans per grab were lowest at the IA and upstream of the IA, the latter of which would not be consistent with an impact of jetting, there was no significant difference in mean abundance of crustaceans across sampling areas (1-way ANOVA; $F = 0.60$, $df = 4, 25$, $P = 0.66$), probably because of the very high variance in mean crustacean abundances at the downstream stations as illustrated in Figure 9.10. The mean abundances of polychaetes and insects did not vary significantly according to sampling area (1-way ANOVA; both $P > 0.33$).

With the exception of 20m downstream of the IA, Table 9.3 showed that all sampling areas were dominated by the infaunal clam, *Macoma balthica*, which is a suspension-feeding and facultative deposit-feeding bivalve. The dominance of *M. balthica* decreased downstream of the IA. The D20 sampling area was dominated by insect larvae, *Chironomus sp.* Thus, the combined evidence from ANOVA and Berger-Parker diversity indices suggests that jetting may have negatively impacted the relative abundance of mollusks, but the impact was not large enough to alter the overall dominant species group, which was *Macoma balthica*. The mean numbers of species appeared to be unaffected by the jetting disturbance.

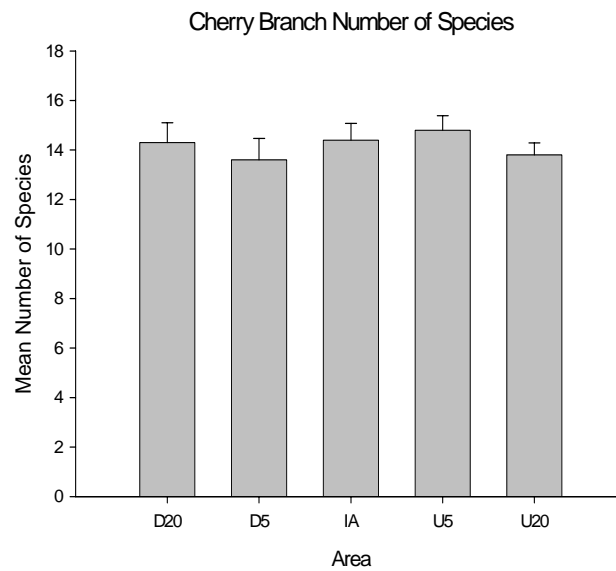
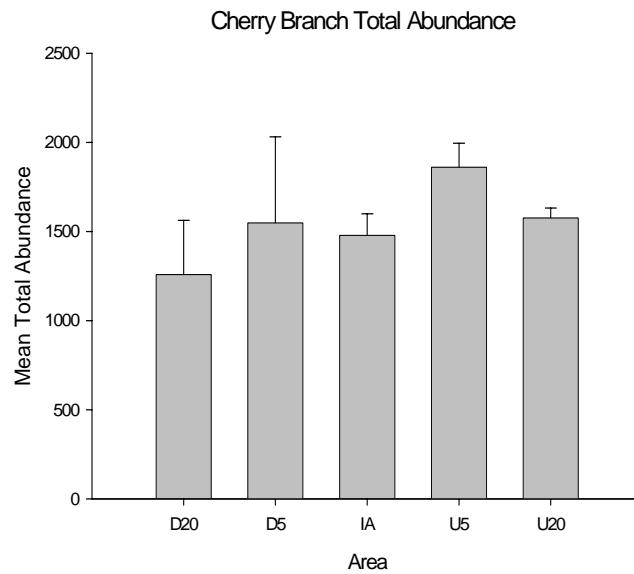


Figure 9-9 Mean (+ SE) total abundance and number of species of macrobenthic organisms ($> 500 \mu\text{m}$) collected with petite Ponar grab samples ($N = 5$) at Cherry Point in March 2004. See text for results of statistical analyses.

Cherry Branch Ferry Basin

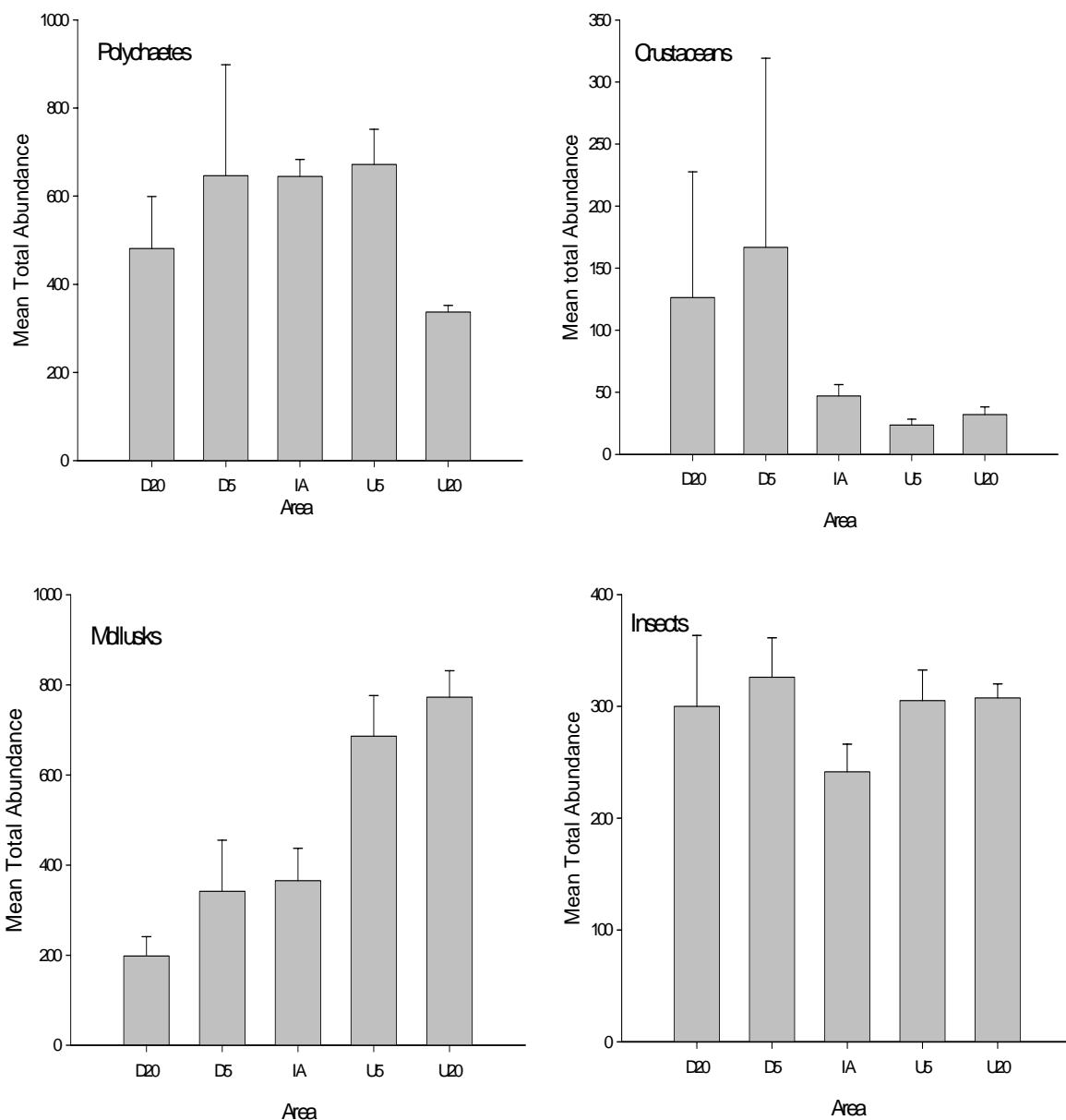


Figure 9-10 Mean (+ SE) total abundance of organisms within the dominant taxonomic groups (> 500 μ m) collected with petite Ponar grab samples (N = 5) at Cherry Point in March 2004. See text for results of statistical analyses.

Table 9-3 Berger-Parker Diversity Index at Cherry Branch

Site	Area	# of Sp	N	Nmax	d	1/d	Dominant species
CB	D20	17	6291	1476	0.235	4.262	<i>Chironomus sp.</i>
	D5	21	7742	1618	0.209	4.785	<i>M. balthica</i>
	IA	18	7390	1717	0.232	4.304	<i>M. balthica</i>
	U5	19	9303	3288	0.353	2.829	<i>M. balthica</i>
	U20	18	7880	3746	0.475	2.104	<i>M. balthica</i>

9.3 Summary of Environmental Impact of Pile Jetting On Macrobenthos

The goal of this study was to begin to assess the environmental impact of jetting pilings on estuarine and freshwater macrobenthos. Macrobenthos are useful organisms to assess sediment- and water-quality-related impacts because they are generally sessile and integrate overlying water quality in terms of growth and survival (Kerans and Karr 1994). Although we expected to see the largest decrease in mean abundance and diversity of macrobenthos in the impact area and the sampling areas located 5 m downstream of the IA, this was generally not the case. The key findings were: (1) the mean number of macrobenthic organisms was significantly lower at the impact area (IA) compared to sampling areas that were 5 m and 20 m upstream and downstream of the IA at only one of three sites (i.e., Swan Quarter), (2) the mean number of macrobenthic species did not vary significantly according to sampling area, including the impact areas, (3) at the White Oak River, jetting had no statistically significant effect on the mean number organisms nor the mean number of macrobenthic species; however, species adapted to disturbed habitats (tube-building oligochaetes) had colonized the impact area and areas downstream of the IA, (4) at the Swan Quarter Ferry, jetting may have negatively impacted the relative abundance and dominance of polychaetes, with significantly lower overall abundances of polychaetes in the impact area, and a shift from *M. californiensis* to *S. viridis* after jetting disturbance within the IA, and (5) at the Cherry Point Ferry, jetting may have negatively impacted the relative abundance of mollusks, primarily the infaunal clam, *M. balthica*, with significantly lower abundances 20 m downstream of the IA, followed by the IA and 5 m downstream of the IA, and significantly higher abundances upstream of the IA. Thus, 4-9 months after jetting, the mean abundance and species composition of macrobenthos, primarily polychaetes and molluscan bivalves, sometimes showed a negative response to jetting disturbances, however, this biological response to disturbance was isolated in space to < 5 m away from the general impact area, including downstream areas, and did not negatively alter the overall numbers of macrobenthic species. The spatially isolated nature of the impact on macrobenthos observed in this study is consistent with the scale of impact by jetting on the sediment thickness, where sediment thickness from a jetted piling declines to background levels at ~ 6 m from the impact area (M. Gabr and L. Denton, unpubl. data).

Although macrobenthos are good bio-indicators of negative changes in water quality, they are also very resilient to physical disturbance events, and are capable of relatively rapid recolonization after major disturbances (Burkholder et al. 2004 and

references therein). Thus, although jetting pilings may negatively impact macrobenthic organisms such as mollusks and polychaetes, this impact will likely be isolated in space to < 5 m from an impact area (this study), and recovery should occur within 1-2 years (Burkholder et al. 2004).

CHAPTER 10 - EFFECTS OF PILE JETTING ON TIDAL MARSH VEGETATION

by

Dr. Stephen W. Broome
Department of Soil Science
NC State University

Raleigh, NC 27695-8208

Utilization of Jetting for pile installation in tidal marshes directly affects marsh vegetation by burial where sediment is deposited, by changing the elevation, which determines the plant species that can successfully recolonize the affected area, and by altering the physical and chemical properties of the root zone. Elevation relative to tidal inundation and salinity are the two major environmental factors that determine zonation of plant species within tidal marshes. In North Carolina, and along the east coast of the United States, zonation of vegetation in regularly flooded salt marshes is very distinct. The elevation zone from mean high water to mean high tide is nearly a monoculture dominated by *Spartina alterniflora* (smooth cordgrass). Immediately above mean high tide, *Spartina patens* (salt marsh hay) is dominant followed by a shrub zone on the landward side. Common shrub species are *Myrica cerifera* (wax myrtle), *Baccharis halimifolia* (eastern baccharis), and *Juniperus virginiana* (eastern red cedar). In irregularly flooded brackish-water marshes, plant species diversity is greater and zonation may be less pronounced, but plant species and growth are affected by changes in elevation.

10.1 Methods

Effects of jetting for pile installation, which occurred in 2003, on tidal marsh vegetation was assessed at the Swan Quarter and White Oak River sites on April 28 and 29, 2004. The Sampson county site was also visited; however, at that site pile jetting occurred on the upland adjacent to a wetland. Subsequent construction work, grading and seeding erased any apparent jetting effects on the upland or the wetland.

Jetting effects on vegetation at Swan Quarter and White Oak River were assessed by listing each plant species present, recording plant species that were recolonizing spoil deposits, and taking soil samples from spoil deposits and adjacent undisturbed reference marshes. Soil samples were returned to the laboratory, dried in a forced air oven at 35 degrees C, passed through a 2-mm sieve and analyzed by the N.C. Department of Agriculture Soil Testing lab for plant available nutrients, pH and sodium.

10.2 Results for Given Sites

10.2.1 Swan Quarter Marsh

The test area at Swan Quarter is near the ferry terminal in a small brackish-water marsh that has vegetation typical of the Pamlico Sound shoreline as shown in Fig. 10.1. The upper marsh on the left of Figure 10.1 is dominated by *Spartina patens* and *Distichlis spicata* which transitions into the upland shrub zone (April 28, 2004). Plant species observed at the site are described in Table 10.1 and Figure 10.2 and 10.3. The four jetting installations at the site were designated SQ-7, SQ-8, SQ-9 and SQ-10. At SQ-7, sediment deposited near the jetted pile hole was 14 cm deep and consisted of sand with small amounts of clay inclusions and some shell fragments. The spoil covered an area within a radius of about 3 meters around the hole. Shoots of *Scirpus robustus*, which were buried by the jetting spoil, were emerging from the sand. Very little *Distichlis spicata* was coming through the sand, but probably will come back from the edges of the spoil as rhizomes and stolons grow.

Table 10-1 Plant species observed in marshes at Swan Quarter and White Oak River

		Scientific Name	Common name
Swan Quarter	Low and mid marsh	<i>Spartina alterniflora</i> <i>Spartina patens</i> <i>Juncus roemerianus</i> <i>Distichlis spicata</i> <i>Scirpus robustus</i> <i>Scirpus pungens (Scirpus americanus)</i>	smooth cordgrass saltmeadow cordgrass black needle rush salt grass salt-marsh bulrush
	Marsh/upland edge	<i>Phragmites australis</i> <i>Festuca arundinacea</i> <i>Melilotus officinalis</i> <i>Rhus radicans</i> <i>Myrica cereifera</i> <i>Baccharis halimifolia</i> <i>Pinus taeda</i>	common reed tall fescue sweet clover poison ivy wax myrtle groundsel tree loblolly pine
White Oak River	Low and mid marsh	<i>Spartina alterniflora</i> <i>Spartina cynosuroides</i> <i>Spartina patens</i> <i>Juncus roemerianus</i> <i>Distichlis spicata</i> <i>Scirpus robustus</i> <i>Scirpus pungens (Scirpus americanus)</i>	smooth cordgrass big cordgrass saltmeadow cordgrass black needle rush salt grass salt-marsh bulrush three-square bulrush
	Higher elevations	<i>Myrica cerifera</i> <i>Juniperus virginiana</i> <i>Rhus radicans</i> <i>Pinus taeda</i>	wax myrtle red cedar poison ivy loblolly pine



Figure 10-1 . Irregularly flooded brackish-water marsh at Swan Quarter showing spoil from pile jetting installations.



Figure 10-2 *Juncus roemerianus* patch along the shoreline at Swan Quarter.



Figure 10-3 *Spartina alterniflora* is present along small creeks at the Swan Quarter.

Spoil was 10 cm deep covering 1-2 meters in each direction around the SQ-8 jetting hole. There was a second deposit of sand around a blowout that occurred approximately 3 meters from the jetting hole. This deposit of spoil was 18 cm deep. No vegetation was growing on either of these deposits, but there was evidence that *D. spicata* was beginning to grow in around the edges. The SQ-9 jetting hole was similar to SQ-8 with a 12-cm deep sand deposit adjacent to the hole, and an 18-inch blowout deposit 3 meters from the hole. There were a few *D. spicata* shoots emerging from the sand and *D. spicata* was growing in around the edges of each sand deposit. Sand deposited around SQ-10 was 14 cm deep with a few inclusions of fine material and covered an area 2 to 3 meters around the hole. Shoots of *Phragmites australis* and *Juncus roemerianus* were emerging from the sand.

Chemical properties and plant nutrient availability of sandy spoil deposited on the marsh surface at Swan Quarter was very different from the adjacent reference areas as described in Table 10.2. The spoil has higher pH and lower humic matter, P, Ca, Mg, and Na. Plant growth in tidal marshes is often limited by nitrogen and phosphorus availability. The property that would most likely affect plant growth on the spoil at this location is plant-available P. Nitrogen was not included in the soil test, but is also likely to be deficient. The coarse texture of the spoil and the low humic matter are indicators that point to extremely low plant-available N. The effects of the poor nutrient status of the spoil may be less if plant roots can reach the underlying natural marsh soil to absorb N and P. Applying N and P fertilizers would accelerate restoration of vegetation on the spoil deposits at this site.

Table 10-2 Results of analyses of soil samples from Swan Quarter

Sample ID	Wt/Vol (g/cm ³)	pH	Matter (g/100 cm ³)	P (mg/dm ³)	K (meq/100 cm ³)	Ca (meq/100 cm ³)	Mg (meq/100 cm ³)	Na (meq/100 cm ³)
SQ-7	1.26	7.5	0.22	4.4	0.34	6.6	4.4	10.1
control	0.81	5.5	6.58	11.6	0.99	4.4	9.0	12.6
SQ-8	1.28	7.3	0.6	11.8	0.53	10.2	3.7	9.1
SQ-8 washout	1.42	6.9	0.18	4.8	0.10	4.0	1.0	1.4
control	0.56	4.8	1.87	8.2	1.11	14.5	9.5	19.1
SQ-9	1.26	7.4	0.27	0.0	0.32	7.2	3.1	9.9
SQ-9 washout	1.39	3.9	0.13	10.2	0.08	1.0	1.3	2.2
control	0.71	5.3	5.23	14.1	0.86	3.2	6.6	11.6
SQ-10	1.38	6.4	0.13	6.1	0.26	5.4	2.0	5.4
control	0.91	5.5	2.37	14.7	0.97	6.5	6.9	9.0

SQ- Swan Quarter

WO- White Oak River

10.2.2 White Oak River

The White Oak River marsh is also brackish water, but the mix of plant species is different from that at Swan Quarter. *Spartina cynosuroides* and *Juncus roemerianus*, as shown in Figure 10.4 and Figure 10.5, are the dominant plant species, and most of the site appears to be lower and wetter with more frequent tidal inundation than Swan Quarter. Vegetation includes *Juncus roemerianus*, *Spartina alterniflora*, and *Scirpus* spp. growing in a drainage ditch, *Juncus roemerianus*, the previous year's seed stalks of *Spartina cynosuroides* and shrubs scattered across the marsh.

The three pile jetting installations within the marsh were designated WO-4, WO-5 and WO-6. The WO-4 and WO-5 sites were close together so they were combined for sampling purposes. The sand deposit near the WO-4 and WO-5 sites was 12 cm deep. There was also some fill sand that was trucked in to fill the hole, and this was sampled separately. New shoots from plants were beginning to emerge around the outer edges of the sand deposits. On the edge toward the marsh, emerging plant species were *Juncus roemerianus*, *Distichlis spicata*, *Scirpus robustus* and *Polygonum* spp. On the landward edge toward the highway, emerging plants were *Scirpus americanus*, *D. spicata*, and *Juncus roemerianus*.



Figure 10-4 White Oak River spoil from pile jetting installation



Figure 10-5 Vegetation at White Oak River Marsh. *Spartina alterniflora* (center)

Sand deposited around the WO-6 pile jetting installation was 6-10 cm deep, but the spoil deposit impacted a relatively small area. A thick organic surface layer at this site reduced the depth of sand penetrated by pile jetting. Uplift of the surface by jetting was about equal to the thickness of the spoil at this site. Plants recolonizing the area were *J. roemerianus*, *S. robustus*, and *Spartina patens*.

Results of soil analyses from White Oak River indicated much higher plant available P levels in both the spoil and the natural marsh than at Swan Quarter as listed in Table 10.3. The spoil from the WO-6 jetting installation was exceptionally high in P, and P levels in all of the samples were adequate to support plant growth. Generally the natural marsh soils had higher humic matter, K, Ca, Mg and Na contents, but the only plant nutrient that might be limit plant growth on the spoil would be nitrogen. Plant nutrients are not likely to be a limiting factor in plant growth on the spoil at White Oak River.

Table 10.3 Results of analyses of soil samples from White Oak River marshes

Sample ID	Wt/Vol (g/cm ³)	pH	Matter (g/100 cm ³)	P (mg/dm ³)	K (meq/100 cm ³)	Ca (meq/100 cm ³)	Mg (meq/100 cm ³)	Na (meq/100 cm ³)
WO-4/5	1.42	6.8	0.22	29.7	0.19	4.2	1.6	3.2
WO-4/5 fill	1.38	6.8	0.18	35.5	0.14	3.4	1.2	2.8
control	0.63	5.5	2.68	42.6	0.97	8.4	11.3	6.4
control	0.64	4.7	2.68	45.4	1.18	8.9	12.5	9.2
WO-6 white	1.43	4.6	0.13	453.0	0.08	5.4	0.8	0.8
WO-6 brown	1.40	4.5	0.18	208.4	0.06	3.9	0.6	0.6
control	0.47	5.2	2.29	46.4	0.46	11.0	11.1	5.0
control	0.48	4.6	2.44	41.9	0.60	8.5	7.3	3.8

SQ- Swan Quarter

WO- White Oak River

10.3 Summary of Effects of Pile Jetting On Tidal Marsh Vegetation

Sediments deposited around pile jetting installations in two brackish-water marshes resulted in sandy spoil deposits on the marsh surface, uplift of the marsh surface, and some blowout deposits of sand. The potential effects on marsh vegetation (and benthic organisms) are burial of existing vegetation, increased elevation of the surface (changing tidal inundation), and a change in physical and chemical properties of soil in the root zone of plants that may grow on the spoil. The long-term impact of the elevation change on marsh vegetation is likely to be minimal in these marshes even if the spoil deposits are not removed. The elevation changes due to uplift of the original surface plus the spoil deposit does not exceed the maximum elevation of some plant community in each marsh.

The change in elevation may result in a different assemblage of plants in the impacted area, but it is still within the maximum elevation limits of marsh vegetation at each site.

Spoil deposited at each of the jetting installations was deep enough to bury existing vegetation, but there was evidence of regrowth by shoots coming up through the spoil deposits or rhizomes growing into the affected area from the edges. Although physical and chemical properties of the spoil were very different than the reference marsh soil, the spoil will eventually support plant growth. Tidal flushing and deposition of sediment by tidal action modify soil properties and nutrient availability over time. At Swan Quarter, where the sandy spoil is very phosphorus deficient, applying and incorporating phosphate fertilizer would enhance establishment of vegetation. An assessment of recovery of vegetation at the end of this growing season (2004) and a year from now (summer or fall of 2005) could more conclusively determine the extent of recovery of vegetation at the pile jetting sites and determine whether mitigation is needed.

Effects of spoil deposits on the marsh vegetation could be mitigated by removal, but removal activity might cause additional damage to surrounding vegetation. Another approach to mitigation would be to plant marsh vegetation adapted to the elevation created by the deposit and enhancing growth by adding nitrogen and phosphorus fertilizers.

CHAPTER 11 - SUMMARY AND CONCLUSIONS

Work presented in this report described the development of pile jetting model for the computation of jetting-induced debris zone on the surface in various soil profiles through implementation of a laboratory and field testing programs, and comprehensive data analyses. The study is systematically performed to characterize the surface disturbance and associated ecological impacts due to pile jetting process. From the laboratory testing program, the physical phenomenon of jetting was observed and a model for computing the disturbance created by jetted-pile installations was presented. Field testing encompassed four test sites in different geographical locations of Eastern North Carolina. A total of 26 jetted pile installations were performed to aid in model development and verify the behavior observed during laboratory experimentations. The laboratory and field testing results were used to develop a phenomenological model that is empirical in nature. Based on the analyses of data and environmental impacts, the following conclusions are advanced.

- i. Installation of piles using jetting approach stems from the simultaneous erosion of soils beneath the pile tip and transport of these soil particles through the annulus to the ground surface. The pile advances only after a sufficient area of soil has been eroded to cause a tip bearing capacity failure as side friction is reduced due to the return water and liquefaction jetting annulus.
- ii. Optimization of water flowrate (Q_w) and jet nozzle velocity (V_j) for a given soil profile provides minimal debris zone dimensions for jetted installations. In general, higher jet velocities with longer flow rates will produce smaller debris zones.
- iii. Given equal jetting parameters, the extent of the debris zone for sands with smaller average particle sizes ($D_{50} = 0.15$ mm) were approximately 100% further from the pile center than sands with larger average particle size ($D_{50} = 0.5$ mm).
- iv. Based on results from the field research program, it was determined that the diameter of the debris zones created from the jetting process was generally equivalent to the jetted depth of pile. Furthermore, the volume of debris material measured around the annulus of pile was generally equal to, or slightly more in case of dense profiles than, the inserted volume of pile for a particular installation.
- v. A proposed phenomenological model provides an estimate of debris zone characteristics. The model was verified through data obtained from field testing. The results of the verification study indicate that the results from the model agree fairly with field data. In 11 cases, the model results over predicted the measured debris volume and diameters. In six

- cases, the model under predicted the measured values by approximately 20% on the average.
- vi. A model component, capable of estimating the change in bedform length due to under water current velocity, was proposed based upon published literature on sediment transport. The proposed procedure, while not verified by field testing, should give a conservative estimate of the extent of distribution of the plume of fine particles during underwater jetting applications, based on an assumed flow depth.
 - vii. A design procedure was outlined for implementing the proposed three part jetting model that include insertion rate, volume and size of disturbance zone, and change in bedform due to under current velocities. A spreadsheet was developed and presented for determination of the insertion characteristics and debris volume and lateral extent.
 - viii. At only one of three sites (i.e., Swan Quarter), the mean number of macrobenthic organisms was significantly lower at the impact area compared to sampling areas that were 5 m and 20 m upstream and downstream).
 - ix. The mean number of macrobenthic species did not vary significantly according to sampling area, including the impact areas, and at the White Oak River jetting had no statistically significant effect on the mean number organisms nor the mean number of macrobenthic species; however, species adapted to disturbed habitats (tube-building oligochaetes) had colonized the impact area and areas downstream.
 - x. It seems that 4-9 months after jetting, the mean abundance and species composition of macrobenthos, primarily polychaetes and molluscan bivalves, sometimes showed a negative response to jetting disturbances, however, this biological response to disturbance was isolated in space to < 5 m away from the general impact area, including downstream areas, and did not negatively alter the overall numbers of macrobenthic species.
 - xi. The spatially isolated nature of the impact on macrobenthos observed in this study is consistent with the scale of impact by jetting on the sediment thickness, where sediment thickness from a jetted piling declines to background levels at ~ 6 m from the impact area.
 - xii. It seems that on land, the long-term impact of elevation change due to jetting on marsh vegetation is likely to be minimal even if the spoil deposits are not removed. The elevation changes due to uplift of the original surface plus the spoil deposit does not exceed the maximum elevation of some plant community in each marsh.
 - xiii. While spoil deposited at each of the jetting installations was deep enough to bury existing vegetation, there was evidence of regrowth by shoots coming up through the spoil deposits or rhizomes growing into the affected area from the edges.

- xiv. At Swan Quarter, where the sandy spoil is very phosphorus deficient, applying and incorporating phosphate fertilizer would enhance establishment of vegetation. An assessment of recovery of vegetation at the end of this growing season (2004) and a year from now (summer or fall of 2005) could more conclusively determine the extent of recovery of vegetation at the pile jetting sites and determine whether mitigation is needed.

Work in this report presents a first documented study to characterize the surface disturbance and associated ecological impact due to pile jetting process. While the results presented herein are applicable to site conditions encountered in this study, monitoring of the installations and associated disturbance zones and documentation of employed pumps capacity should be performed to add data to the data base collected during this research. The addition of more jetting data with a larger variety of subsurface profiles will further verify the insertion model. Research should also be further conducted on the effects of jetting and surface water currents in order to develop a better model for estimation of plume and sediment transport in areas of fast moving currents. As field jetting for construction is conducted in the future, it is also recommended that the environmental impact of alternative installation methods (such as driving) or foundation type (such as drilled shafts) be evaluated so that engineers will have the ability to perform realistic cost-benefit analyses for structures to be installed in environmentally sensitive areas.

REFERENCES

- Adamus, P.R., L.T. Stockwell, E.J. Clairain, M.E. Morrow, L.P. Rozas, and R.D. Smith (1991) "Wetland Evaluation Technique (WET)" Volume 1: Literature Review and Evaluation Rationale, Environmental Laboratory, Report No. WRP-DE-2, Waterways Experiment Station, Vicksburg, MS.
- Allen, J. R. L., "Fundamental properties of fluids and their relation to sediment transport processes," In Pye (ed.) *Sediment Transport and Depositional Processes*, Blackwell, 1994.
- Allen, J.R.L. (1985) *Principles of Physical Sedimentology*, George Allen & Unwin Publishers Ltd., London.
- ASTM D 422 Test Method for Particle-Size Analysis of Soils, ASTM, Vol. 4.08, Soil and Rock; Dimension Stone; Geosynthetics.
- ASTM D 854 Test Method for Specific Gravity of Soils, ASTM, Vol. 4.08, Soil and Rock; Dimension Stone; Geosynthetics.
- ASTM D 3080 Test Method for Direct Shear Test of Soils Under Consolidated Drained Conditions, ASTM, Vol. 4.08, Soil and Rock; Dimension Stone; Geosynthetics.
- ASTM D 4221 Test Method for Despersive Characteristics of Clay Soil by Double Hydrometer, ASTM, Vol. 4.08, Soil and Rock; Dimension Stone; Geosynthetics.
- ASTM D 4253 Test Methods for Maximum Index Density and Unit Weight of Soils Using a Vibratory Table, ASTM, Vol. 4.08, Soil and Rock; Dimension Stone; Geosynthetics.
- ASTM D 4254 Test Methods for Minimum Index Density and Unit Weight of Soils and Calculation of Relative Density, ASTM, Vol. 4.08, Soil and Rock; Dimension Stone; Geosynthetics.
- Berger, W. H. and F. L. Parker. 1970. Diversity of planktonic Foraminifera in deep sea sediments. *Science* 168:1345-1347.
- Burkholder, J, D. Eggleston, H Glasgow, et al. 2004. Comparative impacts of two major hurricane seasons on the Neuse River and western Pamlico Sound ecosystems. *Proceedings of the National Academy of Sciences* 101:9291-9296.
- Clayton, CRI (1990) "SPT Energy Transmission: Theory, Measurement, and Significance," *Ground Engineering*, Volume 2, No. 10, pp. 35-43.

Coduto, D.P., (2001) *Foundation Design, Principles and Practices* (2nd ed), Prentice-Hall, Inc., New Jersey.

Day, J. H. 1973. *New Polychaeta from Beaufort, with key to all species recorded from North Carolina*. NOAA Technical Report NMFS CIRC-375.

Decker, R. S., and Dunning, L. P. "Development and Use of the Soil Conservation Service Dispersion Test," *Dispersive Clays, Related Piping, and Erosion in Geotechnical Projects*, ASTM STP 623, 1977, pp. 94-109.

Epler, J. H. 2001. *Identification Manual for the Larval Chironomidae (Diptera) of North and South Carolina*. Special Publication SJ2001-Sp13, EPA WQ Program Sec. 104(b)(93), EPA Region 4 and Human Health and Ecological Criteria Division. North Carolina Department of Environment and Natural Resources, Division of Water Quality.

Federal Regulations 40446 (August 14, 1991) "Proposed Revisions to the Federal Manual for Delineating Wetlands.

Fox, R. S. and Bynum, K. H. 1975. *The Amphipod Crustaceans of North Carolina Estuarine Waters*. Science, Vol. 16, No. 4, pp.223-237, December 1975.

Gunaratne, M., R.A. Hameed, C. Kuo, S. Putcha, and D.V. Reddy (1999) *Investigation of the Effects of Pile Jetting and Preforming*, Research Report No. 772, Florida Department of Transportation, in cooperation with Federal Highway Administration.

Holtz, R.D., and W.D. Kovacs (1981) *An Introduction to Geotechnical Engineering*, Prentice-Hall, Inc., New Jersey.

Kerans, B. L. and J. R. Karr. 1994. A benthic index of biotic integrity (B-IBI) for rivers of the Tennessee Valley. *Ecol. Appl.* 4:768-785.

Matlin, A. (1983) *Wide Flange, Concrete Sheet Pile Warves*, Proceedings of ASCE Specialty Conference, Ports, 1983, New Orleans, LA., Mar 21-23, 389-401.

McGregor, T.H. (1963) *T-shaped Concrete Sheet Piles Renew Deteriorated Bulkhead*. *Engineering News-Record*, January 3, 20-21.

Milligan, M. R. 1997. *Identification Manual for the Aquatic Oligochaeta of Florida, Vol. I Freshwater Oligochaetes*. State of Florida Department of Environmental Protection, Clean Water Act 205 (j)(1). DEP Contract No. WM550.

Mitchell, J.K. (1976) *Fundamentals of Soil Behavior*, John Wiley & Sons, Inc., New York, 422 pp.

Munson, B.R., T.H. Okiishi, and D.F. Young (1998) Fundamentals of Fluid Mechanics, Third Edition, John Wiley & Sons, Inc., Canada.

North Carolina Department of Transportation Soils and Foundations Design reference Manual, Version 2001.

North Carolina Division of Water Quality (NCDWQ). 1997. Master List of Benthic Macroinvertebrates, tolerance values for use of the North Carolina Biotic Index. Technical Manual Procedures for the collection and processing of Freshwater Macroinvertebrates. January 1997.

Open University Oceanography Course Team, Waves, Tides and Shallow Water Processes, Boston, Butterworth and Heinemann, 1999.

Roback, S. S. 1980. The immature chironomids of the eastern United States IV. Tanypodinae: Procladiini. Proc. Acad. Nat. Sci. Philad. 132, pp. 1-63.

Shestopal, A.O. (1959) Jetting of Pipes, Piles, and Sheet Piles. Hydroproject Institute, Moscow, U.S.S.R.

Skempton, A.W., (1953) The Colloidal Activity of Clays, Proceedings of the Third International Conference on Soil Mechanics and Foundation Engineering, Vol I, pp 57-61.

Smith, Alex (2003) "Jetting Techniques for Pile Installation and Environmental Impact Minimization," Master of Science, North Carolina State University, Raleigh, NC.

Tsinker, G.P. (1988) Pile Jetting, Journal of Geotechnical Engineering, ASCE, Vol. 144, No. 3 March 1988, pp. 326-334.

US Fish and Wildlife Service (1981) "Habitat Evaluation Procedure Handbook" (870 FW 1.9A), Washington, D.C.

Van Rijn, Leo C., "Sediment Transport, Part I: Bed Load Transport," Journal of Hydraulic Engineering, Vol. 110, No. 10, 1431 – 1455, 1984(a).

Van Rijn, Leo C., "Sediment Transport, Part II: Suspended Load Transport," Journal of Hydraulic Engineering, Vol. 110, No. 11, 1613 – 1641, 1984(b).

Van Rijn, Leo C., "Sediment Transport, Part III: Bed Forms and Alluvial Roughness," Journal of Hydraulic Engineering, Vol. 110, No. 12, 1733 – 1754, 1984(c).

APPENDIX I

(Lab Data)

A. Laboratory Testing Medium

B. Data Analysis and Model Development Data

APPENDIX A
Laboratory Testing Medium

Characteristics of Laboratory Testing Medium

Index density

<u>Specimen</u>	<u>H1 (in.)</u>	<u>H2 (in.)</u>	<u>Avg. 1&2 (in.)</u>	<u>H3 (in.)</u>	<u>H4 (in.)</u>	<u>Avg. 3&4 (in.)</u>
<i>Mortar - 1</i>	0.475	0.436	0.456	0.412	0.381	0.397
<i>Mortar - 2</i>	0.313	0.316	0.315	0.561	0.573	0.567
<i>Concrete - 1</i>	0.268	0.266	0.267	0.617	0.613	0.615
<i>Concrete - 2</i>	0.426	0.476	0.451	0.329	0.289	0.309
<i>Cherry Branch</i>	1.352	1.357	1.355	1.459	1.232	1.346

<u>Specimen</u>	<u>Avg. (in.)</u>	<u>Height of Sample (in.)</u>	<u>Volume (ft³)</u>	<u>Weight (lbs.)</u>	<u>Density (lb./ft.³)</u>	<u>Avg. max (pcf)</u>
<i>Mortar - 1</i>	0.4260	5.190	0.0848	9.136	107.7	108.0
<i>Mortar - 2</i>	0.4408	5.175	0.0846	9.155	108.2	
<i>Concrete - 1</i>	0.4410	5.175	0.0846	9.713	114.8	114.8
<i>Concrete - 2</i>	0.3800	5.236	0.0856	9.821	114.8	
<i>Cherry Branch</i>	1.3500	4.740	0.0773	7.902	102.2	102.0

<u>Specimen</u>	<u>Height of Sample (in.)</u>	<u>Specimen Diameter (in.)</u>	<u>Specimen Area (in²)</u>	<u>Specimen Volume (in³)</u>	<u>Specimen Volume (ft³)</u>	<u>Specimen Weight (lb)</u>
<i>Mortar - 1</i>	6.098	5.996	28.24	172.19	0.100	8.98
<i>Mortar - 2</i>	6.098	5.996	28.24	172.19	0.100	8.98
<i>Concrete - 1</i>	6.098	5.996	28.24	172.19	0.100	9.38
<i>Concrete - 2</i>	6.098	5.996	28.24	172.19	0.100	9.38
<i>Cherry Branch-1</i>	6.090	5.990	28.18	171.62	0.099	8.13
<i>Cherry Branch2</i>	6.090	5.990	28.18	171.62	0.099	8.16

<u>Specimen</u>	<u>Density (lb./ft.³)</u>	<u>Avg. min (pcf)</u>
<i>Mortar - 1</i>	90.120	90.1
<i>Mortar - 2</i>	90.120	
<i>Concrete - 1</i>	94.134	94.1
<i>Concrete - 2</i>	94.134	
<i>Cherry Branch-1</i>	81.860	82.0
<i>Cherry Branch2</i>	82.162	

Appendix A-1 Maximum and Minimum Index Density

Effective Angle of Internal Friction

Mortar Sand		Concrete Sand	
Normal Stress (psf)	Shear Stress at Failure (psf)	Normal Stress (psf)	Shear Stress at Failure (psf)
277	245	277	367
504	428	504	612
1008	836	1008	958
2006	1549	2006	1692

Cherry Branch Sand		Mortar Sand + Kaolinite	
Normal Stress (psf)	Shear Stress at Failure (psf)	Normal Stress (psf)	Shear Stress at Failure (psf)
277	265	504	408
504	428	277	183
1008	754	1008	550
2006	1304	2006	1162

Appendix A-2 Direct Shear Test Data for Testing Material

Permeability

Unit Weight Information

Measurement	Specimen	
	Diameter (cm)	Length (cm)
1	7.21	13
2	7.26	13
3	7.26	13
Average	7.25	13

Sample Name: **Concrete Sand**
 Date: **7/21/2003**

rho=2.65	Vs (cm ³) =	321.69
	Vv (cm ³) =	214.59
	e =	0.67

Specimen Area (cm²) **41.25**
 Specimen Volume (cm³) **536.28**

Weight of Dry Soil (lb):	2.004
Dry Unit Weight (pcf):	104.9
Void Ratio:	0.667
Relative Density:	57

Pore Volume (cm³) **214.59**

Beaker Tare gm **115.35**

Test No.	Cell Pressure (psi)	Head Pressure (psi)	Mass of Pore (gm)	Flow Volume (ft ³)	Time (s)	Q/At
1.00	10.00	11.00	315.89	200.54	54.00	0.09
2.00	10.00	11.00	320.66	205.31	61.30	0.08
3.00	10.00	11.00	323.39	208.04	65.90	0.08
4.00	10.00	11.00	312.72	197.37	69.70	0.07
5.00	10.00	11.00	237.75	122.40	36.00	0.08
6.00	10.00	11.00	314.37	199.02	83.00	0.06
7.00	10.00	11.00	314.85	199.50	105.80	0.05
8.00	10.00	11.00	314.06	198.71	128.20	0.04
9.00	10.00	11.00	314.36	199.01	157.60	0.03
10.00	10.00	11.00	319.63	204.28	190.65	0.03
11.00	10.00	11.00	315.28	199.93	180.20	0.03
12.00	10.00	11.00	315.33	199.98	210.80	0.02
13.00	10.00	11.00	312.90	197.55	178.30	0.03
14.00	10.00	11.00	312.10	196.75	197.00	0.02
15.00	10.00	11.00	311.80	196.45	215.00	0.02
16.00	10.00	11.00	310.20	194.85	215.00	0.02
17.00	10.00	11.00	285.20	169.85	213.00	0.02
18.00	10.00	11.00	212.20	96.85	126.00	0.02

Appendix A-3 Falling Head Permeability Data (Concrete sand)
 Continued

dstandpipe = 7.6cm
 Area of Standpipe, a (cm²) = 45.4

=QL/hAt
 Constant Head
 =(2.3aL/At)
 log(h1/h2)
 Falling Head

Test No.	h/L	h	k (cm/s)	h1 (cm)	h2 (cm)	k (cm/s)
1.00	5.41	70.34	0.0166	74.76	70.34	0.0161
2.00	5.41	70.34	0.0150	74.86	70.34	0.0145
3.00	5.41	70.34	0.0141	74.92	70.34	0.0137
4.00	5.41	70.34	0.0127	74.69	70.34	0.0123
5.00	5.41	70.34	0.0152	73.03	70.34	0.0149
6.00	5.41	70.34	0.0107	74.72	70.34	0.0104
7.00	5.41	70.34	0.0084	74.73	70.34	0.0082
8.00	5.41	70.34	0.0069	74.72	70.34	0.0067
9.00	5.41	70.34	0.0057	74.72	70.34	0.0055
10.00	5.41	70.34	0.0048	74.84	70.34	0.0046
11.00	5.41	70.34	0.0050	74.74	70.34	0.0048
12.00	5.41	70.34	0.0043	74.74	70.34	0.0041
13.00	5.41	70.34	0.0050	74.69	70.34	0.0048
14.00	5.41	70.34	0.0045	74.67	70.34	0.0043
15.00	5.41	70.34	0.0041	74.67	70.34	0.0040
16.00	5.41	70.34	0.0041	74.63	70.34	0.0039
17.00	5.41	70.34	0.0036	74.08	70.34	0.0035
18.00	5.41	70.34	0.0034	72.47	70.34	0.0034

0.0047 0.0045 10⁻²

97.033

Appendix A-3 Falling Head Permeability Data (Concrete sand)

Unit Weight Information

Measurement	Specimen	
	Diameter (cm)	Length (cm)
1	7.201	13.8
2	7.201	13.8
3	7.203	13.8
Average	7.202	13.8

Sample Name: Mortar Sand
Date: 1/17/2003

rho=2.65	Vs (cm ³) =	341.05
	Vv (cm ³) =	221.09
	e =	0.65

Specimen Area (cm²) **40.73**
 Specimen Volume (cm³) **562.14**

Weight of Dry Soil (lb):	1.99
Dry Unit Weight (pcf):	100.60
Void Ratio:	0.65
Relative Density:	62.70

Pore Volume (cm³)	221.09
-------------------------------------	--------

Beaker Tare gm 119.69

Test No.	Cell Pressure (psi)	Head Pressure (psi)	Mass of Pore (gm)	Flow Volume (cm ³)	Time (s)	Q/At
1.00	5.00	7.50	338.38	218.69	79.00	0.07
2.00	5.00	6.00	341.38	221.69	87.81	0.06
3.00	5.00	6.00	341.92	222.23	91.60	0.06
4.00	5.00	6.00	342.32	222.63	89.70	0.06
5.00	5.00	6.00	341.32	221.63	90.75	0.06
6.00	5.00	6.00	295.62	175.93	66.72	0.06
7.00	10.00	11.00	339.77	220.08	64.00	0.08
8.00	10.00	11.00	342.11	222.42	64.06	0.09
9.00	10.00	11.00	338.21	218.52	63.10	0.09
10.00	10.00	11.00	338.20	218.51	63.70	0.08
11.00	10.00	11.00	338.80	219.11	64.00	0.08
12.00	10.00	11.00	335.58	215.89	65.46	0.08
13.00	10.00	11.00	336.99	217.30	66.47	0.08
14.00	10.00	11.00	335.06	215.37	64.20	0.08

Appendix A-4 Falling Head Permeability Data (Mortar sand)

Continued

dstandpipe = 7.6cm
 Area of Standpipe, a (cm²) = 45.4

=QL/hAt
 Constant Head
 =(2.3aL/At)
 log(h1/h2)
 Falling Head

Test No.	h/L	h	k (cm/s)	h1 (cm)	h2 (cm)	k (cm/s)
1.00	12.74	175.85	0.01	180.66	175.85	0.005
2.00	5.10	70.34	0.01	75.22	70.34	0.012
3.00	5.10	70.34	0.01	75.23	70.34	0.011
4.00	5.10	70.34	0.01	75.24	70.34	0.012
5.00	5.10	70.34	0.01	75.22	70.34	0.011
6.00	5.10	70.34	0.01	74.21	70.34	0.012
7.00	5.10	70.34	0.02	75.19	70.34	0.016
8.00	5.10	70.34	0.02	75.24	70.34	0.016
9.00	5.10	70.34	0.02	75.15	70.34	0.016
10.00	5.10	70.34	0.02	75.15	70.34	0.016
11.00	5.10	70.34	0.02	75.16	70.34	0.016
12.00	5.10	70.34	0.02	75.09	70.34	0.015
13.00	5.10	70.34	0.02	75.12	70.34	0.015
14.00	5.10	70.34	0.02	75.08	70.34	0.016
			0.02			0.016

10⁻²

% error
 96.620

Appendix A-4 Falling Head Permeability Data (Mortar sand)

Measurement	Specimen	
	Diameter (cm)	Length (cm)
1	7.19	13.5
2	7.20	13.5
3	7.20	13.5
Average	7.20	13.5

Sample Name: **Cherry Branch**

Date: **7/17/2003**

rho=2.61

Vs (cm ³)	321.7
Vv (cm ³)	227.2
e =	0.7

Specimen Area (cm²) : **40.7**

Specimen Volume (cm³) : **548.9**

Weight of Dry Soil (lb):	1.851
Dry Unit Weight (pcf):	95.4
Void Ratio:	0.706
Relative Density:	72

Pore Volume (cm³) **227.22**

Beaker Tare gm **103.75**

Test No.	Cell Pressure (psi)	Head Pressure (psi)	Mass of Pore (gm)	Flow Volume (cm ³)	Time (s)	Q/At	h/L
1.00	5.00	7.50	336.34	232.59	91.00	0.06	13.03
2.00	5.00	6.00	333.09	229.34	87.00	0.06	5.21
3.00	5.00	6.00	334.55	230.80	90.50	0.06	5.21
4.00	5.00	6.00	333.02	229.27	91.53	0.06	5.21
5.00	5.00	6.00	331.42	227.67	85.20	0.07	5.21
6.00	5.00	6.00	251.73	147.98	103.30	0.04	5.21
7.00	10.00	11.00	330.03	226.28	83.00	0.07	5.21
8.00	10.00	11.00	332.25	228.50	86.40	0.07	5.21
9.00	10.00	11.00	330.73	226.98	87.50	0.06	5.21
10.00	10.00	11.00	331.06	227.31	105.20	0.05	5.21
11.00	10.00	11.00	330.44	226.69	88.30	0.06	5.21
12.00	10.00	11.00	329.89	226.14	91.70	0.06	5.21
13.00	10.00	11.00	329.93	226.18	94.27	0.06	5.21
14.00	10.00	11.00	329.67	225.92	98.04	0.06	5.21
15.00	10.00	11.00	331.44	227.69	105.21	0.05	5.21
16.00	10.00	11.00	331.82	228.07	108.70	0.05	5.21
17.00	10.00	11.00	329.55	225.80	114.90	0.05	5.21
18.00	10.00	11.00	328.26	224.51	112.30	0.05	5.21
19.00	10.00	11.00	330.84	227.09	117.80	0.05	5.21
20.00	10.00	11.00	331.20	227.45	123.70	0.05	5.21
21.00	10.00	11.00	329.84	226.09	128.20	0.04	5.21
22.00	10.00	11.00	329.30	225.55	214.30	0.03	5.21
23.00	10.00	11.00	328.82	225.07	140.00	0.04	5.21
	10.00	11.00	252.94	149.19	99.00	0.04	5.21

Appendix A-5 Falling Head Permeability Data (Cherry Branch Sand)

Continued

Unit Weight Information

Measurement	Specimen	
	Diameter (cm)	Length (cm)
1	7.20344	13
2	7.2136	13
3	7.1882	13
Average	7.2017	13

Sample Name: **Kaolin + Sand**
 Date: **7/22/2003**

$\rho = 2.65$

V_s (cm ³) =	340.11
V_v (cm ³) =	189.44
$e =$	0.56

Specimen Area (cm²) **40.735**
 Specimen Volume cm³) **529.552**

Weight of Dry Soil (lb):	
Dry Unit Weight (pcf):	
Void Ratio:	
Relative Density:	

Pore Volume (cm³) **189.4424**

Beaker Tare gm **101.02**

Test No.	Cell Pressure (psi)	Head Pressure (psi)	Mass of Pore (gm)	Flow Volume (ft ³)	Time (s)	Q/At	h/L
1.00	10.00	11.00	340.4	239.42	1332.0	0.00	5.41
2.00	10.00	11.00	327.3	226.26	1424.0	0.00	5.41
3.00	10.00	11.00	331.6	230.58	1051.0	0.01	5.41
4.00	10.00	11.00	317.2	216.19	1078.0	0.00	5.41

dstandpipe = 7.6cm
 Area of Standpipe, a (cm²) = **45.4**

=QL/hAt =(2.3aL/At) log(h1/h2)
 Constant Head Falling Head

Test No.	h	k (cm/s)	h1 (cm)	h2 (cm)	k (cm/s)
1.00	70.34	0.0008	75.61	70.34	0.0008
2.00	70.34	0.0007	75.32	70.34	0.0007
3.00	70.34	0.0010	75.42	70.34	0.0010
4.00	70.34	0.0009	75.10	70.34	0.0009
		0.00086			0.00083

10^{-3}

Appendix A-6 Falling Head Permeability Data (Mortar sand + Kaolinite Sand)

APPENDIX B
Data Analysis and Model Development Data

Data Analysis and Model Development Data

Depth Analysis							
	Depth (ft)	Time (min)	Vj/IR	Qw/Qp	Depth (ft)	Time (min)	Vj/IR
5/29/2003 10DW8-.5	0.50	1.10	1176.47	9.04	1.00	3.70	4264.72
6/2/2003 10DW8-.625	0.50				1.00		
6/25/03 10DW8-.625	0.50	4.63	7435.31	47.24	1.00		
5/29/2003 20DW8-.8125	0.50	0.65	519.78	8.74	1.00	2.03	1707.86
5/29/2003 20DW8-.5	0.50	0.33	588.24	5.50	1.00	0.89	2941.18
5/30/2003 20DW8-.625	0.50	0.48	941.18	8.08	1.00	1.42	2007.85
6/3/2003 20DW8-.625	0.50	0.49	878.43	8.22	1.00	1.43	1819.61

	Qw/Qp	Depth (ft)	Time (min)
5/29/2003 10DW8-.5	14.67	1.50	n/a
6/2/2003 10DW8-.625		1.50	
6/25/03 10DW8-.625		1.50	
5/29/2003 20DW8-.8125	14.50	1.50	5.18
5/29/2003 20DW8-.5	7.17	1.50	1.57
5/30/2003 20DW8-.625	11.32	1.50	4.14
6/3/2003 20DW8-.625	11.39	1.50	3.00

	Vj/IR	Qw/Qp	Depth (ft)	Time (min)	Vj/IR	Qw/Qp	Depth (ft)
5/29/2003 10DW8-.5	n/a	n/a	2.00	n/a	n/a	n/a	2.50
6/2/2003 10DW8-.625			2.00	n/a	n/a	n/a	2.50
6/25/03 10DW8-.625			2.00	n/a	n/a	n/a	2.50
5/29/2003 20DW8-.8125	4937.94	28.30	2.00	n/a	n/a	n/a	2.50
5/29/2003 20DW8-.5	2156.87	8.26	2.00	2.75	1470.59	10.79	2.50
5/30/2003 20DW8-.625	1631.38	21.76	2.00	5.98	2321.57	25.55	2.50
6/3/2003 20DW8-.625	3011.77	17.79	2.00	3.00	3011.77	17.79	2.50

	Time (min)	Vj/IR	Qw/Qp
5/29/2003 10DW8-.5	n/a	n/a	n/a
6/2/2003 10DW8-.625	n/a	n/a	n/a
6/25/03 10DW8-.625	n/a	n/a	n/a
5/29/2003 20DW8-.8125	n/a	n/a	n/a
5/29/2003 20DW8-.5	5.60	1470.59	17.49
5/30/2003 20DW8-.625	n/a	n/a	n/a
6/3/2003 20DW8-.625			

Appendix B-1 Data Analysis and Model Development Data (Concrete Sand)

Continued

Bearing Pressure Analysis

	Depth (ft)	Time (min)	Qw/Qp	qapp/s'v	Depth (ft)	Time (min)	Qw/Qp
5/29/2003 10DW8-.5	0.5	1.1	9.0	59.5	1.0	3.7	14.7
6/2/2003 10DW8-.625	0.5				1.0		
6/25/03 10DW8-.625	0.5	4.6	47.2	74.0	1.0		
5/29/2003 20DW8-.8125	0.5	0.7	8.7	47.5	1.0	2.0	14.5
5/29/2003 20DW8-.5	0.5	0.3	5.5	59.9	1.0	0.9	7.2
5/30/2003 20DW8-.625	0.5	0.5	8.1	61.4	1.0	1.4	11.3
6/3/2003 20DW8-.625	0.5	0.5	8.2	61.3	1.0	1.4	11.4

	qapp/s'v	Depth (ft)	Time (min)
5/29/2003 10DW8-.5	27.8	1.5	n/a
6/2/2003 10DW8-.625		1.5	
6/25/03 10DW8-.625		1.5	
5/29/2003 20DW8-.8125	24.5	1.5	5.2
5/29/2003 20DW8-.5	27.5	1.5	1.6
5/30/2003 20DW8-.625	28.4	1.5	4.1
6/3/2003 20DW8-.625	28.4	1.5	3.0

	Qw/Qp	qapp/s'v	Depth (ft)	Time (min)	Qw/Qp	qapp/s'v	Depth (ft)
5/29/2003 10DW8-.5	n/a		2.0	n/a	n/a		2.5
6/2/2003 10DW8-.625			2.0	n/a	n/a		2.5
6/25/03 10DW8-.625			2.0	n/a	n/a		2.5
5/29/2003 20DW8-.8125	28.3	18.3	2.0	n/a	n/a		2.5
5/29/2003 20DW8-.5	8.3	17.5	2.0	2.8	10.8	12.7	2.5
5/30/2003 20DW8-.625	21.8	18.1	2.0	6.0	25.5	14.5	2.5
6/3/2003 20DW8-.625	17.8	20.6	2.0				2.5

	Time (min)	Qw/Qp	qapp/s'v
5/29/2003 10DW8-.5	n/a	n/a	
6/2/2003 10DW8-.625	n/a	n/a	
6/25/03 10DW8-.625	n/a	n/a	
5/29/2003 20DW8-.8125	n/a	n/a	
5/29/2003 20DW8-.5	5.6	17.5	9.79478
5/30/2003 20DW8-.625	n/a	n/a	
6/3/2003 20DW8-.625			

Appendix B-1 Data Analysis and Model Development Data (Concrete Sand)

Full Depth Tests - Mortar Sand

Test Description	Jet Velocity (ft/min)	Pile Dia. (in)	Ap (ft ²)	Dj (in)	Aj (ft ²)	Final Depth of Insertion (ft)
4/15/2003 10DU8-.8125	186	8	0.35	0.81	0.0072	0.76
4/15/2003 20DU8-.8125	370	8	0.35	0.81	0.0072	2.43
4/16/2003 10DU8-.5	490	8	0.35	0.50	0.0027	1.21
4/16/2003 20DU8-.5	978	8	0.35	0.50	0.0027	2.90
4/17/2003 20DU8-.5	978	8	0.35	0.50	0.0027	2.92
4/17/2003 20DU8-.625	626	8	0.35	0.63	0.0043	2.56
4/11/2003 10DU8-.8125	186	8	0.35	0.81	0.0072	0.49
5/8/2003 20DU8-.625	626	8	0.35	0.63	0.0043	2.36
45 Deg 7-7-03 10 DU8 0.5	490	8	0.35	0.50	0.0027	2.83
45 Deg 7-8-03 10 DU8 0.625	314	8	0.35	0.63	0.0043	3.00
45 Deg 7-8-03 10 DU8 0.8125	186	8	0.35	0.81	0.0072	2.00

Test Description	Ap/Aj	Q (ft ³ /min)	Pile Volume (ft ³)	Time	Qw/Qp (Total)
4/15/2003 10DU8-.8125	48.47	1.34	0.27	7.00	35.28
4/15/2003 20DU8-.8125	48.47	2.67	0.85	6.45	20.30
4/16/2003 10DU8-.5	128.00	1.34	0.42	5.83	18.45
4/16/2003 20DU8-.5	128.00	2.67	1.01	2.90	7.65
4/17/2003 20DU8-.5	128.00	2.67	1.02	4.42	11.57
4/17/2003 20DU8-.625	81.92	2.67	0.89	4.45	13.28
4/11/2003 10DU8-.8125	48.47	1.34	0.17	2.07	16.18
5/8/2003 20DU8-.625	81.92	2.67	0.82	3.97	12.85
45 Deg 7-7-03 10 DU8 0.5	128.00	1.34	0.99	6.78	9.17
45 Deg 7-8-03 10 DU8 0.625	81.92	1.34	1.05	8.83	11.28
45 Deg 7-8-03 10 DU8 0.8125	48.47	1.34	0.70	10.67	20.43

Test Description	Depth (ft)	Time (min)	Qw/Qp	qapp/s' v	Depth (ft)	Time (min)
4/15/2003 10DU8-.8125	0.50	3.00	22.51	59.71	1.00	
4/15/2003 20DU8-.8125	0.50				1.00	
4/16/2003 10DU8-.5	0.50	0.77	5.87	61.79	1.00	3.45
4/16/2003 20DU8-.5	0.50				1.00	
4/17/2003 20DU8-.5	0.50	0.32	4.41	56.22	1.00	0.68
4/17/2003 20DU8-.625	0.50	0.38	5.67	52.76	1.00	0.94
4/11/2003 10DU8-.8125	0.50	2.07	16.06		1.00	
5/8/2003 20DU8-.625	0.50	0.38	6.07	62.55	1.00	0.83
45 Deg 7-7-03 10 DU8 0.5	0.50	0.29	2.44	65.67	1.00	0.63
45 Deg 7-8-03 10 DU8 0.625	0.50	0.41	3.41	68.19	1.00	1.04
45 Deg 7-8-03 10 DU8 0.8125	0.50	0.47	3.90	66.52	1.00	1.26

Appendix B-2 Data Analysis and Model Development Data (Motar Sand)

Continued

Test Description	Qw/Qp	qapp/s'v	Depth (ft)	Time (min)	Qw/Qp	qapp/s'v
4/15/2003 10DU8-.8125			1.50			
4/15/2003 20DU8-.8125	4.89	28.48	1.50			
4/16/2003 10DU8-.5	13.21	29.92	1.50			
4/16/2003 20DU8-.5			1.50			
4/17/2003 20DU8-.5	4.98	28.49	1.50	1.26	6.21	18.74
4/17/2003 20DU8-.625	7.08	28.31	1.50	1.61	8.10	18.44
4/11/2003 10DU8-.8125			1.50			
5/8/2003 20DU8-.625	6.41	29.73	1.50	1.72	8.85	19.15
45 Deg 7-7-03 10 DU8 0.5	2.50	30.37	1.50	1.39	3.66	19.39
45 Deg 7-8-03 10 DU8 0.625	4.16	31.54	1.50	2.51	6.59	20.14
45 Deg 7-8-03 10 DU8 0.8125	5.03	30.77	1.50	4.24	11.14	19.64

Test Description	Depth (ft)	Time (min)	Qw/Qp	qapp/s'v	Depth (ft)	Time (min)
4/15/2003 10DU8-.8125	2.00				2.50	
4/15/2003 20DU8-.8125	2.00				2.50	
4/16/2003 10DU8-.5	2.00				2.50	
4/16/2003 20DU8-.5	2.00				2.50	
4/17/2003 20DU8-.5	2.00	1.83	6.84	13.76	2.50	2.61
4/17/2003 20DU8-.625	2.00	3.09	11.71	13.47	2.50	4.38
4/11/2003 10DU8-.8125	2.00				2.50	
5/8/2003 20DU8-.625	2.00	2.98	11.50	13.91	2.50	
45 Deg 7-7-03 10 DU8 0.5	2.00	2.77	5.41	14.03	2.50	4.23
45 Deg 7-8-03 10 DU8 0.625	2.00	3.66	7.16	14.57	2.50	5.38
45 Deg 7-8-03 10 DU8 0.8125	2.00	9.59	18.76	14.21		

Test Description	Qw/Qp	qapp/s'v	Depth	Time	Qw/Qp	qapp/s'v
4/15/2003 10DU8-.8125			3.00			
4/15/2003 20DU8-.8125			3.00			
4/16/2003 10DU8-.5			3.00			
4/16/2003 20DU8-.5			3.00			
4/17/2003 20DU8-.5	8.08	11.17	3.00	4.21	11.16	9.31
4/17/2003 20DU8-.625	13.31	10.48	3.00			
4/11/2003 10DU8-.8125			3.00			
5/8/2003 20DU8-.625			3.00			
45 Deg 7-7-03 10 DU8 0.5	6.60	10.85	3.00	6.23	8.54	9.36
45 Deg 7-8-03 10 DU8 0.625	8.37	11.27	3.00	8.46	10.95	9.08
45 Deg 7-8-03 10 DU8 0.8125				3.00		

Continued

Test Description	Jet Velocity (ft/min)	qapp/s'v	Qw/Qp	qapp/s'v	Qw/Qp	qapp/s'v
4/15/2003 10DU8-.8125	186					
4/15/2003 20DU8-.8125	370					
4/16/2003 10DU8-.5	490	56.50	5.87	29.92	13.21	26.47
4/16/2003 20DU8-.5	978					
4/17/2003 20DU8-.5	978	56.22	4.41	29.84	5.06	25.33
4/17/2003 20DU8-.625	626	53.58	5.67	30.99	6.29	26.04
4/11/2003 10DU8-.8125	186					
5/8/2003 20DU8-.625	626	53.00	6.08	29.73	6.41	26.25

Test Description	Qw/Qp	qapp/s'v	Qw/Qp	qapp/s'v	Qw/Qp	qapp/s'v
4/15/2003 10DU8-.8125						
4/15/2003 20DU8-.8125						
4/16/2003 10DU8-.5	16.60					
4/16/2003 20DU8-.5						
4/17/2003 20DU8-.5	5.17	20.57	5.76	14.78	6.50	9.98
4/17/2003 20DU8-.625	7.35	20.28	7.78	15.22	9.79	10.48
4/11/2003 10DU8-.8125						
5/8/2003 20DU8-.625	6.90	20.38	8.01	15.33	10.97	

Appendix B-2 Data Analysis and Model Development Data (Mortar Sand)

Full Tests - Cherry Branch Sand

Test Description	Depth	Time	Vj/IR	Qw/Qp	Depth	Time	Vj/IR
5/21/2003 10DU8-.8125	0.50	3.45	1744.99	26.91	1.00		
5/22/2003 10DU8-.625	0.50	2.37	1537.26	18.09	1.00	5.13	1725.5
5/22/2003 20DU8-.8125	0.50	0.78	445.53	13.58	1.00	1.64	779.7
5/27/2003 10DU8-.5	0.50	1.21	1225.49	11.03	1.00	2.68	1666.7
6/27/2003 10DU8-.5	0.50	0.70	392.16	5.85	1.00	1.15	490.2

Test Description	Qw/Qp	Depth	Time	Vj/IR	Qw/Qp
5/21/2003 10DU8-.8125		1.50			
5/22/2003 10DU8-.625	19.61	1.50	8.51	2509.81	21.71
5/22/2003 20DU8-.8125	13.42	1.50	2.64	705.42	14.08
5/27/2003 10DU8-.5	11.18	1.50	4.47	2058.83	12.05
6/27/2003 10DU8-.5	4.60	1.50	2.08	1225.49	5.47

Test Description	Depth	Time	Vj/IR	Qw/Qp	Depth	Time	Vj/IR
5/21/2003 10DU8-.8125	2.00				2.50		
5/22/2003 10DU8-.625	2.00	12.00	1725.49	22.97	2.50	14.98	4015.70
5/22/2003 20DU8-.8125	2.00	3.86	1485.09	15.26	2.50	5.60	1150.95
5/27/2003 10DU8-.5	2.00	6.58	1421.57	13.14	2.50	8.65	2254.91
6/27/2003 10DU8-.5	2.00	3.90	1813.73	7.63	2.50	5.98	2058.83

Test Description	Qw/Qp	Depth	Time	Vj/IR	Qw/Qp
5/21/2003 10DU8-.8125		3.00			
5/22/2003 10DU8-.625	24.57	3.00			
5/22/2003 20DU8-.8125	17.60	3.00	7.28	1485.09	18.99
5/27/2003 10DU8-.5	13.69	3.00			
6/27/2003 10DU8-.5	9.31	3.00	8.94	3333.34	11.58

Test Description	Depth	Time	Vj/IR	Qw/Qp
5/21/2003 10DU8-.8125	3.50			
5/22/2003 10DU8-.625	3.50			
5/22/2003 20DU8-.8125	3.50	9.56	2351.40	21.3017
5/27/2003 10DU8-.5	3.50			
6/27/2003 10DU8-.5	3.50			

Appendix B-3 Data Analysis and Model Development Data (Cherry Branch Sand)

Full Depth Tests - Mortar Sand + Kaolinite

Test Description	Jet Velocity (ft/min)	Pile Dia. (in)	Ap (ft ²)	Dj (in)	Aj (ft ²)	Final Depth of Insertion (ft)	Ap/Aj
7-15-03 10KM8-0.5	490	8.00	0.35	0.50	0.0027	2.33	128.00
8-5-0310KM8-0.8125	186	8.00	0.35	0.81	0.0072	0.92	48.47
8-6-0310KM8-.625	314	8.00	0.35	0.63	0.0043	2.00	81.92

Test Description	Q (ft ³ /min)	Pile Volume (ft ³)	Time	Qw/Qp (Total)
7-15-03 10KM8-0.5	1.34	0.81	5.67	9.30
8-5-0310KM8-0.8125	1.34	0.32	6.30	26.32
8-6-0310KM8-.625	1.34	0.70	8.75	16.76

Test Description	Depth (ft)	Time (min)	Qw/Qp	Depth (ft)	Time (min)	Qw/Qp	Depth (ft)
7-15-03 10KM8-0.5	0.50	0.32	2.65	1.00	1.34	5.36	1.50
8-5-0310KM8-0.8125	0.50	1.62	13.51	1.00	5.68		1.50
8-6-0310KM8-.625	0.50	0.79	6.62	1.00	2.35	9.39	1.50

Test Description	Time (min)	Qw/Qp	Depth (ft)	Time (min)	Qw/Qp
7-15-03 10KM8-0.5	2.66	6.98	2.00	4.77	9.32
8-5-0310KM8-0.8125			2.00		
8-6-0310KM8-.625	4.34	11.40	2.00	8.04	15.73

Appendix B-4 Data Analysis and Model Development Data (Mortar + Kaolinite sand)

APPENDIX II

(Field Data)

C. White Oak River site

D. Cherry Branch Ferry Basin site

E. Sampson County Bridge Replacement site

F. Swan Quarter Ferry Basin site

G. Model Development Spreadsheet

APPENDIX C
Measured Field Data- White Oak River site

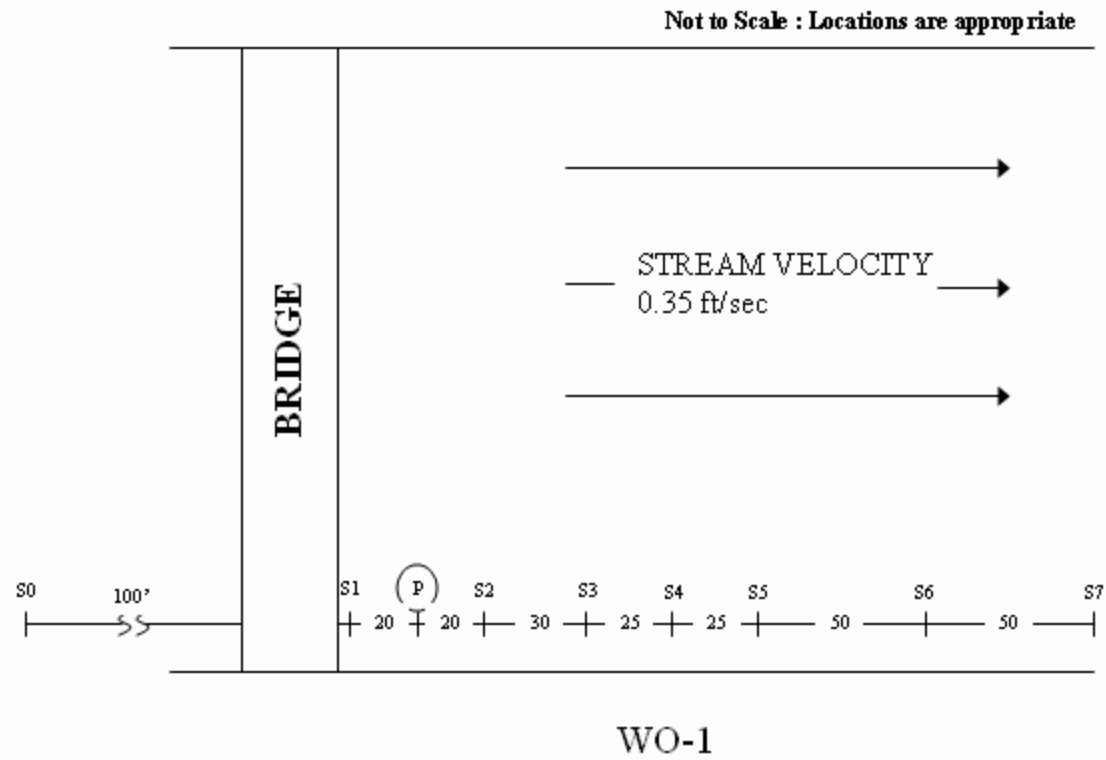


Figure C- 1 WO-1 Field Drawing

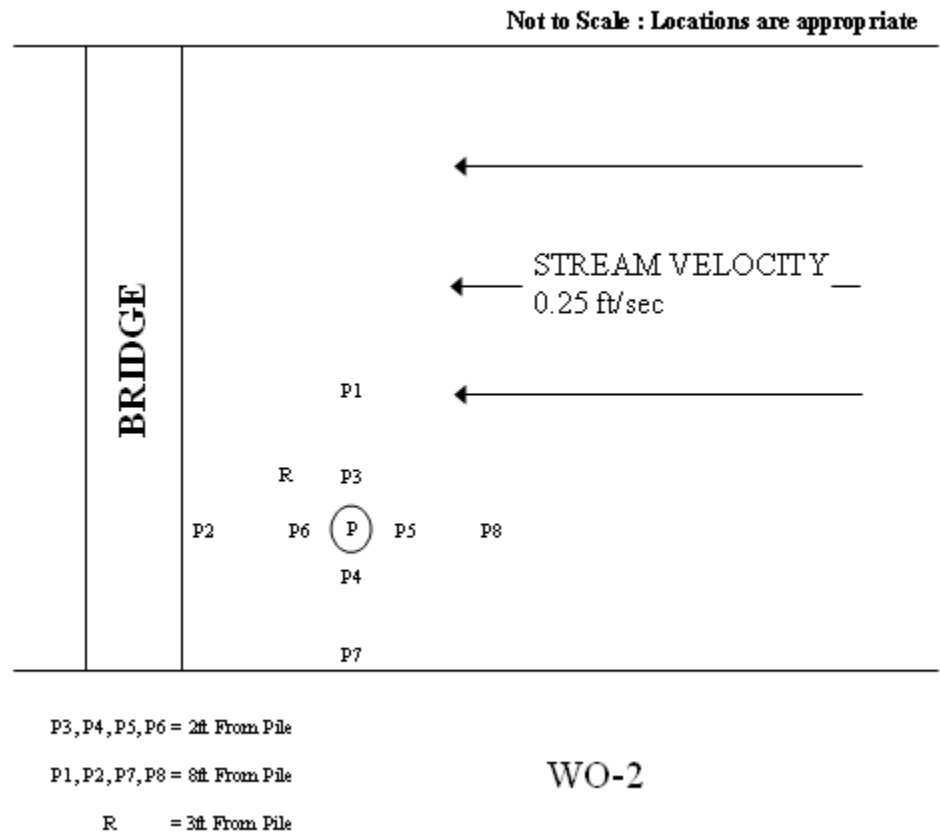


Figure C- 2. WO-2 Field Drawing

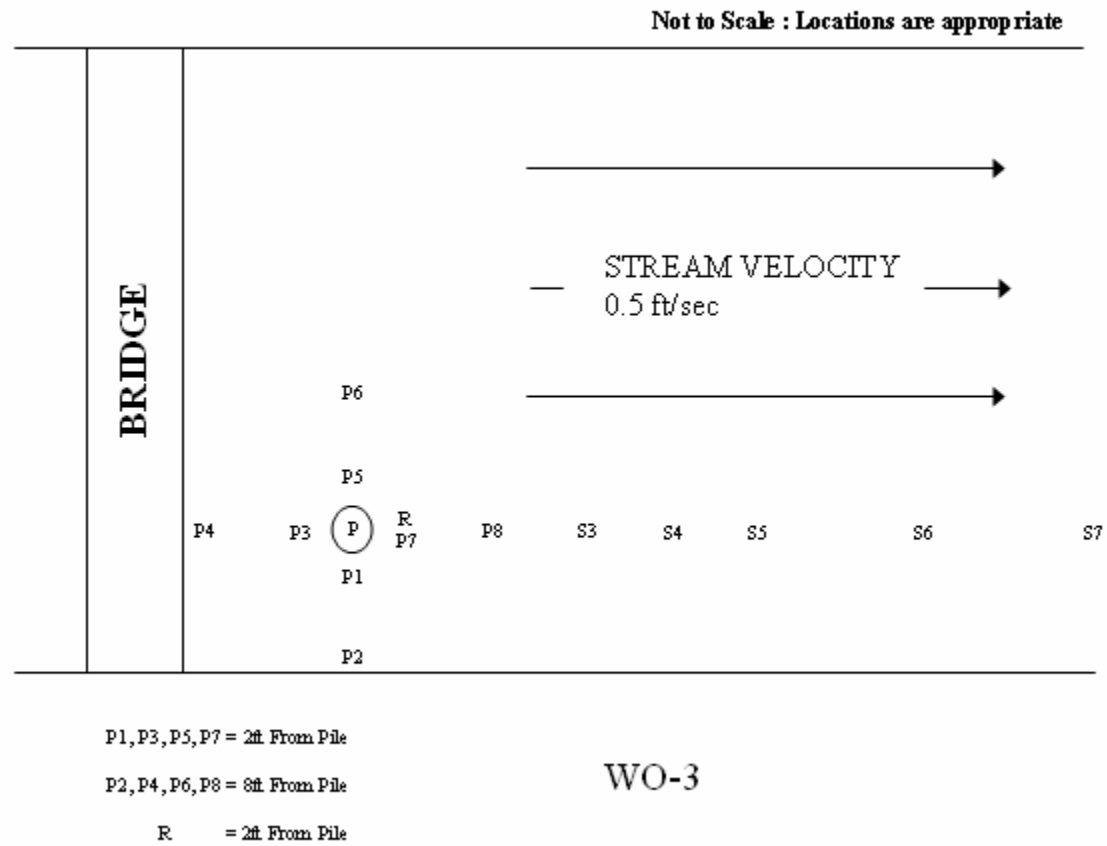


Figure C- 3. WO-3 Field Drawing

Date: 6/17/2003		Underwater					Spoil Volume Calculation													
Pile ID: WO-2																				
Avg Flowrate (cfm): 35.49																				
Nozzles (in): 1.5																				
Prejet Survey					PostJet Survey					Difference										
	North	South	East	West		North	South	East	West		North	South	East	West		North	South	East		
0	10.6	10.6	10	9.9	0	10	10.4	9.5	9	0	0.6	0.2	0.5	0.9	0	xxxxxxx	xxxxxxx	xxxxxxx		
1	10.8	10.6	10.1	9.8	1	10	10.4	9.4	9	1	0.8	0.2	0.7	0.8	1	6.59734457	1.884956	5.654867		
2	10.9	10.54	10.2	9.5	2	10	10.1	9.1	9.3	2	0.9	0.44	1.1	0.2	2	13.3517688	5.026548	14.13717		
3	11.1	10.3	10.3	9.7	3	10.2	10	9.4	9.4	3	0.9	0.3	0.9	0.3	3	19.7920337	8.136725	21.99115		
4	11.3	10	10.4	9.7	4	10.6	10	10	9.5	4	0.7	0	0.4	0.2	4	22.6194671	4.24115	18.37832		
5	11.4	9.9	10.3	9.6	5	11.2	9.8	10.1	9.5	5	0.2	0.1	0.2	0.1	5	15.5508836	1.727876	10.36726		
6	11.4	9.9	10.3	9.6	6	11.4	9.9	10.4	9.5	6	0	0	-0.1	0.1	6	4.08407045	2.042035	2.042035		
7	11.5	9.8	10.4	9.6	7	11.6	9.7	10.4	9.4	7	-0.1	0.1	0	0.2	7	-2.3561945	2.356194	-2.356194		
8	11.7	9.7	10.4	9.6	8	11.9	9.6	10.5	9.4	8	-0.2	0.1	-0.1	0.2	8	-8.0110613	5.340708	-2.670354		
9	12	9.7	10.4	9.6	9	12.1	9.5	10.5	9.4	9	-0.1	0.2	-0.1	0.2	9	-8.9535391	8.953539	-5.969026		
10	12	9.5	10.4	9.5	10	12.1	9.4	10.6	9.4	10	-0.1	0.1	-0.2	0.1	10	-6.5973446	9.896017	-9.896017		
11	12.1	9.5	10.5	9.5	11	12.1	9.3	10.6	9.4	11	0	0.2	-0.1	0.1	11	-3.6128316	10.83849	-10.83849		
12	12.1	9.4	10.6	9.5	12	12.1	9.2	10.6	9.4	12	0	0.2	0	0.1	12	0	15.70796	-3.926991		
13	12.2	9.3	10.6	9.6	13	12.2	9.1	10.6	9.3	13	0	0.2	0	0.3	13	0	16.9646	0		
14	12.3	9.2	10.6	9.5	14	12.3	9.2	10.6	9.2	14	0	0	0	0.3	14	0	9.110619	0		
15	12.3			9.4	15	12.3			9.2	15	0	0	0	0.2	15	0	0	0		
16	12.3			9.4	16	12.3			9.2	16	0	0	0	0.2	16	0	0	0		
17	12.2			9.4	17	12.2			9.2	17	0	0	0	0.2	17	0	0	0		
18	12.3			9.4	18	12.3			9.3	18	0	0	0	0.1	18	0	0	0		
19	12.4			9.4	19	12.4			9.4	19	0	0	0	0	19	0	0	0		
20	12.5				20	12.5				20	0	0	0	0	20	0	0	0		
21					21					21	0	0	0	0	21	0	0	0		
22					22					22	0	0	0	0	22	0	0	0		
23					23					23	0	0	0	0	23	0	0	0		
24					24					24	0	0	0	0	24	0	0	0		
25					25					25	0	0	0	0	25	0	0	0		
26					26					26	0	0	0	0	26	0	0	0		
27					27					27	0	0	0	0	27	0	0	0		
28					28					28	0	0	0	0	28	0	0	0		
29					29					29	0	0	0	0	29	0	0	0		
30					30					30	0	0	0	0	30	0	0	0		
																	52.4645973	102.2274	36.91371	
																	Avg Spoil Area (ft^2) 392.6991		Avg Spoil Volume (ft^3) 104.725	

Figure C- 5. WO-2 Survey Measurements and Volume Calculation.

Date: 6/17/2003		Underwater	Spoil Volume Calculation																
Pile ID: WO-3																			
Avg Flowrate (cfm): 44.52																			
Nozzles (in): 2.5																			
Prejet Survey				PostJet Survey				Difference											
	North	South	East	West		North	South	East	West		North	South	East	West		North	South	East	
0	10.4	10	9.3	9.1	0	9.7	9.3	8.6	8.3	0	0.7	0.7	0.7	0.8	xxxxxxx	xxxxxxx	xxxxxxx		
1	10.4	9.9	9.3	9.1	1	9.9	9.4	8.8	8.4	1	0.5	0.5	0.5	0.7	5.6548678	5.654867	5.654867		
2	10.4	9.8	9.2	9.1	2	10.2	9.5	8.9	8.3	2	0.2	0.3	0.3	0.8	5.49778714	6.283185	6.283185		
3	10.6	9.7	9.2	9.1	3	10.4	9.6	9	8.5	3	0.2	0.1	0.2	0.6	4.39822972	4.39823	5.497787		
4	10.6	9.5	9.2	9	4	10.5	9.5	9.1	8.7	4	0.1	0	0.1	0.3	4.24115008	1.413717	4.24115		
5	10.8	9.6	9.4	8.9	5	10.7	9.5	9.1	8.9	5	0.1	0.1	0.3	0	3.45575192	1.727876	6.911504		
6	11	9.5	9.3	9	6	10.8	9.5	9.1	8.9	6	0.2	0	0.2	0.1	6.12610567	2.042035	10.21018		
7	11.1	9.5	9.3	8.8	7	11	9.5	9.1	9	7	0.1	0	0.2	-0.2	7.06858347	0	9.424778		
8	11.2	9.4	9.4		8	11.2	9.4	9.3		8	0	0	0.1	0	2.67035376	0	8.011061		
9	11.4	9.3	9.4		9	11.4	9.3	9.3		9	0	0	0.1	0	0	0	5.969026		
10	11.7	9.2	9.5		10	11.6	9	9.4		10	0.1	0.2	0.1	0	3.29867229	6.597345	6.597345		
11	12	8.9	9.4		11	11.8	8.9	9.4		11	0.2	0	0	0	10.8384947	7.225663	3.612832		
12	12		9.4		12	12		9.2		12	0	0	0.2	0	7.85398163	0	7.853982		
13	12.1		9.6		13	12.1		9.6		13	0	0	0	0	0	0	8.4823		
14	12.2		9.8		14	12.2		9.8		14	0	0	0	0	0	0	0	0	
15	12.3		10.4		15	12.3		10.4		15	0	0	0	0	0	0	0	0	
16	12.4		9.5		16	12.4		9.5		16	0	0	0	0	0	0	0	0	
17	12.4		9.2		17	12.4		9.2		17	0	0	0	0	0	0	0	0	
18	12.4		9.4		18	12.4		9.4		18	0	0	0	0	0	0	0	0	
19	12.4				19	12.4				19	0	0	0	0	0	0	0	0	
20	12.4				20	12.4				20	0	0	0	0	0	0	0	0	
21					21					21	0	0	0	0	0	0	0	0	
22					22					22	0	0	0	0	0	0	0	0	
23					23					23	0	0	0	0	0	0	0	0	
24					24					24	0	0	0	0	0	0	0	0	
25					25					25	0	0	0	0	0	0	0	0	
26					26					26	0	0	0	0	0	0	0	0	
27					27					27	0	0	0	0	0	0	0	0	
28					28					28	0	0	0	0	0	0	0	0	
29					29					29	0	0	0	0	0	0	0	0	
30					30					30	0	0	0	0	0	0	0	0	
												61.1039771 35.34292 88.74999							
Avg Spoil Area (ft^2)												343.219				Avg Spoil Volume (ft^3) 57.92311			

Figure C- 6. WO-3 Survey Measurements and Volume Calculation.

Date:	6/18/2003	On Land	Spoil Volume Calculation		
Pile ID:	WO-4				
Avg Flowrate (cfm):	52.11				
Nozzles (in):	2				
Prejet Survey					
	North	South	East	West	
0	2.7	2.7	2.7	2.7	
1	2.7	2.7	2.7	2.7	
2	2.7	2.7	2.7	2.8	
3	2.7	2.6	2.7	2.8	
4	2.7	2.6	2.7	2.7	
5	2.7	2.5	2.7	2.8	
6	2.7	2.5	2.7	2.8	
7	2.7	2.5	2.7	2.8	
8		2.5	2.7	2.8	
9		2.4	2.6	2.8	
10		2.4	2.6	2.9	
11		2.4	2.6	2.8	
12		2.4	2.6	2.8	
13		2.4		2.8	
14					
15					
16					
17					
18					
19					
20					
21					
22					
23					
24					
25					
26					
27					
28					
29					
30					
PostJet Survey					
	North	South	East	West	
0	2.3	2.3	2.3	2.3	
1	2.4	2.3	2.4	2.3	
2	2.4	2.3	2.3	2.4	
3	2.5	2.3	2.4	2.4	
4	2.6	2.3	2.4	2.4	
5	2.7	2.3	2.3	2.4	
6	2.8	2.3	2.4	2.5	
7	2.7	2.3	2.4	2.5	
8		2.3	2.5	2.6	
9		2.4	2.6	2.7	
10		2.3	2.6	2.8	
11		2.4	2.6	2.8	
12		2.4	2.6	2.8	
13		2.4		2.8	
14					
15					
16					
17					
18					
19					
20					
21					
22					
23					
24					
25					
26					
27					
28					
29					
30					
Difference					
	North	South	East	West	
0	0.4	0.4	0.4	0.4	
1	0.3	0.4	0.3	0.4	
2	0.3	0.4	0.4	0.4	
3	0.2	0.3	0.3	0.4	
4	0.1	0.3	0.3	0.3	
5	0	0.2	0.4	0.4	
6	-0.1	0.2	0.3	0.3	
7	0	0.2	0.3	0.3	
8	0	0.2	0.2	0.2	
9	0	0	0	0.1	
10	0	0.1	0	0.1	
11	0	0	0	0	
12	0	0	0	0	
13	0	0	0	0	
14	0	0	0	0	
15	0	0	0	0	
16	0	0	0	0	
17	0	0	0	0	
18	0	0	0	0	
19	0	0	0	0	
20	0	0	0	0	
21	0	0	0	0	
22	0	0	0	0	
23	0	0	0	0	
24	0	0	0	0	
25	0	0	0	0	
26	0	0	0	0	
27	0	0	0	0	
28	0	0	0	0	
29	0	0	0	0	
30	0	0	0	0	
	North	South	East		
0	xxxxxxx	xxxxxxx	xxxxxxx		
1	3.29867229	3.769911	3.298672		
2	4.71238898	6.283185	5.497787		
3	5.49778714	7.696902	7.696902		
4	4.24115008	8.4823	8.4823		
5	1.72787596	8.63938	12.09513		
6	-2.0420352	8.168141	14.29425		
7	-2.3561945	9.424778	14.13717		
8	0	10.68142	13.35177		
9	0	5.969026	5.969026		
10	0	3.298672	0		
11	0	3.612832	0		
12	0	0	0		
13	0	0	0		
14	0	0	0		
15	0	0	0		
16	0	0	0		
17	0	0	0		
18	0	0	0		
19	0	0	0		
20	0	0	0		
21	0	0	0		
22	0	0	0		
23	0	0	0		
24	0	0	0		
25	0	0	0		
26	0	0	0		
27	0	0	0		
28	0	0	0		
29	0	0	0		
30	0	0	0		
	North	South	East		
0	15.0796447	76.02654	84.823		
Avg Spoil Area (ft^2)		251.3274		Avg Spoil Volume (ft^3) 69.4292	

Figure C- 7. WO-4 Survey Measurements and Volume Calculation.

Date: 6/18/2003		On Land		
Pile ID: WO-5				
Avg Flowrate (cfm): 47.22				
Nozzles (in): 2.5				

Prejet Survey					PostJet Survey					Difference					Spoil Volume Calculation		
	North	South	East	West		North	South	East	West		North	South	East	West	North	South	East
0					0					0	0	0	0	0	xxxxxxx	xxxxxxx	xxxxxxx
1					1					1	0	0	0	0	0	0	0
2					2					2	0	0	0	0	0	0	0
3					3					3	0	0	0	0	0	0	0
4					4					4	0	0	0	0	0	0	0
5					5					5	0	0	0	0	0	0	0
6					6					6	0	0	0	0	0	0	0
7					7					7	0	0	0	0	0	0	0
8					8					8	0	0	0	0	0	0	0
9					9					9	0	0	0	0	0	0	0
10					10					10	0	0	0	0	0	0	0
11					11					11	0	0	0	0	0	0	0
12					12					12	0	0	0	0	0	0	0
13					13					13	0	0	0	0	0	0	0
14					14					14	0	0	0	0	0	0	0
15					15					15	0	0	0	0	0	0	0
16					16					16	0	0	0	0	0	0	0
17					17					17	0	0	0	0	0	0	0
18					18					18	0	0	0	0	0	0	0
19					19					19	0	0	0	0	0	0	0
20					20					20	0	0	0	0	0	0	0
21					21					21	0	0	0	0	0	0	0
22					22					22	0	0	0	0	0	0	0
23					23					23	0	0	0	0	0	0	0
24					24					24	0	0	0	0	0	0	0
25					25					25	0	0	0	0	0	0	0
26					26					26	0	0	0	0	0	0	0
27					27					27	0	0	0	0	0	0	0
28					28					28	0	0	0	0	0	0	0
29					29					29	0	0	0	0	0	0	0
30					30					30	0	0	0	0	0	0	0
No spoil zone measured due to water escaping from hole created at WO-4.																	
															0	0	0
															Avg Spoil Volume (ft^3)		
															0		

Figure C- 8. WO-5 Survey Measurements and Volume Calculation.

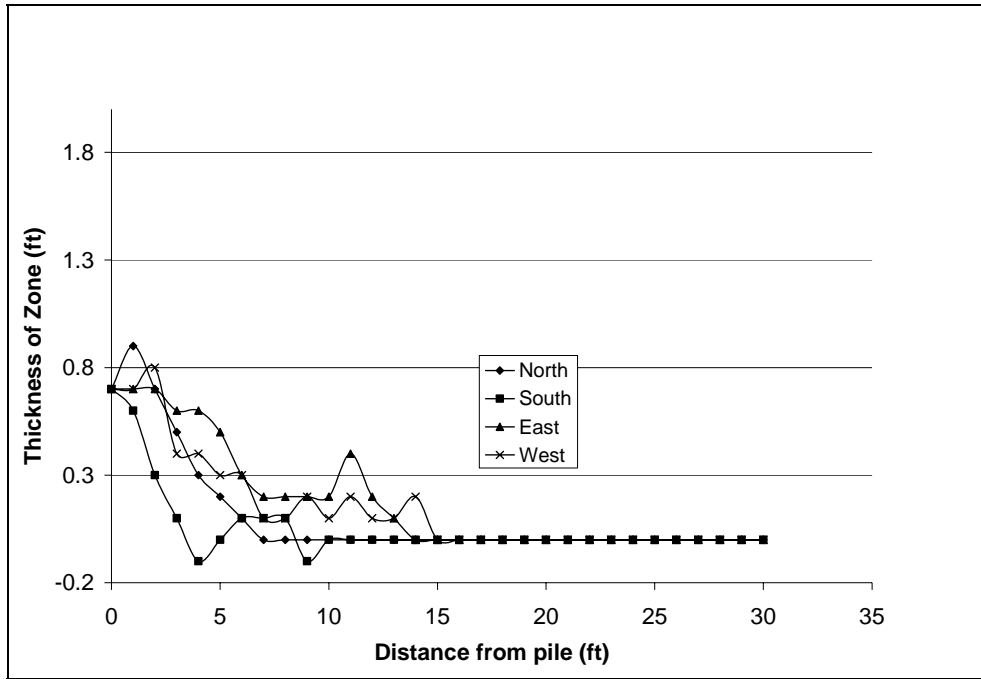


Figure C- 10. WO-1 Debris Zone Profile.

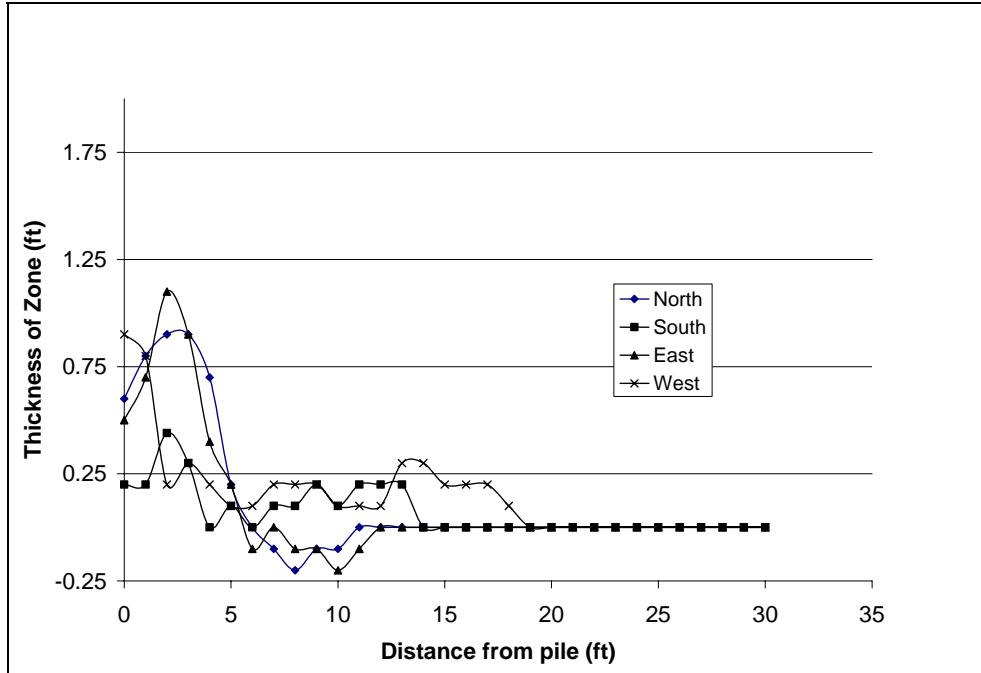


Figure C- 11. WO-2 Debris Zone Profile.

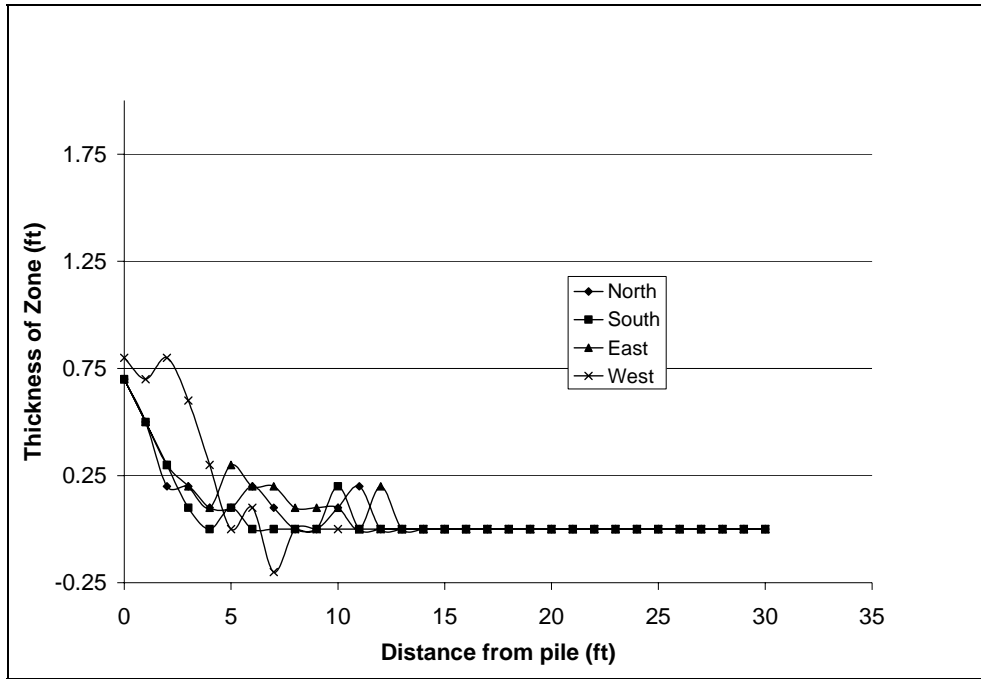


Figure C- 12. WO-3 Debris Zone Profile.

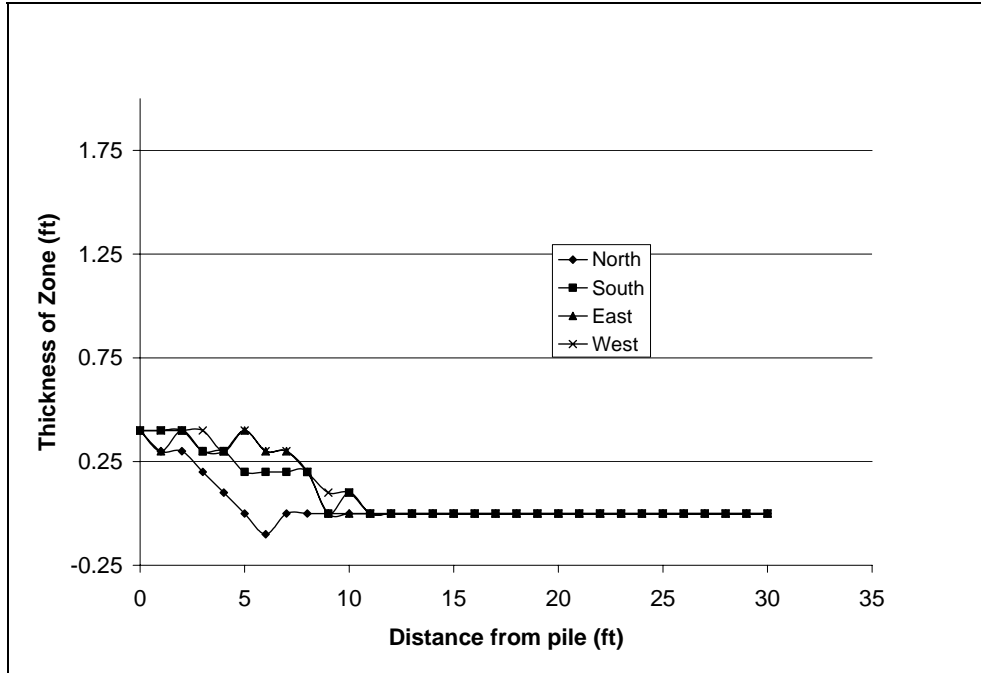


Figure C- 13. WO-4 Debris Zone Profile.

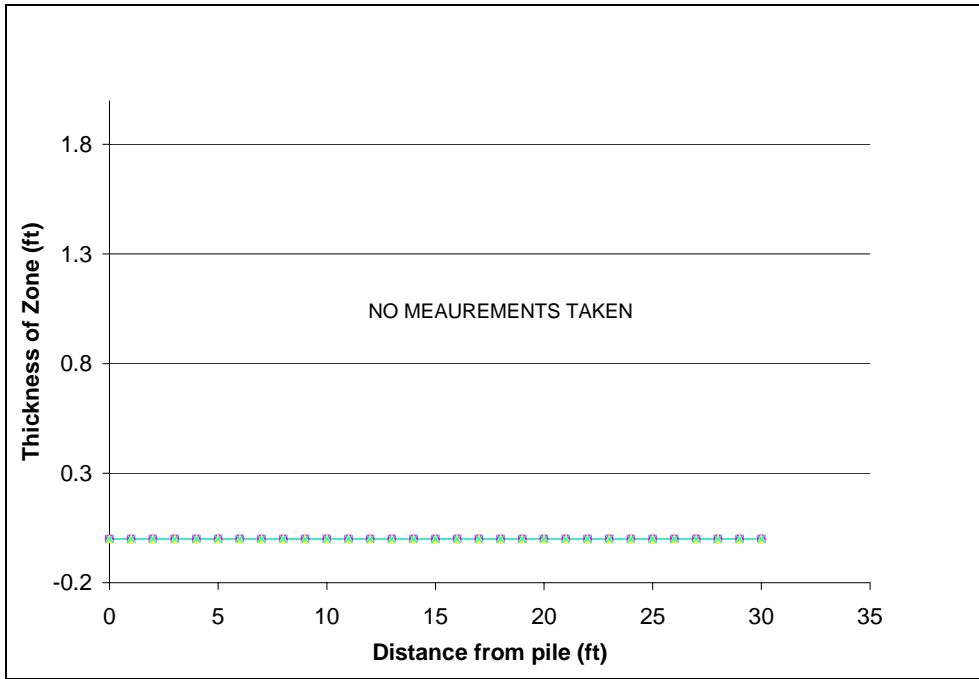


Figure C- 14. WO-5 Debris Zone Profile (not measured).

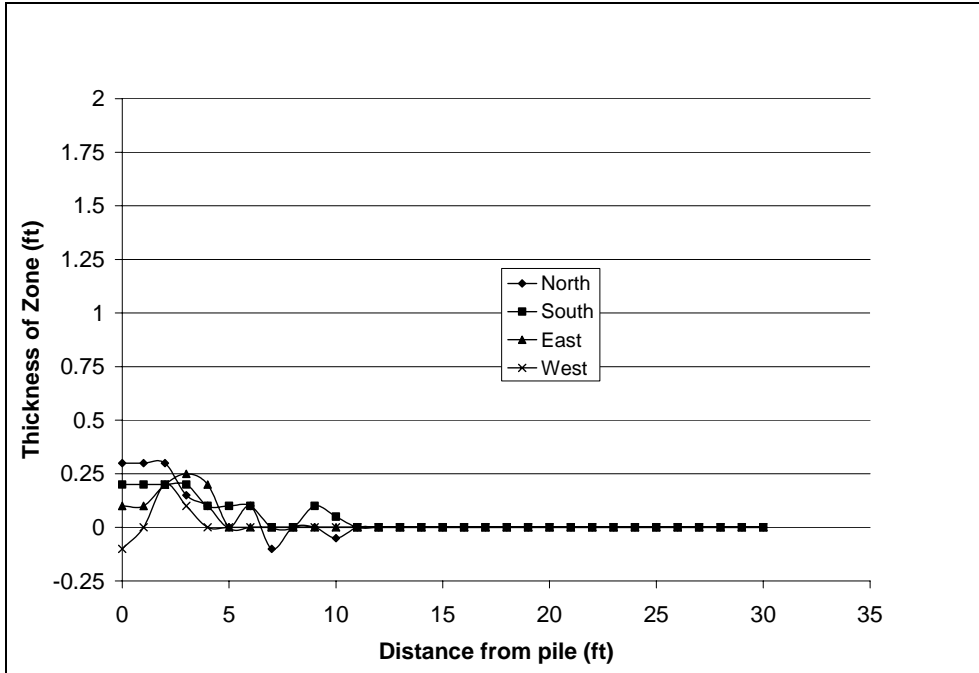


Figure C- 15. WO-6 Spoil Zone Profile.

WO-1

Q _w (cfm)	35.497
----------------------	--------

Depth (ft)	Time (sec)	Min	Insertion rate	
0	0	0	xxxxxxxxxxxx	
1	35	0.583333	1.71	
2	39	0.65	15.00	
3	45	0.75	10.00	
4	50	0.833333	12.00	
5	58	0.966667	7.50	
6	64	1.066667	10.00	
7	68	1.133333	15.00	
8	73	1.216667	12.00	
9	82	1.366667	6.67	
10	89	1.483333	8.57	
11	93	1.55	15.00	
12	96	1.6	20.00	
13	105	1.75	6.67	freefall
14	110	1.833333	12.00	
15	117	1.95	8.57	
16	125	2.083333	7.50	
17	133	2.216667	7.50	
18	141	2.35	7.50	
19	153	2.55	5.00	
20	201	3.35	1.25	

Figure C- 16. WO-1 Measured Insertion Data.

WO-2				
Q _w (cfm)	35.497			
Depth (ft)	Time			Insertion rate
	min	sec	min	
0	0	0	0.00	XXXXXXXXXX
1	0	9	0.15	6.67
2	0	17	0.28	7.50
3	0	22	0.37	12.00
4	0	27	0.45	12.00
5	0	32	0.53	12.00
6	0	37	0.62	12.00
7	0	42	0.70	12.00
8	0	47	0.78	12.00
9	0	50	0.83	20.00
10	0	53	0.88	20.00
11	0	57	0.95	15.00
12	1	0	1.00	20.00
13	1	5	1.08	12.00
14	1	10	1.17	12.00
15	1	16	1.27	10.00
16	1	20	1.33	15.00
17	1	24	1.40	15.00
18	1	29	1.48	12.00
19	1	36	1.60	8.57
20	1	45	1.75	6.67
21	2	26	2.43	1.46
22	2	43	2.72	3.53
23	2	55	2.92	5.00
24	3	53	3.88	1.03
25	4	23	4.38	2.00
26	4	46	4.77	2.61
27	5	25	5.42	1.54

Test ran until 9:57

freefall

Figure C- 17. WO-2 Measured Insertion Data.

WO-3				
Q_w (cfm)	44.526			
Depth (ft)	Time			Insertion rate
	min	sec	min	
0	0	0	0.00	xxxxxxxxxxx
1	0	20	0.33	3.00
2	0	23	0.38	20.00
3	0	28	0.47	12.00
4	0	33	0.55	12.00
5	0	36	0.60	20.00
6	0	41	0.68	12.00
7	0	43	0.72	30.00
8	0	45	0.75	30.00
9	0	51	0.85	10.00
10	0	53	0.88	30.00
11	0	58	0.97	12.00
12	1	3	1.05	12.00
13	1	8	1.13	12.00
14	1	11	1.18	20.00
15	1	15	1.25	15.00
16	1	20	1.33	12.00
17	1	23	1.38	20.00
18	1	30	1.50	8.57
19	1	33	1.55	20.00
20	1	39	1.65	10.00
21	1	52	1.87	4.62
22	2	33	2.55	1.46
23	4	45	4.75	0.45
24	5	37	5.62	1.15
25	6	2	6.03	2.40
26	7	15	7.25	0.82
27	8	5	8.08	1.20
28	8	51	8.85	1.30
29	13	0	13.00	0.24

freefall

Figure C- 18. WO-3 Measured Insertion Data.

WO-4

Q _w (cfm)	52.11506
----------------------	----------

Depth (ft)	Time			Insertion rate
	min	sec	min	
0	0	0	0.00	xxxxxxxxxxx
1	0	4	0.07	15.00
2	0	8	0.13	15.00
3	0	11	0.18	20.00
4	0	14	0.23	20.00
5	0	16	0.27	30.00
6	0	18	0.30	30.00
7	0	21	0.35	20.00
8	0	26	0.43	12.00
9	0	28	0.47	30.00
10	0	34	0.57	10.00
11	0	37	0.62	20.00
12	0	39	0.65	30.00
13	0	42	0.70	20.00
14	0	48	0.80	10.00
15	0	50	0.83	30.00
16	0	53	0.88	20.00
17	0	56	0.93	20.00
18	1	1	1.02	12.00
19	1	4	1.07	20.00
20	1	8	1.13	15.00
21	1	12	1.20	15.00
22	1	54	1.90	1.43
23	2	37	2.62	1.40
24	4	32	4.53	0.52
25	5	11	5.18	1.54
26	6	1	6.02	1.20
27	10	30	10.50	0.22

freefall

Test ran to 14:48

Figure C- 19. WO-4 Measured Insertion Data.

WO-5				
Q_w (cfm)	47.22222			
Depth (ft)	Time			Insertion rate
	min	sec	min	
0	0	0	0.00	xxxxxxxxxxx
1	0	6	0.10	10.00
2	0	8	0.13	30.00
3	0	11	0.18	20.00
4	0	15	0.25	15.00
5	0	19	0.32	15.00
6	0	23	0.38	15.00
7	0	26	0.43	20.00
8	0	29	0.48	20.00
9	0	36	0.60	8.57
10	0	41	0.68	12.00
11	0	46	0.77	12.00
12	0	53	0.88	8.57
13	0	59	0.98	10.00
14	1	2	1.03	20.00
15	1	5	1.08	20.00
16	1	8	1.13	20.00
17	1	10	1.17	30.00
18	1	13	1.22	20.00
19	1	15	1.25	30.00
20	1	17	1.28	30.00
21	1	25	1.42	7.50
22	4	30	4.50	0.32
23	5	12	5.20	1.43
24	7	23	7.38	0.46
25	8	46	8.77	0.72
26	10	26	10.43	0.60
27	14	50	14.83	0.23

freefall

Figure C- 20. WO-5 Measured Insertion Data.

WO-6

Q _w (cfm)	43.01739
----------------------	----------

Depth (ft)	Time		min	Insertion rate
	min	sec		
0	0	0	0.00	xxxxxxxxxx
1	0	33	0.55	1.82
2	1	30	1.50	1.05
3	1	38	1.63	7.50
4	2	26	2.43	1.25
5	3	11	3.18	1.33
6	3	25	3.42	4.29
7	4	0	4.00	1.71
8	4	39	4.65	1.54
9	5	11	5.18	1.88
10	5	40	5.67	2.07
11	6	30	6.50	1.20
12	7	5	7.08	1.71
13	7	49	7.82	1.36
14	8	38	8.63	1.22
15	9	11	9.18	1.82
16	10	0	10.00	1.22
17	10	42	10.70	1.43
18	11	8	11.13	2.31
19	11	25	11.42	3.53
20	11	33	11.55	7.50
21	15	20	15.33	0.26

freefall

Test ran to 17:25

Figure C- 21. WO-6 Measured Insertion Data.

Date	6/17/2003							
Time	11:06am							
Velocity (ft/sec)	0.35							
	Flowing from S0 towards S7							
	Location							
	S0	S1	S2	S3	S4	S5	S6	S7
Elapsed time	Prejet	Prejet	Prejet	Prejet	Prejet	Prejet	Prejet	Prejet
Turbidity	6.7	6.2	6.3	5.9	7.5	7.4	6.8	6.2
pH	6.46	6.52	6.44	6.45	6.41	6.23	6.5	6.41
dO	3.85	3.6	3.74	3.7	3.63	3.6	3.72	3.75
Salinity	0	0	0	0	0	0	0	0
Conductivity	163	181	165	166	163	163	162	162
Temp C	26.5	26.2	26.2	26.2	26.2	27.1	26.2	26.4
Temp F	79.7	79.2	79.2	79.2	79.2	80.8	79.2	79.5
Distance	-100	-20	20	50	75	100	150	200
Elapsed time	30	1	5	12	15	20	23	25
Turbidity	6.5	6.4	6	5.8	6.2	6.5	5.8	7
pH	6.52	6.4	6.45	6.49	6.49	6.49	6.52	6.46
dO	3.87	4.04	4.2	3.97	4.02	4.01	3.97	4.02
Salinity	0	0	0	0	0	0	0	0
Conductivity	172	175	172	173	173	173	171	168
Temp C	26.8	27	26.9	26.7	26.8	26.8	26.6	26.6
Temp F	80.2	80.6	80.4	80.1	80.2	80.2	79.9	79.9
Distance	-100	-20	20	50	75	100	150	200
Elapsed time		36	43					
Turbidity		6.6	5.6					
pH		6.52						
dO		4.05						
Salinity		0						
Conductivity		169						
Temp C		26.9						
Temp F		80.4						
Distance		-20	20					

Figure C- 22. WO-1 Measured Water Quality Data.

Test ID	WO-2							
Date	6/17/2003							
Time	2:30pm							
Stream Velocity (ft/sec)	0.25							
	Flowing from S7 towards S0							
	Location							
	R	R	R	R	R	R	R	R
Elapsed time	Prejet	:15	:30	:45	1	1:30	2	2:30
dO	3.9	3.96	3.92	3.93	3.98	3.93	3.82	3.9
Temp C	27.2							
Temp F	81.0							
Distance (ft)	3	3	3	3	3	3	3	3
Elapsed time	3	3:30	4	4:30	5	5:30	6	6:30
dO	3.99	3.99	3.97	4.03	4	3.96	3.96	3.98
Distance (ft)	3	3	3	3	3	3	3	3
Elapsed time	7	7:30	8	8:30	9	10	11	15
dO	3.95	3.96	3.9	3.92	3.96	3.96	3.95	3.82
Distance (ft)	3	3	3	3	3	3	3	3
	Location							
	P1	P2	P3	P4	P5	P6	P7	P8
Elapsed time	2	2	2	2	2	2	2	2
Turbidity	44.2	8.8	8.6	82.4	19.3	15	7.9	11.6
Distance (ft)	8	8	2	2	2	2	8	8
Elapsed time	4	4	4	4	4	4	4	4
Turbidity	39.7	8.7	7	83.9	22.2	14.2	7.1	11.7
Distance (ft)	8	8	2	2	2	2	8	8
Elapsed time	6	6	6	6				
Turbidity	41.7	8.7	7.8	81.3				
Distance (ft)	8	8	2	2				
Prejet								
Turbidity	66							

Figure C- 23. WO-2 Measured Water Quality Data.

Test ID	WO-3	
Date	6/17/2003	
Time	3:44pm	
Stream Velocity (ft/sec)	0.5	Flowing from S0 towards S7

	Location							
	R	R	R	R	R	R	R	R
Elapsed time	Prejet	:15	:30	:45	1	2	3	4
pH	6.51	nr	nr	nr	6.55	6.54	6.53	6.54
dO	3.94	3.91	3.68	3.78	3.75	3.75	3.66	3.73
Salinity	0	nr	nr	nr	0	0	0	0
Conductivity	174	nr	nr	nr	187	183	190	172
Temp C	27.2	nr	nr	nr	27	27.1	27	26.8
Temp F	81.0	nr	nr	nr	80.6	80.8	80.6	80.2
Distance (ft)	2	2	2	2	2	2	2	2

	Location						
	R	R	R	R	R	R	R
Elapsed time	5	6	7	8	10	12	13
pH	6.54	6.52	6.52	6.51	6.52	6.52	6.52
dO	3.71	3.58	3.62	3.6	3.63	3.68	3.59
Salinity	0	0	0	0	0	0	0
Conductivity	173	183	182	191	175	194	171
Temp C	26.9	26.9	26.9	26.9	26.8	26.8	26.9
Temp F	80.4	80.4	80.4	80.4	80.2	80.2	80.4
Distance (ft)	2	2	2	2	2	2	2

	Location				
	S3	S4	S5	S6	S7
Elapsed time	28	32	17	20	23
Turbidity	8.9	7.7	56.6	13.5	21.1
pH	6.63	6.54	6.62	6.53	6.55
dO	3.75	3.47	3.83	3.69	3.78
Salinity	0	0	0	0	0
Conductivity	171	166	171	181	168
Temp C	26.7	26.6	26.7	26.8	26.5
Temp F	80.1	79.9	80.1	80.2	79.7
Distance (ft)	50	75	100	150	200

	Location								
	R	P1	P2	P3	P4	P5	P6	P7	P8
Elapsed time	0	<5	<5	<5	<5	<5	<5	nr	<5
Turbidity	6.4	16.2	6.4	21.8	6.5	6.92	7.71	nr	9.6
Distance (ft)	2	2	8	2	8	2	8	nr	8

Figure C- 24. WO-3 Measured Water Quality Data.

APPENDIX D
Measured Field Data- Cherry Branch Ferry Basin Site

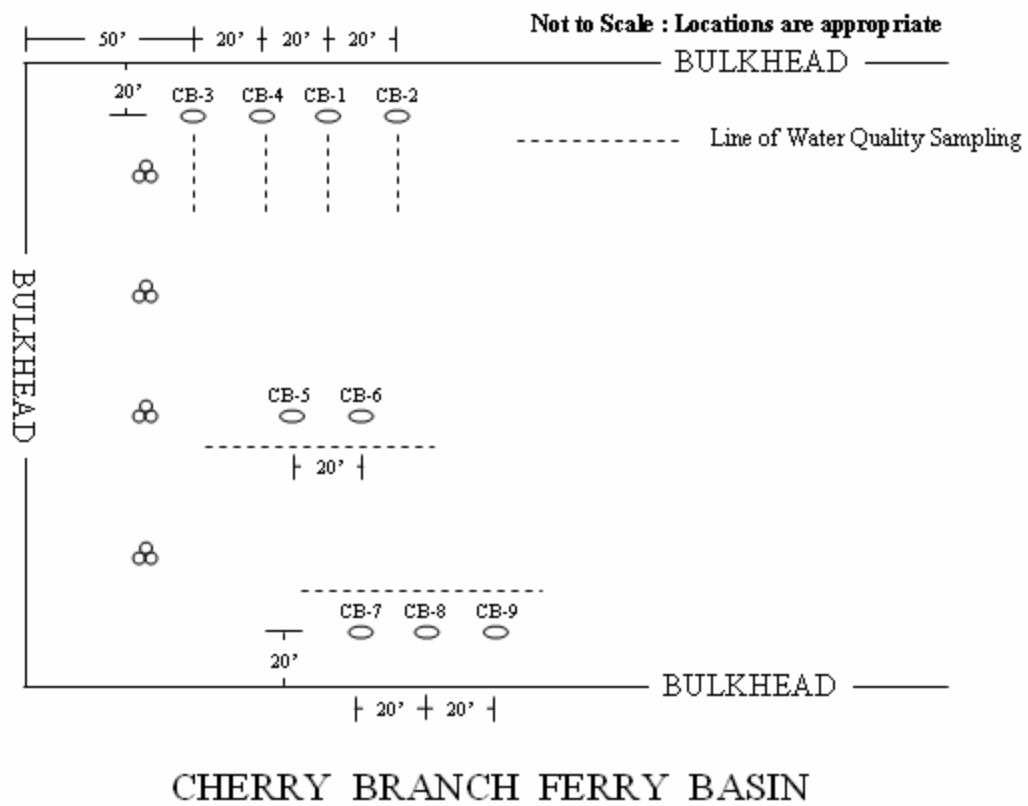


Figure D- 1. Cherry Branch Ferry Basin Field Drawing.

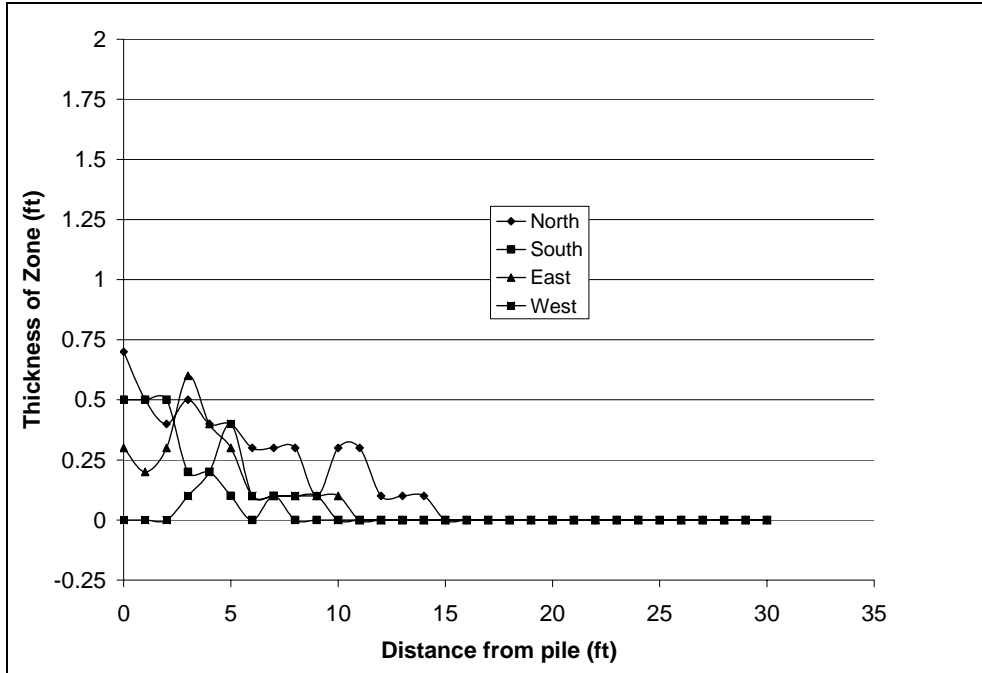


Figure D- 11. CB-1 Debris Zone Profile.

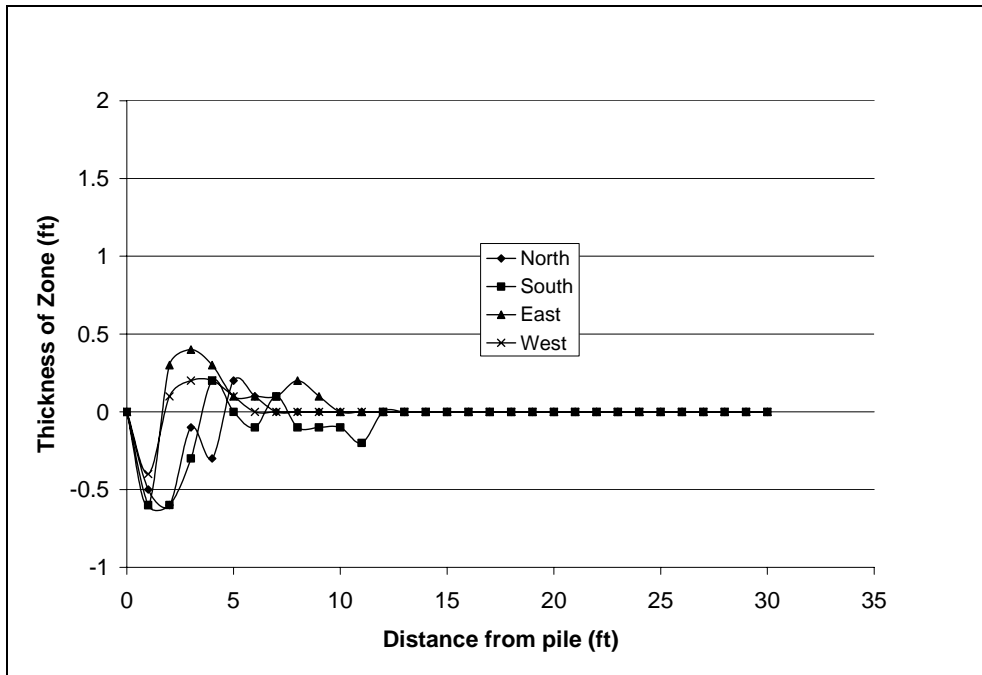


Figure D- 12. CB-2 Debris Zone Profile.

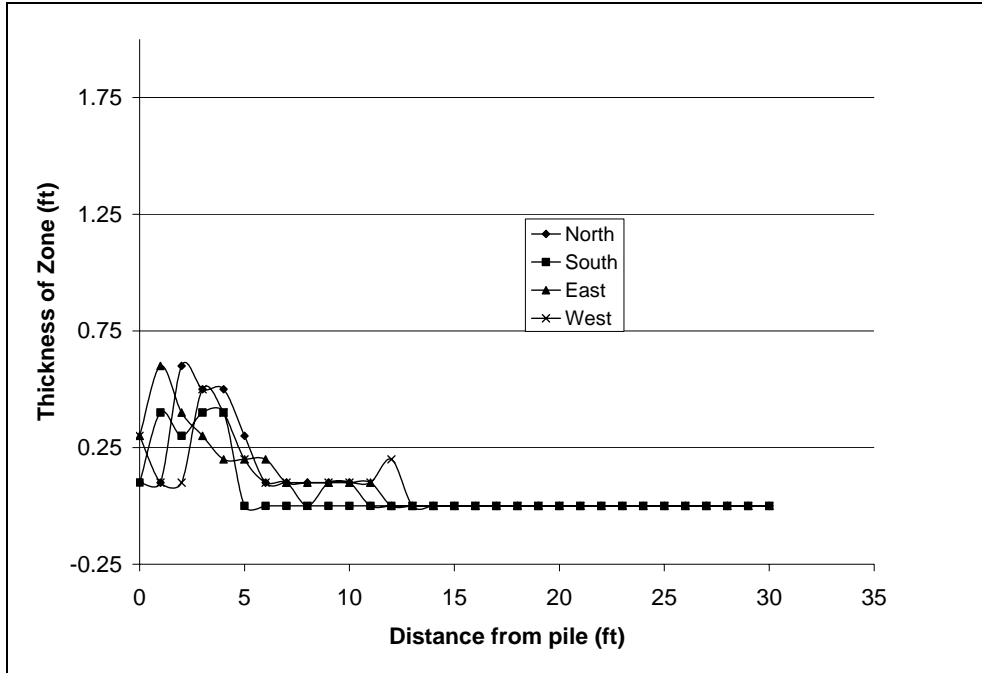


Figure D- 13. CB-3 Debris Zone Profile.

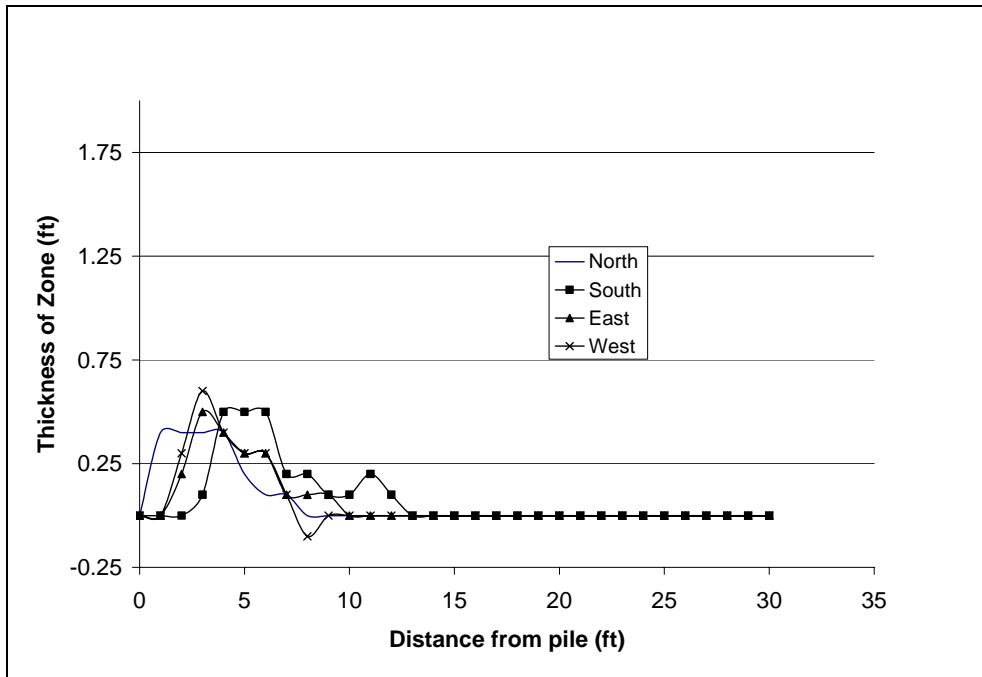


Figure D- 14. CB-4 Debris Zone Profile.

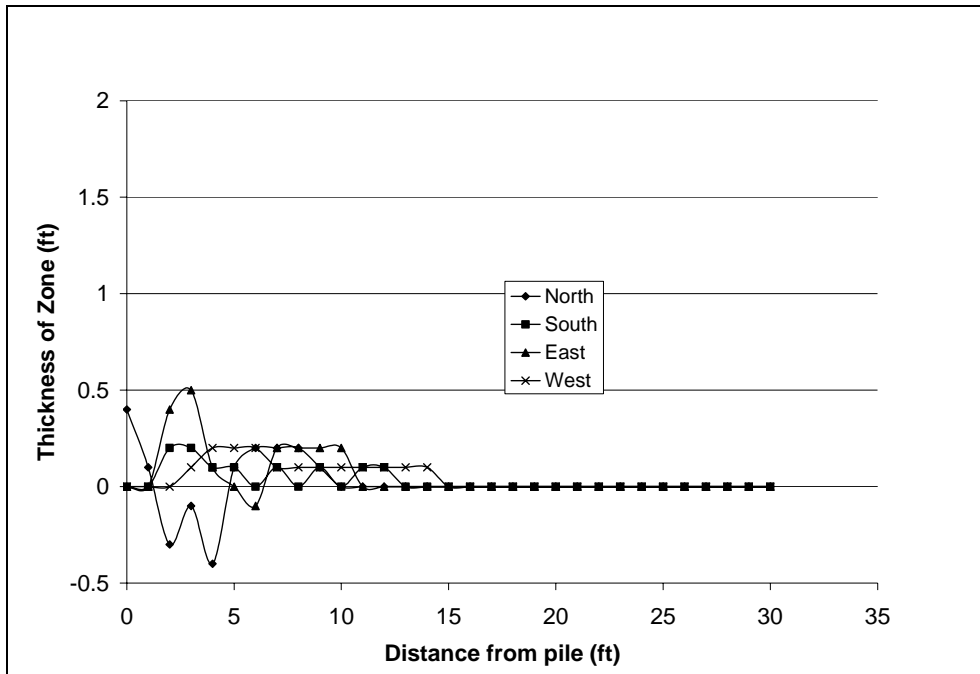


Figure D- 15. CB-5 Debris Zone Profile.

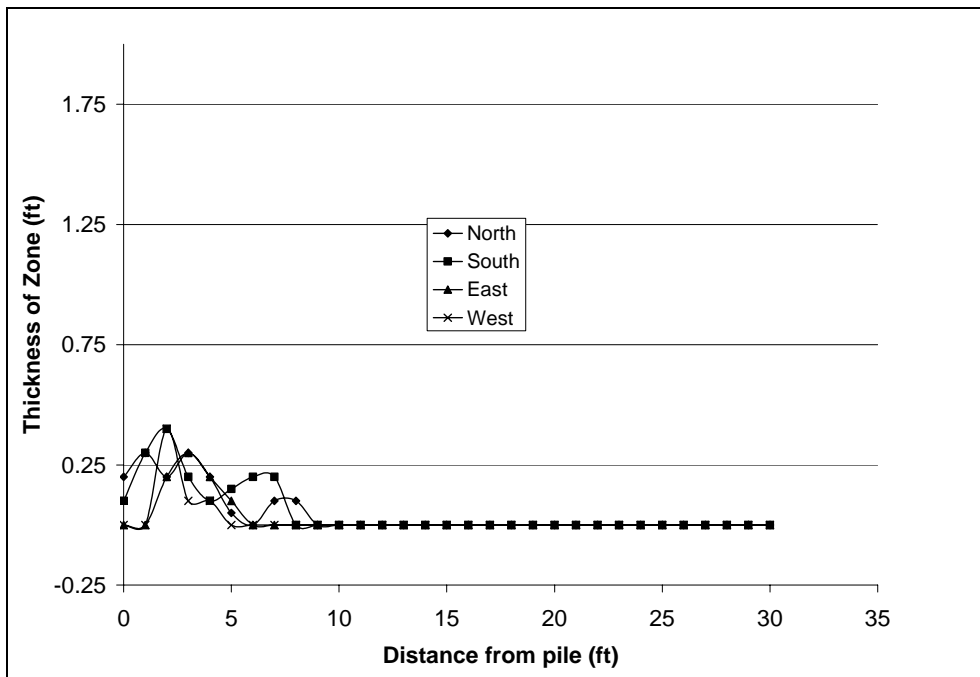


Figure D- 16. CB-6 Debris Zone Profile.

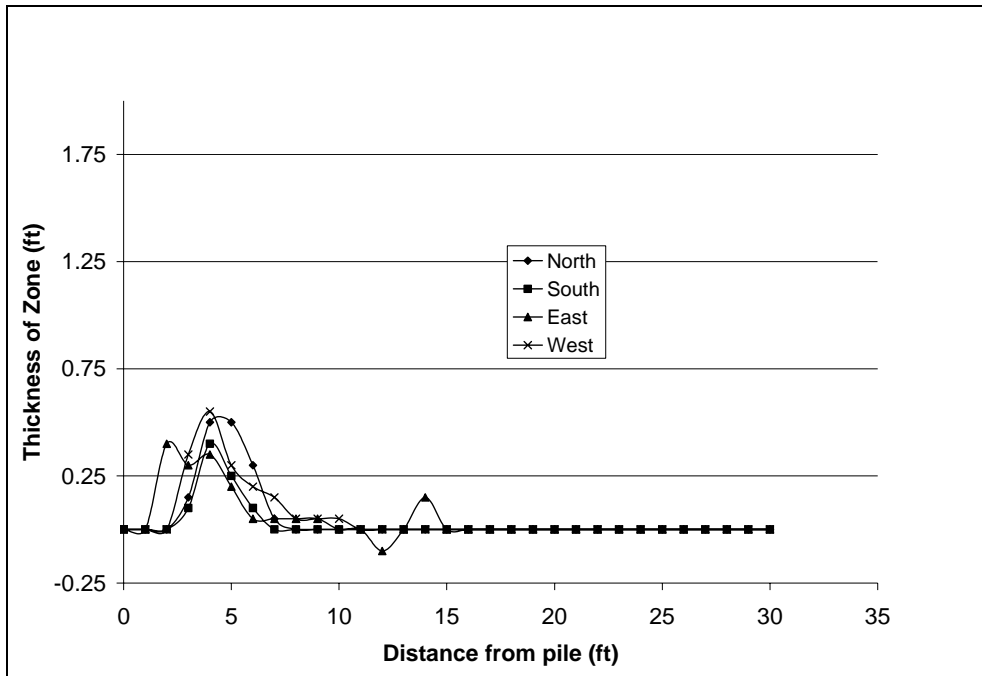


Figure D- 17. CB-7 Debris Zone Profile.

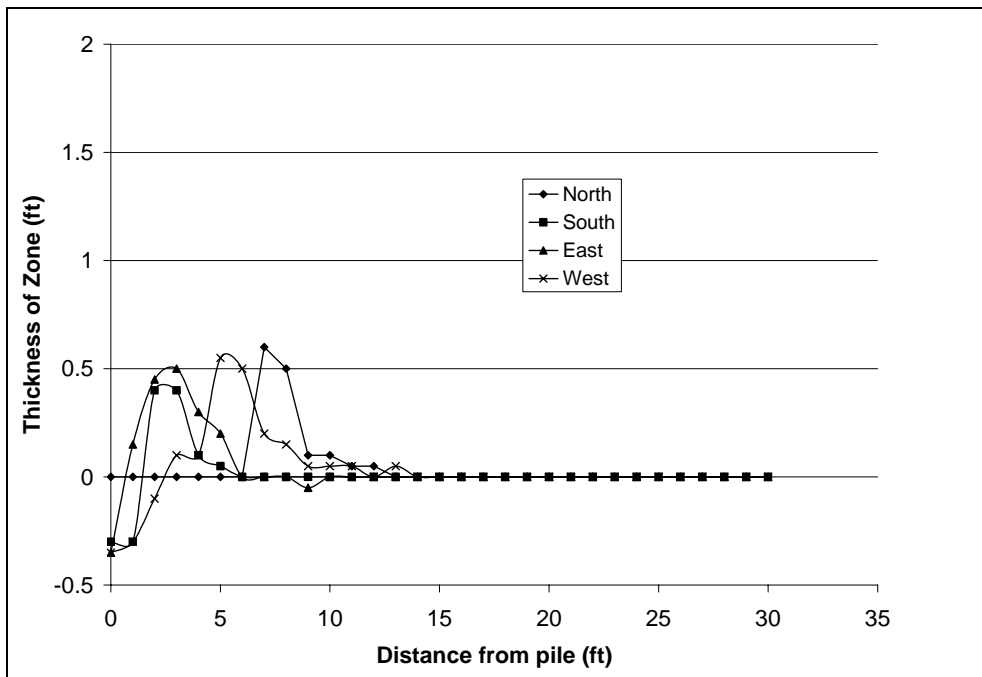


Figure D- 18. CB-8 Debris Zone Profile.

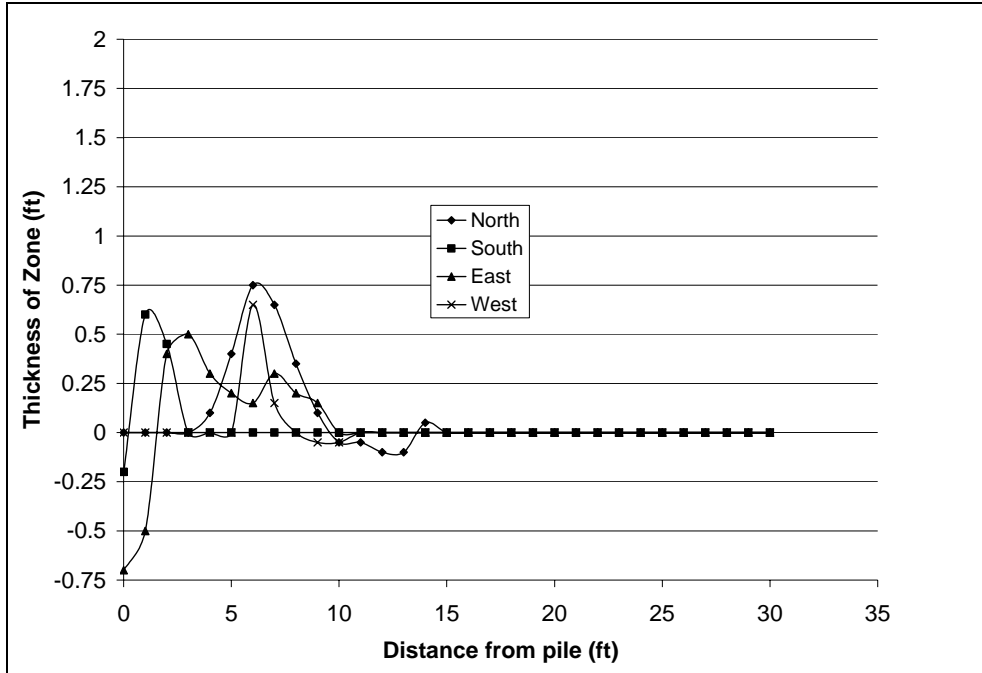


Figure D- 19. CB-9 Debris Zone Profile.

Test CB-1					
Q_w (cfm)	42.000				
Depth (ft)	Time (sec) Min		Insertion rate		
0.001	0	0	XXXXXXXXXX		
1	2	0.033333	30.00		
2	4	0.066667	30.00		
3	6	0.1	30.00		
4	7	0.116667	60.00		
5	8	0.133333	60.00		
6	314	5.233333	0.20		
7	423	7.05	0.55		
8	430	7.166667	8.57		
9	437	7.283333	8.57		
10	512	8.533333	0.80		
				Total time	13:25

Figure D- 20. CB-1 Measured Insertion Data.

Test CB-2			
Q _w (cfm)		44.000	
Depth (ft)	Time (sec)	Min	Insertion rate
0.001	0	0	xxxxxxxxxxx
1	3.5	0.058333	17.14
2	7	0.116667	17.14
3	35	0.583333	2.14
4	86	1.433333	1.18
5	229	3.816667	0.42
6	390	6.5	0.37
7	470	7.833333	0.75
8	549	9.15	0.76
9	606	10.1	1.05
10	761	12.68333	0.39
10.5	901	15.01667	0.43
Total time 15:01			

Figure D- 21. CB-2 Measured Insertion Data.

Test CB-3			
Q _w (cfm)		77.000	
Depth (ft)	Time (sec)	Min	Insertion rate
0.001	6	0.1	xxxxxxxxxxx
1	10	0.166667	15.00
2	14	0.233333	15.00
3	17	0.283333	20.00
4	21	0.35	15.00
5	25	0.416667	15.00
6	28	0.466667	20.00
7	31	0.516667	20.00
8	35	0.583333	15.00
9	39	0.65	15.00
10	42	0.7	20.00
11	46	0.766667	15.00
12	49	0.816667	20.00
13	70	1.166667	2.86
14	90	1.5	3.00
15	111	1.85	2.86
16	178	2.966667	0.90

Figure D- 22. CB-3 Measured Insertion Data.

Test CB-4

Q_w (cfm)	77.400		
-------------	--------	--	--

Depth (ft)	Time (sec)	Min	Insertion rate
0.001	13	0.216667	xxxxxxxxxxx
1	18	0.3	12.00
2	20	0.333333	30.00
3	25	0.416667	12.00
4	29	0.483333	15.00
5	37	0.616667	7.50
6	43	0.716667	10.00
7	47	0.783333	15.00
8	61	1.016667	4.29
9	82	1.366667	2.86
10	110	1.833333	2.14
11	132	2.2	2.73
12	156	2.6	2.50
13	190	3.166667	1.76
14	209	3.483333	3.16
15	245	4.083333	1.67
16	329	5.483333	0.71

Figure D- 23. CB-4 Measured Insertion Data.

Test CB-5

Q_w (cfm)	81.300		
-------------	--------	--	--

Depth (ft)	Time (sec)	Min	Insertion rate
0.001	0	0	xxxxxxxxxxx
1	2	0.033333	30.00
2	4	0.066667	30.00
3	8	0.133333	15.00
4	11	0.183333	20.00
5	14	0.233333	20.00
6	18	0.3	15.00
7	21	0.35	20.00
8	25	0.416667	15.00
9	29	0.483333	15.00
10	33	0.55	15.00
11	39	0.65	10.00
12	137	2.283333	0.61
13	183	3.05	1.30
14	269	4.483333	0.70

Total time 6:08

Figure D- 24. CB-5 Measured Insertion Data.

Test CB-6			
Q_w (cfm)		77.700	
Depth (ft)	Time (sec)	Min	Insertion rate
0.001	0	0	xxxxxxxxxxx
1	8	0.133333	7.50
2	16	0.266667	7.50
3	19	0.316667	20.00
4	21	0.35	30.00
5	23	0.383333	30.00
6	27	0.45	15.00
7	32	0.533333	12.00
8	34	0.566667	30.00
9	37	0.616667	20.00
10	39	0.65	30.00
11	44	0.733333	12.00
12	59	0.983333	4.00
13	118	1.966667	1.02
14	345	5.75	0.26
Total time 5:45			

Figure D- 25. CB-6 Measured Insertion Data.

Test CB-7			
Q_w (cfm)		82.200	
Depth (ft)	Time (sec)	Min	Insertion rate
0.001	0	0	xxxxxxxxxxx
1	4	0.066667	15.00
2	7	0.116667	20.00
3	10	0.166667	20.00
4	20	0.333333	6.00
5	36	0.6	3.75
6	44	0.733333	7.50
7	47	0.783333	20.00
8	52	0.866667	12.00
9	119	1.983333	0.90
10	180	3	0.98
2' free fall	Total time 5:11		

Figure D- 26. CB-7 Measured Insertion Data.

Test CB-8			
Q _w (cfm)		89.400	
Depth (ft)	Time (sec)	Min	Insertion rate
0.001	0	0	xxxxxxxxxxx
1	3	0.05	20.00
2	8	0.133333	12.00
3	13	0.216667	12.00
4	28	0.466667	4.00
5	40	0.666667	5.00
6	44	0.733333	15.00
7	52	0.866667	7.50
8	63	1.05	5.45
9	103	1.716667	1.50
10	203	3.383333	0.60
11	360	6	0.38
12	610	10.16667	0.24
2' free fall		Total time 11:50	

Figure D- 27. CB-8 Measured Insertion Data.

Test CB-9			
Q _w (cfm)		90.500	
Depth (ft)	Time (sec)	Min	Insertion rate
0.001	0	0	xxxxxxxxxxx
1	4	0.066667	15.00
2	8	0.133333	15.00
3	17	0.283333	6.67
4	36	0.6	3.16
5	57	0.95	2.86
6	66	1.1	6.67
7	72	1.2	10.00
8	88	1.466667	3.75
9	135	2.25	1.28
10	390	6.5	0.24
2' free fall		Total time 7:00	

Figure D- 28. CB-9 Measured Insertion Data.

Test ID	CB-1				
Date	9/3/2003				
	Location				
	S1	S2	S3	S4	S5
Elapsed time	Prejet	Prejet	Prejet	Prejet	
Turbidity	9.9	9	9.5	9	
pH				5.67	
dO					
Salinity	9.4	9.5	9.3	9.4	
Conductivity			15.7	15.78	
Temp C			29.1	29.1	
Temp F			84.4	84.4	
Distance	15	25	35	50	5
Elapsed time	After	After	After	After	During
Turbidity	10.8	10.2	12.2	11.6	12
pH	7.3	7.3	7.23	7.15	6.99
dO					
Salinity	9.4	9.4	9.3	9.3	9.3
Conductivity	15.78	15.88	15.79	15.7	15.7
Temp C	29.2	29.2	29.3	29.2	29.2
Temp F	84.6	84.6	84.7	84.6	84.6
Distance	15	25	35	50	5

Figure D- 29. CB-1 Measured Water Quality Data.

Test ID	CB-2				
Date	9/3/2003				
	Location				
	S1, 25'	S2, 10'	S3, 10'	S4, 25'	S5
Elapsed time	Prejet	Prejet	Prejet	Prejet	
Turbidity	12.5	12.2	11.8	12.5	
pH	6.25	6.8	7.09	7.55	
dO					
Salinity	9.2	9.2	9.3	9.3	
Conductivity	15.5	15.7	15.66	15.63	
Temp C	29.5	29.5	29.2	30.3	
Temp F	85.1	85.1	84.6	86.5	
Distance	15	25	35	50	5
Elapsed time	After	After	After	After	During
Turbidity	21.6	16.5	10.6	9.4	18.2
pH	7.1	7.18	7.51	7.9	
dO					
Salinity	9.2	9.2	9.3	9.2	
Conductivity	15.5	15.7	15.7	15.64	
Temp C	29.5	29.7	29.3	29.5	
Temp F	85.1	85.5	84.7	85.1	
Distance	15	25	35	50	5

Figure D- 30. CB-2 Measured Water Quality Data.

Test ID	CB-3			
Date	9/8/2003			
	Location			
	S1	S2	S3	S4
Elapsed time	Prejet	Prejet	Prejet	Prejet
Turbidity	11.8	10.3	8.8	11.3
pH				
dO	4.48	9.25	4.8	12.5
Salinity	8.4	8.5	8.5	8.5
Conductivity	14.42	14.51	14.51	14.5
Temp C	24.6	24.5	24.5	24.5
Temp F	76.3	76.1	76.1	76.1
Distance	15	25	35	50
Elapsed time	After	After	After	After
Turbidity	8.7	8.8	7.4	7.8
pH				
dO	7.75	5	7.75	6.2
Salinity	8.5	8.5	8.5	8.5
Conductivity	14.5	14.51	14.5	14.5
Temp C	24.6	24.6	24.6	24.6
Temp F	76.3	76.3	76.3	76.3
Distance	15	25	35	50

Figure D- 31. CB-3 Measured Water Quality Data.

Test ID	CB-4			
Date	9/8/2003			
	Location			
	S1	S2	S3	S4
Elapsed time	Prejet	Prejet	Prejet	Prejet
Turbidity	11.1	8.8	10.8	8.5
pH				
dO	4.57	4.48	4.25	4.38
Salinity	8.5	8.5	8.5	8.5
Conductivity	14.51	14.51	14.5	14.5
Temp C	24.3	24.6	24.3	24.3
Temp F	75.7	76.3	75.7	75.7
Distance	15	25	35	50
Elapsed time	After	After	After	After
Turbidity	8.6	8.7	14.5	8.7
pH				
dO	4.42	6.2	4.32	4.29
Salinity	8.5	8.5	8.5	8.5
Conductivity	14.51	14.51	14.51	14.51
Temp C	24.4	24.4	24.4	24.4
Temp F	75.9	75.9	75.9	75.9
Distance	15	25	35	50

Figure D- 32. CB-4 Measured Water Quality Data.

Test ID	CB-5			
Date	9/8/2003			
	Location			
	S1	S2	S3	S4
Elapsed time	Prejet	Prejet	Prejet	Prejet
Turbidity	5.4	4.2	5.6	7.2
pH				
dO	4.85	4.83	4.89	4.85
Salinity	7.3	7.3	7.3	7.3
Conductivity	12.67	12.69	12.69	12.66
Temp C	24.3	24.3	24.4	24.4
Temp F	75.7	75.7	75.9	75.9
Distance	25	10	10	25
Elapsed time	After	After	After	After
Turbidity	7.1	4.5	5.5	7.5
pH				
dO	4.85	4.89	4.83	4.85
Salinity	7.3	7.3	7.3	7.3
Conductivity	12.66	12.69	12.69	12.67
Temp C	24.4	24.4	24.3	24.3
Temp F	75.9	75.9	75.7	75.7
Distance	25	10	10	25

Figure D- 33. CB-5 Measured Water Quality Data.

Test ID	CB-7			
Date	9/10/2003			
	Location			
	S1, 25'	S2, 10'	S3, 10'	S4, 25'
Elapsed time	Prejet	Prejet	Prejet	Prejet
Turbidity	28.5	10.5	11.2	7.2
pH				
dO	5.21	5	4.9	5.12
Salinity	6.9	6.9	6.9	6.8
Conductivity	11.93	11.92	11.91	11.88
Temp C	24.7	24	24	24
Temp F	76.5	75.2	75.2	75.2
Distance	25	10	10	25
Elapsed time	After	After	After	After
Turbidity	34.9	26.7	11	24.1
pH	6.67	6.72	6.69	6.71
dO	5.18	5.17	5.19	5.28
Salinity	6.9	6.9	6.9	6.9
Conductivity	11.89	11.93	11.9	11.88
Temp C	24	24	24	24
Temp F	75.2	75.2	75.2	75.2
Distance	25	10	10	25

Figure D- 34. CB-7 Measured Water Quality Data.

Test ID	CB-8			
Date	9/10/2003			
	Location			
	S1-25'	S2-10'	S3-10'	S4-25'
Elapsed time	Prejet	Prejet	Prejet	Prejet
Turbidity	18.4	16.5	22.5	17.5
pH				
dO	5.5	5.35	5.7	5.5
Salinity	6.9	6.9	6.9	6.9
Conductivity				
Temp C	24	24	24	24
Temp F	75.2	75.2	75.2	75.2
Distance	25	10	10	25
Elapsed time	After	After	After	After
Turbidity	20.5	22.4	18.1	17.5
pH				
dO	5.44	5.45	5.4	5.4
Salinity	6.9	6.9	6.9	6.9
Conductivity				
Temp C	24	24	24	24
Temp F	75.2	75.2	75.2	75.2
Distance	25	10	10	25

Figure D- 35. CB-8 Measured Water Quality Data.

Test ID	CB-9			
Date	9/10/2003			
	Location			
	S1	S2	S3	S4
Elapsed time	Prejet	Prejet	Prejet	Prejet
Turbidity	22.1	21.5	21.4	13.5
pH				
dO	5.32	5.45	5.37	5.5
Salinity	6.9	6.9	6.9	6.9
Conductivity				
Temp C	24	24	24	24
Temp F	75.2	75.2	75.2	75.2
Distance	25	10	10	25
Elapsed time	After	After	After	After
Turbidity	16.5	12.5	14.2	12.6
pH				
dO	5.44	5.44	5.45	5.44
Salinity	6.9	6.9	6.9	6.9
Conductivity				
Temp C	24	24	24	24
Temp F	75.2	75.2	75.2	75.2
Distance	25	10	10	25

Figure D- 36. CB-9 Measured Water Quality Data.

APPENDIX E
Measured Field Data- Sampson County Site

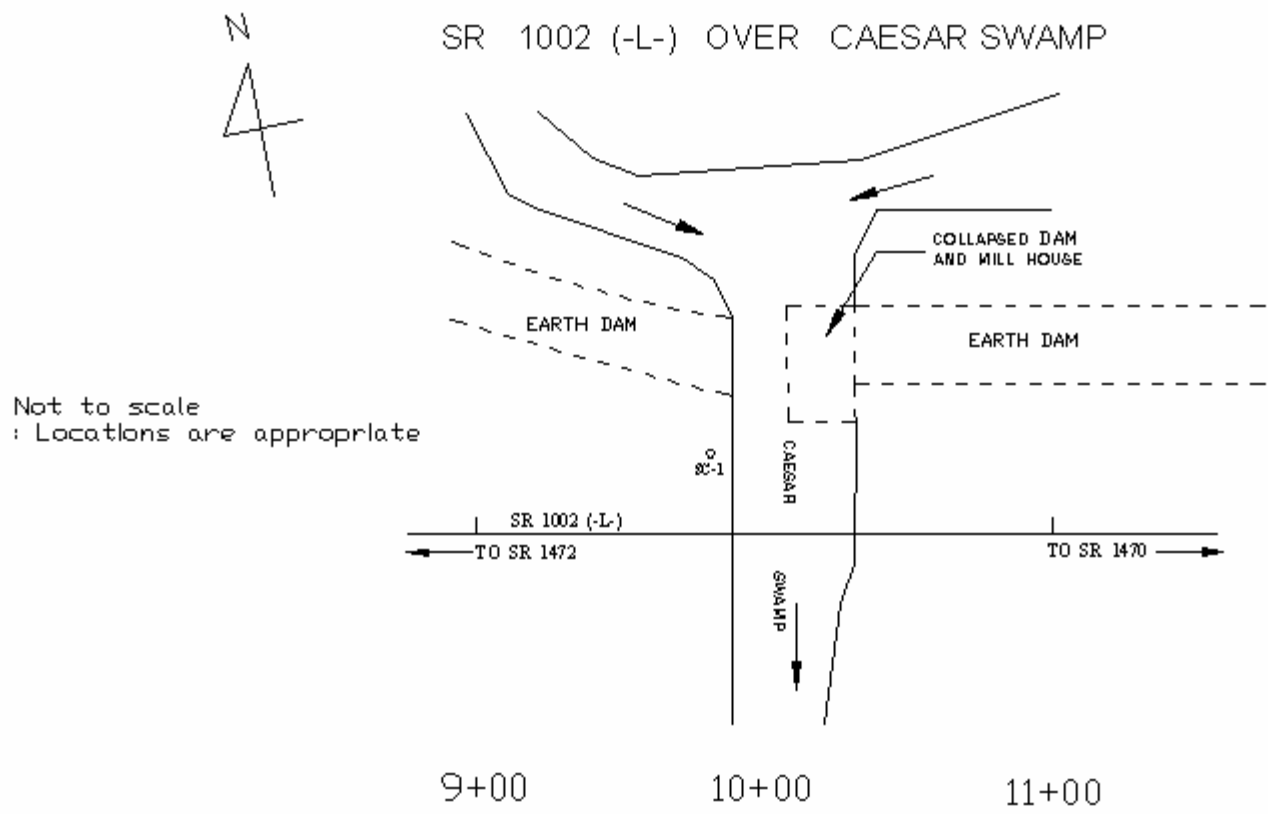


Figure E- 1. Sampson County Field Drawing.

Date:	10/27/2003
Pile ID:	SC-1
Avg Flowrate (cfm):	
Nozzles (in):	2

Prejet Survey					PostJet Survey					Difference					Spoil Volume Calculation		
	North	South	East	West	North	South	East	West	North	South	East	West	North	South	East		
0									0	0	0	0	xxxxxxx	xxxxxxx	xxxxxxx		
1									0	0	0	0	0	0	0		
2									0	0	0	0	0	0	0		
3									0	0	0	0	0	0	0		
4									0	0	0	0	0	0	0		
5									0	0	0	0	0	0	0		
6									0	0	0	0	0	0	0		
7									0	0	0	0	0	0	0		
8									0	0	0	0	0	0	0		
9									0	0	0	0	0	0	0		
10									0	0	0	0	0	0	0		
11									0	0	0	0	0	0	0		
12									0	0	0	0	0	0	0		
13									0	0	0	0	0	0	0		
14									0	0	0	0	0	0	0		
15									0	0	0	0	0	0	0		
16									0	0	0	0	0	0	0		
17									0	0	0	0	0	0	0		
18									0	0	0	0	0	0	0		
19									0	0	0	0	0	0	0		
20									0	0	0	0	0	0	0		
21									0	0	0	0	0	0	0		
22									0	0	0	0	0	0	0		
23									0	0	0	0	0	0	0		
24									0	0	0	0	0	0	0		
25									0	0	0	0	0	0	0		
26									0	0	0	0	0	0	0		
27									0	0	0	0	0	0	0		
28									0	0	0	0	0	0	0		
29									0	0	0	0	0	0	0		
30									0	0	0	0	0	0	0		

Not Measured

	0	0	0
Avg Spoil Volume (ft ³)	0		

Figure E- 2. SC-1 Survey Measurements and Volume Calculation.

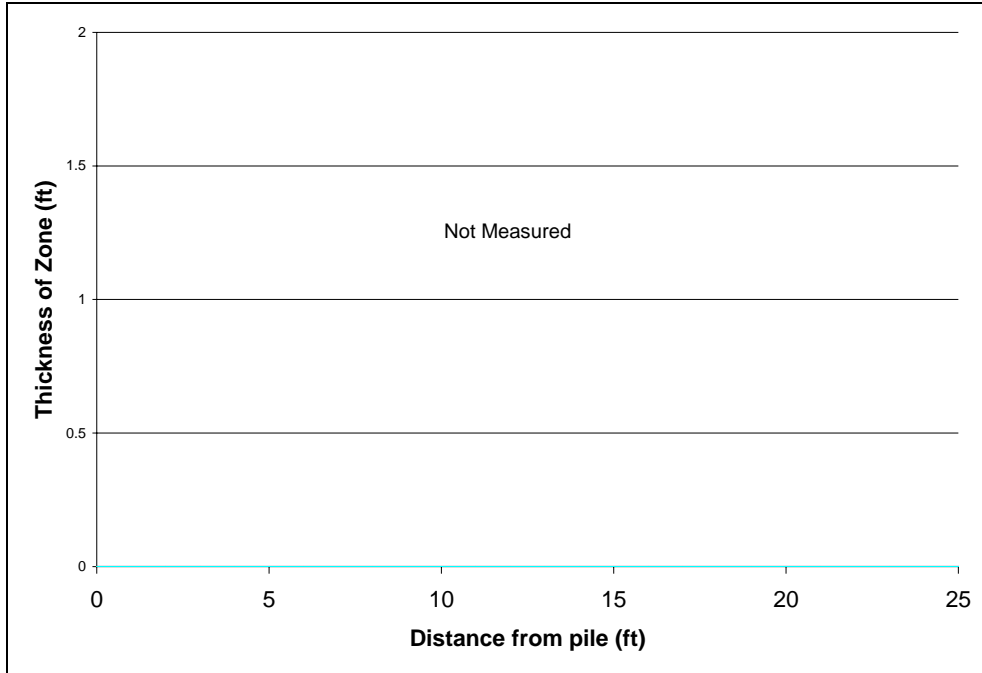
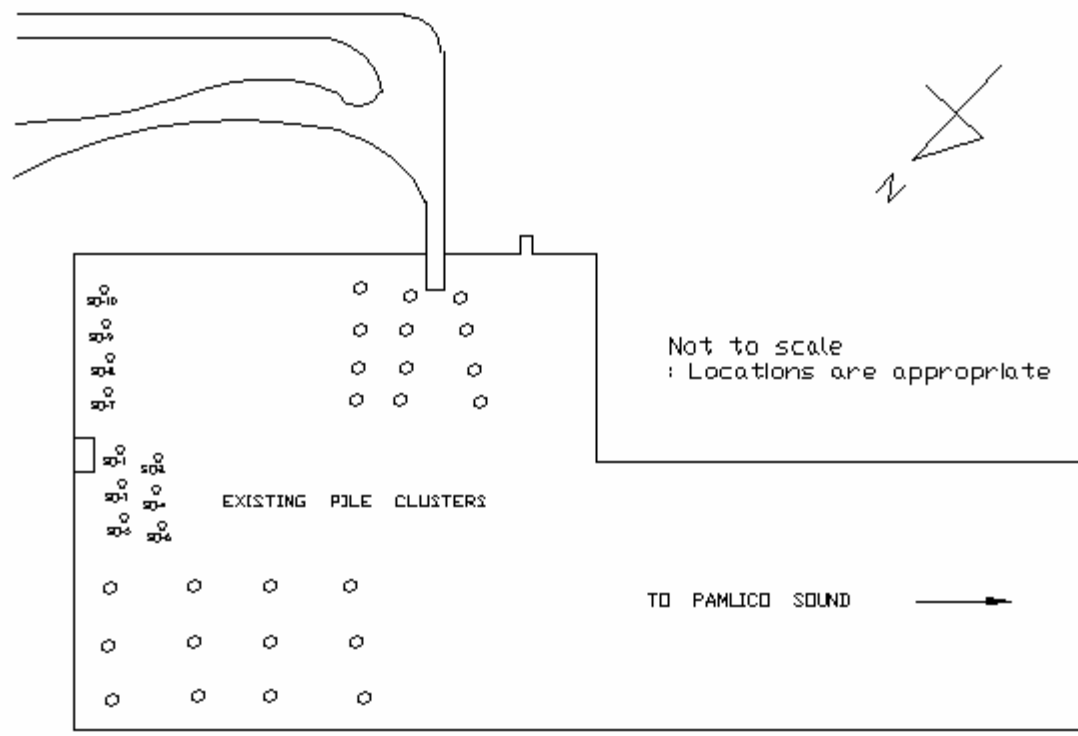


Figure E- 3. SC-1 Debris Zone Profile (not measured).

Test SC-1							
Back Pressure 125 psi							
Q _w (cfm)	179.000						
Depth (ft)	Time (sec)	Min	Insertion rate		L/D	(lv/Qw)(L/D)	IP
0.001	0	0	xxxxxxxxxxx		0.0005	8.7751E-09	1.03E-09
1	55	0.916667	1.09		0.5	0.00877514	0.001032
2	88	1.466667	1.82		1	0.03510056	0.004128
3	123	2.05	1.71		1.5	0.07897626	0.009288
4	194	3.233333	0.85		2	0.14040223	0.016511
6	314	5.233333	0.50		3	0.31590503	0.03715
8	324	5.4	6.00		4	0.56160894	0.066045
9	332	5.533333	7.50		4.5	0.71078631	0.083588
10	335	5.583333	20.00		5	0.87751397	0.103196
11	340	5.666667	12.00		5.5	1.0617919	0.124867
12	344	5.733333	15.00		6	1.26362011	0.148602
13	351	5.85	8.57		6.5	1.4829986	0.174401
14	353	5.883333	30.00		7	1.71992737	0.202263
15	365	6.083333	5.00		7.5	1.97440642	0.23219
16	466	7.766667	0.59		8	2.24643575	0.264181
17	780	13	0.19		8.5	2.53601536	0.298235

Figure E- 4. SC-1 Measured Insertion Data.

APPENDIX F
Measured Field Data- Swan Quarter Ferry Basin Site



SWAN QUARTER FERRY

Figure F- 1. Swan Quarter Ferry Basin Field Drawing.

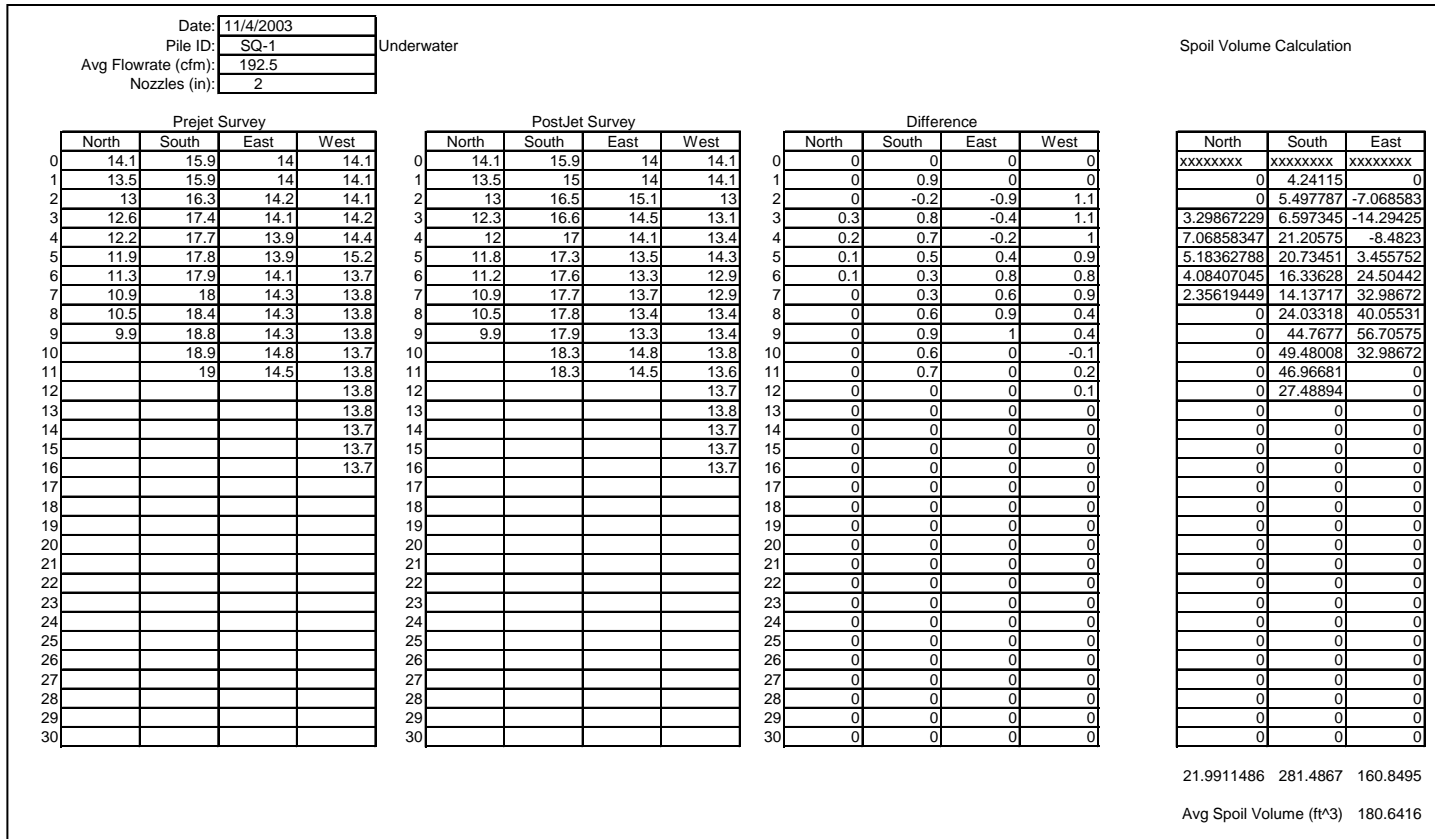


Figure F- 2. SQ-1 Survey Measurements and Volume Calculation.

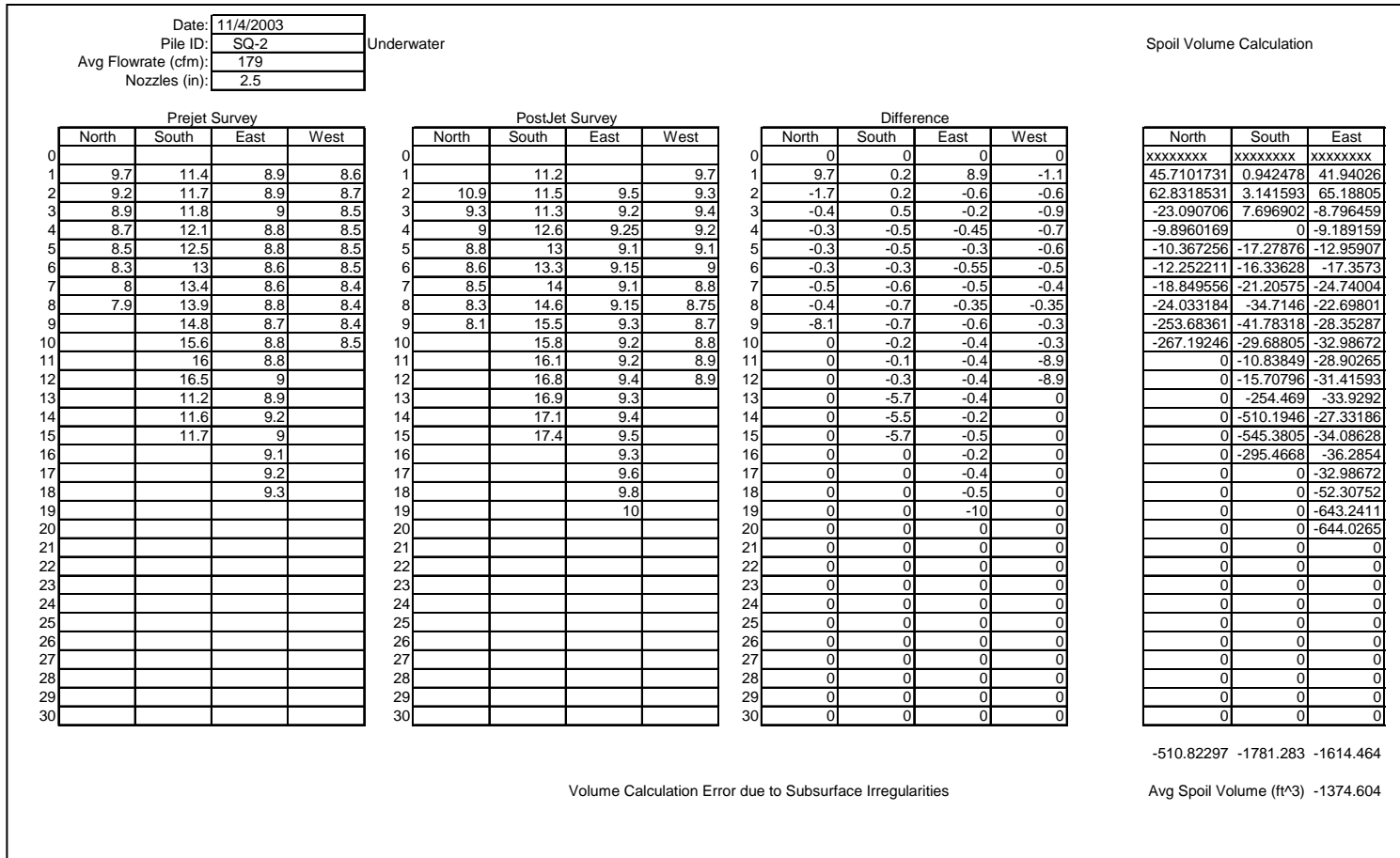


Figure F- 3. SQ-2 Survey Measurements and Volume Calculation (INACCURATE SURVEY)

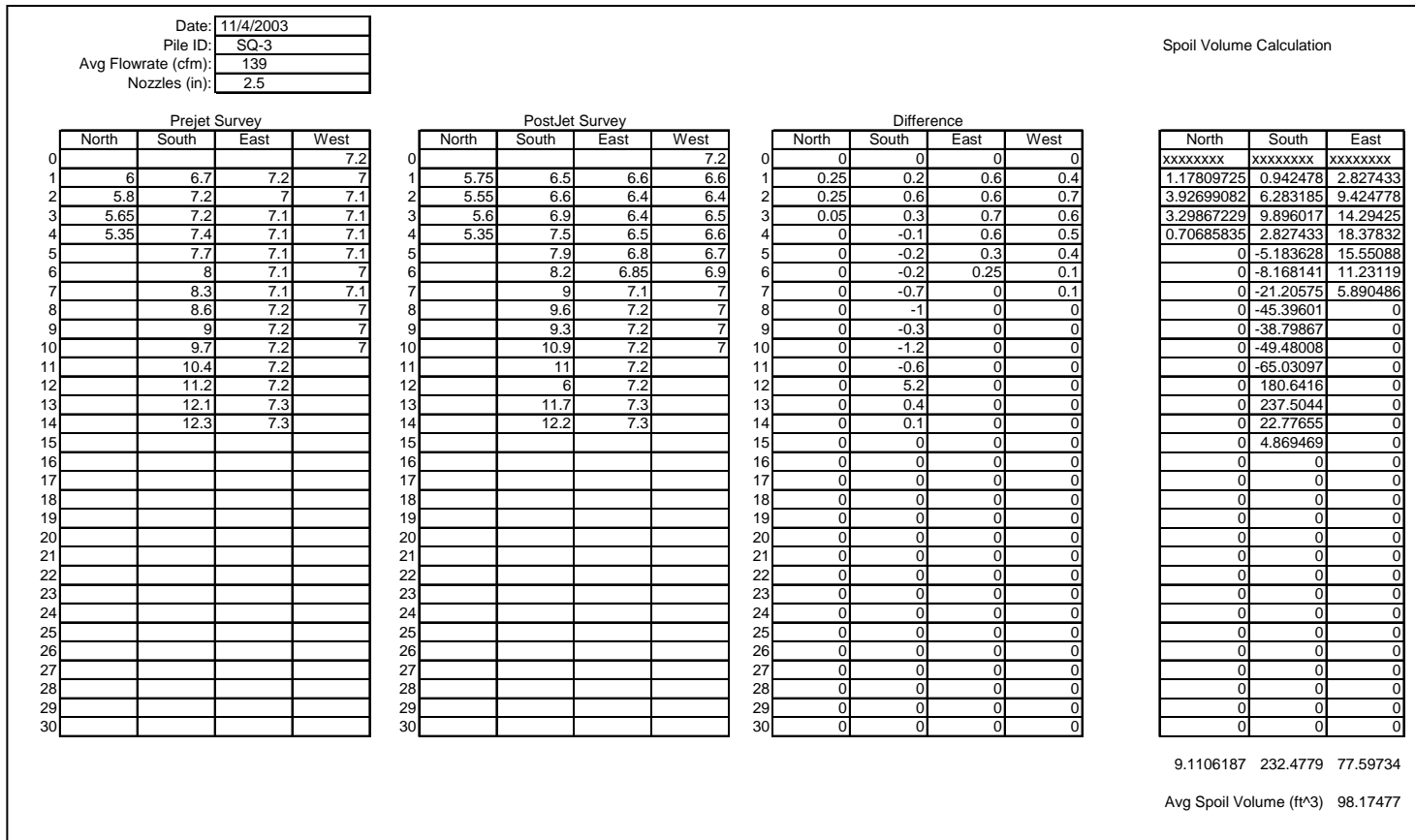


Figure F- 4. SQ-3 Survey Measurements and Volume Calculation (INACCURATE SURVEY).

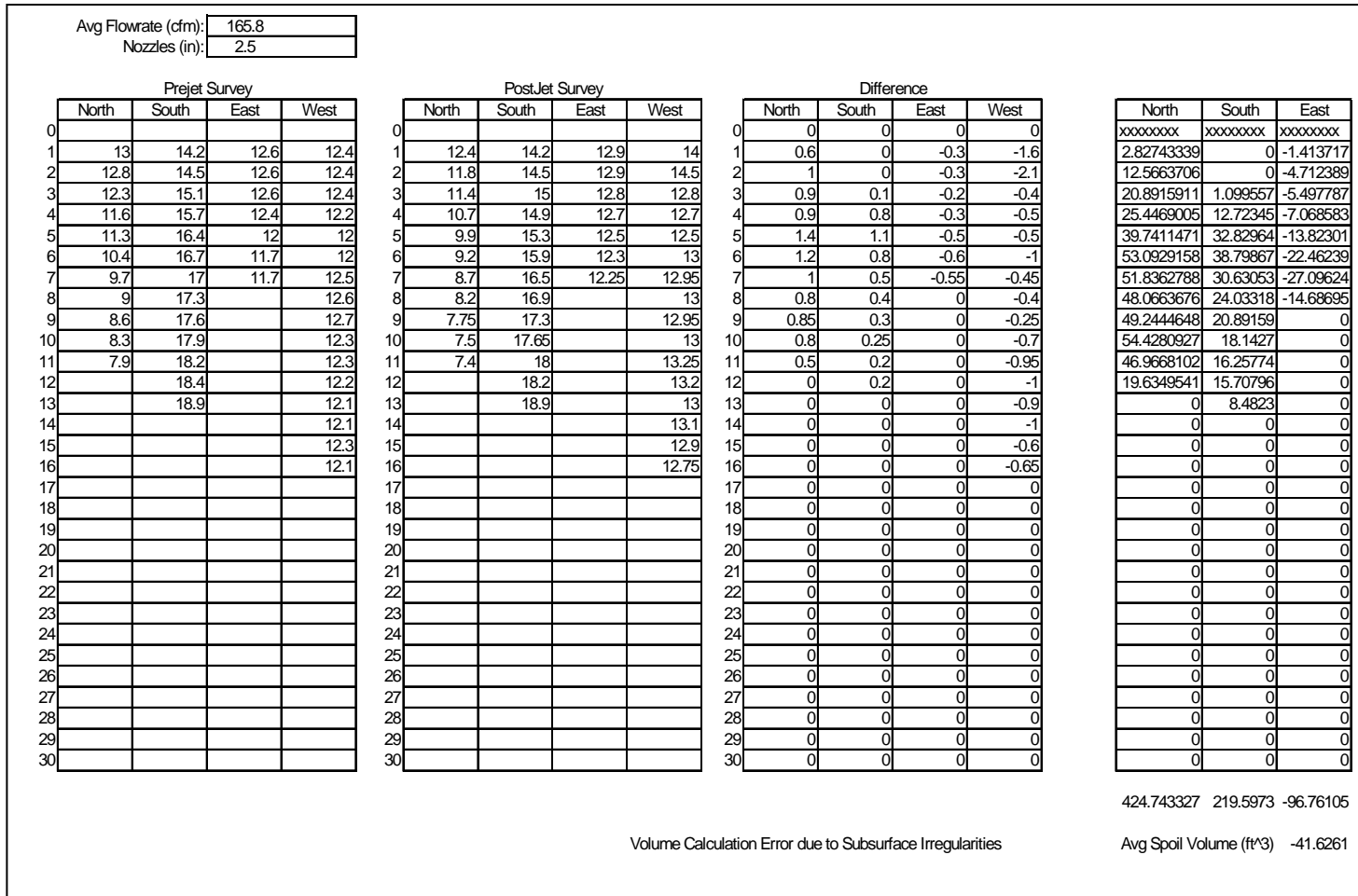


Figure F- 5. SQ-4 Survey Measurements and Volume Calculation (INACCURATE SURVEY).

Date:	11/5/2003
Pile ID:	SQ-5
Avg Flowrate (cfm):	184
Nozzles (in):	2

Spoil Volume Calculation

Prejet Survey					PostJet Survey					Difference								
	North	South	East	West		North	South	East	West		North	South	East	West		North	South	East
0	8.1	8.1	7.3		0	8.1	8.1			0	0	0	7.3	0	xxxxxxx	xxxxxxx	xxxxxxx	
1	7.9	8.4	7.2	7.3	1	8	7.6	6.75	6.95	1	-0.1	0.8	0.45	0.35	-0.4712389	3.769911	36.52101	
2	7.75	8.5	7.1	7.3	2	7.8	7.8	6.35	6.4	2	-0.05	0.7	0.75	0.9	-1.1780972	11.78097	9.424778	
3	7.3	8.7	7.15	7.3	3	7.5	7.95	6.25	6.35	3	-0.2	0.75	0.9	0.95	-2.7488936	15.94358	18.1427	
4	7.3	8.8	7.1	7.3	4	7	8.1	6.45	6.5	4	0.3	0.7	0.65	0.8	1.41371669	20.49889	21.91261	
5	7	8.9	7.1	7.3	5	7	8.4	6.5	6.6	5	0	0.5	0.6	0.7	5.18362788	20.73451	21.59845	
6	6.8	9	7	7.3	6	6.8	8.65	6.45	6.6	6	0	0.35	0.55	0.7	0	17.3573	23.48341	
7		9.25	7	7.4	7		9	6.55	6.75	7	0	0.25	0.45	0.65	0	14.13717	23.56194	
8		9.45	7	7.3	8		9.35	6.55	6.9	8	0	0.1	0.45	0.4	0	9.346238	24.03318	
9		9.8	7	7.3	9		9.55	6.5	6.85	9	0	0.25	0.5	0.45	0	10.4458	28.35287	
10		9.2	6.9	7.3	10		9.85	6.5	6.95	10	0	-0.65	0.4	0.35	0	-13.19469	29.68805	
11		10.6	6.9	7.4	11		10.3	6.5	7	11	0	0.3	0.4	0.4	0	-12.64491	28.90265	
12		11.3		7.4	12		11.05		6.95	12	0	0.25	0	0.45	0	21.59845	15.70796	
13		11.6			13		11.8			13	0	-0.2	0	0	0	2.120575	0	
14		12.3			14		12.2			14	0	0.1	0	0	0	-4.555309	0	
15		12.65			15		12.5			15	0	0.15	0	0	0	12.17367	0	
16		13.3			16		12.9			16	0	0.4	0	0	0	28.50995	0	
17		13.5			17		13.1			17	0	0.4	0	0	0	43.9823	0	
18		13.6			18		13.45			18	0	0.15	0	0	0	31.96571	0	
19		13.8			19		13.8			19	0	0	0	0	0	9.189159	0	
20		14.4			20		14.4			20	0	0	0	0	0	0	0	0
21					21					21	0	0	0	0	0	0	0	0
22					22					22	0	0	0	0	0	0	0	0
23					23					23	0	0	0	0	0	0	0	0
24					24					24	0	0	0	0	0	0	0	0
25					25					25	0	0	0	0	0	0	0	0
26					26					26	0	0	0	0	0	0	0	0
27					27					27	0	0	0	0	0	0	0	0
28					28					28	0	0	0	0	0	0	0	0
29					29					29	0	0	0	0	0	0	0	0
30					30					30	0	0	0	0	0	0	0	0

2.19911486 243.1593 281.3296

Avg Spoil Volume (ft^3) 207.2273

Figure F- 6. SQ-5 Survey Measurements and Volume Calculation (INACCURATE SURVEY).

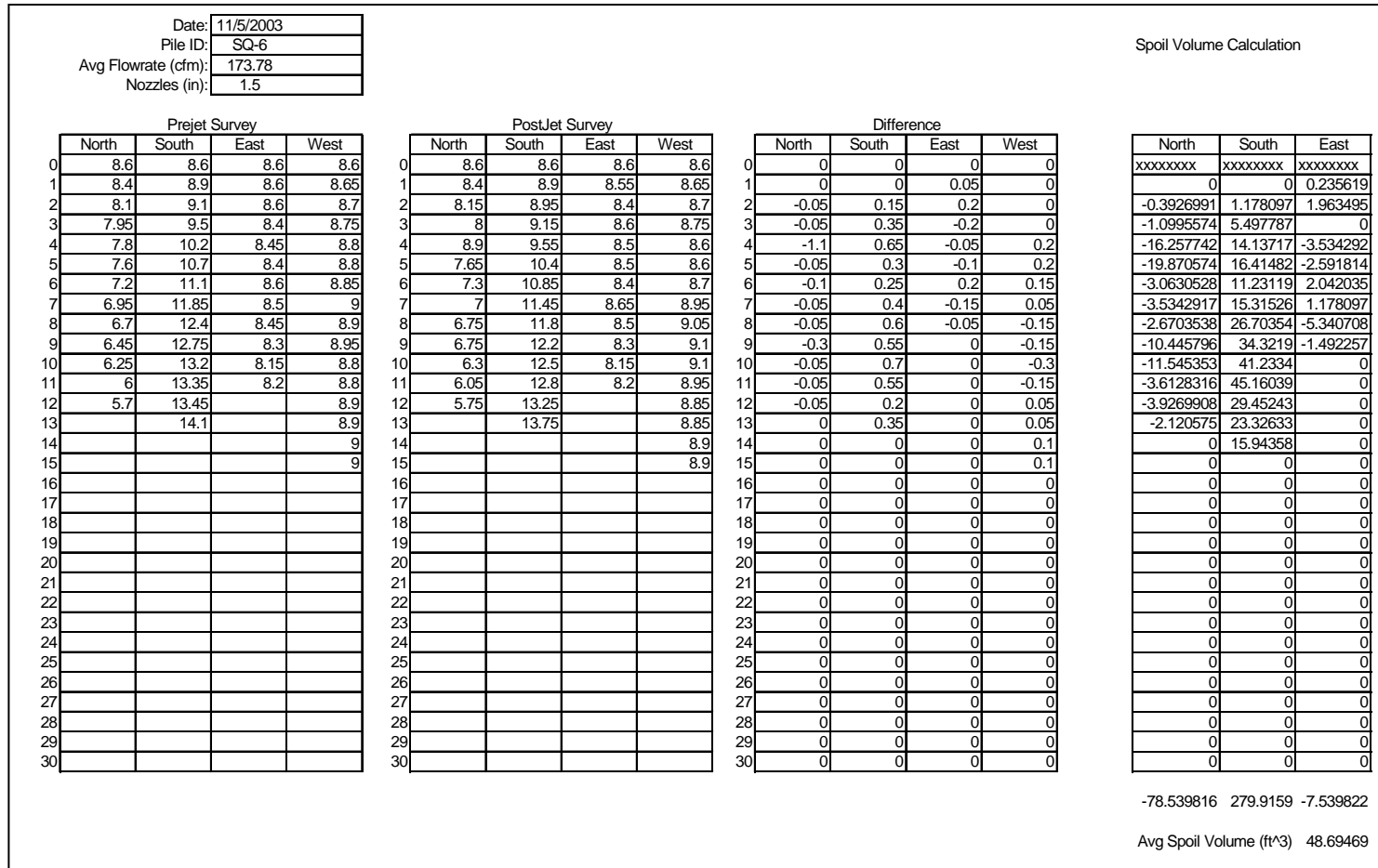


Figure F- 7. SQ-6 Survey Measurements and Volume Calculation (INACCURATE SURVEY).

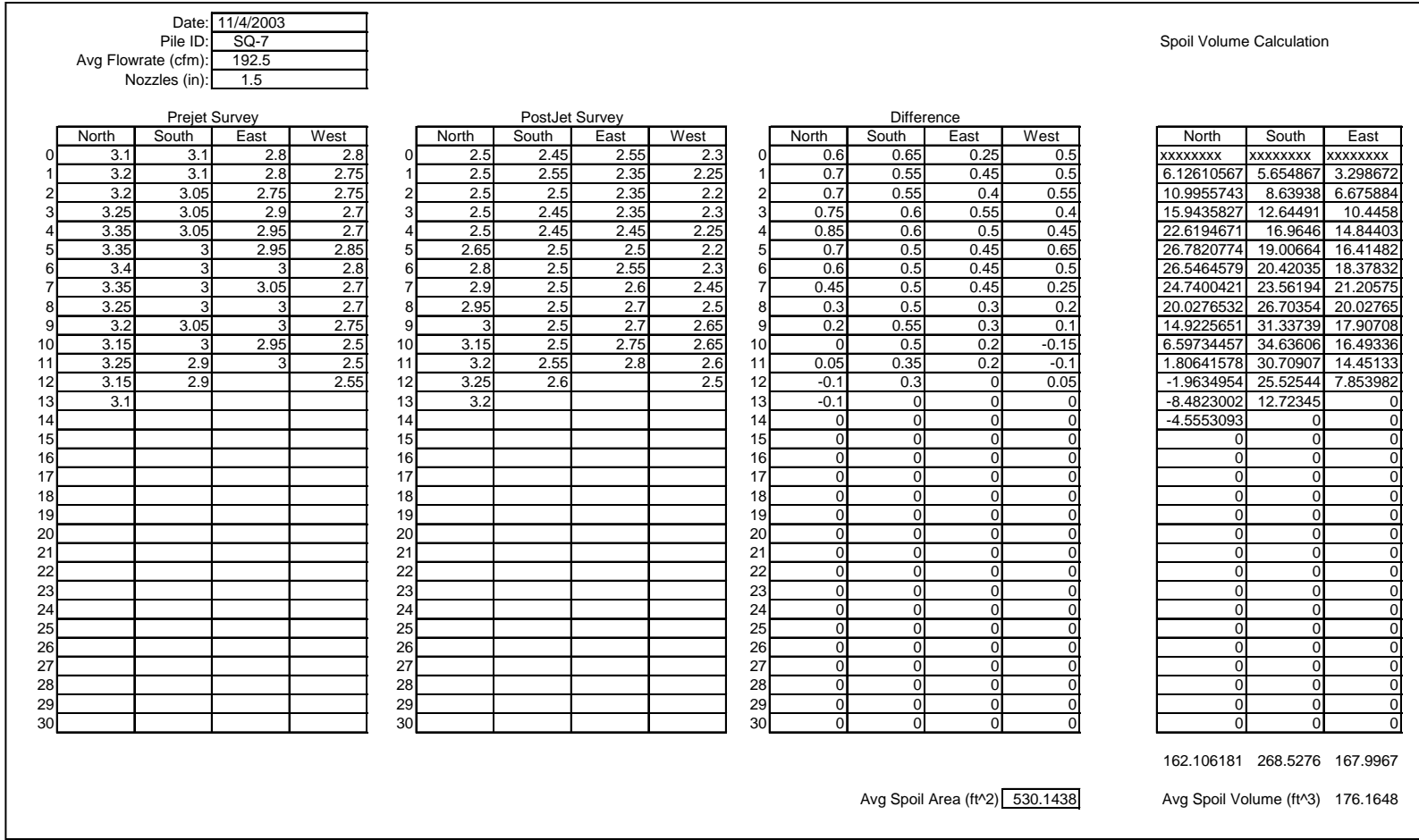


Figure F- 8. SQ-7 Survey Measurements and Volume Calculation.

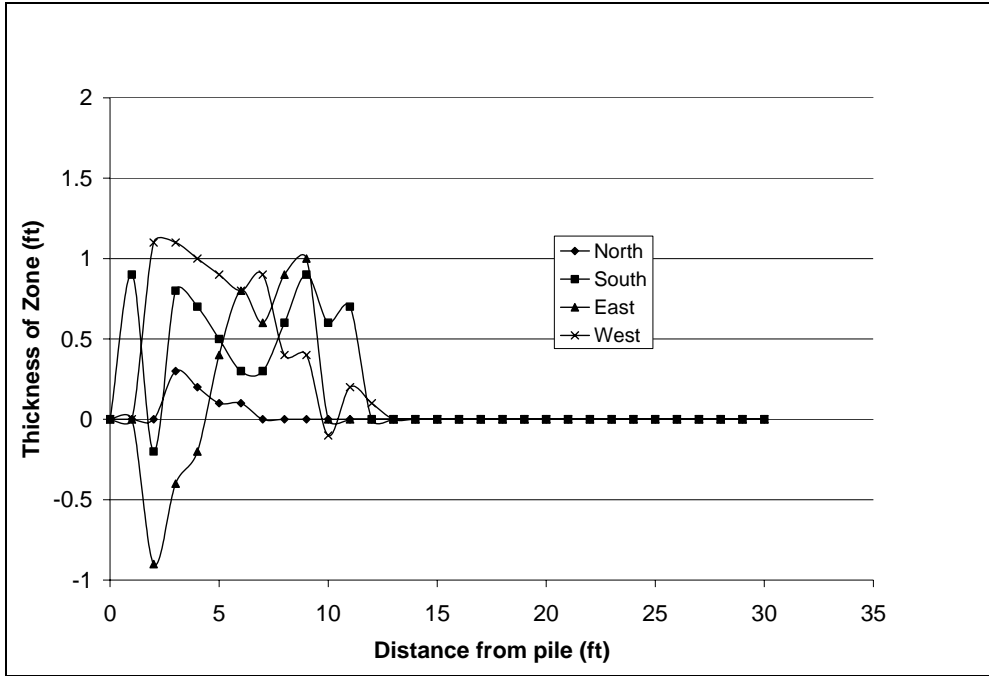


Figure F- 12. SQ-1 Debris Zone Profile.

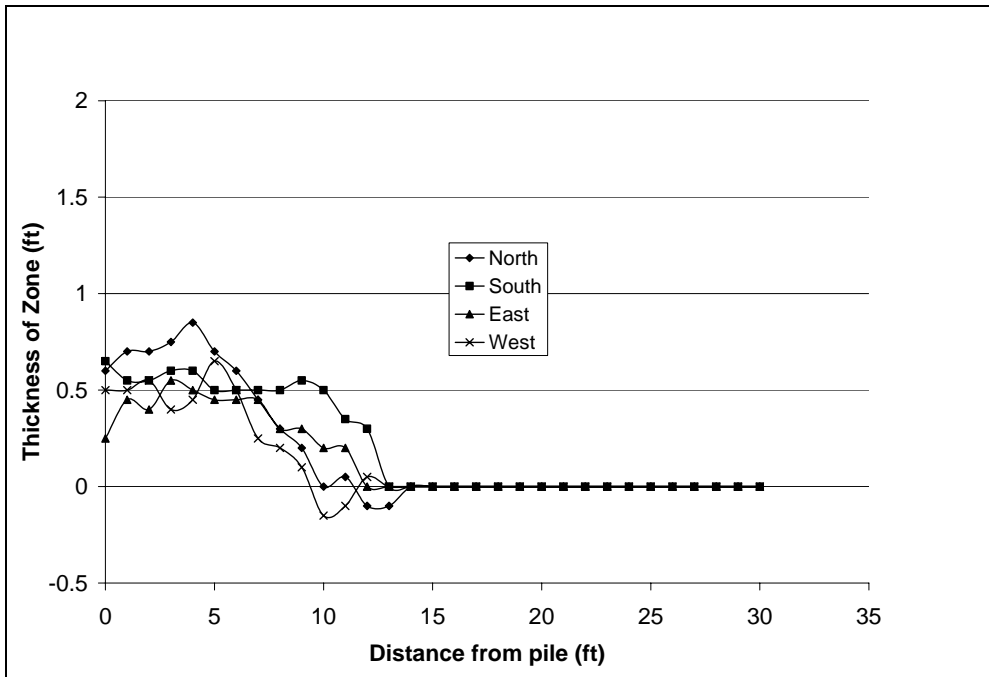


Figure F- 13. SQ-7 Debris Zone Profile.

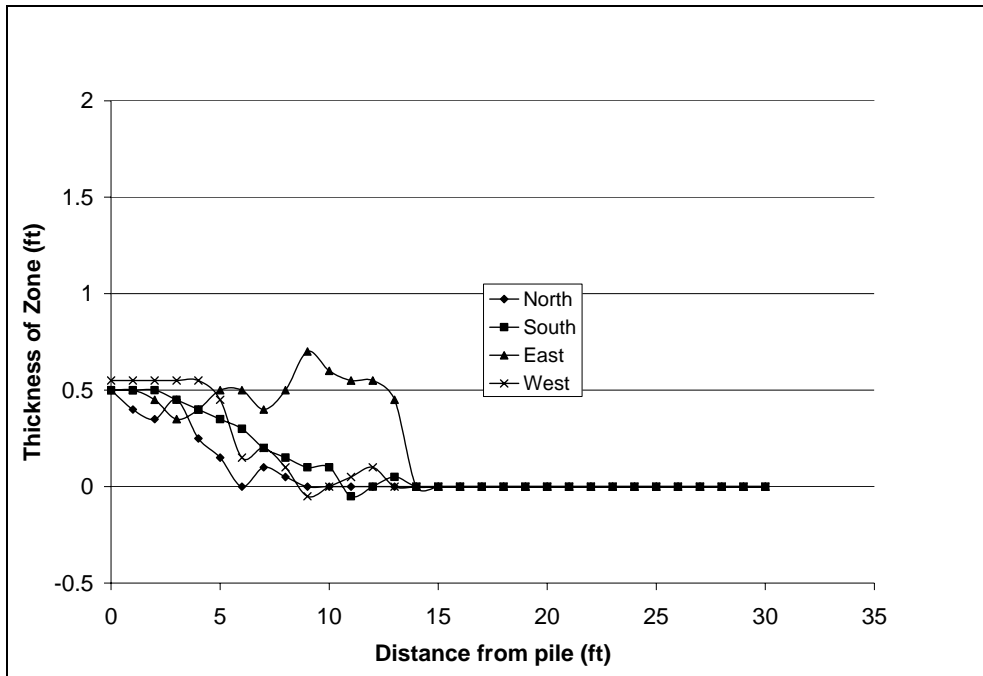


Figure F- 14. SQ-8 Debris Zone Profile.

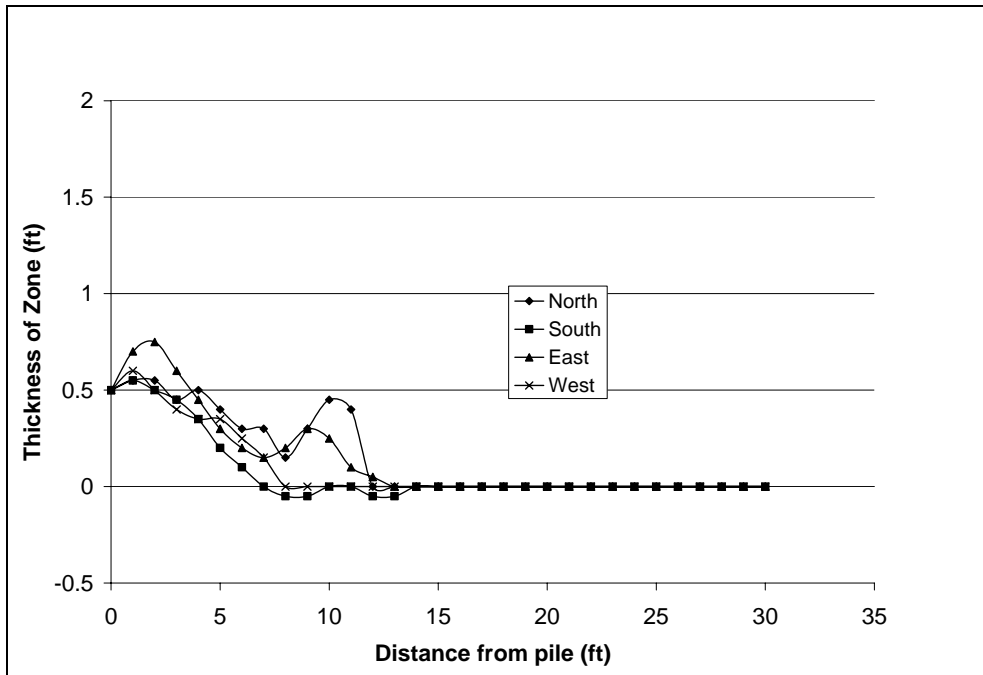


Figure F- 15. SQ-9 Debris Zone Profile.

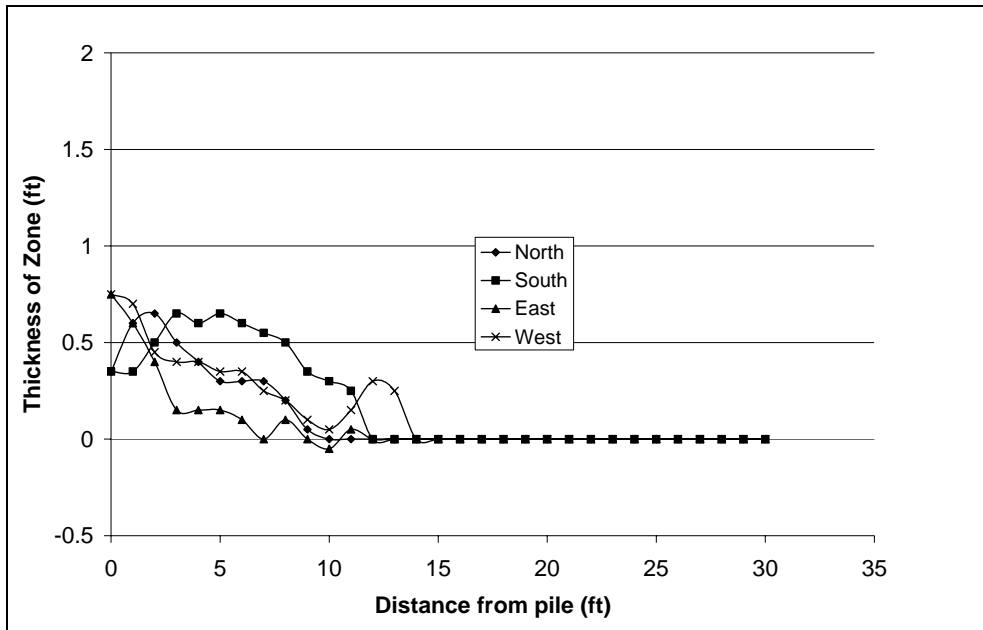


Figure F- 16. SQ-10 Debris Zone Profile.

Test SQ-1							
Back Pressure 112.5 psi							
Q _w (cfm)	192.500						
Depth (ft)	Time (sec)	Min	Insertion rate		L/D	(lv/Qw)(L/D)	IP
0.001	0	0	xxxxxxxxxxx		0.0005	8.1597E-09	1.07E-09
1	2.5	0.041667	24.00		0.5	0.00815974	0.001066
2	5	0.083333	24.00		1	0.03263896	0.004265
3	9	0.15	15.00		1.5	0.07343766	0.009596
4	13	0.216667	15.00		2	0.13055584	0.017059
5	18	0.3	12.00		2.5	0.20399351	0.026655
6	23	0.383333	12.00		3	0.29375065	0.038383
7	26.5	0.441667	17.14		3.5	0.39982727	0.052244
8	30	0.5	17.14		4	0.52222338	0.068237
9	33	0.55	20.00		4.5	0.66093896	0.086363
10	36	0.6	20.00		5	0.81597403	0.106621
11	59	0.983333	2.61		5.5	0.98732857	0.129011
12	82	1.366667	2.61		6	1.1750026	0.153534
13	85	1.416667	20.00		6.5	1.3789961	0.180189
14	107	1.783333	2.73		7	1.59930909	0.208976
15	115	1.916667	7.50		7.5	1.83594156	0.239896
16	123	2.05	7.50		8	2.08889351	0.272949
17	132	2.2	6.67		8.5	2.35816494	0.308134
18	141	2.35	6.67		9	2.64375584	0.345451
19	146	2.433333	12.00		9.5	2.94566623	0.3849
20	152	2.533333	10.00		10	3.2638961	0.426482
21	167	2.783333	4.00		10.5	3.59844545	0.470197
22	181	3.016667	4.29		11	3.94931429	0.516044
23	196	3.266667	4.00		11.5	4.3165026	0.564023
24	210	3.5	4.29		12	4.70001039	0.614135
25	223	3.716667	4.62		12.5	5.09983766	0.666379
26	236	3.933333	4.62		13	5.51598442	0.720755
27	260	4.333333	2.50		13.5	5.94845065	0.777264
28	284	4.733333	2.50		14	6.39723636	0.835906
29	300	5	3.75		14.5	6.86234156	0.896679
30	316	5.266667	3.75		15	7.34376623	0.959585

Figure F- 17. SQ-1 Measured Insertion Data.

Test SQ-2							
Back Pressure 100 psi							
Q _w (cfm)	179.000						
Depth (ft)	Time (sec)	Min	Insertion rate		L/D	(lv/Qw)(L/D)	IP
0.001	0	0	xxxxxxxxxxx		0.0005	8.77514E-09	1.28995E-09
1	4	0.066667	15.00		0.5	0.00877514	0.001289946
2	8	0.133333	15.00		1	0.035100559	0.005159782
3	28	0.466667	3.00		1.5	0.078976257	0.01160951
4	49	0.816667	2.86		2	0.140402235	0.020639128
5	59	0.983333	6.00		2.5	0.219378492	0.032248638
6	68	1.133333	6.67		3	0.315905028	0.046438039
7	75	1.25	8.57		3.5	0.429981844	0.063207331
8	83	1.383333	7.50		4	0.561608939	0.082556514
9	87	1.45	15.00		4.5	0.710786313	0.104485588
10	91	1.516667	15.00		5	0.877513966	0.128994553
11	96	1.6	12.00		5.5	1.061791899	0.156083409
12	101	1.683333	12.00		6	1.263620112	0.185752156
13	111	1.85	6.00		6.5	1.482998603	0.218000795
14	122	2.033333	5.45		7	1.719927374	0.252829324
15	142	2.366667	3.00		7.5	1.974406425	0.290237744
16	163	2.716667	2.86		8	2.246435754	0.330226056
17	170	2.833333	8.57		8.5	2.536015363	0.372794258
18	176	2.933333	10.00		9	2.843145251	0.417942352
19	188	3.133333	5.00		9.5	3.167825419	0.465670337
20	199	3.316667	5.45		10	3.510055866	0.515978212
21	210	3.5	5.45		10.5	3.869836592	0.568865979
22	222	3.7	5.00		11	4.247167598	0.624333637
23	232	3.866667	6.00		11.5	4.642048883	0.682381186
24	243	4.05	5.45		12	5.054480447	0.743008626
25	268	4.466667	2.40		12.5	5.484462291	0.806215957
26	295	4.916667	2.22		13	5.931994413	0.872003179
27	317	5.283333	2.73		13.5	6.397076816	0.940370292
28	338	5.633333	2.86		14	6.879709497	1.011317296
29	403	6.716667	0.92		14.5	7.379892458	1.084844191
30	468	7.8	0.92		15	7.897625698	1.160950978
31	478	7.966667	6.00		15.5	8.432909218	1.239637655
32	489	8.15	5.45		16	8.985743017	1.320904223
33	534	8.9	1.33		16.5	9.556127095	1.404750683

Figure F- 18. SQ-2 Measured Insertion Data.

Test SQ-3							
Back Pressure 98 psi							
Q _w (cfm)	139.000						
Depth (ft)	Time (sec)	Min	Insertion rate		L/D	(Iv/Qw)(L/D)	IP
0.001	0	0	xxxxxxxxxxx		0.0005	1.13E-08	1.7E-09
1	2.5	0.041667	24.00		0.5	0.01130036	0.001695
2	5	0.083333	24.00		1	0.04520144	0.00678
3	18	0.3	4.62		1.5	0.10170324	0.015255
4	32	0.533333	4.29		2	0.18080576	0.027121
5	121	2.016667	0.67		2.5	0.28250899	0.042376
6	210	3.5	0.67		3	0.40681295	0.061022
7	222	3.7	5.00		3.5	0.55371763	0.083058
8	234	3.9	5.00		4	0.72322302	0.108483
9	239	3.983333	12.00		4.5	0.91532914	0.137299
10	243	4.05	15.00		5	1.13003597	0.169505
11	248	4.133333	12.00		5.5	1.36734353	0.205102
12	253	4.216667	12.00		6	1.6272518	0.244088
13	258	4.3	12.00		6.5	1.90976079	0.286464
14	264	4.4	10.00		7	2.2148705	0.332231
15	267	4.45	20.00		7.5	2.54258094	0.381387
16	270	4.5	20.00		8	2.89289209	0.433934
17	318	5.3	1.25		8.5	3.26580396	0.489871
18	365	6.083333	1.28		9	3.66131655	0.549197
19	396	6.6	1.94		9.5	4.07942986	0.611914
20	427	7.116667	1.94		10	4.52014388	0.678022
21	457	7.616667	2.00		10.5	4.98345863	0.747519
22	486	8.1	2.07		11	5.4693741	0.820406
23	506	8.433333	3.00		11.5	5.97789029	0.896684
24	526	8.766667	3.00		12	6.50900719	0.976351
25	546	9.1	3.00		12.5	7.06272482	1.059409
26	567	9.45	2.86		13	7.63904317	1.145856
27	619	10.31667	1.15		13.5	8.23796223	1.235694
28	671	11.18333	1.15		14	8.85948201	1.328922
29	716	11.93333	1.33		14.5	9.50360252	1.42554
30	760	12.66667	1.36		15	10.1703237	1.525549

Figure F- 19. SQ-3 Measured Insertion Data.

Test SQ-4
Back Pressure 100 psi

Q _w (cfm)	139						
Q _w (cfm)	165.800						
Depth (ft)	Time (sec)	Min	Insertion rate		L/D	(lv/Qw)(L/D)	IP
0.001	0	0	xxxxxxxxxxx		0.0005	1.13004E-08	1.66E-09
1	4	0.066667	15.00		0.5	0.01130036	0.001661
2	8	0.133333	15.00		1	0.045201439	0.006645
3	12	0.2	15.00		1.5	0.101703237	0.01495
4	16	0.266667	15.00		2	0.180805755	0.026578
5	20	0.333333	15.00		2.5	0.282508993	0.041529
6	34	0.566667	4.29		3	0.40681295	0.059802
7	48	0.8	4.29		3.5	0.553717626	0.081396
8	53	0.883333	12.00		4	0.723223022	0.106314
9	58	0.966667	12.00		4.5	0.915329137	0.134553
10	69	1.15	5.45		5	1.130035971	0.166115
11	80	1.333333	5.45		5.5	1.367343525	0.200999
12	113	1.883333	1.82		6	1.627251799	0.239206
13	159	2.65	1.30		6.5	1.909760791	0.280735
14	201	3.35	1.43		7	2.214870504	0.325586
15	225	3.75	2.50		7.5	2.542580935	0.373759
16	240	4	4.00		8	2.892892086	0.425255
17	257	4.283333	3.53		8.5	2.737917672	0.402474
18	274	4.566667	3.53		9	3.069499397	0.451216
19	292	4.866667	3.33		9.5	3.420028649	0.502744
20	310	5.166667	3.33		10	3.789505428	0.557057
21	330	5.5	3.00		10.5	4.177929735	0.614156
22	372	6.2	1.43		11	4.585301568	0.674039
23	399	6.65	2.22		11.5	5.011620929	0.736708
24	450	7.5	1.18		12	5.456887817	0.802163
25	480	8	2.00		12.5	5.921102232	0.870402
26	520	8.666667	1.50		13	6.404264174	0.941427
26.5	593	9.883333	0.82		13.25	6.652950467	0.977984
26.5	630	10.5	1.62		13.25	6.652950467	0.977984

**new flowrate

Figure F- 20. SQ-4 Measured Insertion Data.

Test SQ-5
Back Pressure 75 psi

Q _w (cfm)	184.500						
Depth (ft)	Time (sec)	Min	Insertion rate		L/D	(lv/Qw)(L/D)	IP
0.001	0	0	xxxxxxxxxxx		0.0005	8.514E-09	1.66866E-09
20	140	2.333333			10	3.4054201	0.667462331
22	170	2.833333			11	4.1205583	0.80762942
24	192	3.2			12	4.9038049	0.961145756
26	220	3.666667			13	5.7551599	1.128011339
28	252	4.2			14	6.6746233	1.308226168
30	298	4.966667			15	7.6621951	1.501790244
34	338	5.633333			17	9.841664	1.928966136

Figure F- 21. SQ-5 Measured Insertion Data.

Test SQ-6
Back Pressure 75 psi

Q _w (cfm)	173.780					
Depth (ft)	Time (sec)	Min		L/D	lv/Qw)(L/D	IP
0.001	0	0		0.0005	9.04E-09	1.7716E-09
2	24	0.4		1	0.036155	0.00708636
4	34	0.566667		2	0.14462	0.02834545
6	40	0.666667		3	0.325394	0.06377726
8	46	0.766667		4	0.578479	0.11338179
10	53	0.883333		5	0.903873	0.17715905
12	79	1.316667		6	1.301577	0.25510903
16	119	1.983333		8	2.313914	0.45352717
18	132	2.2		9	2.928548	0.57399533
22	197	3.283333		11	4.374744	0.85744981
24	267	4.45		12	5.206307	1.02043614
25	380	6.333333		12.5	5.649204	1.10724407

Figure F- 22. SQ-6 Measured Insertion Data.

Test SQ-7
Back Pressure 75 psi

Q _w (cfm)	192.500					
Depth (ft)	Time (sec)	Min		L/D	lv/Qw)(L/D	IP
0.001	0	0		0.0005	8.16E-09	1.59931E-09
4	145	2.416667		2	0.130556	0.025588945
6	270	4.5		3	0.293751	0.057575127
8	293	4.883333		4	0.522223	0.102355782
20	384	6.4		10	3.263896	0.639723636
22	410	6.833333		11	3.949314	0.7740656
24	423	7.05		12	4.70001	0.921202036
26	436	7.266667		13	5.515984	1.081132945
28	473	7.883333		14	6.397236	1.253858327
30	510	8.5		15	7.343766	1.439378182
32	535	8.916667		16	8.355574	1.637692509
34	570	9.5		17	9.43266	1.848801309

Figure F- 23. SQ-7 Measured Insertion Data.

Test SQ-8
Back Pressure 75 psi

Q _w (cfm)	160.400	Depth (ft)	Time (sec)	Min	L/D	(lv/Qw)(L/D)	IP
		0.001	0	0	0.0005	9.7927E-09	1.919E-09
		4	97	1.616667	2	0.15668329	0.0307099
		6	121	2.016667	3	0.35253741	0.0690973
		8	132	2.2	4	0.62673317	0.1228397
		10	136	2.266667	5	0.97927057	0.191937
		14	140	2.333333	7	1.91937032	0.3761966
		16	162	2.7	8	2.50693267	0.4913588
		18	193	3.216667	9	3.17283666	0.621876
		20	220	3.666667	10	3.91708229	0.7677481
		22	255	4.25	11	4.73966958	0.9289752
		24	280	4.666667	12	5.6405985	1.1055573
		26	308	5.133333	13	6.61986908	1.2974943
		28	348	5.8	14	7.6774813	1.5047863
		32	450	7.5	16	10.0277307	1.9654352

Figure F- 24. SQ-8 Measured Insertion Data.

Test SQ-9
Back Pressure 125 psi

Q _w (cfm)	165.800	Depth (ft)	Time (sec)	Min	L/D	(lv/Qw)(L/D)	IP
		0.001	0	0	0.0005	9.4738E-09	1.11E-09
		8	42	0.7	4	0.60632087	0.071303
		12	60	1	6	1.36422195	0.160433
		14	65	1.083333	7	1.85685766	0.218366
		16	71	1.183333	8	2.42528347	0.285213
		18	97	1.616667	9	3.0694994	0.360973
		20	120	2	10	3.78950543	0.445646
		22	145	2.416667	11	4.58530157	0.539231
		28	210	3.5	14	7.42743064	0.873466
		30	240	4	15	8.52638721	1.002703
		31.5	260	4.333333	15.75	9.4003419	1.10548

Figure F- 25. SQ-9 Measured Insertion Data.

Test SQ-10						
Back Pressure		78 psi				
Q _w (cfm)	175.000					
Depth (ft)	Time (sec)	Min		L/D	(lv/Qw)(L/D)	IP
0.001	0	0		0.0005	8.9757E-09	1.6916E-09
6	130	2.166667		3	0.32312571	0.06089677
8	150	2.5		4	0.57444571	0.10826092
14	168	2.8		7	1.75924	0.33154908
16	180	3		8	2.29778286	0.43304369
18	211	3.516667		9	2.90813143	0.54807092
22	270	4.5		11	4.34424571	0.81872323
24	300	5		12	5.17001143	0.97434831
26	335	5.583333		13	6.06758286	1.143506
30	440	7.333333		15	8.07814286	1.52241923
32	535	8.916667		16	9.19113143	1.73217477
32.5	547	9.116667		16.25	9.48059821	1.78672813

Figure F- 26. SQ-10 Measured Insertion Data.

Test ID	SQ-1				
Date	11/4/2003				
	Location				
	C, 10'	B-1, 40'	B-2, 100'	B-3, 200'	B-4, 350'
Elapsed time	Prejet	Prejet	Prejet	Prejet	
Turbidity	12.3	11	12.2	12.7	14.3
pH					
dO	6.6	6.8	6.93	6.65	6.75
Salinity					
Conductivity					
Temp C	19.8	19.7	19.7	19.7	19.7
Temp F	67.6	67.5	67.5	67.5	67.5
Distance	10	40	100	200	350
Elapsed time	4min	19min	17min	14.5min	11min
Turbidity	12.6	12.5	16.8	19.8	20.2
pH					
dO					
Salinity					
Conductivity					
Temp C	19.7	19.7	19.7	19.7	19.7
Temp F	67.5	67.5	67.5	67.5	67.5
Distance	10	40	100	200	350
Elapsed time	28min	43min	41min	37min	35min
Turbidity	15.2	15.6	14.9	19.2	15.4
pH					
dO	6.94	7.15	7.1	6.92	6.8
Salinity					
Conductivity					
Temp C	19.7	19.7	19.7	19.7	19.7
Temp F	67.5	67.5	67.5	67.5	67.5
Distance	10	40	100	200	350
Elapsed time	120min	120min	120min	120min	120min
Turbidity	12.3	14.2	12.2	13.3	15.3
pH					
dO	7.4	7.29	7.26	7.28	6.74
Salinity					
Conductivity					
Temp C	19.7	19.7	19.7	19.7	19.7
Temp F	67.5	67.5	67.5	67.5	67.5
Distance	10	40	100	200	350

Turbidity Caused by incoming Ferry

Turbidity Caused by incoming Ferry

Turbidity Caused by incoming Ferry

Figure F- 27. SQ-1 Measured Water Quality Data.

Test ID	SQ-2				
Date	11/4/2003				
	Location				
	C, 10'	B-1, 40'	B-2, 100'	B-3, 200'	B-4, 350'
Elapsed time	Prejet	Prejet	Prejet	Prejet	
Turbidity	12.3	14.2	12.2	13.3	15.3
pH					
dO	7.4	7.29	7.26	7.28	6.74
Salinity					
Conductivity					
Temp C	19.7	19.7	19.7	19.7	19.7
Temp F	67.5	67.5	67.5	67.5	67.5
Distance	10	40	100	200	350
Elapsed time	2min	11min	9.5min	5min	7min
Turbidity	16.7	13.3	13.2	12.9	13
pH					
dO					
Salinity					
Conductivity					
Temp C	19.7	19.7	19.7	19.7	19.7
Temp F	67.5	67.5	67.5	67.5	67.5
Distance	10	40	100	200	350
Elapsed time	30min				
Turbidity	14.1				
Elapsed time	70min	70min	70min	70min	70min
Turbidity	16.1	15	15.6	16.9	18.3
pH					
dO					
Salinity					
Conductivity					
Temp C	19.7	19.7	19.7	19.7	19.7
Temp F	67.5	67.5	67.5	67.5	67.5
Distance	10	40	100	200	350

Ferry Came in before reading was taken

Figure F- 28. SQ-2 Measured Water Quality Data.

Test ID	SQ-3				
Date	11/4/2003				
	Location				
	C, 10'	B-1, 40'	B-2, 100'	B-3, 200'	B-4, 350'
Elapsed time	Prejet	Prejet	Prejet	Prejet	
Turbidity	16.1	15	15.6	16.9	18.3
Temp C	19.7	19.7	19.7	19.7	19.7
Temp F	67.5	67.5	67.5	67.5	67.5
Distance	10	40	100	200	350
Elapsed time	4m in	9m in	10m in	11m in	12m in
Turbidity	25	16	14.7	15.7	16
Temp C	19.7	19.7	19.7	19.7	19.7
Temp F	67.5	67.5	67.5	67.5	67.5
Distance	10	40	100	200	350
Elapsed time	35m in	40m in	42m in	44m in	47m in
Turbidity	19.6	16.6	15.8	15.4	14.4
Temp C	19.7	19.7	19.7	19.7	19.7
Temp F	67.5	67.5	67.5	67.5	67.5
Distance	10	40	100	200	350
Elapsed time	58m in				
Turbidity	17.6				
Elapsed time	85m in				
Turbidity	15.8				

Figure F- 29. SQ-3 Measured Water Quality Data.

Test ID	SQ-4			
Date	11/4/2003			
	Location			
	C	C	C	C
Elapsed time	Prejet	4min	35min	50min
Turbidity	15.8	21.3	22.8	16.1
Temp C	19.7	19.7	19.7	20.7
Temp F	67.5	67.5	67.5	69.3
Distance	10'	10'	10'	10'

Figure F- 30. SQ-4 Measured Water Quality Data.

Test ID	SQ-5				
Date	11/5/2003				
	Location				
	C	C	C	C	C
Elapsed time	Prejet	15min	35min	55min	65min
Turbidity	16.5	68.9	35.6	22.8	21.8
dO	5.77	6.96	7.19	7.12	7.14
Temp C	19.7	19.7	19.7	19.7	19.7
Temp F	67.5	67.5	67.5	67.5	67.5
Distance	10'	10'	10'	10'	10'

Figure F- 31. SQ-5 Measured Water Quality Data.

Test ID	SQ-6				
Date	11/5/2003				
	Location				
	C	C	C	C	C
Elapsed time	Prejet	4min	16min	27min	75min
Turbidity	21.8	38.8	35.5	33.9	23.7
Temp C	19.7	19.7	19.7	19.7	19.7
Temp F	67.5	67.5	67.5	67.5	67.5
Distance	10'	10'	10'	10'	10'

Figure F- 32. SQ-10 Measured Water Quality Data.

APPENDIX G
Model Development Spreadsheets

SQ-1				SQ-2			
Depth (ft)	Navg	Min	IP	Depth (ft)	Navg	Min	IP
0.001	0	0	1.06621E-09	0.001	0	0	1.28995E-09
1	0	0.041667	0.001066206	1	0	0.066666667	0.001289946
2	0	0.0833333	0.004264824	2	0	0.133333333	0.005159782
3	0	0.15	0.009595855	3	0	0.466666667	0.01160951
4	0	0.216667	0.017059297	4	0	0.816666667	0.020639128
5	0	0.3	0.026655152	5	0	0.983333333	0.032248638
6	0	0.383333	0.038383418	6	0	1.133333333	0.046438039
7	0	0.441667	0.052244097	7	0	1.25	0.063207331
8	0	0.5	0.068237188	8	0	1.383333333	0.082556514
9	0	0.55	0.086362691	9	0	1.45	0.104485588
10	0	0.6	0.106620606	10	0	1.516666667	0.128994553
11	23	0.983333	0.129010933	11	0	1.6	0.156083409
12	23	1.366667	0.153533673	12	0	1.683333333	0.185752156
13	23	1.416667	0.180188824	13	0	1.85	0.218000795
14	23	1.783333	0.208976388	14	23	2.033333333	0.252829324
15	17	1.916667	0.239896364	15	23	2.366666667	0.290237744
16	17	2.05	0.272948752	16	23	2.716666667	0.330226056
17	17	2.2	0.308133552	17	17	2.833333333	0.372794258
18	17	2.35	0.345450764	18	17	2.933333333	0.417942352
19	17	2.433333	0.384900388	19	17	3.133333333	0.465670337
20	17	2.533333	0.426482424	20	17	3.316666667	0.515978212
21	17	2.783333	0.470196873	21	17	3.5	0.568865979
22	19	3.016667	0.516043733	22	17	3.7	0.624333637
23	19	3.266667	0.564023006	23	17	3.866666667	0.682381186
24	19	3.5	0.614134691	24	20	4.05	0.743008626
25	19	3.716667	0.666378788	25	20	4.466666667	0.806215957
26	19	3.933333	0.720755297	26	20	4.916666667	0.872003179
27	19	4.333333	0.777264218	27	20	5.283333333	0.940370292
28	19	4.733333	0.835905552	28	20	5.633333333	1.011317296
29	19	5	0.896679297	29	20	6.716666667	1.084844191
30	19	5.266667	0.959585455	30	20	7.8	1.160950978
				31	20	7.966666667	1.239637655
Pb	112.5			32	20	8.15	1.320904223
Qw	192.5			33	20	8.9	1.404750683
				Pb	100		
				Qw	179		

Figure G- 1. SQ-1, SQ-2 Insertion Data used to develop slope parameter, m.

SQ-3				SQ-4			
Depth (ft)	Navg	Min	IP	Depth (ft)	Navg	Min	IP
0.001	0		0 1.69505E-09	0.001	3		0 1.66115E-09
1	0	0.0416667	0.001695054	1	3	0.066667	0.001661153
2	0	0.0833333	0.006780216	2	3	0.133333	0.006644612
3	0	0.3	0.015255486	3	3	0.2	0.014950376
4	0	0.5333333	0.027120863	4	3	0.266667	0.026578446
5	0	2.0166667	0.042376349	5	3	0.333333	0.041528822
6	0	3.5	0.061021942	6	3	0.566667	0.059801504
7	0	3.7	0.083057644	7	3	0.8	0.081396491
8	0	3.9	0.108483453	8	3	0.883333	0.106313784
9	0	3.9833333	0.137299371	9	3	0.966667	0.134553383
10	0	4.05	0.169505396	10	3	1.15	0.166115288
11	0	4.1333333	0.205101529	11	3	1.333333	0.200999498
12	0	4.2166667	0.24408777	12	23	1.883333	0.239206014
13	0	4.3	0.286464119	13	23	2.65	0.280734836
14	0	4.4	0.332230576	14	23	3.35	0.325585964
15	0	4.45	0.38138714	15	17	3.75	0.373759397
16	23	4.5	0.433933813	16	17	4	0.425255137
17	23	5.3	0.489870594	17	17	4.283333	0.402473898
18	23	6.0833333	0.549197482	18	17	4.566667	0.451216411
19	23	6.6	0.611914478	19	17	4.866667	0.502744211
20	17	7.1166667	0.678021583	20	17	5.166667	0.557057298
21	17	7.6166667	0.747518795	21	17	5.5	0.614155671
22	17	8.1	0.820406115	22	20	6.2	0.674039331
23	17	8.4333333	0.896683543	23	20	6.65	0.736708277
24	17	8.7666667	0.976351079	24	20	7.5	0.802162509
25	17	9.1	1.059408723	25	20	8	0.870402028
26	17	9.45	1.145856475	26	20	8.666667	0.941426834
27	20	10.316667	1.235694335	26.5	20	9.883333	0.977983719
28	20	11.183333	1.328922302	26.5	20	10.5	0.977983719
29	20	11.933333	1.425540378				
30	20	12.666667	1.525548561				
Pb	98			Pb	100		
Qw	139			Qw	139+160		

Figure G- 2. SQ-3, SQ-4 Insertion Data used to develop slope parameter, m.

SQ-10				SQ-9			
Depth (ft)	Navg	Min	IP	Depth (ft)	Navg	Min	IP
0.001	---	0	1.69158E-09	0.001	---	0	1.11E-09
6	---	2.166667	0.060896769	8	6	0.7	0.071303
8	6	2.5	0.108260923	12	6	1	0.160433
14	6	2.8	0.331549077	14	18	1.083333	0.218366
16	6	3	0.433043692	16	18	1.183333	0.285213
18	18	3.516667	0.548070923	18	18	1.616667	0.360973
22	18	4.5	0.818723231	20	18	2	0.445646
24	18	5	0.974348308	22	18	2.416667	0.539231
26	18	5.583333	1.143506	28	25	3.5	0.873466
30	25	7.333333	1.522419231	30	25	4	1.002703
32	25	8.916667	1.732174769	31.5	25	4.333333	1.10548
32.5	25	9.116667	1.786728125				
Pb	78			Pb	125		
Qw	175			Qw	165.8		

Figure G- 3. SQ-10, SQ-9 Insertion Data used to develop slope parameter, m.

SC-1			
Depth (ft)	Navg	Min	IP
0.001	---	0	1.03E-09
1	---	0.916667	0.001032
2	---	1.466667	0.004128
3	---	2.05	0.009288
4	---	3.233333	0.016511
6	13	5.233333	0.03715
8	13	5.4	0.066045
9	13	5.533333	0.083588
10	13	5.583333	0.103196
11	13	5.666667	0.124867
12	13	5.733333	0.148602
13	13	5.85	0.174401
14	13	5.883333	0.202263
15	13	6.083333	0.23219
16	50	7.766667	0.264181
17	50	13	0.298235
Pb	125		
Qw	165.8		

Figure G- 4. SC-1 Insertion Data used to develop slope parameter, m.

Pile Insertion Spreadsheet		ROBUST CHECK							
Vc (ft ³)	192.5								
D (ft)	2								
A (ft ²)	3.14								
Pb (psi)	112.5								
Pa (psi)	14.7								
Depth (ft)	N value	m	L/D	lv (ft ³)	(lv/Vc)(L/D)/ (Pb/Pa)	Time req (min)	Prev Increment	Incremental	
0.1	15	0.231226	0.05	0.314	1.0657E-05	4.60889E-05	0	4.60889E-05	
1	15	0.231226	0.5	3.14	0.0010657	0.004608888	4.60889E-05	0.004562799	
2	15	0.231226	1	6.28	0.00426279	0.018435551	0.004608888	0.013826663	
3	15	0.231226	1.5	9.42	0.00959127	0.04147999	0.018435551	0.023044439	
4	15	0.231226	2	12.56	0.01705115	0.073742205	0.04147999	0.032262215	
5	15	0.231226	2.5	15.7	0.02664242	0.115222195	0.073742205	0.04147999	
6	15	0.231226	3	18.84	0.03836509	0.165919961	0.115222195	0.050697766	
7	15	0.231226	3.5	21.98	0.05221915	0.225835502	0.165919961	0.059915541	
8	15	0.231226	4	25.12	0.06820461	0.294968819	0.225835502	0.069133317	
9	15	0.231226	4.5	28.26	0.08632145	0.373319912	0.294968819	0.078351093	
10	15	0.231226	5	31.4	0.1065697	0.46088878	0.373319912	0.087568868	
11	15	0.231226	5.5	34.54	0.12894933	0.557675424	0.46088878	0.096786644	
12	15	0.231226	6	37.68	0.15346036	0.663679843	0.557675424	0.106004419	
13	15	0.231226	6.5	40.82	0.18010279	0.778902038	0.663679843	0.115222195	
14	15	0.231226	7	43.96	0.20887661	0.903342009	0.778902038	0.124439971	
15	15	0.231226	7.5	47.1	0.23978182	1.036999755	0.903342009	0.133657746	
16	15	0.231226	8	50.24	0.27281842	1.179875276	1.036999755	0.142875522	
17	15	0.231226	8.5	53.38	0.30798642	1.331968574	1.179875276	0.152093297	
18	15	0.231226	9	56.52	0.34528582	1.493279647	1.331968574	0.161311073	
19	15	0.231226	9.5	59.66	0.38471661	1.663808495	1.493279647	0.170528849	
20	15	0.231226	10	62.8	0.42627879	1.843555119	1.663808495	0.179746624	
21	15	0.231226	10.5	65.94	0.46997236	2.032519519	1.843555119	0.1889644	
22	15	0.231226	11	69.08	0.51579733	2.230701695	2.032519519	0.198182175	
23	15	0.231226	11.5	72.22	0.5637537	2.438101645	2.230701695	0.207399951	
24	15	0.231226	12	75.36	0.61384145	2.654719372	2.438101645	0.216617727	
25	15	0.231226	12.5	78.5	0.66606061	2.880554874	2.654719372	0.225835502	
26	15	0.231226	13	81.64	0.72041115	3.115608152	2.880554874	0.235053278	
27	15	0.231226	13.5	84.78	0.77689309	3.359879205	3.115608152	0.244271053	
28	15	0.231226	14	87.92	0.83550642	3.613368034	3.359879205	0.253488829	
29	15	0.231226	14.5	91.06	0.89625115	3.876074639	3.613368034	0.262706605	
30	15	0.231226	15	94.2	0.95912727	4.147999019	3.876074639	0.27192438	

≅ 4.147999019

Figure G-5. Insertion Prediction Spreadsheet, (Robust Check).

Pile Insertion Spreadsheet		SQ-1						
Vc (ft ³)	192.5							
D (ft)	2							
A (ft ²)	3.14							
Pb (psi)	112.5							
Pa (psi)	14.7							
Depth (ft)	N value	m	L/D	lv (ft ³)	(lv/vc)(L/D)/ (Pb/Pa)	Time req (min)	Prev Increment	Incremental
0.1	2	0.77495	0.05	0.314	1.0657E-05	1.37518E-05	0	1.37518E-05
1	2	0.77495	0.5	3.14	0.0010657	0.001375182	1.37518E-05	0.00136143
2	2	0.77495	1	6.28	0.00426279	0.005500729	0.001375182	0.004125547
3	2	0.77495	1.5	9.42	0.00959127	0.012376641	0.005500729	0.006875911
4	2	0.77495	2	12.56	0.01705115	0.022002917	0.012376641	0.009626276
5	2	0.77495	2.5	15.7	0.02664242	0.034379557	0.022002917	0.012376641
6	2	0.77495	3	18.84	0.03836509	0.049506562	0.034379557	0.015127005
7	2	0.77495	3.5	21.98	0.05221915	0.067383932	0.049506562	0.01787737
8	2	0.77495	4	25.12	0.06820461	0.088011666	0.067383932	0.020627734
9	2	0.77495	4.5	28.26	0.08632145	0.111389765	0.088011666	0.023378099
10	2	0.77495	5	31.4	0.1065697	0.137518229	0.111389765	0.026128463
11	23	0.134196	5.5	34.54	0.12894933	0.960906242	0.79413739	0.166768852
12	23	0.134196	6	37.68	0.15346036	1.143557842	0.960906242	0.1826516
13	21	0.158586	6.5	40.82	0.18010279	1.135677889	0.967678201	0.167999688
14	19	0.18741	7	43.96	0.20887661	1.11454436	0.961010188	0.153534172
15	17	0.221472	7.5	47.1	0.23978182	1.082671306	0.943127004	0.139544302
16	15	0.261726	8	50.24	0.27281842	1.042381981	0.916156038	0.126225943
17	13	0.309296	8.5	53.38	0.30798642	0.99576669	0.882063228	0.113703463
18	14	0.284518	9	56.52	0.34528582	1.213579834	1.082483247	0.131096587
19	15	0.261726	9.5	59.66	0.38471661	1.469921466	1.319264695	0.150656771
20	16	0.240759	10	62.8	0.42627879	1.770559439	1.597929893	0.172629545
21	17	0.221472	10.5	65.94	0.46997236	2.12203576	1.924748988	0.197286771
22	18	0.20373	11	69.08	0.51579733	2.531763064	2.306833701	0.224929363
23	19	0.18741	11.5	72.22	0.5637537	3.008132482	2.752242195	0.255890287
24	20	0.172397	12	75.36	0.61384145	3.560634208	3.270096347	0.290537861
25	21	0.158586	12.5	78.5	0.66606061	4.199992192	3.870712804	0.329279388
26	22	0.145882	13	81.64	0.72041115	4.938314569	4.565749416	0.372565152
27	23	0.134196	13.5	84.78	0.77689309	5.789261573	5.368368756	0.420892817
28	24	0.123445	14	87.92	0.83550642	6.768232922	6.293420663	0.474812259
29	25	0.113556	14.5	91.06	0.89625115	7.892576834	7.357645943	0.534930891
30	26	0.104459	15	94.2	0.95912727	9.181823102	8.579903587	0.601919514

≡ 5.207855225

Figure G- 6. SQ-1 Insertion Prediction Spreadsheet (upper N-value zone neglected).

Pile Insertion Spreadsheet SQ-2

Vc (ft³) 179
D (ft) 2
A (ft²) 3.14
Pb (psi) 100
Pa (psi) 14.7

Depth (ft)	N value	m	L/D	lv (ft ³)	(lv/Vc)(L/D)/ (Pb/Pa)	Time req (min)	Prev Increment	Incremental
0.001	2	0.77495	0.0005	0.00314	1.2893E-09	1.66376E-09	0	1.66376E-09
1	2	0.77495	0.5	3.14	0.00128933	0.001663759	1.66376E-09	0.001663758
2	2	0.77495	1	6.28	0.00515732	0.006655037	0.001663759	0.004991278
3	2	0.77495	1.5	9.42	0.01160397	0.014973834	0.006655037	0.008318796
4	2	0.77495	2	12.56	0.02062927	0.026620149	0.014973834	0.011646315
5	2	0.77495	2.5	15.7	0.03223324	0.041593982	0.026620149	0.014973834
6	2	0.77495	3	18.84	0.04641587	0.059895335	0.041593982	0.018301352
7	2	0.77495	3.5	21.98	0.06317715	0.081524206	0.059895335	0.021628871
8	2	0.77495	4	25.12	0.08251709	0.106480595	0.081524206	0.024956389
9	2	0.77495	4.5	28.26	0.1044357	0.134764503	0.106480595	0.028283908
10	2	0.77495	5	31.4	0.12893296	0.16637593	0.134764503	0.031611427
11	2	0.77495	5.5	34.54	0.15600888	0.201314875	0.16637593	0.034938945
12	2	0.77495	6	37.68	0.18566346	0.239581339	0.201314875	0.038266464
13	2	0.77495	6.5	40.82	0.2178967	0.281175321	0.239581339	0.041593982
14	23	0.134196	7	43.96	0.2527086	1.883137106	1.623725361	0.259411744
15	23	0.134196	7.5	47.1	0.29009916	2.161764534	1.883137106	0.278627429
16	21	0.158586	8	50.24	0.33006838	2.081319036	1.829284309	0.252034727
17	19	0.18741	8.5	53.38	0.37261626	1.988242511	1.761211359	0.227031152
18	17	0.221472	9	56.52	0.41774279	1.886206965	1.68245004	0.203756925
19	15	0.261726	9.5	59.66	0.46544799	1.778379148	1.596107601	0.182271547
20	13	0.309296	10	62.8	0.51573184	1.667439051	1.504863744	0.162575307
21	14	0.284518	10.5	65.94	0.56859436	1.998444795	1.81264834	0.185796455
22	15	0.261726	11	69.08	0.62403553	2.384308885	2.17247979	0.211829095
23	16	0.240759	11.5	72.22	0.68205536	2.83293374	2.591946938	0.240986802
24	17	0.221472	12	75.36	0.74265385	3.353256827	3.079640385	0.273616442
25	18	0.20373	12.5	78.5	0.80583101	3.955377517	3.64527592	0.310101597
26	19	0.18741	13	81.64	0.87158682	4.650698745	4.29983242	0.350866325
27	20	0.172397	13.5	84.78	0.93992128	5.452085151	5.055705847	0.396379305
28	21	0.158586	14	87.92	1.01083441	6.374039547	5.926881161	0.447158387
29	22	0.145882	14.5	91.06	1.0843262	7.432899762	6.929124153	0.503775608
30	23	0.134196	15	94.2	1.16039665	8.647058138	8.080195437	0.5668627
31	24	0.123445	15.5	97.34	1.23904575	10.0372062	9.400089057	0.637117147
32	25	0.113556	16	100.48	1.32027352	11.62660732	10.91129847	0.715308849
33	26	0.104459	16.5	103.62	1.40407994	13.44140036	12.63911292	0.802287441

≡ 7.21 min

Figure G- 7. SQ-2 Insertion Prediction Spreadsheet (upper N-value zone neglected).

Pile Insertion Spreadsheet		SQ-3						
Vc (ft ³)	139							
D (ft)	2							
A (ft ²)	3.14							
Pb (psi)	98							
Pa (psi)	14.7							
Depth (ft)	N value	m	L/D	lv (ft ³)	(lv/Vc)(L/D)/ (Pb/Pa)	Time req (min)	Prev Increment	Incremental
0.001	2	0.77495	0.0005	0.00314	1.6942E-09	2.18626E-09	0	2.18626E-09
1	2	0.77495	0.5	3.14	0.00169424	0.002186264	2.18626E-09	0.002186262
2	2	0.77495	1	6.28	0.00677698	0.008745057	0.002186264	0.006558793
3	2	0.77495	1.5	9.42	0.0152482	0.019676378	0.008745057	0.010931321
4	2	0.77495	2	12.56	0.02710791	0.034980228	0.019676378	0.01530385
5	2	0.77495	2.5	15.7	0.04235612	0.054656606	0.034980228	0.019676378
6	2	0.77495	3	18.84	0.06099281	0.078705513	0.054656606	0.024048907
7	2	0.77495	3.5	21.98	0.08301799	0.107126948	0.078705513	0.028421435
8	2	0.77495	4	25.12	0.10843165	0.139920911	0.107126948	0.032793964
9	2	0.77495	4.5	28.26	0.13723381	0.177087403	0.139920911	0.037166492
10	2	0.77495	5	31.4	0.16942446	0.218626424	0.177087403	0.04153902
11	2	0.77495	5.5	34.54	0.2050036	0.264537973	0.218626424	0.045911549
12	2	0.77495	6	37.68	0.24397122	0.31482205	0.264537973	0.050284077
13	2	0.77495	6.5	40.82	0.28632734	0.369478656	0.31482205	0.054656606
14	2	0.77495	7	43.96	0.33207194	0.42850779	0.369478656	0.059029134
15	2	0.77495	7.5	47.1	0.38120504	0.491909453	0.42850779	0.063401663
16	23	0.134196	8	50.24	0.43372662	3.232049398	2.840668416	0.391380982
17	23	0.134196	8.5	53.38	0.48963669	3.648680766	3.232049398	0.416631368
18	21	0.158586	9	56.52	0.54893525	3.461432414	3.087512246	0.373920168
19	19	0.18741	9.5	59.66	0.6116223	3.263554499	2.929062763	0.334491735
20	17	0.221472	10	62.8	0.67769784	3.059965151	2.761618548	0.298346602
21	15	0.261726	10.5	65.94	0.74716187	2.854748807	2.589341321	0.265407485
22	13	0.309296	11	69.08	0.82001439	2.65123054	2.415687331	0.235543209
23	14	0.284518	11.5	72.22	0.8962554	3.150078622	2.882113522	0.2679651
24	15	0.261726	12	75.36	0.97588489	3.728651502	3.424403897	0.304247605
25	16	0.240759	12.5	78.5	1.05890288	4.398179168	4.053361921	0.344817247
26	17	0.221472	13	81.64	1.14530935	5.171341105	4.781195548	0.390145557
27	18	0.20373	13.5	84.78	1.23510432	6.062442139	5.621688458	0.440753681
28	19	0.18741	14	87.92	1.32828777	7.087608662	6.590391218	0.497217444
29	20	0.172397	14.5	91.06	1.42485971	8.265007511	7.704834588	0.560172923
30	21	0.158586	15	94.2	1.52482014	9.615090039	8.98476747	0.630322569

≅ 5.751363676

Figure G- 8. SQ-3 Insertion Prediction Spreadsheet (upper N-value zone neglected).

Pile Insertion Spreadsheet SQ-4

Vc (ft³) 139
D (ft) 2
A (ft²) 3.14
Pb (psi) 100
Pa (psi) 14.7

Depth (ft)	N value	m	L/D	lv (ft ³)	(lv/Qw)(L/D)	Time req (min)	Prev Increment	Incremental
					/(Pb/Pa)			
0.001	2	0.77495	0.0005	0.00314	1.6604E-09	2.14254E-09	0	2.14254E-09
1	2	0.77495	0.5	3.14	0.00166036	0.002142539	2.14254E-09	0.002142537
2	2	0.77495	1	6.28	0.00664144	0.008570156	0.002142539	0.006427617
3	2	0.77495	1.5	9.42	0.01494324	0.019282851	0.008570156	0.010712695
4	2	0.77495	2	12.56	0.02656576	0.034280623	0.019282851	0.014997773
5	2	0.77495	2.5	15.7	0.04150899	0.053563474	0.034280623	0.019282851
6	2	0.77495	3	18.84	0.05977295	0.077131402	0.053563474	0.023567928
7	2	0.77495	3.5	21.98	0.08135763	0.104984409	0.077131402	0.027853006
8	2	0.77495	4	25.12	0.10626302	0.137122493	0.104984409	0.032138084
9	2	0.77495	4.5	28.26	0.13448914	0.173545655	0.137122493	0.036423162
10	23	0.134196	5	31.4	0.16603597	1.23726891	1.002187817	0.235081093
11	23	0.134196	5.5	34.54	0.20090353	1.497095381	1.23726891	0.259826471
12	21	0.158586	6	37.68	0.2390918	1.507646118	1.26684153	0.240804588
13	19	0.18741	6.5	40.82	0.28060079	1.49725733	1.275769559	0.221487771
14	17	0.221472	7	43.96	0.3254305	1.469395265	1.266978571	0.202416695
15	15	0.261726	7.5	47.1	0.37358094	1.427374403	1.243401702	0.183972701
16	13	0.309296	8	50.24	0.42505209	1.374257681	1.207843665	0.166414016
17	14	0.284518	8.5	53.38	0.47984396	1.686512793	1.493935207	0.192577585
18	15	0.261726	9	56.52	0.53795655	2.055419141	1.833383122	0.222036018
19	16	0.240759	9.5	59.66	0.59938986	2.489580522	2.234415759	0.255164763
20	17	0.221472	10	62.8	0.66414388	2.998765848	2.706386177	0.29237967
21	18	0.20373	10.5	65.94	0.73221863	3.594055204	3.259914017	0.334141187
22	19	0.18741	11	69.08	0.8036141	4.288003241	3.907044275	0.380958966
23	20	0.172397	11.5	72.22	0.87833029	5.094821872	4.661424926	0.433396946
24	21	0.158586	12	75.36	0.95636719	6.030584472	5.538505531	0.492078941
25	22	0.145882	12.5	78.5	1.03772482	7.113454014	6.55575922	0.557694795
26	23	0.134196	13	81.64	1.12240317	8.363937833	7.732930689	0.631007144
26.5	24	0.123445	13.25	83.21	1.16598761	9.445380054	9.09231316	0.353066894

≅ 5.654506243

Figure G- 9. SQ-4 Insertion Prediction Spreadsheet (upper N-value zone neglected).

Pile Insertion Spreadsheet SQ-9

Vc (ft³) 165.8
D (ft) 2
A (ft²) 3.14
Pb (psi) 125
Pa (psi) 14.7

Depth (ft)	N value	m	L/D	lv (ft ³)	(lv/Vc)(L/D)/ (Pb/Pa)	Time req (min)	Prev Increment	Incremental
0.001	2	0.77495	0.0005	0.00314	1.1136E-09	1.43697E-09	0	1.43697E-09
1	2	0.77495	0.5	3.14	0.00111358	0.001436974	1.43697E-09	0.001436973
2	2	0.77495	1	6.28	0.00445433	0.005747897	0.001436974	0.004310923
3	2	0.77495	1.5	9.42	0.01002224	0.012932768	0.005747897	0.007184871
4	2	0.77495	2	12.56	0.01781732	0.022991588	0.012932768	0.01005882
5	2	0.77495	2.5	15.7	0.02783957	0.035924356	0.022991588	0.012932768
6	2	0.77495	3	18.84	0.04008897	0.051731073	0.035924356	0.015806717
7	2	0.77495	3.5	21.98	0.05456555	0.070411738	0.051731073	0.018680665
8	2	0.77495	4	25.12	0.07126929	0.091966352	0.070411738	0.021554614
9	2	0.77495	4.5	28.26	0.09020019	0.116394915	0.091966352	0.024428562
10	2	0.77495	5	31.4	0.11135826	0.143697425	0.116394915	0.027302511
11	2	0.77495	5.5	34.54	0.1347435	0.173873885	0.143697425	0.030176459
12	2	0.77495	6	37.68	0.1603559	0.206924293	0.173873885	0.033050408
13	2	0.77495	6.5	40.82	0.18819546	0.242848649	0.206924293	0.035924356
14	2	0.77495	7	43.96	0.2182622	0.281646954	0.242848649	0.038798305
15	4	0.655762	7.5	47.1	0.25055609	0.382083852	0.332837489	0.049246363
16	4	0.655762	8	50.24	0.28507715	0.434726516	0.382083852	0.052642664
17	4	0.655762	8.5	53.38	0.32182538	0.490765481	0.434726516	0.056038965
18	26	0.104459	9	56.52	0.36080077	3.45398255	3.080867151	0.373115399
19	26	0.104459	9.5	59.66	0.40200333	3.848418829	3.45398255	0.394436279
20	22.6	0.138753	10	62.8	0.44543305	3.21025046	2.89725104	0.31299942
21	19.2	0.184306	10.5	65.94	0.49108994	2.664534278	2.416811136	0.247723141
22	15.8	0.244814	11	69.08	0.53897399	2.201566866	2.005973115	0.19559375
23	12.4	0.325186	11.5	72.22	0.58908521	1.811531905	1.657431838	0.154100068
24	9	0.431945	12	75.36	0.64142359	1.484966291	1.363797167	0.121169124
25	12.6	0.319801	12.5	78.5	0.69598914	2.17632149	2.005697885	0.170623605
26	16.2	0.236772	13	81.64	0.75278186	3.179352272	2.939489896	0.239862376
27	19.8	0.1753	13.5	84.78	0.81180174	4.630932001	4.294252445	0.336679556
28	23.4	0.129787	14	87.92	0.87304878	6.726758863	6.254856137	0.471902726
29	27	0.096091	14.5	91.06	0.93652299	9.746186418	9.085624437	0.660561981
30	27.2	0.0945	15	94.2	1.00222437	10.60556831	9.910314385	0.695253922
31	27.4	0.092935	15.5	97.34	1.07015291	11.51509543	10.78416846	0.730926973
31.5	27.6	0.091396	15.75	98.91	1.10495236	12.08976834	11.70901222	0.380756121

≡ 5.64 min

Figure G- 10. SQ-9 Insertion Prediction Spreadsheet (upper N-value zone neglected).

Pile Insertion Spreadsheet SQ-10

Vc (ft³) 175
D (ft) 2
A (ft²) 3.14
Pb (psi) 78
Pa (psi) 14.7

Depth (ft)	N value	m	L/D	lv (ft ³)	(lv/Vc)(L/D) (Pb/Pa)	Time req (min)	Prev Increment	Incremental
0.001	2	0.77495	0.00	0.00	0.00	0.00	0.00	0.00
1	2	0.77495	0.50	3.14	0.00	0.00	0.00	0.00
2	2	0.77495	1.00	6.28	0.01	0.01	0.00	0.01
3	2	0.77495	1.50	9.42	0.02	0.02	0.01	0.01
4	2	0.77495	2.00	12.56	0.03	0.03	0.02	0.02
5	2	0.77495	2.50	15.70	0.04	0.05	0.03	0.02
6	2	0.77495	3.00	18.84	0.06	0.08	0.05	0.02
7	2	0.77495	3.50	21.98	0.08	0.11	0.08	0.03
8	2	0.77495	4.00	25.12	0.11	0.14	0.11	0.03
9	2	0.77495	4.50	28.26	0.14	0.18	0.14	0.04
10	2	0.77495	5.00	31.40	0.17	0.22	0.18	0.04
11	2	0.77495	5.50	34.54	0.20	0.26	0.22	0.05
12	2	0.77495	6.00	37.68	0.24	0.31	0.26	0.05
13	2	0.77495	6.50	40.82	0.29	0.37	0.31	0.05
14	2	0.77495	7.00	43.96	0.33	0.43	0.37	0.06
15	4	0.655762	7.50	47.10	0.38	0.58	0.51	0.07
16	4	0.655762	8.00	50.24	0.43	0.66	0.58	0.08
17	4	0.655762	8.50	53.38	0.49	0.75	0.66	0.09
18	26	0.104459	9.00	56.52	0.55	5.24	4.68	0.57
19	26	0.104459	9.50	59.66	0.61	5.84	5.24	0.60
20	22.6	0.138753	10.00	62.80	0.68	4.87	4.40	0.48
21	19.2	0.184306	10.50	65.94	0.75	4.05	3.67	0.38
22	15.8	0.244814	11.00	69.08	0.82	3.34	3.05	0.30
23	12.4	0.325186	11.50	72.22	0.89	2.75	2.52	0.23
24	9	0.431945	12.00	75.36	0.97	2.25	2.07	0.18
25	12.6	0.319801	12.50	78.50	1.06	3.30	3.05	0.26
26	16.2	0.236772	13.00	81.64	1.14	4.83	4.46	0.36
27	19.8	0.1753	13.50	84.78	1.23	7.03	6.52	0.51
28	23.4	0.129787	14.00	87.92	1.33	10.21	9.50	0.72
29	27	0.096091	14.50	91.06	1.42	14.80	13.79	1.00
30	27.2	0.0945	15.00	94.20	1.52	16.10	15.05	1.06
31	27.4	0.092935	15.50	97.34	1.62	17.48	16.37	1.11
32	27.6	0.091396	16.00	100.48	1.73	18.94	17.78	1.17
32.5	27.8	0.089882	16.25	102.05	1.79	19.87	19.26	0.61

◦ 9.76 min

Figure G- 11. SQ-10 Insertion Prediction Spreadsheet (upper N-value zone neglected).

Pile Insertion Spreadsheet

SC-1

Vc (ft³) 139
 D (ft) 2
 A (ft²) 3.14
 Pb (psi) 125
 Pa (psi) 14.7

Depth (ft)	N value	m	L/D	lv (ft ³)	(lv/Qw)(L/D) /(Pb/Pa)	Time req (min)	Prev Increment	Incremental
0.001	2	0.77495	0.0005	0.00314	1.3283E-09	1.71403E-09	0	1.71403E-09
1	2	0.77495	0.5	3.14	0.00132829	0.001714031	1.71403E-09	0.001714029
2	2	0.77495	1	6.28	0.00531315	0.006856125	0.001714031	0.005142093
3	2	0.77495	1.5	9.42	0.01195459	0.01542628	0.006856125	0.008570156
4	2	0.77495	2	12.56	0.0212526	0.027424499	0.01542628	0.011998218
5	2	0.77495	2.5	15.7	0.03320719	0.042850779	0.027424499	0.01542628
6	13	0.309296	3	18.84	0.04781836	0.154603989	0.107363881	0.047240108
7	13	0.309296	3.5	21.98	0.0650861	0.210433207	0.154603989	0.055829218
8	13	0.309296	4	25.12	0.08501042	0.274851536	0.210433207	0.064418329
9	13	0.309296	4.5	28.26	0.10759131	0.347858976	0.274851536	0.073007439
10	13	0.309296	5	31.4	0.13282878	0.429455525	0.347858976	0.08159655
11	13	0.309296	5.5	34.54	0.16072282	0.519641186	0.429455525	0.09018566
12	13	0.309296	6	37.68	0.19127344	0.618415957	0.519641186	0.098774771
13	13	0.309296	6.5	40.82	0.22448063	0.725779838	0.618415957	0.107363881
14	13	0.309296	7	43.96	0.2603444	0.84173283	0.725779838	0.115952992
15	13	0.309296	7.5	47.1	0.29886475	0.966274932	0.84173283	0.124542102
16	13	0.309296	8	50.24	0.34004167	1.099406145	0.966274932	0.133131213

° 0.992042264

Figure G- 12. SC-1 Insertion Prediction Spreadsheet.

Jetting Model Spreadsheet

C_c = Coeff of Curvature of the grain size distribution

$$C_c = (D_{30})^2 / (D_{10} * D_{60})$$

Q_w = Pump Flowrate

A = Area of Pile

P_b = Pump pressure

P_a = Atmospheric Pressure

Qw (gal/min)	1200
Diam (ft)	2
A (ft ²)	3.14
Pb (psi)	100
Pa (psi)	14.7

C _c	1.05
D50 (mm)	0.17
Total Depth(ft)	30

Incremental
Insertion Time

Depth (ft)	N value	m	L/D	lv (ft ³)	IP	Time req (min)	Prev Increment	(min)
0.1	30	0.093459	0.05	0.314	1.4387E-05	0.000153938	0	0.0002
1	30	0.093459	0.5	3.14	0.00143869	0.015393807	0.000153938	0.0152
2	30	0.093459	1	6.28	0.00575476	0.061575226	0.015393807	0.0462
3	30	0.093459	1.5	9.42	0.01294822	0.138544259	0.061575226	0.0770
4	30	0.093459	2	12.56	0.02301906	0.246300904	0.138544259	0.1078
5	30	0.093459	2.5	15.7	0.03596727	0.384845163	0.246300904	0.1385
6	30	0.093459	3	18.84	0.05179287	0.554177034	0.384845163	0.1693
7	30	0.093459	3.5	21.98	0.07049586	0.754296519	0.554177034	0.2001
8	30	0.093459	4	25.12	0.09207622	0.985203617	0.754296519	0.2309
9	30	0.093459	4.5	28.26	0.11653397	1.246898327	0.985203617	0.2617
10	30	0.093459	5	31.4	0.1438691	1.539380651	1.246898327	0.2925
11	30	0.093459	5.5	34.54	0.17408161	1.862650588	1.539380651	0.3233
12	30	0.093459	6	37.68	0.2071715	2.216708137	1.862650588	0.3541
13	30	0.093459	6.5	40.82	0.24313877	2.6015533	2.216708137	0.3848
14	30	0.093459	7	43.96	0.28198343	3.017186076	2.6015533	0.4156
15	30	0.093459	7.5	47.1	0.32370547	3.463606464	3.017186076	0.4464
16	30	0.093459	8	50.24	0.36830489	3.940814466	3.463606464	0.4772
17	30	0.093459	8.5	53.38	0.41578169	4.448810081	3.940814466	0.5080
18	30	0.093459	9	56.52	0.46613587	4.987593309	4.448810081	0.5388
19	30	0.093459	9.5	59.66	0.51936744	5.55716415	4.987593309	0.5696
20	30	0.093459	10	62.8	0.57547639	6.157522603	5.55716415	0.6004
21	30	0.093459	10.5	65.94	0.63446272	6.78866867	6.157522603	0.6311
22	30	0.093459	11	69.08	0.69632643	7.45060235	6.78866867	0.6619
23	30	0.093459	11.5	72.22	0.76106752	8.143323643	7.45060235	0.6927
24	30	0.093459	12	75.36	0.828686	8.866832549	8.143323643	0.7235
25	30	0.093459	12.5	78.5	0.89918186	9.621129068	8.866832549	0.7543
26	30	0.093459	13	81.64	0.97255509	10.4062132	9.621129068	0.7851
27	30	0.093459	13.5	84.78	1.04880572	11.22208494	10.4062132	0.8159
28	30	0.093459	14	87.92	1.12793372	12.0687443	11.22208494	0.8467
29	30	0.093459	14.5	91.06	1.2099391	12.94619127	12.0687443	0.8774
30	30	0.093459	15	94.2	1.29482187	13.85442586	12.94619127	0.9082

Π 14 TOTAL TIME (min)

Qw (ft ³ /min)	Q _p (ft ³ /min)	V _{total} (ft ³)	Q _w /Q _p	a _{volume}	b _{volume}	a _{area}	b _{area}	Predicted		
								V _{debris}	A _{debris}	D _{debris}
160.41666	6.80	2222.48	23.59	1.41	-0.97	11.37	-0.94	144.26	655.44	28.89

Q_p must be >= Apile * 1foot

Figure G- 13. Example of Proposed Jetting Model Spreadsheet.

APPENDIX H
Environmental Impact of Pile Jetting on Macrobenthos

TAXA

POLYCHAETA

Amphectis floridium (*Hobsonia floridia*)

Eteone heteropoda

Heteromastus filiformis

Mediomastus californiensis

Notomastus hemipodus

Neanthes succinea

Polydora websteri

Streblospio benedicti

Scolecopelides viridis

CRUSTACEA

Callinectes sapidus

Rithropanopeus harrisi

Edotea sp.

Cumacea sp.

Cyathura polita

Mysis sp.

Sphaeroma quadridentatum

Tanaidacea (*Tanais* sp.)

Corophium lacustre

Melita nitida

Gammarus tigrinus

MOLLUSCA

Macoma balthica

Macoma mitchelli

Macoma tenta

Mulinia lateralis

Mytilopsis leucophaeta

Rangia cuneata

Tellina alternata

Littodorinops tenuipes

Crassostrea virginica

INSECTA (DIPTERA)

Ceratopogonidae *Culcoides* sp.

Chironomus plumosus

Cryptochironomus fulvus

Cryptotendipedes sp.

Dicrotendipedes modestus

Polypelilum halterale

Polypelilum scalaenum

Continued

Procladius bellus type
Cladotanytarsus sp.
Micropsectra sp. D
Rheotanytarsus sp.
Coelotanypus scapularis
Tanypus neopunctipennis

OTHER

Barnacle
Cerebratus lacteus
Lineus socialis
Turbellaria
Leech

OLIGOCHAETA

Limnodrilus hoffmansteri
Tubificex tubifex
Nais communis complex

MEIOFAUNA Observed**

Foraminifera
Calanoid copepoda
Harpacticoida
Nematoda

Colonials

Encrusting Bryozoa
Colonial hydroid

Vertebrates

FISH

**not included in species totals

APPENDIX H-1. List of macrobenthic families and species enumerated from benthic Ponor grab samples taken from the White Oak River, Swan Quarter Ferry terminal basin, and Cherry Point ferry terminal basin, North Carolina during March 2004.

2004 DOT Jetting Sample Summary

Location	Date	sample	Salinity		DO mg/l	pH	Turbidity NTU	Start time	GPS N	GPS W	Water depth M	Grab depth cm
			temp C	ppt								
White Oak River	3/29/2004	WOR1-1	15.3	0.2	8.25	7.08	8.3	9:15	34.77453	77.15411	0.7	5.8
White Oak River	3/29/2004	WOR1-2							34.77449	77.15405	1.2	6.5
White Oak River	3/29/2004	WOR1-3							34.77448	77.15402	1.1	5.1
White Oak River	3/29/2004	WOR1-4							34.77451	77.15395	1.3	4.0
White Oak River	3/29/2004	WOR1-5							34.77456	77.15406	0.35	7.5
White Oak River	3/29/2004	WOR2-1	15.7	0.1	8.45	7.07	7.1	11:17	34.77469	77.15407	0.7	5.0
White Oak River	3/29/2004	WOR2-2							34.77470	77.15405	0.8	3.0
White Oak River	3/29/2004	WOR2-3							34.77470	77.15401	1.1	6.5
White Oak River	3/29/2004	WOR2-4							34.77470	77.15399	1.3	5.0
White Oak River	3/29/2004	WOR2-5							34.77471	77.15391	1.3	5.5
White Oak River	3/29/2004	WOIA-1	16	0.1	8.35	7.5	6.9	13:12	34.77480	77.15399	0.9	6.0
White Oak River	3/29/2004	WOIA-2							34.77477	77.15401	0.9	6.5
White Oak River	3/29/2004	WOIA-3							34.77479	77.15401	0.4	6.0
White Oak River	3/29/2004	WOIA-4							34.77476	77.15400	0.6	3.0
White Oak River	3/29/2004	WOIA-5							34.77478	77.15404	0.4	5.5
White Oak River	3/29/2004	WOR3-1	16.3	0.1	8.46	6.89	12.6	14:22	34.77481	77.15403	0.1	1.0
White Oak River	3/29/2004	WOR3-2							34.77493	77.15400	0.2	5.5
White Oak River	3/29/2004	WOR3-3							34.77489	77.15402	0.2	6.0
White Oak River	3/29/2004	WOR3-4							34.77488	77.15392	0.6	6.0
White Oak River	3/29/2004	WOR3-5							34.77489	77.15400	0.5	6.0
White Oak River	3/29/2004	WOR4-1	16.7	0.1	8.34	7.13	8.9	15:19	34.77502	77.15403	0.2	5.0
White Oak River	3/29/2004	WOR4-2							34.77501	77.15399	0.6	6.5
White Oak River	3/29/2004	WOR4-3							34.77503	77.15398	0.5	5.0
White Oak River	3/29/2004	WOR4-4							34.77502	77.15396	0.8	4.5
White Oak River	3/29/2004	WOR4-5							34.77500	77.15402	0.5	6.0

Appendix H-2 Jetting Sample summary : White Oak

Continued-Cherry Branch

Cherry Branch	3/30/2004	CBR1-1	12.2	2.8	9.03	7.67	17.8	10:33	34.93562	76.80997	2.7	3.0
Cherry Branch	3/30/2004	CBR1-2							34.93568	76.81007	2.7	7.0
Cherry Branch	3/30/2004	CBR1-3							34.93566	76.80986	2.7	7.5
Cherry Branch	3/30/2004	CBR1-4							34.93572	76.81009	2.7	6.0
Cherry Branch	3/30/2004	CBR1-5							34.93568	76.80999	2.7	6.0
Cherry Branch	3/30/2004	CBR2-1	13.3	2.7	9.1	7.18	15.8	11:35	34.93575	76.81006	2.7	5.5
Cherry Branch	3/30/2004	CBR2-2							34.93575	76.81003	2.7	7.0
Cherry Branch	3/30/2004	CBR2-3							34.93577	76.80999	2.7	6.5
Cherry Branch	3/30/2004	CBR2-4							34.93578	76.81007	2.7	2.0
Cherry Branch	3/30/2004	CBR2-5							34.93581	76.81007	2.7	6.0
Cherry Branch	3/30/2004	CBIA-1	14	2.9	8.73	7.32	17.7	12:46	34.93580	76.81005	2.6	5.0
Cherry Branch	3/30/2004	CBIA-2							34.93588	76.81003	2.6	8.5
Cherry Branch	3/30/2004	CBIA-3							34.93588	76.80997	2.5	6.5
Cherry Branch	3/30/2004	CBIA-4							34.93590	76.80998	2.5	7.0
Cherry Branch	3/30/2004	CBIA-5							34.93588	76.80996	2.5	5.0
Cherry Branch	3/30/2004	CBR3-1	14.3	2.6	8.7	7.17	17.4	13:45	34.93592	76.81002	2.5	6.0
Cherry Branch	3/30/2004	CBR3-2							34.93592	76.81004	2.5	7.0
Cherry Branch	3/30/2004	CBR3-3							34.93595	76.81001	2.5	7.5
Cherry Branch	3/30/2004	CBR3-4							34.93595	76.81004	2.6	8.0
Cherry Branch	3/30/2004	CBR3-5							34.93595	76.81005	2.6	6.5
Cherry Branch	3/30/2004	CBR4-1	13.8	2.9	8.93	7.15	15.7	14:46	34.93600	76.81007	2.5	6.5
Cherry Branch	3/30/2004	CBR4-2							34.93603	76.81005	2.5	7.0
Cherry Branch	3/30/2004	CBR4-3							34.93600	76.81008	2.5	4.0
Cherry Branch	3/30/2004	CBR4-4							34.93601	76.81001	2.5	8.0
Cherry Branch	3/30/2004	CBR4-5							34.93601	76.80997	2.5	8.0

Continued-Swan Quarter

Swan Quarter	3/31/2004	SQR1-1	12.8	9	9.24	7.22	13.2	9:25	35.39542	76.32788	3.4	5.0
Swan Quarter	3/31/2004	SQR1-2							35.39542	76.32791	3.5	5.0
Swan Quarter	3/31/2004	SQR1-3							35.39545	76.32787	2.5	5.0
Swan Quarter	3/31/2004	SQR1-4							35.39543	76.32785	2.4	4.0
Swan Quarter	3/31/2004	SQR1-5							35.39546	76.32781	1.5	4.0
Swan Quarter	3/31/2004	SQR2-1	12.7	9	9.67	nodata	15.8	9:54	35.39534	76.32773	2.4	4.5
Swan Quarter	3/31/2004	SQR2-2							35.39526	76.32766	3.1	3.0
Swan Quarter	3/31/2004	SQR2-3						12:40	35.39533	76.32773	3.5	5.5
Swan Quarter	3/31/2004	SQR2-4							35.39531	76.32774	3.4	6.0
Swan Quarter	3/31/2004	SQR2-5							35.39532	76.32772	3.4	6.0
Swan Quarter	3/31/2004	SQIA-1	12.8	9	9.98	7.11	nodata	10:54	35.39523	76.27580	2	3.0
Swan Quarter	3/31/2004	SQIA-2							35.39522	76.32760	2	3.5
Swan Quarter	3/31/2004	SQIA-3							35.39525	76.32761	5.3	3.5
Swan Quarter	3/31/2004	SQIA-4							35.39525	76.32757	1.6	2.0
Swan Quarter	3/31/2004	SQIA-5							39.39525	76.32759	1.5	2.0
Swan Quarter	3/31/2004	SQR3-1	12.8	9	10.06	7.21	nodata	11:20	35.39504	76.32743	2.9	5.5
Swan Quarter	3/31/2004	SQR3-2							35.39505	76.32745	3	5.5
Swan Quarter	3/31/2004	SQR3-3							35.39503	76.32747	3	6.0
Swan Quarter	3/31/2004	SQR3-4							35.39508	76.32740	2.7	5.0
Swan Quarter	3/31/2004	SQR3-5							35.39508	76.32737	3.3	6.5
Swan Quarter	3/31/2004	SQR4-1	13.2	8.9	10.35	7.31	14.3	12:06	35.39493	76.32727	2.7	6.5
Swan Quarter	3/31/2004	SQR4-2							35.39492	76.32729	2.7	6.5
Swan Quarter	3/31/2004	SQR4-3							35.39492	76.32726	2.8	6.5
Swan Quarter	3/31/2004	SQR4-4							35.39496	76.32730	2.8	6.0
Swan Quarter	3/31/2004	SQR4-5							35.39495	76.32731	2.9	7.5

Appendix H-2 Jetting Sample summary